

NORTHWESTERN UNIVERSITY

A Strategy for the Convergent and Stereoselective Assembly of Polycyclic Molecules

A DISSERTATION

SUBMITTED TO THE GRADUATE SCHOOL
IN PARTIAL FULFILLMENT OF THE REQUIREMENTS

for the degree

DOCTOR OF PHILOSOPHY

Field of Chemistry

By

Emily Elizabeth Robinson

EVANSTON, ILLINOIS

September 2018

ABSTRACT

A Strategy for the Convergent and Stereoselective Assembly of Polycyclic Molecules

Emily Elizabeth Robinson

Fused polycyclic scaffolds with three-dimensional complexity from an array of stereocenters compose the core structures of countless natural product families with a variety of desirable biological activity. The development of synthetic methods and strategies to afford rapid access to these structures is essential to expose a wealth of untapped biological potential.

Oxidative enolate coupling is a powerful tool in the context of this task, forging a new carbon–carbon bond between two fragments. This reaction serves as the foundation for the strategy developed herein, facilitating the convergent and stereoselective construction of fused polycyclic scaffolds when employed in an oxidative coupling–ring-closing metathesis sequence. The established tandem successfully assembled several fused structures with four contiguous stereocenters, varying in substitution pattern and carbocyclic composition. Demonstrated selective manipulations of the prepared compounds reinforced the value of the strategy to complex molecule synthesis.

The developed strategy was successfully applied to the concise synthesis of marine diterpenoid (+)-7,20-diisocyanoadociane. Execution of the established sequence enabled the convergent construction of much of the natural product's all-*trans* perhydropyrene core structure, while exploiting the pseudo-symmetry within the molecule to amplify the efficiency of the final stages of the synthesis.

Thesis advisor: Professor Regan J. Thomson

Acknowledgements

First and foremost, I am so grateful to my advisor, Regan. Aside from your brilliance as a chemist, your dedication to mentorship was one of the biggest reasons that I joined your group. You have greatly aided my development as a chemist and problem solver, and have shown me overwhelming support, kindness, and patience during the most rewarding, and most challenging days. I'll never forget you coming with me to take that NMR of the final step in our DICA synthesis, or how unbelievably kind you were on the worst day of my graduate career. Allowing me to leave for a summer to complete an internship when it was not in your best interest highlights how much you care about what is best for your students. The list truly does go on and on.

I would like to thank my committee members, Professors Scheidt and Nguyen, as their support has meant, and continues to mean, a great deal to my personal and scientific development.

All past and present members of the Thomson group have astounded me with their intelligence, kindness, and friendship. It's very special that everyone I've ever known in the group has truly wanted to help each other out. I want to thank Jordan for being a great friend. To Marvin and Weiwei: I cannot imagine making it through the past five years without you two by my side.

I would never have accomplished this goal without the unwavering love and support of my family. My parents, Dan, Matt, Kristen, and Becca constantly cheer me on and build me up, and sharing this with them is an honor for me. To Dan and Kristen: having you two in Chicago during this time has been nothing short of a miracle for me. Lastly, to my partner in crime, Zach: You are my rock. No one inspires me, makes me laugh, or knows me to the core the way that you do, and I am so lucky to have you in my life. You have been by my side through the most difficult, and the absolute best days of this journey, and I share a huge part of this with you.

List of Abbreviations

Ac	acetyl
AcO	acetate
Ac ₂ O	acetic anhydride
acac	acetyl acetate
ACN	acetonitrile
AIBN	2,2'-azobis(2-methylpropionitrile)
ATR	attenuated total reflectance
9-BBN	9-borabicyclononane
BDSB	bromodiethylsulfonium bromopentachloroantimonate
BHT	dibutylhydroxytoluene
Bn	benzyl
BP	1,1'-biphenyl
bpy	2,2'-bipyridine
Bu or <i>n</i> Bu	butyl
BuLi	<i>n</i> -butyl lithium
Bz	benzoyl
CAN	ceric ammonium nitrate
Cbz	carboxybenzyl
cod	1,4-cyclooctadiene
Cp	cyclopentadienyl

CrO ₃ •DMP	chromium(IV) oxide-3,5-dimethylpyrazole
cy	cyclohexane
dba	dibenzylideneacetone
DBU	1,8-diazabicyclo[5.4.0]undec-7-ene
DCB	1,2-dichlorobenzene
DCE	dichloroethane
DCM	dichloromethane
DCTMB	1,4-dicyano-2,3,5,6-tetramethylbenzene
DDQ	2,3-dichloro-5,6-dicyano-1,4-benzoquinone
DEAD	diethyl azodicarboxylate
DIAD	diisopropyl azodicarboxylate
DIBAL	diisobutylaluminum hydride
DICA	diisocyanoadociane
DMAP	4-dimethylaminopyridine
DME	1,2-dimethoxyethane
DMF	dimethylformamide
DMP	Dess–Martin periodinane
DMPU	1,3-dimethyl-3,4,5,6-tetrahydro-2(1 <i>H</i>)-pyrimidinone
DMS	dimethylsulfide
DMSO	dimethyl sulfoxide
Mn(dpm) ₃	tris(2,2,6,6-tetramethyl-3,5-heptanedionato)manganese(III)

DTBP	2,6-di- <i>tert</i> -butylpyridine
dr	diastereomeric ratio
ee	enantiomeric excess
EI	electron impact
ESI	electrospray ionization
Et	ethyl
EtCN	propionitrile
EtOAc	ethyl acetate
equiv	equivalents
FT	Fourier transform
GC	gas chromatography
hfacac	hexafluoroacetylacetate
HFIP	hexafluoroisopropanol
HMPA	hexamethylphosphoramide
HRMS	high-resolution mass spectrometry
HPLC	high-pressure liquid chromatography
IBX	2-iodoxybenzoic acid
IPNBSH	<i>N</i> -isopropylidene- <i>N'</i> -2-nitrobenzenesulfonyl hydrazine
iPr or i-Pr	isopropyl
IR	infrared spectroscopy
<i>J</i>	coupling constant

KHMDS	potassium bis(trimethylsilyl)amide
LAH	lithium aluminum hydride
LBA	Lewis acid-assisted Brønsted acid
LDA	lithium diisopropylamide
LHMDS	lithium bis(trimethylsilyl)amide
LRMS	low resolution mass spectrometry
<i>m</i> CPBA	<i>meta</i> -chloroperoxybenzoic acid
Me	methyl
Mes	mesitylene
MOM	methoxymethyl
Ms	methanesulfonyl
MSA	methanesulfonic acid
NaHMDS	sodium bis(trimethylsilyl)amide
Nap	naphthyl
NBS	<i>N</i> -bromosuccinimide
NIS	<i>N</i> -iodosuccinimide
NMP	<i>N</i> -methylpyrrolidone
NMR	nuclear magnetic resonance spectrometry
NOE	nuclear Overhauser effect
PBQ	<i>p</i> -benzoquinone
PCC	pyridinium chlorochromate

PDC	pyridinium dichromate
Ph	phenyl
PMB	<i>p</i> -methoxybenzyl
Pr or <i>n</i> Pr	propyl
pTsOH or TsOH	toluenesulfonic acid
Red-Al	sodium bis(2-methoxyethoxy)aluminum hydride
SI	selectivity index
SOMO	singly occupied molecular orbital
TADA	transannular Diels–Alder
TBACN	tetrabutylammonium cerium(IV) nitrate
TBAF	tetrabutylammonium fluoride
TBDPS	<i>tert</i> -butyldiphenylsilyl
TBHP	<i>tert</i> -butyl hydrogen peroxide
TBS	<i>tert</i> -butyldimethylsilyl
^t Bu	<i>tert</i> -butyl
TES	triethylsilyl
Tf	(trifluoromethyl)sulfonyl
TFA	trifluoroacetic acid
TFAA	trifluoroacetic anhydride
TFE	trifluoroethanol
THF	tetrahydrofuran

TIPS	triisopropylsilyl
TLC	thin layer chromatography
TMS	trimethylsilyl
TMSCN	trimethylsilyl cyanide
Tr	triphenylmethyl
Ts	toluenesulfonyl

Table of Contents

1	Chapter 1	22
1.1	Introduction	22
1.2	Synthesis from linear precursors – polyene cyclization cascades	23
1.2.1	Cationic polyene cascades	24
1.2.2	Radical-based cyclizations	32
1.2.3	Pericyclic cyclizations	37
1.3	Synthesis from macrocyclic species – transannular reactions	39
1.3.1	Transannular Diels–Alder reactions	39
1.3.2	Radical-mediated macrocyclization–transannular cyclization cascade	41
1.4	Synthesis from building blocks – convergent and modular fragment coupling	43
1.4.1	Robinson annulation and similar domino transformations	44
1.4.2	Diels–Alder cycloaddition	47
1.4.3	Tethered cyclic species in convergent polycyclic assembly	51
1.5	Conclusion	54
2	Chapter 2	56
2.1	Introduction	56
2.2	Oxidative enolate coupling as a powerful tool	56
2.2.1	Coupling of metal enolates	58
2.2.2	Coupling of enol silanes	62
2.2.3	Coupling of enamines	69

	11
2.2.4 Electrochemical oxidative coupling	71
2.3 Development of a strategy for the construction of fused polycycles	72
2.4 Substrate preparation	74
2.5 Realization of the couple and close strategy	77
2.5.1 Optimization of the process	77
2.5.2 Scaffolds constructed through the developed strategy	79
2.5.3 Challenging systems for the strategy	86
2.6 Selective functionalization of prepared substrates	89
2.7 Investigation of the bioactivity of the prepared compounds	90
2.8 Conclusion	92
2.9 Experimental Section	93
2.9.1 General information	93
2.9.2 Starting material experimental procedures and characterization data	94
2.9.3 Oxidative coupling experimental procedures and characterization data	111
2.9.4 Ring-closing metathesis experimental procedures and characterization data	127
2.9.5 Challenging systems	139
2.9.6 Selective functionalization of prepared scaffolds	141
2.9.7 Cell viability assays	149
3 Chapter 3	152
3.1 Introduction	152
3.2 Isocyanoterpenes	152

	12	
3.2.1	Structure of isocyanoterpenes	152
3.2.2	Biosynthesis of diterpenoid isonitriles	154
3.2.3	Bioactivity of isocyanoterpenes	157
3.3	Previous syntheses of 7,20-diisocyanoadociane	161
3.3.1	Corey's synthesis	162
3.3.2	Mander's synthesis	165
3.3.3	Miyaoka's synthesis	168
3.3.4	Vanderwal's synthesis	171
3.3.5	Shenvi's synthesis	174
3.4	Implementation of the couple and close strategy to DICA	177
3.4.1	General strategy	177
3.4.2	Initial late-stage strategy	180
3.4.3	Strategic departure from symmetry	182
3.4.4	Strategic return to symmetry	186
3.4.5	Successful synthesis of Corey dione	191
3.5	Conclusion	192
3.6	Experimental Section	193
3.6.1	General information	193
3.6.2	Construction of the key diketone intermediate III-109	194
3.6.3	Triflate strategy – model system	200
3.6.4	Olefination strategy – model system	209

	13
3.6.5 Successful synthesis of Corey dione	213
4 Chapter 4	217
4.1 Introduction	217
4.2 Further methodology development	217
4.3 Potential natural product targets	218
4.3.1 Quassin	218
4.3.2 Fichtelite	219
4.3.3 Cassaine	219
4.3.4 Conifer oleoresin diterpenoids	220
4.3.5 Phytoalexin diterpenoids	221
4.3.6 Acylglycerol diterpenes	221
4.3.7 Furan-containing diterpenes	222
4.3.8 Bicyclic compounds	223
4.3.9 Steroid core	224
4.3.10 Larger polycyclic scaffolds	225
4.4 Conclusion	225
References	227

List of Figures

Figure 1.1 General strategies for the synthesis of fused tricyclic scaffolds.....	23
Figure 1.2 Biosynthesis of cholesterol.....	24
Figure 1.3 Complementary radical-based cyclization approaches.....	42
Figure 1.4 Structures of common bicyclic building blocks.....	44
Figure 2.1 Suite of enone substrates.....	74
Figure 2.2 Model for coupling stereoselectivity.....	80
Figure 2.3 Scaffolds prepared from the developed three-step strategy.....	82
Figure 2.4 Inaccessible scaffolds due to unsuccessful oxidative coupling.....	87
Figure 2.5 Anticancer compounds with similar carbocyclic cores containing enones.....	91
Figure 3.1 Diterpene 7,20-diisocyanoadociane III-1.....	152
Figure 3.2 Various ICT carbocyclic scaffolds.....	153
Figure 3.3 Common malaria therapeutics.....	158
Figure 3.4 Antimalarial activity of nitrogenous terpene natural products.....	160
Figure 3.5 Shenvi's late-stage strategy for selective isonitrile installation.....	174
Figure 4.1 Generally desirable carbocyclic scaffolds.....	217
Figure 4.2 Quassin.....	218
Figure 4.3 Fichtelite.....	219
Figure 4.4 Cassaine.....	220
Figure 4.5 Conifer oleoresin hydrocarbons.....	220
Figure 4.6 Bioactive pimarane diterpenoids.....	221

Figure 4.7 Phytoalexins from rice plants	221
Figure 4.8 Bioactive acylglycerols isolated from mollusks	222
Figure 4.9 Furan-containing diterpenes	223
Figure 4.10 Putative bicyclic natural product targets	224
Figure 4.11 Cybastacine B	225

List of Schemes

Scheme 1.1 Johnson's a) acetal- and b) allylic alcohol-promoted cationic polyene cyclization..	25
Scheme 1.2 Johnson's cyclization with asymmetric induction.....	26
Scheme 1.3 Corey's strategy for accessing the tricyclic core of dammarenediol II	26
Scheme 1.4 Newhouse's polyene cyclization	27
Scheme 1.5 a) Yamamoto's and b) Corey's enantioselective polyene cyclizations	28
Scheme 1.6 Ishihara's chiral nucleophile-promoted enantioselective cyclization.....	28
Scheme 1.7 Snyder's use of BDSB for the synthesis of tricyclic products.....	29
Scheme 1.8 Livinghouse's sulfenium ion-promoted cyclization.....	30
Scheme 1.9 Canesi's oxidative dearomatization cyclization	30
Scheme 1.10 Negishi's palladium-catalyzed cyclization cascade.....	31
Scheme 1.11 Gagné's platinum-catalyzed cyclization cascade	31
Scheme 1.12 a) Carreira's iridium-catalyzed and b) Toste's gold-catalyzed cyclizations	32
Scheme 1.13 Julia's radical-based cyclization	33
Scheme 1.14 Demuth's photoinduced electron transfer strategy	34
Scheme 1.15 Pattenden's acyl selenide-promoted cyclization	34
Scheme 1.16 Wang's cyclization cascade	35
Scheme 1.17 a) Snider's and b) Zoretic's use of Mn(III).....	35
Scheme 1.18 a) Cuerva's and b) Oltra's use of titanocene complexes.....	36
Scheme 1.19 MacMillan's application of SOMO to polyene cyclizations.....	37
Scheme 1.20 Vollhardt's cobalt-catalyzed cyclization cascade	38

	17
Scheme 1.21 Mukai's bis(allene)-promoted cyclization cascade	38
Scheme 1.22 Deslongchamps's TADA strategy	40
Scheme 1.23 Deslongchamps's access to <i>trans-anti-trans</i> stereoisomers.....	41
Scheme 1.24 Deslongchamps's synthesis of (+)-cassaine	41
Scheme 1.25 Pattenden's macrocyclic cyclization strategies	43
Scheme 1.26 Mori's Robinson annulation strategy.....	45
Scheme 1.27 Gribble's Robinson annulation strategy.....	45
Scheme 1.28 She's cyclization strategy.....	46
Scheme 1.29 Ramana's convergent domino strategy	46
Scheme 1.30 Deslongchamps's second synthesis of (+)-cassaine	47
Scheme 1.31 Valenta's Diels–Alder approach.....	48
Scheme 1.32 a) Danishefsky's and b) Hashimoto's Diels–Alder strategies.....	48
Scheme 1.33 Crawford's Diels–Alder sequence.....	49
Scheme 1.34 Taber's synthesis of fichtelite.....	50
Scheme 1.35 Tanner's Diels–Alder strategy.....	50
Scheme 1.36 Vanderwal's Diels–Alder strategy.....	51
Scheme 1.37 Carreira's synthesis of (+)-sarcophytin.....	51
Scheme 1.38 Marvel's tethered fragment approach	52
Scheme 1.39 Overman's intramolecular Heck cyclization.....	52
Scheme 1.40 Taber's linked fragment strategy	53
Scheme 1.41 Tang's tethered fragment approach	53

	18
Scheme 1.42 Micalizio's synthesis of the steroidal core	54
Scheme 2.1 Oxidative enolate coupling	57
Scheme 2.2 Ivanoff's preliminary oxidative coupling report	58
Scheme 2.3 Rathke's oxidative coupling.....	59
Scheme 2.4 Saegusa's oxidative coupling.....	59
Scheme 2.5 Thomson's biaryl synthesis.....	60
Scheme 2.6 Baran's cross-coupling with equal stoichiometries of coupling partners.....	60
Scheme 2.7 Schäfer's enantioselective dimerization	61
Scheme 2.8 Daugulis's catalytic oxidative coupling	62
Scheme 2.9 Coupling of enol silanes.....	63
Scheme 2.10 Rathke's unsymmetrical silyl bis-enol ether formation.....	64
Scheme 2.11 Schmittel's silyl bis-enol ether coupling.....	65
Scheme 2.12 Thomson's oxidative coupling methods development.....	66
Scheme 2.13 Thomson's diastereoselective coupling of cyclic ketones	67
Scheme 2.14 Thomson's synthesis of propolisbenzofuran B	69
Scheme 2.15 Narasaka's early contribution.....	69
Scheme 2.16 MacMillan's application of SOMO catalysis.....	70
Scheme 2.17 Jia's pyrrole synthesis.....	71
Scheme 2.18 Itoh's electrochemical coupling	71
Scheme 2.19 Moeller's electrochemical coupling strategy.....	72
Scheme 2.20 General couple and close strategy	73

	19
Scheme 2.21 Synthesis of substrates II-118–II-123	75
Scheme 2.22 Production of substrates II-124–II-127	76
Scheme 2.23 Silyl bis-enol ether preparation	78
Scheme 2.24 Initial couple and close result	79
Scheme 2.25 Formation of the 6,8,6-fused system	85
Scheme 2.26 Coupling of saturated systems	88
Scheme 2.27 Attempted Diels–Alder to fashion the fused ring system	89
Scheme 2.28 Elaboration of prepared scaffolds	90
Scheme 2.29 General method A for synthesis of symmetrical silyl bis-enol ethers	111
Scheme 2.30 General method B for synthesis of unsymmetrical silyl bis-enol ethers	112
Scheme 2.31 General method C for the oxidative coupling of silyl bis-enol ethers	113
Scheme 2.32 Oxidative coupling control experiment without the silicon tether	126
Scheme 2.33 General method D for the ring-closing metathesis of coupled products	127
Scheme 2.34 Epimerization of the minor stereochemistry to the major, <i>all-trans</i> II-195	144
Scheme 3.1 Proposed biosynthesis of diisocyanoadociane III-1	155
Scheme 3.2 Proposed isonitrile incorporation	155
Scheme 3.3 Origin of isonitrile, formamide, and isothiocyanate functionalities	156
Scheme 3.4 Corey's synthesis	163
Scheme 3.5 Mander's synthesis	166
Scheme 3.6 Completion of Mander's formal synthesis	167
Scheme 3.7 Miyaoka's synthesis	169

	20
Scheme 3.8 Vanderwal's synthesis	172
Scheme 3.9 Enantioselective synthesis with chiral pool materials	173
Scheme 3.10 Shenvi's synthesis	175
Scheme 3.11 General strategy to access Corey's intermediate III-45	178
Scheme 3.12 Access to the key diketone intermediate III-109	179
Scheme 3.13 Initial late-stage strategy	180
Scheme 3.14 Attempts to form bis(triflate) III-119	181
Scheme 3.15 Access to bis(triflate) III-119 and attempted manipulations	182
Scheme 3.16 First strategy from monotriflate III-120	183
Scheme 3.17 Second strategy from monotriflate III-120	184
Scheme 3.18 Third strategy from monotriflate III-120	185
Scheme 3.19 Revised strategy returning to symmetry	186
Scheme 3.20 Yoon's reductive cyclization of enones	190
Scheme 3.21 Successful reductive ring closure	191
Scheme 3.22 Successful synthesis of Corey dione III-45	192
Scheme 4.1 Access to the steroid nucleus	225

List of Tables

Table 2.1 Cell Assay Results	92
Table 3.1 Olefination of diketone III-117	187
Table 3.2 Double allylic oxidation of bis(olefin) III-139	189

Chapter 1

An Analysis of Strategies for the Synthesis of Fused Tricyclic Scaffolds

1 Chapter 1

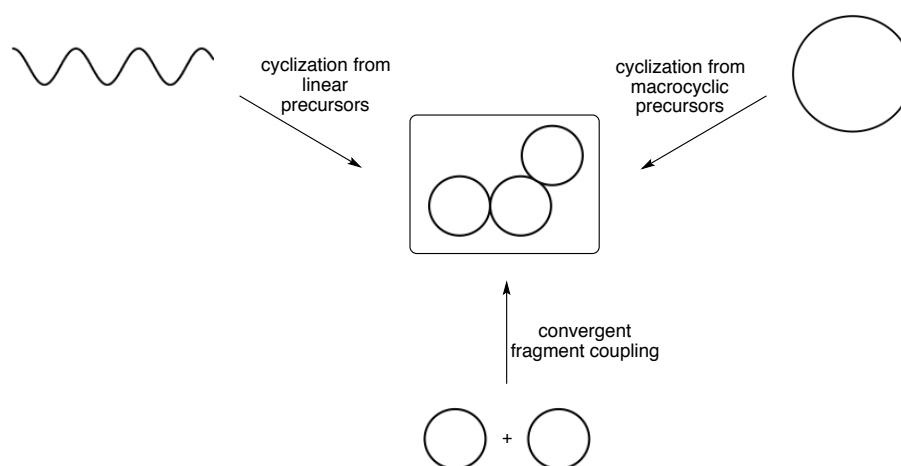
1.1 Introduction

Fused polycyclic structures with an array of stereogenic centers are incredibly common among naturally occurring compounds, and as such, the synthesis of these scaffolds has been central to the research of many synthetic groups in various contexts. The development of novel reactions and strategies to build the core structures of bioactive steroids, terpenes, and other natural products has been explored to advance the boundaries of synthetic chemistry, and to enable biological research through the synthesis of small molecules with attractive properties. Although these molecules have been of great interest to the chemical community for a long time, rapid access to the three-dimensionally complex carbocyclic cores comprising numerous natural product families is recently thought to have enhanced priority due to the acknowledged reservoir of untapped biological potential that these molecules represent to drug discovery.¹⁻³ While high-throughput compound screening has been an invaluable tool for the rapid discovery of novel therapeutic agents, these libraries are largely composed of small molecules lacking the sp^3 -centers present in many biologically active natural products that express more potent and selective activities.⁴⁻⁹ In fact, a study by Schmidt and Feher comparing drugs and combinatorial library compounds to natural products revealed the huge disparity that exists in the number of stereogenic centers per molecule between these classes of compounds.¹⁰ In 2003, 71% of compounds in combinatorial libraries and 45% of drugs on the market did not contain a single stereogenic center. The average number of stereogenic centers in natural products was 6.2/molecule, while that for drugs and combinatorial library compounds was 2.3/molecule and 0.4/molecule, respectively. The advent of transition metal-catalyzed coupling provided facile access to a large variety of these sp^2 -

rich compounds, but with the renewed scientific interest in natural products as inspiration for drug development comes a revived need for methods and strategies to rapidly afford architecturally complex scaffolds in a modular manner.¹¹

Three-dimensionally complex fused carbocyclic scaffolds have inspired great synthetic innovation spanning from many decades ago through today, as evidenced by the varied strategies that have been developed to build the mentioned structures. Three general strategic themes emerge from the literature and will be discussed herein. As depicted in Figure 1.1, the fused tricyclic scaffold is generally accessed from the cyclization of a linear precursor, the cyclization within a macrocyclic precursor, or the convergent coupling of two fragments.

Figure 1.1 General strategies for the synthesis of fused tricyclic scaffolds

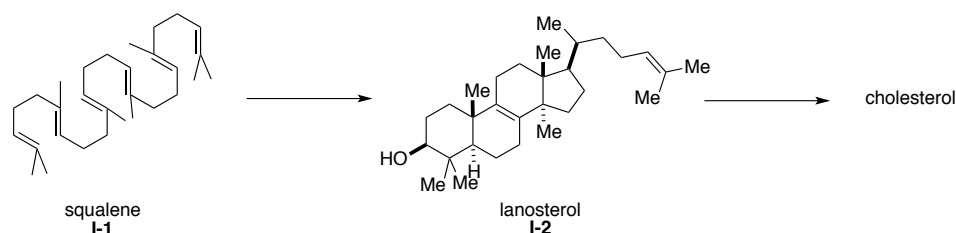


1.2 *Synthesis from linear precursors – polyene cyclization cascades*

The synthesis of fused polycyclic scaffolds from linear polyene precursors has captured the attention of scientists around the world who are inspired by nature's remarkable ability to convert squalene **I-1** to lanosterol **I-2** in the biosynthesis of cholesterol (Figure 1.2). The biosynthesis of these steroid and terpenoid compounds has been extensively examined and reviewed.¹²⁻¹⁵ This

extraordinary transformation forms four rings and perfectly sets seven stereocenters, providing one single product out of the possible 128 stereochemical outcomes.¹⁶ Early synthetic work in this area in the 1950s and beyond sought to discover whether this transformation was achievable without enzymatic facilitation.

Figure 1.2 Biosynthesis of cholesterol



1.2.1 Cationic polyene cascades

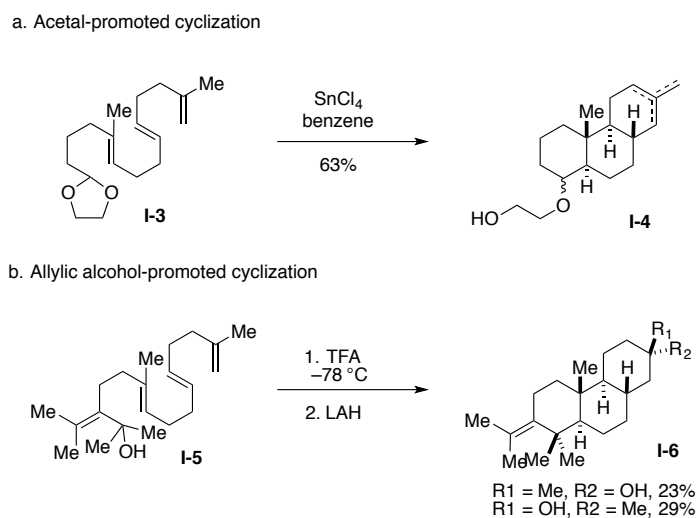
In 1955, Stork¹⁷ and Eschenmoser¹⁸ each rationalized that the stereospecific nature of this cyclization was the result of inherent stereoelectronic factors rather than enzymatic control, whereby the electrophilic addition of a carbenium ion to the neighboring alkene occurs in an antiparallel fashion, leading to the all-*trans* geometry of the carbon backbone from *E*-polyenes. This hypothesis, named the Stork–Eschenmoser hypothesis by Johnson,¹⁶ formed the basis for the spark in synthetic interest to replicate this biological process in the absence of enzymes. The subsequent contributions by Johnson to this area of research are unparalleled, paving the way to our current knowledge of steroids.¹⁹⁻²² Johnson and coworkers' initial acid-catalyzed cyclization attempts proved to be challenging due to promiscuous protonation of the polyene substrate, leading to a mixture of different cyclized and isomerized products. Thus, they pioneered investigations into polyenes equipped with functional groups conducive to the formation of a cyclizable cationic center under conditions that would not disturb the alkenes – a strategy that has been adopted by

many. Although this work spans decades and provides access to countless fused ring systems, the research with respect to 6,6,6-tricyclic scaffolds will be primarily discussed herein.

1.2.1.1 Acetal and allylic alcohol-promoted cyclization

Johnson and coworkers' preliminary results employing a trienyl sulfonate ester functional handle provided the desired tricyclic product in 3% yield and was uniquely selective for the all-*trans* stereochemistry, however the poor yield rendered this approach synthetically impractical.¹⁹ Motivated to discover a worthy initiating functional group for the cascade, Johnson and coworkers achieved the successful cyclization of polyenic acetals (i.e. **I-3**) in the presence of SnCl₄ (Scheme 1.1a),²³⁻²⁴ and of allylic alcohols (i.e. **I-5**) in the presence of formic acid at room temperature,²⁵⁻²⁶ or trifluoroacetic acid at cryogenic temperatures (Scheme 1.1b).²⁷ These methods generated the all-*trans* tricyclic core structures **I-4** and **I-6**, respectively, in synthetically useful yields.

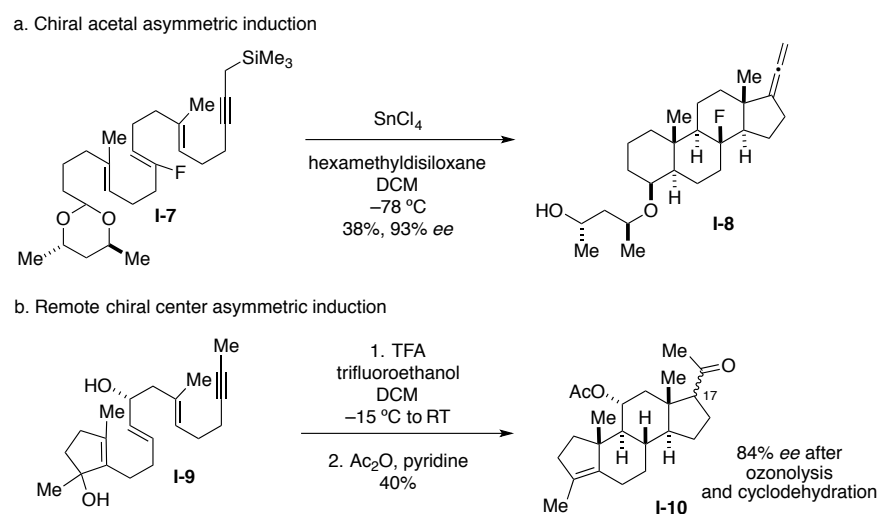
Scheme 1.1 Johnson's a) acetal- and b) allylic alcohol-promoted cationic polyene cyclization



The group rendered this transformation enantioselective by employing a chiral acetal (Scheme 1.2a)²⁸⁻²⁹ or by incorporating a chiral center along the polyene chain (Scheme 1.2b).³⁰⁻³¹ In 2007, Loh and coworkers developed a similar chiral acetal-initiated cyclization to achieve enantiopure

tricyclic structures.³²⁻³³ These strategies have been applied to numerous steroid and natural product syntheses, with representative examples cited herein.^{31, 34-38}

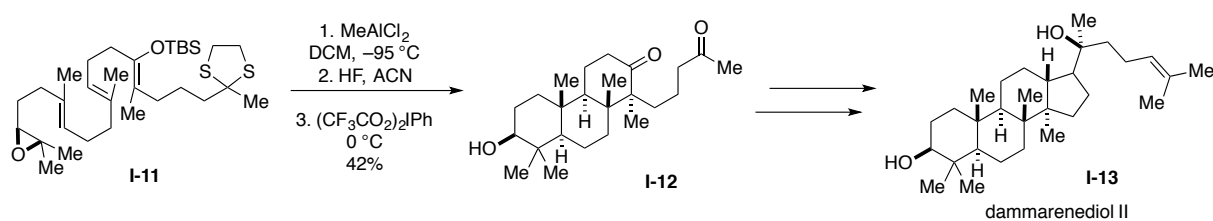
Scheme 1.2 Johnson's cyclization with asymmetric induction



1.2.1.2 Epoxide-promoted cyclization

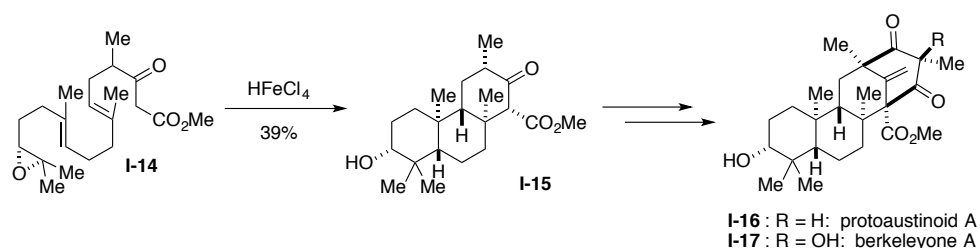
Many investigations of epoxides as enabling functional groups for this cyclization cascade led to the determination that epoxysqualene was indeed the biosynthetic intermediate of the process.³⁹⁻⁴² Corey and coworkers harnessed this reactivity in 1996 by employing methylaluminum dichloride to facilitate the key cyclization to the tricyclic scaffold **I-12** in their synthesis of dammarenediol II **I-13** (Scheme 1.3).⁴³ This strategy has also been successfully applied to the synthesis of sesquiterpene natural products.⁴⁴⁻⁴⁵

Scheme 1.3 Corey's strategy for accessing the tricyclic core of dammarenediol II



More recently, other research groups have also investigated the cyclization of these polyene epoxides, employing different Lewis acid promoters to form a variety of different fused carbocyclic scaffolds.⁴⁶⁻⁴⁸ Most recently, Newhouse and coworkers demonstrated the Brønsted acid-promoted cyclization of linear polyene **I-14** to form tricyclic intermediate **I-15** in 39% yield en route to natural products protoaustinoid A, **I-16**, and berkeleyone A, **I-17** (Scheme 1.4).⁴⁹

Scheme 1.4 Newhouse's polyene cyclization

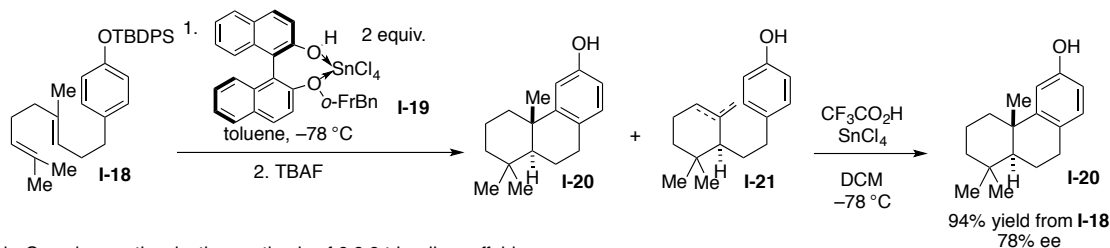


1.2.1.3 Lewis acid-assisted chiral Brønsted acid-promoted cyclization

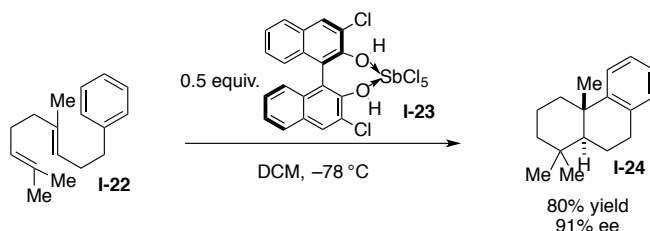
Yamamoto and coworkers rendered this cyclization cascade enantioselective with the use of a Lewis acid-assisted chiral Brønsted acid (chiral LBA).⁵⁰⁻⁵² As shown in Scheme 1.5a, their strategy required two steps to achieve complete cyclization to the tricyclic system. An initial enantioselective cyclization of **I-18** with chiral LBA (**I-19**) provided a mixture of tricyclic **I-20** and monocyclized **I-21**. This mixture converged on the desired tricyclic **I-20** through a diastereoselective formation of the B ring. Since Yamamoto's seminal reports, this concept has been developed further by multiple groups in recent years.⁵³⁻⁵⁴ For example, in 2012, Corey and Surendra enhanced this reactivity by using an antimony-based chiral LBA (**I-23**), allowing for the desired cyclization to occur with good yields in one step (Scheme 1.5b).⁵⁵ Enantioselective polyene cyclizations have been recently reviewed by Sarlah and coworkers.⁵⁶

Scheme 1.5 a) Yamamoto's and b) Corey's enantioselective polyene cyclizations

a. Yamamoto's enantioselective synthesis of 6,6,6 tricyclic scaffolds



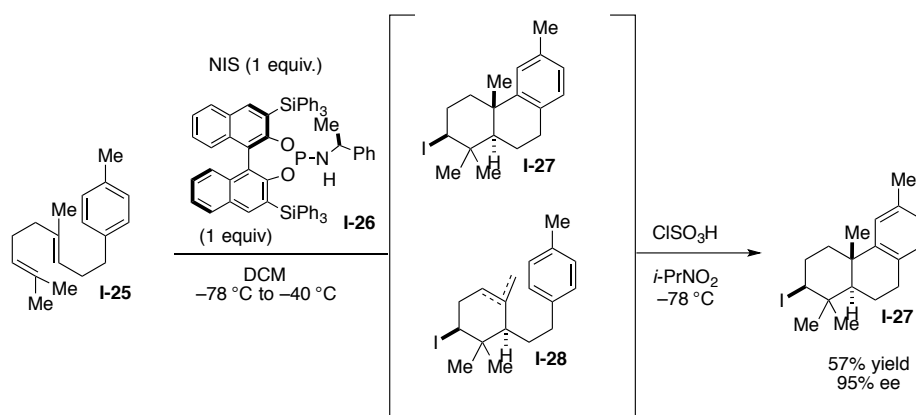
b. Corey's enantioselective synthesis of 6,6,6 tricyclic scaffolds



1.2.1.4 Halogen-promoted cyclization

In 2007, Ishihara and coworkers reported an impressive alternative strategy for this enantioselective cyclization. Instead of a chiral Lewis acid promotor, they developed a chiral nucleophilic promotor to enable the halocyclization.⁵⁷⁻⁵⁸

Scheme 1.6 Ishihara's chiral nucleophile-promoted enantioselective cyclization

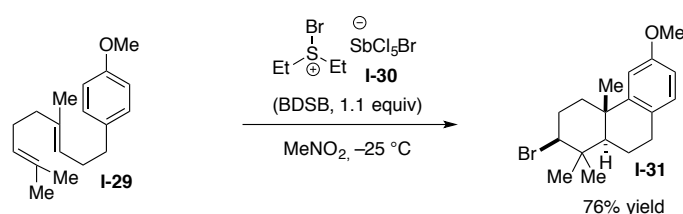


As shown in Scheme 1.6, chiral nucleophilic promotor **I-26** activated the halogenating reagent NIS, which facilitated the enantioselective halocyclization to form an initial mixture of desired

tricyclic product **I-27** and monocyclized adduct **I-28**. Treatment of this mixture with chlorosulphonic acid in 2-nitropropane provided full conversion to **I-27**.

In further development of this halocyclization strategy, Snyder and coworkers established a simple reagent for the halonium-induced cation- π cyclization of linear precursors.⁵⁹⁻⁶⁰ As shown in Scheme 1.7, they demonstrated that a bromine complex with Et_2S and SbCl_5 (BDSB, **I-30**) successfully formed tricyclic species **I-31** and similar scaffolds in high yields and very fast reaction times (5 minutes). Although this process was not enantioselective, the group was able to develop a two-step method using $\text{Hg}(\text{OTf})_2$ with a chiral ligand to provide the same products that would result from asymmetric bromonium-induced cyclization.⁶¹

Scheme 1.7 Snyder's use of BDSB for the synthesis of tricyclic products



1.2.1.5 Aziridine-promoted cyclization

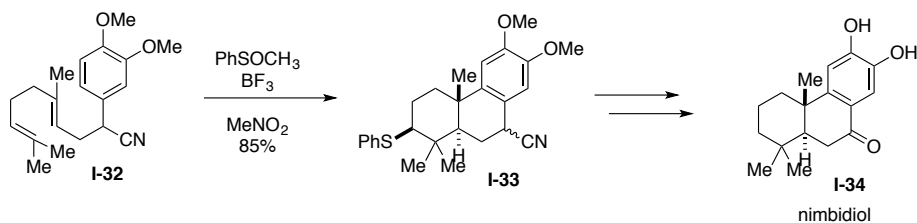
As an alternative to epoxide- or halogen-enabled cyclizations, Loh and coworkers demonstrated the ability for the aziridine functionality to initiate the cyclization of linear polyenes in the presence of a catalytic amount of Lewis acid InBr_3 to form tri- and tetracyclic products in good yields.⁶² When enantioenriched precursors were employed, the cyclization proceeded with retention of the high levels of enantiopurity.

1.2.1.6 Sulfenium ion-promoted cyclization

In the late 1980s, Livinghouse and coworkers reported an efficient cyclization of linear polyene species by employing a sulfenium ion to initiate the cascade that is ultimately terminated

by an aromatic ring.⁶³⁻⁶⁴ As shown in Scheme 1.8, this method allowed for the cyclization of linear precursor **I-32** to tricyclic **I-33**, and thus facilitated the successful synthesis of diterpene nimbidiol **I-34** in traceless fashion, as the enabling sulfur functionality was later reductively removed.

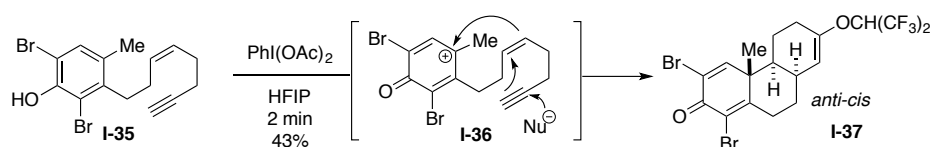
Scheme 1.8 Livinghouse's sulfenium ion-promoted cyclization



1.2.1.7 Oxidant-promoted cyclization

In 2011, Canesi and coworkers reported an oxidative dearomatization to generate a cation that promoted the cyclization cascade of linear polyenes to fused tricyclic structures.⁶⁵ As shown in Scheme 1.9, when polyene **I-35** was treated with hypervalent iodide oxidant $\text{PhI}(\text{OAc})_2$ and hexafluoroisopropanol (HFIP), phenoxonium ion **I-36** was generated and subsequently captured by the proximal alkene in a ring-closing cascade to form tricyclic **I-37** with *anti-cis* stereochemistry. They showed that the *anti-trans* stereoisomer was formed from the corresponding *trans*-**I-35** enyne. Recently, the group has applied this general idea to the polycyclic core structures of other natural product families.⁶⁶⁻⁶⁷

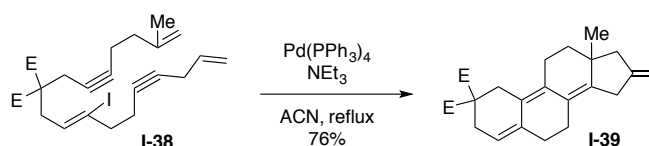
Scheme 1.9 Canesi's oxidative dearomatization cyclization



1.2.1.8 Transition metal-promoted cyclization

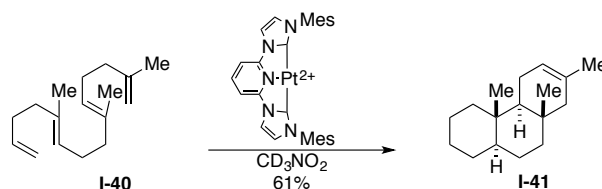
In 1990, Negishi and coworkers reported a palladium-catalyzed cyclization of acyclic precursors such as **I-38**, as shown in Scheme 1.10.⁶⁸

Scheme 1.10 Negishi's palladium-catalyzed cyclization cascade



Gagné and coworkers have elegantly demonstrated the use of platinum catalysts for the cyclization of linear polyenes.⁶⁹ Most recently they showcased the ability for a platinum catalyst equipped with an NHC pincer ligand to enable the cyclization cascade to form *trans-anti-trans* tricycle **I-41** and other similar carbocyclic cores (Scheme 1.11).⁷⁰

Scheme 1.11 Gagné's platinum-catalyzed cyclization cascade

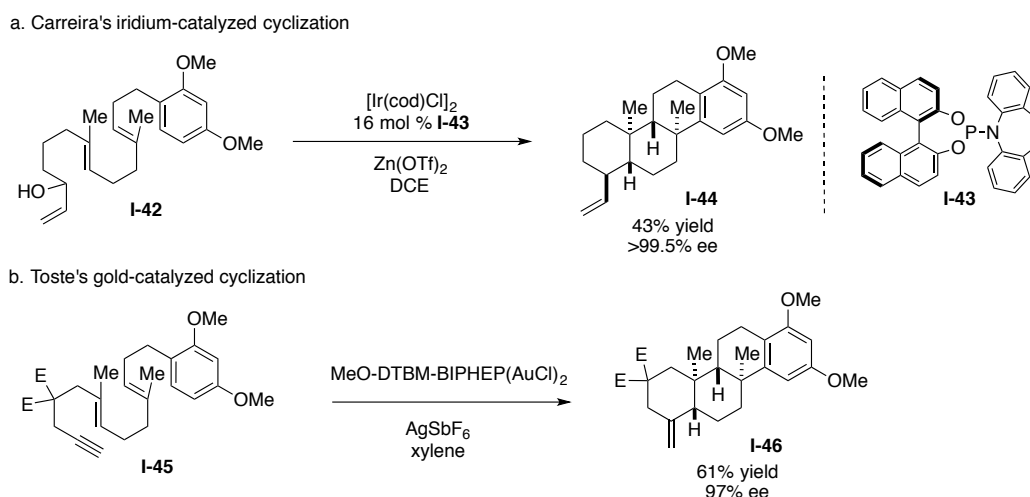


Gagné collaborated with Tantillo in 2017 to determine how closely their platinum-catalyzed method mimics the biological process, developing an energy profile and putative intermediates for the transformation, and ultimately concluding that their approach can indeed be considered biomimetic with the platinum catalyst assuming the responsibilities of the enzyme.⁷¹

In addition to palladium and platinum catalyzed processes, iridium⁷²⁻⁷⁴ and gold⁷⁵⁻⁷⁷ catalysis have been successfully employed in recent years for the cyclization of linear precursors. As shown in Scheme 1.12, Carreira's iridium-catalyzed strategy (a) complements Toste's gold-

catalyzed approach (b) to polyene cyclizations in an enantioselective fashion, providing access to fused *trans-anti-trans* cyclic products.

Scheme 1.12 a) Carreira's iridium-catalyzed and b) Toste's gold-catalyzed cyclizations



1.2.2 Radical-based cyclizations

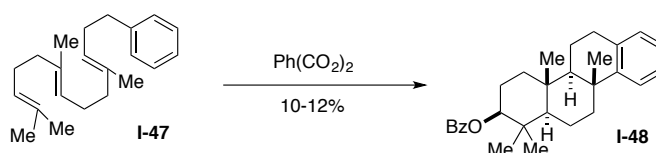
In the early 1960s, Breslow hypothesized, and later rejected, the idea that sterols and terpenes may naturally arrive from their linear polyene counterparts through a radical-based mechanism.⁷⁸⁻⁸⁰ Although epoxysqualene was ultimately proven as the biosynthetic intermediate for the formation of lanosterol in the cholesterol biosynthesis,³⁹⁻⁴⁰ the radical pathway to the carbocyclic structure of terpenes and steroids presents a complementary strategy to the well-explored biomimetic cationic cyclization. Many investigations of this strategy demonstrate that diastereoselective polyene cyclizations do not require a carbenium ion.^{21, 81}

1.2.2.1 Benzyloxy radical-promoted cyclization

Aside from Breslow, early research in the production of tricyclic species through a radical cyclization was conducted by Julia and coworkers in the 1970s.⁸²⁻⁸³ As shown in Scheme 1.13, the

group was able to access the 6,6,6-tricyclic core with an initial addition of a benzyloxy radical to polyene **I-47** which provoked the 6-*endo*-trig polycyclization cascade, terminating with a radical Friedel-Crafts type reaction to form **I-48**.⁸³ Consistent with Breslow's work, the products formed contained the all-*trans* geometry about the ring junctions, paralleling the cation-driven process, and displaying that the *E*-configuration of the linear precursor was translated to the final product. This seminal work from Breslow and Julia suffered from low yields, but provided the proof of concept and inspiration for further exploration into the potential of this strategy.

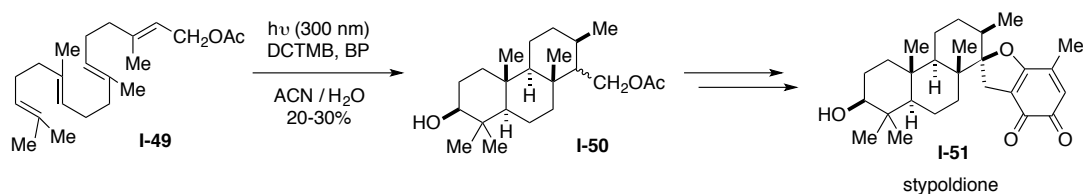
Scheme 1.13 Julia's radical-based cyclization



1.2.2.2 Photoinduced electron transfer cyclization

Supplementary investigations in this area took off in the 1990s. In 1993, Demuth and coworkers presented a photoinduced electron transfer cyclization allowing for the formation of terpene-like skeletons.⁸⁴ As shown in Scheme 1.14, the process was conducted under 300 nm light with 1,4-dicyano-2,3,5,6-tetramethylbenzene (DCTMB) and 1,1'-biphenyl (BP) in acetonitrile and water.⁸⁵ Photoinduced electron transfer from BP to the excited acceptor DCTMB resulted in a radical anion/radical cation pair. Electron transfer from the polyalkene **I-49** to the BP radical cation provided a polyalkene radical cation which was trapped with water, and the resulting beta-hydroxy radical underwent the desired cyclization cascade to form **I-50**. Despite the low yields, the all-*trans* selectivity of the method paralleled the natural cationic process,⁸⁴⁻⁸⁶ and enabled its application to the synthesis of terpenoid stypoldione **I-51**,⁸⁷⁻⁸⁸ as well as a steroid core with asymmetric induction imparted by a remote chiral auxiliary, similar to the cationic cyclizations.⁸⁹

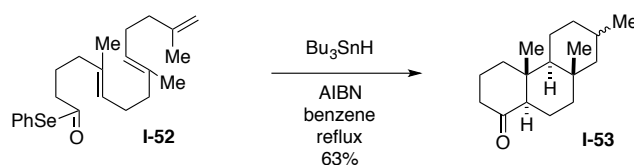
Scheme 1.14 Demuth's photoinduced electron transfer strategy



1.2.2.3 Acyl selenide-promoted cyclization

Pattenden and coworkers pioneered the use of acyl selenides for the synthesis of fused tricyclic species. As shown in Scheme 1.15, they employed Bu₃SnH-AIBN to generate a radical from acyl selenide **I-52**, initiating a series of 6-*endo*-trig cyclizations to form *trans-anti-trans* tricyclic **I-53**.⁹⁰⁻⁹¹ They successfully applied this strategy to the total synthesis of spongian-16-one⁹² and the steroid core.⁹³

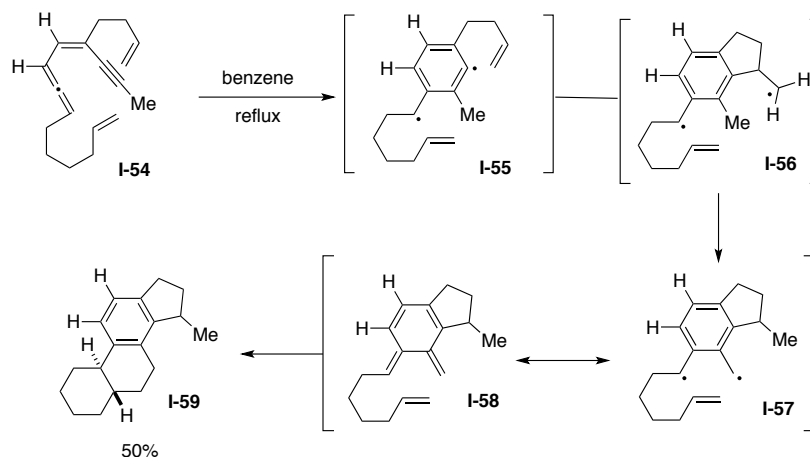
Scheme 1.15 Pattenden's acyl selenide-promoted cyclization



1.2.2.4 Thermally-induced cyclization

In 1993, Wang and coworkers demonstrated the interesting cyclization of acyclic enyne-allenes triggered by heat to form a tetracyclic carbocycle.⁹⁴ As shown in Scheme 1.16, upon heating, **I-54** underwent a cycloaromatization of conjugated enyne-allenes, as had been previously reported by Myers and coworkers.⁹⁵ The authors propose that initial ring closure of the intermediate aryl radical **I-55** provided **I-56**, which then rapidly underwent a 1,5-hydrogen atom transfer to **I-57** faster than the trapping of the radical within **I-56** by the internal double bond. The resonant triene **I-58** then underwent a Diels–Alder reaction to fashion the fused ring system **I-59**.

Scheme 1.16 Wang's cyclization cascade

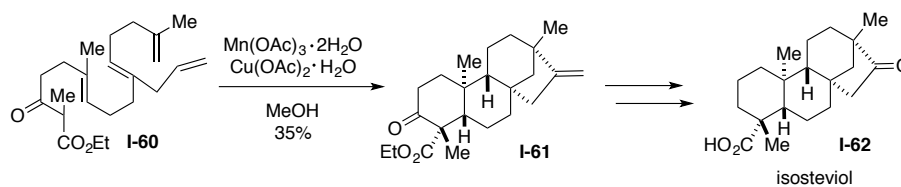


1.2.2.5 Transition metal oxidant-promoted cyclization

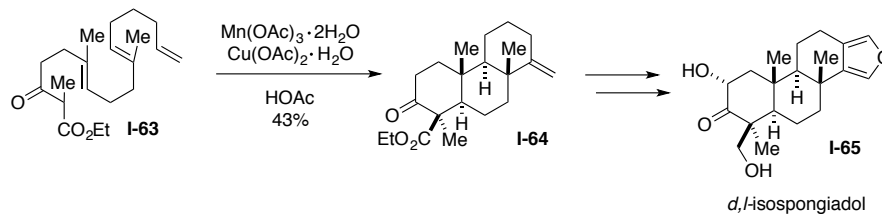
Pioneering work by Snider and coworkers demonstrated Mn(III) complexes to be useful promoters for linear polyene cyclizations, powerful in their ability to both generate a cyclization-initiating radical, as well as oxidize the final radical to an alkene.⁹⁶⁻⁹⁷ The group confirmed the utility of this strategy through the elegant synthesis of isosteviol **I-62**, enabled by the cyclization of linear precursor **I-60** to form tricyclic **I-61**, as shown in Scheme 1.17a.⁹⁸

Scheme 1.17 a) Snider's and b) Zoretic's use of Mn(III)

a. Snider's synthesis of isosteviol



b. Zoretic's synthesis of isospongiadol

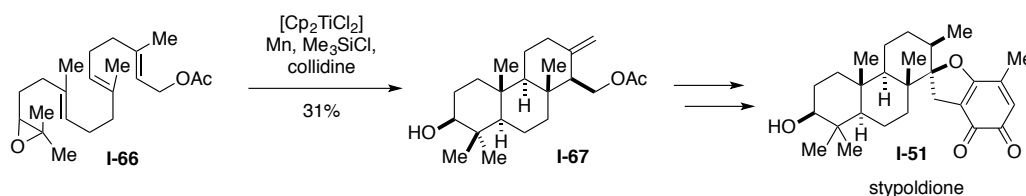


Zoretic and coworkers were also successful in the application of this strategy to the synthesis of natural product carbocyclic cores, such as isospongiadol **I-65** (Scheme 1.17b).⁹⁹⁻¹⁰¹ This general approach employing Mn(III) has been used for the synthesis of triptolide and its analogues by Yang and coworkers, further demonstrating its utility and versatility.¹⁰²⁻¹⁰³

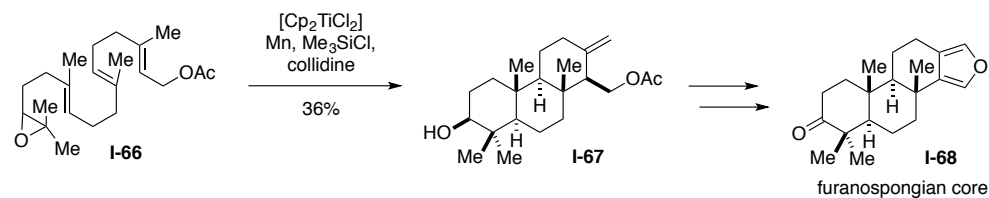
In the 2000s, single-electron transfer Ti(III) complexes were shown to facilitate the radical-based cyclization of linear polyenes to produce fused cyclic systems. Cuerva and coworkers were major contributors to the development of this chemistry, achieving the titanocene-mediated cyclization of epoxy polyenes for the synthesis of terpenoids. As shown in Scheme 1.18a, linear epoxide **I-66** was cyclized to tricyclic **I-67**, enabling the synthesis of stypoldione **I-51**.¹⁰⁴⁻¹⁰⁵ In this transformation, single-electron transfer from the titanocene complex resulted in a β -titanoxy radical that then underwent the cyclization cascade. This same strategy was also successfully applied to the synthesis of furanospongian diterpenes (**I-68**) in 2012 by Oltra and coworkers (Scheme 1.18b).¹⁰⁶

Scheme 1.18 a) Cuerva's and b) Oltra's use of titanocene complexes

a. Cuerva's synthesis of stypoldione

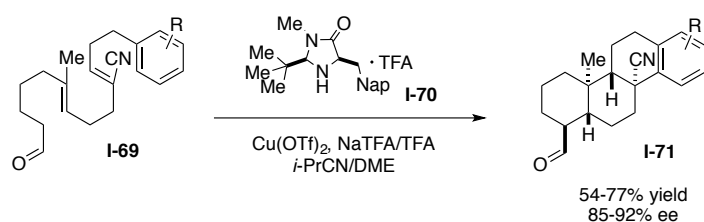


b. Oltra's synthesis of furanospongian diterpenes



In 2010, MacMillan and coworkers applied their SOMO activation platform to the context of enantioselective polyene cyclization (Scheme 1.19).¹⁰⁷ In the presence of imidazolidinone catalyst **I-70** and a copper oxidant, an α -imino radical was generated from **I-69**, which underwent a cascade of 6-*endo*-trig cyclizations terminated by an aromatic ring to form **I-71**. This powerful methodology harnessed the ability for radical polyene cyclization cascades to produce steroid and terpene carbocyclic scaffolds in a catalytic and enantioselective manner for the first time.

Scheme 1.19 MacMillan's application of SOMO to polyene cyclizations



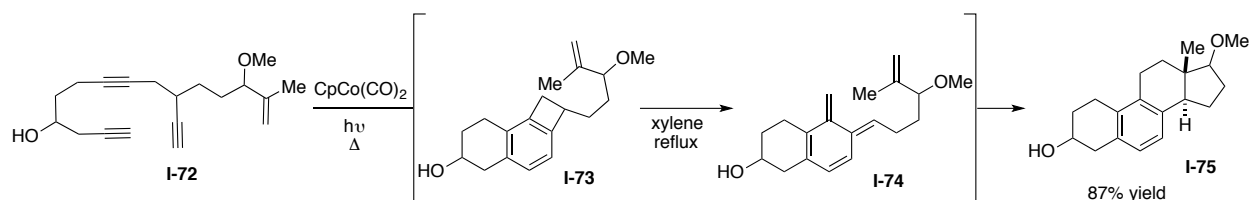
As shown through the examples discussed, radical-based cascades are a very powerful and enabling strategy for the rapid formation of complex structures. This type of transformation has been instrumental to the synthesis of many complex natural products, and has been reviewed by Curran¹⁰⁸ and most recently earlier this year by Maimone.¹⁰⁹

1.2.3 Pericyclic cyclizations

Separate from cationic or radical-enabled cascades, pericyclic cyclization sequences have proven to be a viable approach for the rapid construction of fused polycycles from linear precursors. In the 1980s, Vollhardt and coworkers developed a series of cobalt-catalyzed cyclization cascades to form fused polycyclic structures.¹¹⁰⁻¹¹¹ As shown in Scheme 1.20, their cobalt-mediated, one-pot cyclization cascade began with the intramolecular [2+2+2] cyclization of triyne **I-72** to form cyclobutane intermediate **I-73**, which upon heating, underwent a

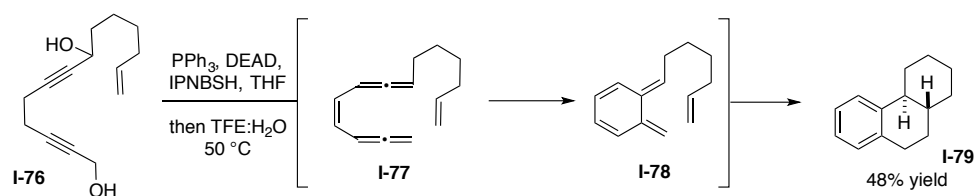
cycloreversion to **I-74** and subsequent [4+2] cycloaddition to furnish carbocyclic scaffold **I-75**. Since these seminal reports, this strategy has been explored by multiple research groups to access various fused carbocyclic scaffolds.¹¹²⁻¹¹⁴

Scheme 1.20 Vollhardt's cobalt-catalyzed cyclization cascade



In an alternative approach, in 2007 Mukai and coworkers designed a strategy to access fused tricyclic systems through a series of pericyclic cyclizations.¹¹⁵ As shown in Scheme 1.21, they took advantage of chemistry developed by Myers¹¹⁶ and Movassaghi¹¹⁷ to transform bis(propargyl alcohol) **I-76** into bis(allene) **I-77** through an initial Mitsunobu reaction with *N*-isopropylidene-*N'*-2-nitrobenzenesulfonyl hydrazine (IPNBSh) as the nucleophile, followed by loss of sulfinic acid to produce an intermittent monoalkyl diazene species which decomposed in a retro-ene fashion to form the allene. This intermediate then underwent a 6π electrocyclic cyclization to **I-78**, followed by a [4+2] cycloaddition to furnish tricyclic product **I-79** in 48% yield.

Scheme 1.21 Mukai's bis(allene)-promoted cyclization cascade



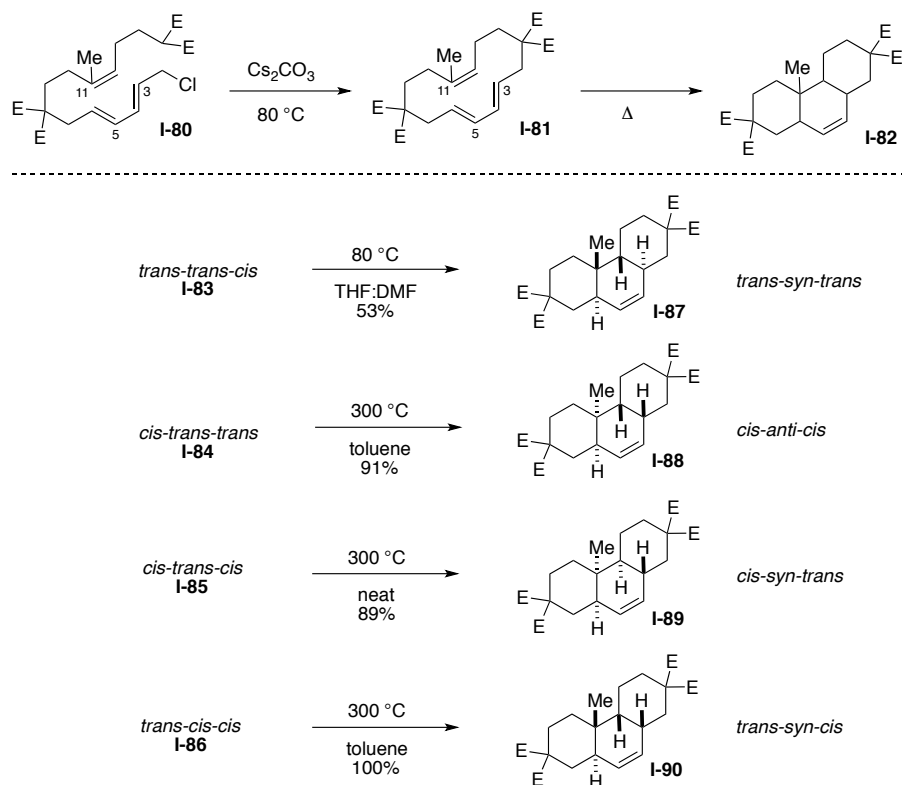
1.3 *Synthesis from macrocyclic species – transannular reactions*

Transannular bond formations within a macrocycle is a powerful strategy that has emerged for the formation of fused polycycles. The earliest examples of this concept were reviewed by McKerverey in 1966.¹¹⁸ In 1981, Olsen and coworkers demonstrated that conjugated trienes within an enclosed macrocycle underwent thermal isomerizations to form fused ring systems of varying size.¹¹⁹ This transannular ring-closing concept has been developed in a variety of contexts which will be discussed herein.

1.3.1 *Transannular Diels–Alder reactions*

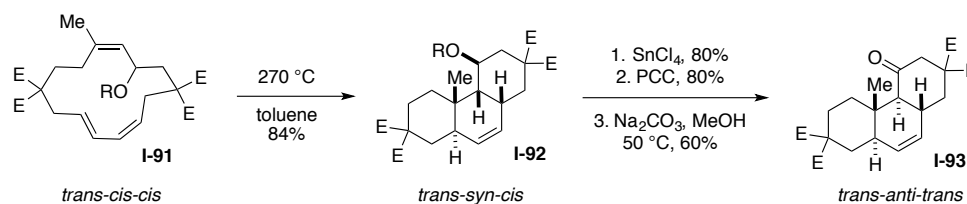
The development of transannular Diels–Alder reactions (TADA) within macrocyclic polyenes to produce fused polycyclic scaffolds was pioneered by Deslongchamps and coworkers.¹²⁰ While this work has been employed for the formation of an assortment of fused carbocyclic systems varying in size, this discussion will focus on the preparation of the 6,6,6-fused ring structure. In the 1980s, Deslongchamps's seminal investigations established the successful application of the TADA strategy for the construction of this scaffold. As shown in Scheme 1.22, the initial disclosure revealed that 14-membered macrocycles (**I-81**) containing a diene and a dienophile successfully underwent a transannular Diels–Alder reaction to fashion the 6,6,6-fused system (**I-82**).¹²¹⁻¹²² The stereochemical outcome of the cyclization to form **I-82** is dependent upon the geometry of the macrocyclic alkenes (**I-81**).¹²³⁻¹²⁷ This understanding of the selectivity for the process enabled a modular strategy for accessing a suite of tricyclic stereoisomers (**I-87–I-90**).

Scheme 1.22 Deslongchamps's TADA strategy



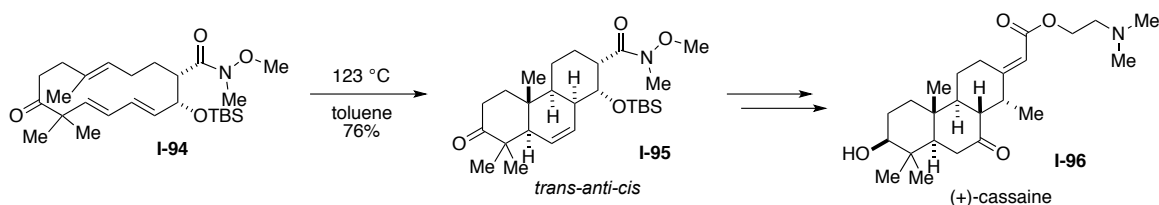
However, the *trans-anti-trans* geometry about the ring junctions, which is prevalent in the largest number of natural products, was unfortunately inaccessible through this strategy. As shown in Scheme 1.23, Deslongchamps and Marinier devised a workaround by incorporating a protected alcohol into the *trans-cis-cis* macrocycle **I-91**.¹²⁸ This transannular Diels–Alder reaction produced *trans-syn-cis* tricyclic product **I-92**, which could be epimerized to the desired, more thermodynamically favorable *trans-anti-trans* product **I-93** following deprotection of the alcohol and oxidation to the ketone. This strategy was implemented with the chiral variant of macrocycle **I-91**, presenting an asymmetric approach to the *trans-anti-trans* tricyclic scaffold.¹²⁹

Scheme 1.23 Deslongchamps's access to *trans-anti-trans* stereoisomers



The application of the transannular Diels–Alder reaction to natural product synthesis was reviewed by Deslongchamps and coworkers in 2001.¹³⁰ Since the publication of that review, a variety of natural products containing the fused 6,6,6-core structure with varying ring junction stereochemistries have been synthesized using this strategy.¹³¹⁻¹³⁵ In one example, as shown in Scheme 1.24, Deslongchamps and coworkers employed the TADA strategy to access tricyclic intermediate **I-95** from macrocycle **I-94** in their synthesis of (+)-cassaine **I-96**.¹³⁵ Because this natural product boasts the *trans-anti-trans* stereochemistry, the TADA approach was used to access the *trans-anti-cis* tricyclic scaffold (**I-95**) which was later epimerized.

Scheme 1.24 Deslongchamps's synthesis of (+)-cassaine



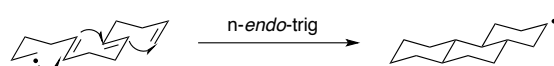
1.3.2 Radical-mediated macrocyclization–transannular cyclization cascade

As was previously discussed, radicals are powerful intermediates for the *n-endo*-trig cyclization cascade of linear polyene frameworks as a “zipper-like” process from one end of the polyene to the other (Figure 1.3a, see Section 1.2.2). It has also been shown that these reactive species have the ability to provide fused polycycles from the outside in, through a

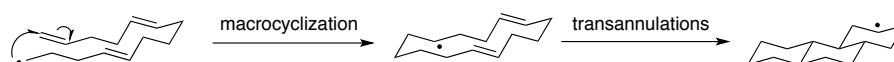
macrocyclization–transannulation approach with an initial *n-endo-trig* macrocyclization followed by a cascade of *n-exo-trig* cyclizations (Figure 1.3b). This strategy, however, has proven to be quite challenging.

Figure 1.3 Complementary radical-based cyclization approaches

a. "Zipper-like" approach



b. Macrocyclization-transannulation approach

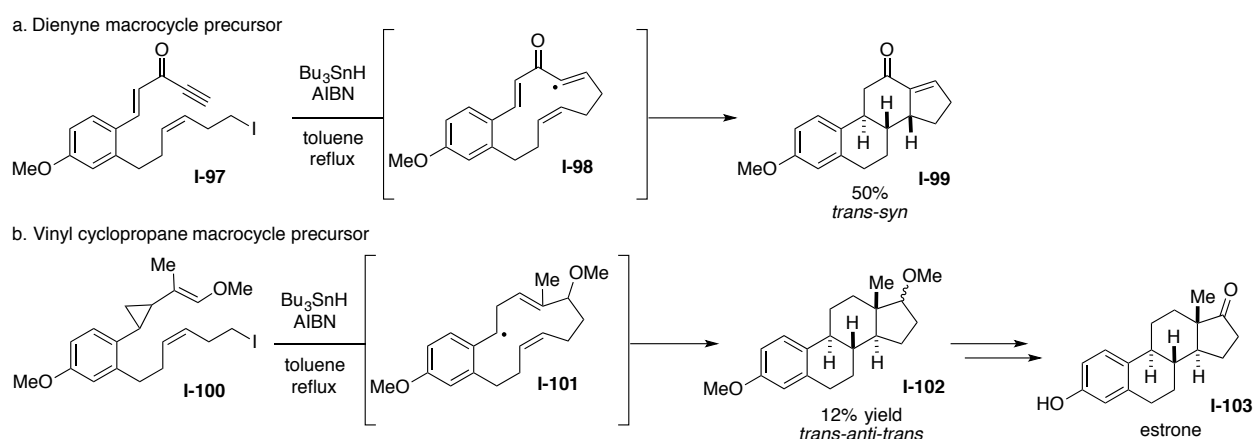


The Pattenden research group was a leader of work in this area, presenting early reports in 1994 of the transannular radical cyclization of macrocycles to form bicyclic systems.¹³⁶ Later that year, they were the first to demonstrate this strategy's ability to furnish a 5,7,5-tricyclic core through a radical-mediated macrocyclization followed by two transannular ring-forming events.¹³⁷ The following year, Curran and Jahn published the first example of a triple transannular radical-based cyclization to form the steroid core, however they only isolated the tetracyclic product in 4% yield.¹³⁸ This initial disclosure demonstrated challenges to this approach that persist today, as the reaction provided a complex mixture of products arriving from an initial macrocyclization and only one ensuing transannular cyclization, with alkene isomerization that prohibited the continued ring-closing cascade. This propensity for 1,5-H abstractions within the macrocycle to arrest a continuous cyclization cascade was reinforced a few years later when Pattenden and Jones reported similar observations under oxidative radical-initiating conditions rather than reductive.¹³⁹

The challenge of a radical-based macrocycle formation–transannular cyclization of completely linear precursors remains unsolved largely due to the demonstrated susceptibility for

reactive radicals in a confined environment to behave in unexpected alternative ways.¹⁴⁰⁻¹⁴¹ However, the Pattenden research group has since established some well-designed methods to access A-aromatic ring steroid scaffolds from ortho-disubstituted aryl polyene species through this general approach.¹⁴²⁻¹⁴³ As shown in Scheme 1.25, they developed a process for two different types of radical precursors to provide complementary polycyclic outcomes. In the presence of Bu₃SnH-AIBN, dienyne **I-97** underwent an initial macrocycle-generating 13-*endo*-dig cyclization to form radical **I-98**, followed by two transannulation reactions to form **I-99** bearing *trans-syn* geometry about the ring junctions in 50% (Scheme 1.25a).

Scheme 1.25 Pattenden's macrocyclic cyclization strategies



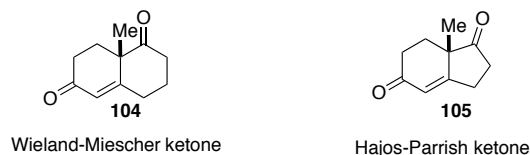
Alternatively, iodovinylcyclopropane **I-100** underwent a separate macrocyclization-transannulation sequence through radical **I-101**, providing the *trans-anti-trans* product **I-102** in 12%, which was successfully converted to estrone **I-103** (Scheme 1.25b).¹⁴³ This strategy was further explored in 2009 by the group for the synthesis of C-nor-D homosteroid ring systems.¹⁴⁴

1.4 Synthesis from building blocks – convergent and modular fragment coupling

Synthetic chemists have placed a real value on achieving convergent syntheses of complex natural products, which greatly improves the efficiency of the synthetic route. While the previous

two sections have focused on the impressively efficient construction of 6,6,6-carbocyclic scaffolds through a cascade of multiple bond formations in a single transformative event, alternative strategies focus on building the core structure in a more convergent manner. This “building block” approach unites different fragments and is therefore potentially more amenable to facile modularity. Among the most common building blocks that have been employed for the convergent synthesis of tricyclic scaffolds is the Wieland-Miescher ketone **I-104**, or similar bicyclic species such as the Hajos-Parrish ketone **I-105** (Figure 1.4). The facile preparation of these species has been widely developed, allowing for their employment in the synthesis of many natural products.¹⁴⁵⁻¹⁴⁶ These convergent “building block” strategies often employ known powerful reactions to construct the desired carbocyclic structure.

Figure 1.4 Structures of common bicyclic building blocks

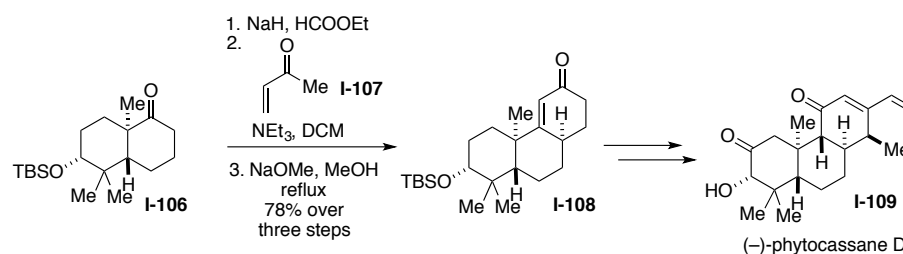


1.4.1 *Robinson annulation and similar domino transformations*

The Robinson annulation has been established as a valuable tool for the synthesis of fused polycyclic species. In some of the earliest examples, the Villarica,¹⁴⁷⁻¹⁴⁸ Ireland,¹⁴⁹⁻¹⁵¹ and Stork¹⁵² research groups displayed that fused tricyclic scaffolds could be achieved using a Robinson annulation from bicyclic building blocks. The power of this approach has been demonstrated in its continued application to the rapid construction of carbocyclic core structures in natural product synthesis. As shown in Scheme 1.26, Mori and Yajima employed this strategy in 2000 to access the tricyclic core of (–)-phytocassane D (**I-108**) from Wieland-Miescher ketone-derived bicyclic building block **I-106** through an initial formylation, followed by Robinson annulation with

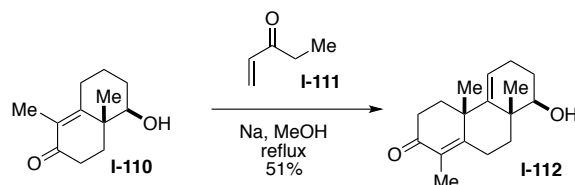
methylvinyl ketone **I-107** with accompanying formyl group removal.¹⁵³⁻¹⁵⁴ This strategy facilitated the successful synthesis of phytocassane D (**I-109**), and as such, enabled the determination of its absolute configuration. Additionally, this convergent approach has been applied in Maier's 2012 synthesis of moluccanic acid methyl ester¹⁵⁵ and Yu's 2015 synthesis of the ABC core structure of aglycon echinoside A.¹⁵⁶

Scheme 1.26 Mori's Robinson annulation strategy



In 2003, Gribble and coworkers displayed the efficiency of this reaction for the formation of tricyclic **I-112** from Wieland-Miescher ketone-derived bicycle **I-110** and ethylvinyl ketone **I-111** in the presence of sodium methoxide at reflux (Scheme 1.27).¹⁵⁷⁻¹⁵⁸ This method was again employed in the Sasaki's 2006 synthesis of brevione B¹⁵⁹ and Takikawa's 2012 synthesis of decaturin C.¹⁶⁰

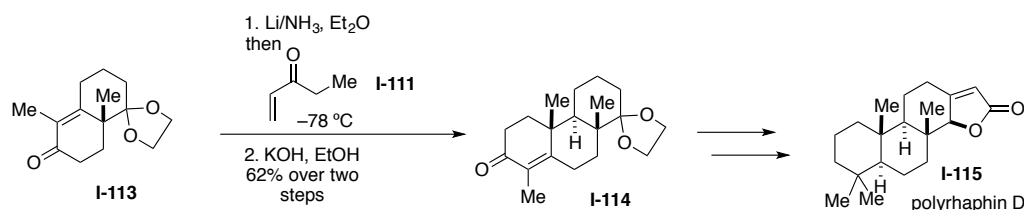
Scheme 1.27 Gribble's Robinson annulation strategy



It has also been revealed that similar products are produced from a dissolving metal reduction of Wieland-Miescher ketone-derived bicyclic enones with in situ capture of a suitable electrophile that can then undergo an intramolecular aldol condensation. This general process was

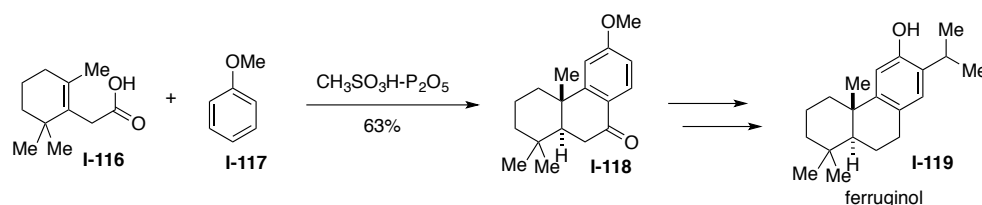
demonstrated in the 1960s by Tsuji and coworkers,¹⁶¹ and has been recently applied in She's 2016 synthesis of isospongian diterpenoid polyrhaphin D (**I-115**, Scheme 1.28)¹⁶² and Williams's 2017 studies toward the synthesis of tetranortriterpenoid gedunin.¹⁶³⁻¹⁶⁴

Scheme 1.28 She's cyclization strategy



Many variations of this domino type of reactivity to construct tricyclic core structures from simple building blocks have been explored over the years to provide tricyclic scaffolds.¹⁶⁵⁻¹⁶⁸ One example is the development of a comparable one-pot domino acylation-cycloalkylation by Ramana and Bhar in 2004, providing rapid access to diterpene core structures and allowing for the completed total syntheses of a number of natural products.¹⁶⁹ As shown in Scheme 1.29, cyclic acid **I-116** and anisole **I-117** underwent an acylation-cycloalkylation sequence in the presence of methanesulfonic acid-phosphorus pentoxide to form tricyclic **I-118**, which was further elaborated to natural product ferruginol **I-119**.

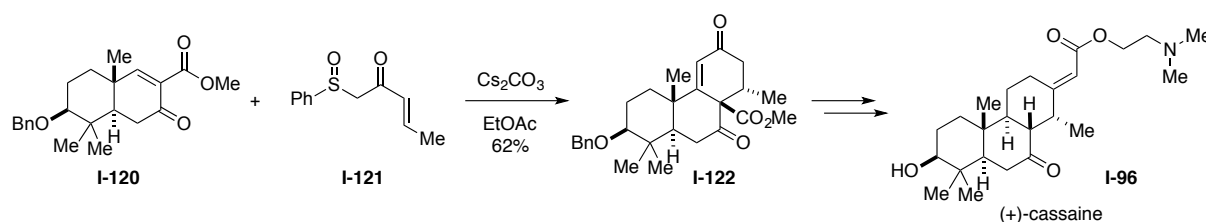
Scheme 1.29 Ramana's convergent domino strategy



In 2013, Deslongchamps and coworkers applied their developed anionic cyclization strategy¹⁷⁰⁻¹⁷¹ to the synthesis of (+)-cassaine **I-96**.¹⁷²⁻¹⁷³ Notably, the group had already successfully constructed this molecule employing their transannular Diels–Alder strategy, as

discussed in Section 1.3.1. In this alternate approach as shown in Scheme 1.30, carvone-derived bicycle **I-120** and Nazarov reagent **I-121** underwent an anionic cyclization in the presence of cesium carbonate to deliver tricyclic **I-122** as a single diastereomer with an axial methyl substituent, which was further elaborated to (+)-cassaine **I-96**. This anionic cyclization is essentially two sequential Michael additions, providing products analogous to those from a Diels–Alder cycloaddition.

Scheme 1.30 Deslongchamps's second synthesis of (+)-cassaine



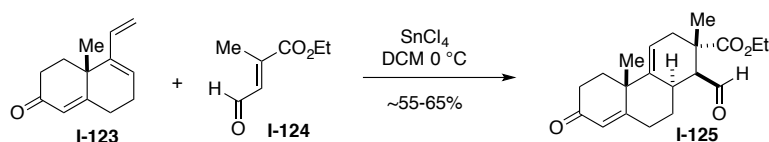
1.4.2 Diels–Alder cycloaddition

The Diels–Alder reaction has been proven to be infinitely useful for the rapid construction of the complexity present in many natural products.¹⁷⁴ As discussed earlier (Section 1.3.1), engaging this transformation within a macrocycle presents one valuable strategy for the production of the polycyclic structures of interest. The Diels–Alder reaction has also proven to be useful in the convergent assembly of different fragments to access the desired scaffolds.

1.4.2.1 Bicyclic Wieland-Miescher or Hajos-Parrish ketone precursors

Pioneering work in the late 1970s by Valenta and coworkers demonstrated the use of the Diels–Alder reaction to unite a bicyclic Wieland-Miescher ketone-derived diene (**I-123**) and a dienophile (**I-124**) in the preparation of tricyclic and steroidal core structures (**I-125**) in good yields (Scheme 1.31).¹⁷⁵⁻¹⁷⁷ A similar approach was employed by Grieco and coworkers for the first synthesis of anticancer agent quassin in 1984.¹⁷⁸

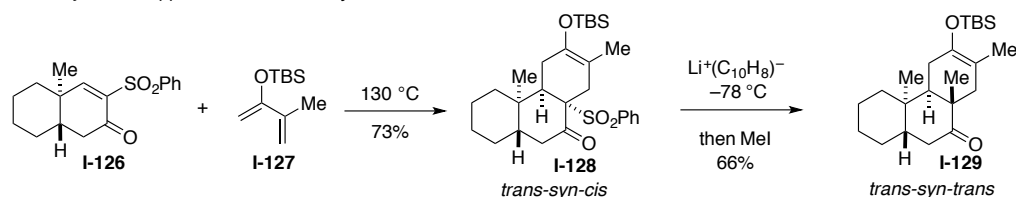
Scheme 1.31 Valenta's Diels–Alder approach



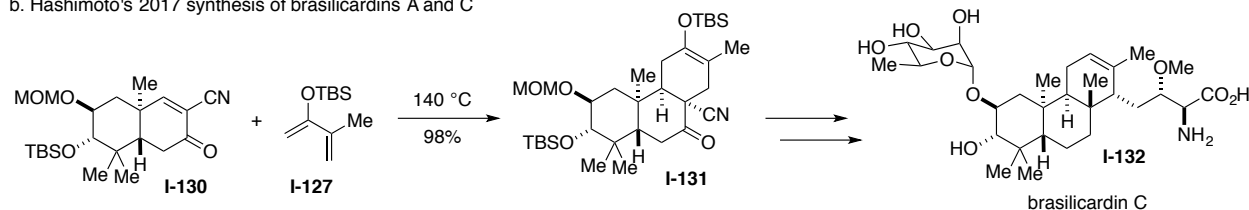
The power of this strategy was further demonstrated more recently in the early 2000s by the Theodorakis group, applying a Diels–Alder reaction with similar building blocks in their synthesis of tricyclic diterpene (–)-acanthoic acid.¹⁷⁹⁻¹⁸⁰ In 2003, Danishefsky and Coltart reported a Diels–Alder strategy to directly access the *trans-syn-trans* stereoisomer of the fused 6,6,6-scaffold.¹⁸¹ As shown in Scheme 1.32a, they established the *syn* relationship through a Diels–Alder reaction between bicyclic sulfone dieneophile **I-126** (accessed from the Wieland-Miescher ketone) and diene **I-127**, providing *trans-syn-cis* tricyclic adduct **I-128**. As planned, they then used the sulfone functionality to facilitate regioselective bridgehead enolate generation, which could be methylated from the less hindered face to access the *trans-syn-trans* perhydrophenanthrene **I-129**.

Scheme 1.32 a) Danishefsky's and b) Hashimoto's Diels–Alder strategies

a. Danishefsky's 2003 approach to the *trans-syn-trans* core



b. Hashimoto's 2017 synthesis of brasilicardins A and C

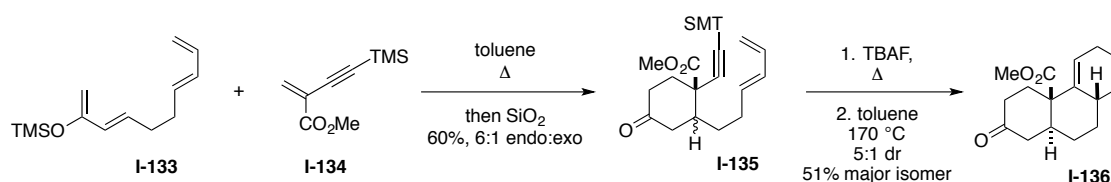


Inspired by this work from Danishefsky and Coltart, in 2017, Hashimoto and coworkers employed a similar approach to build the tricyclic core structure of brasiliocardins A and C (**I-132**), employing the same diene **I-127** in their key Diels–Alder with bicyclic dienophile **I-130** (Scheme 1.32b).¹⁸²

1.4.2.2 Alternative Diels–Alder precursors

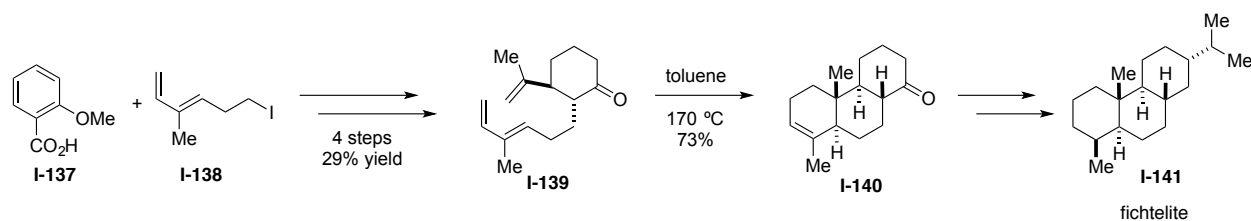
This convergent Diels–Alder strategy has been employed using building blocks outside of those derived from similar species to the bicyclic Wieland-Miescher ketone or the Hajos-Parrish ketone. For example, in the mid 1990s, Crawford and coworkers accessed tricyclic species **I-136** from double diene **I-133** and enyne **I-134** through an initial intermolecular Diels–Alder reaction followed by an intramolecular Diels–Alder (Scheme 1.33).¹⁸³⁻¹⁸⁴

Scheme 1.33 Crawford’s Diels–Alder sequence



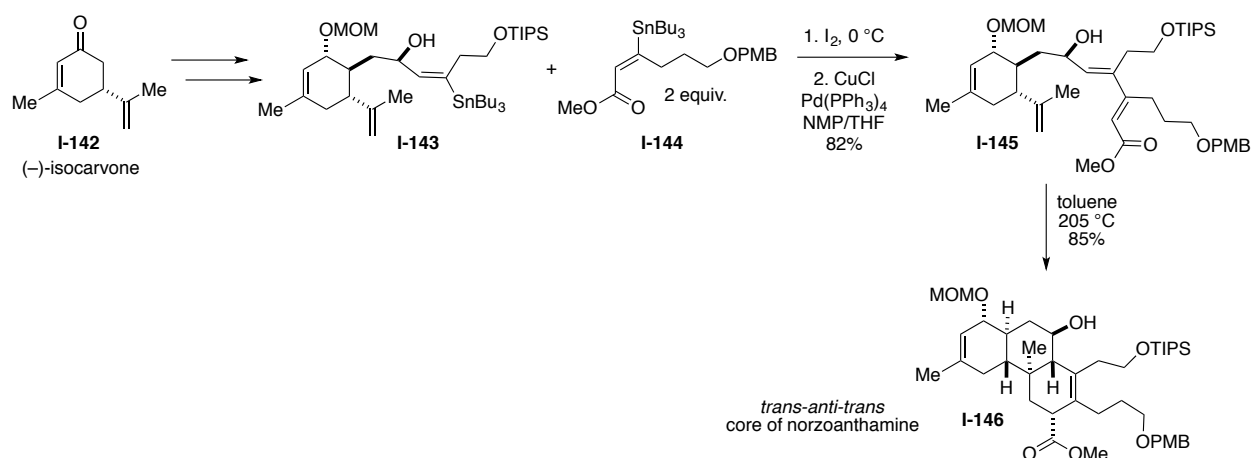
In a slightly different approach, in 1980 Taber and Saleh prepared tethered ketone **I-139** in four steps from fragments **I-137** and **I-138**, which underwent an intramolecular Diels–Alder reaction to achieve tricyclic species **I-140** bearing the *trans-anti-trans* stereochemistry (Scheme 1.34).¹⁸⁵ This stereochemistry was confirmed upon conversion to natural product fichtelite **I-141**, a hydrocarbon that had been synthesized by Johnson and coworkers using their developed cationic polyene cascade as discussed earlier in Section 1.2.1.1.²⁵⁻²⁶

Scheme 1.34 Taber's synthesis of fichtelite



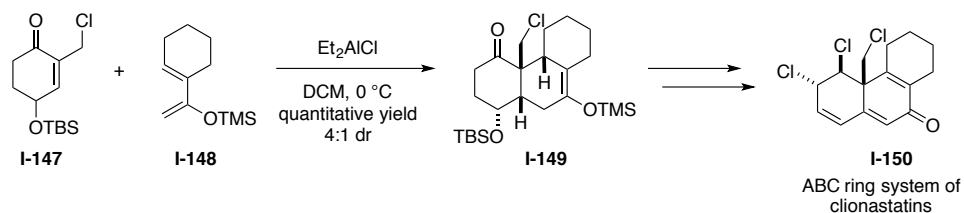
In 2007, Tanner and coworkers employed readily available (–)-isocarvone **I-142** to access their desired dienophile **I-143** and then applied a palladium-catalyzed coupling to convergently append fragment **I-144** to produce the internal diene within **I-145** (Scheme 1.35).¹⁸⁶ An intramolecular Diels–Alder cycloaddition fashioned the fused *trans-anti-trans* ring system **I-146**, which serves as the ABC core structure of marine alkaloid norzoanthamine.

Scheme 1.35 Tanner's Diels–Alder strategy



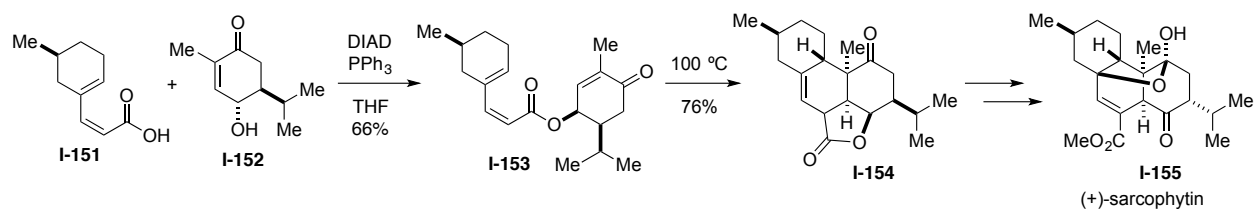
In a different approach in 2014, Vanderwal and Tartakoff were able to efficiently construct the tricyclic core structure of clionastatin natural products (**I-150**) by employing a Lewis acid-promoted Diels–Alder reaction between monocyclic dienophile **I-147** and diene **I-148** to provide tricyclic **I-149** (Scheme 1.36).¹⁸⁷

Scheme 1.36 Vanderwal's Diels–Alder strategy



Finally, in 2017 Carreira and coworkers reported the total synthesis of (+)-sarcophytin **I-155**, enabled by an intramolecular Diels–Alder reaction.¹⁸⁸ As shown in Scheme 1.37, (*S*)-citronellal-derived **I-151** and (*S*)-carvone-derived **I-152** and were combined in a Mitsunobu reaction to afford **I-153**. The key intramolecular Diels–Alder reaction delivered **I-154**, which was converted to the natural product **I-155**.

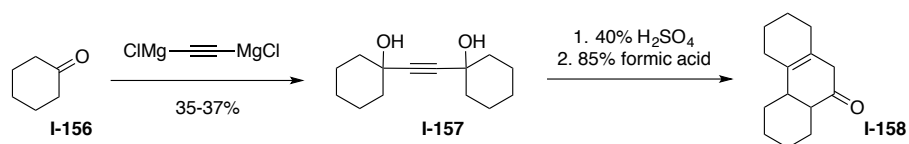
Scheme 1.37 Carreira's synthesis of (+)-sarcophytin



1.4.3 Tethered cyclic species in convergent polycyclic assembly

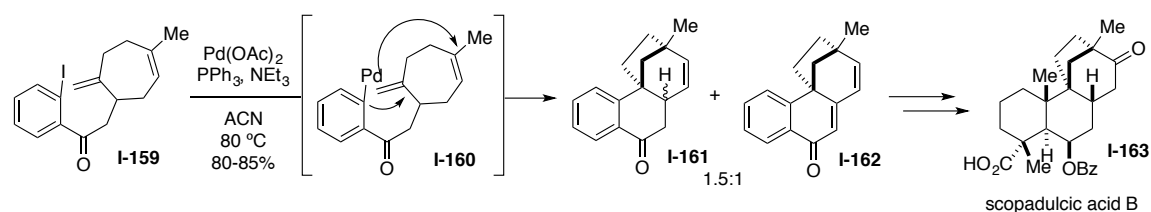
Several research groups over the years have developed a convergent strategy to form fused tricyclic scaffolds by joining two cyclic building blocks together, and then conducting some kind of ring-closing transformation. Earliest examples of this type of an approach date back to the 1930s when Marvel and coworkers reported a method for the synthesis of hydrophenanthrene structures by initially joining two cyclohexanone fragments (**I-156**) with an acetylene tether to provide **I-157** (Scheme 1.38).¹⁸⁹ This tethered species was dehydrated to a dienyne intermediate which cyclized to the tricyclic species **I-158** in the presence of 85% formic acid.

Scheme 1.38 Marvel's tethered fragment approach



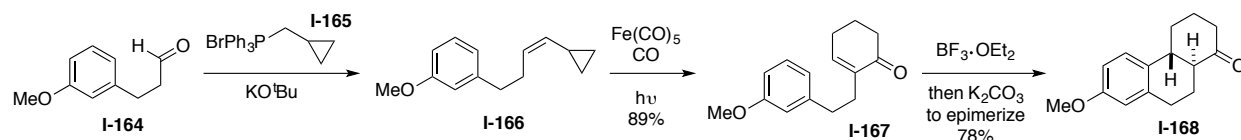
More modern examples of this strategy take advantage of transition metal catalysis for convergent fragment coupling reactions. In the 1990s, Overman and coworkers demonstrated a series of palladium-catalyzed intramolecular Heck cyclizations to fashion a fused polycyclic core from two linked cyclic fragments.¹⁹⁰⁻¹⁹¹ As shown in Scheme 1.39, the aryl iodide tethered to a cycloheptane ring (**I-159**) underwent sequential intramolecular Heck cyclizations to afford a mixture of ketone **I-161** and enone **I-162**, converging on enone **I-162** when treated with DDQ, which was elaborated to natural product scopadulcic acid B **I-163**.

Scheme 1.39 Overman's intramolecular Heck cyclization



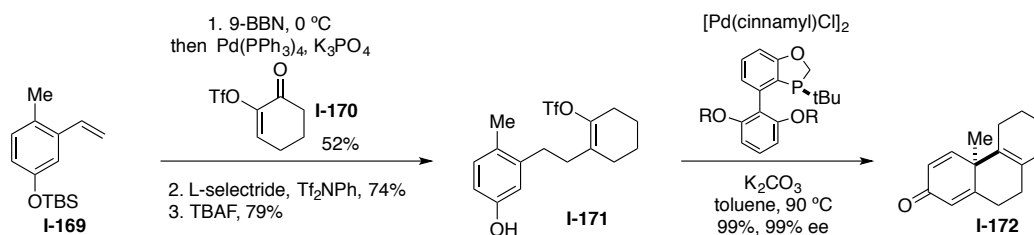
In 2008, Taber and Sheth reported a three-step method to access fused tricyclic structures.¹⁹² As shown in Scheme 1.40, simple aldehydes such as **I-164** were converted to alkenyl cyclopropane species **I-166** through an olefination with cyclopropylmethyl Wittig reagent **I-165**. This alkenyl cyclopropane underwent a key iron-mediated cyclocarbonylation to form 2-substituted cyclohexenones tethered to an aromatic fragment, such as **I-167**. The group demonstrated a subsequent Lewis acid-facilitated cyclization of the tethered species **I-167** and base-promoted epimerization to converge on the *trans*-ring fusion within tricyclic **I-168**.

Scheme 1.40 Taber's linked fragment strategy



In 2015 Tang and coworkers reported an additional modern version of this strategy with their development of a palladium-catalyzed dearomative cyclization. Joining aromatic fragment **I-169** with cyclic vinyl triflate **I-170** formed tethered species **I-171**, which underwent cyclization in the presence of a palladium catalyst and chiral ligand to form tricyclic **I-172** (Scheme 1.41).¹⁹³

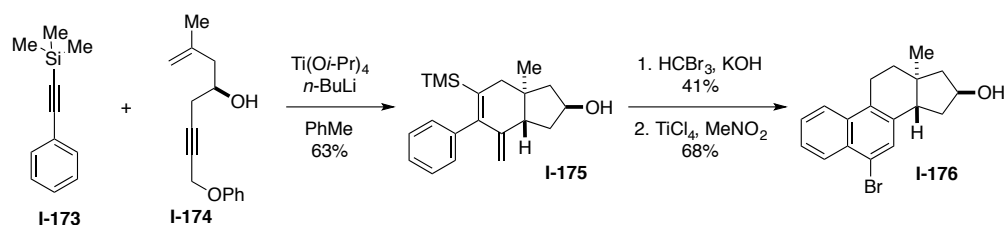
Scheme 1.41 Tang's tethered fragment approach



Most recently in 2018, Micalizio and coworkers devised a convergent route to aromatic steroidal scaffolds that are functionally poised for further modification.¹⁹⁴ Their strategy first constructed the tricyclic A-CD system **I-175** from a metallacycle-facilitated ring-forming cross-coupling between alkyne **I-173** and chiral enyne **I-174** (Scheme 1.42). This powerful transformation formed three new bonds and two stereocenters, providing the substituted *trans*-fused hydrindane system. The final B-ring of the steroid core was then closed from A-CD linked intermediate **I-175** through an initial cyclopropanation to install the required additional carbon atom, providing a vinyl cyclopropane intermediate. In the presence of TiCl_4 , this was converted to a homoallylic cation that participated in an intramolecular Friedel-Crafts alkylation to furnish the tetracyclic core **I-176**. The group observed in their substrate scope development that the

cyclopropanation step proceeded with enhanced yields when the secondary alcohol within **I-175** was protected prior to the transformation.

Scheme 1.42 Micalizio's synthesis of the steroidal core



1.5 Conclusion

The scope of the different strategies that have been developed to afford access to fused 6,6,6-polycyclic scaffolds demonstrates the vast synthetic innovation that these structures have inspired over many years. From elucidating the biosynthesis of steroids, to achieving that remarkable transformation in the absence of enzymes, the cyclization of linear polyenes is an example of how nature can serve as the greatest inspiration for chemists. The development of this synthetic transformation has been heavily explored and elegantly strengthened such that the strategy is a solid approach for the generation of fused polycyclic scaffolds. Alternatively, the construction of fused polycycles from larger macrocycles presents a significant strategy, influential in its ability to forge ring fusions within a contained environment in a single operation. And lastly, the assembly of building blocks offers a powerful avenue to construct complex core structures in a rapid fashion. The convergency of this strategy allows for simpler modification of the prepared scaffolds, and as such it is perhaps the most relevant within the context of the overarching scientific interest in accessing complex structures for novel drug discovery and understanding complex biological processes. It is clear that attention and innovation are being directed toward this goal, as many of the developed methods across all three strategic categories are the result of recent efforts.

Chapter 2

Development of a “Couple and Close” Strategy for the Construction of Fused Polycyclic
Scaffolds

Portions of this chapter appear in the following publication:

Emily E. Robinson and Regan J. Thomson, A Strategy for the Convergent and Stereoselective
Assembly of Polycyclic Molecules. *J. Am. Chem. Soc.* **2018**, *140*, 1956–1965.

2 Chapter 2

2.1 Introduction

As described in Section 1.1, the recently renewed interest in natural products as inspiration for drug discovery has led to a recognized need for the development of novel methods to rapidly access these complex core structures. The intricate biological processes and issues accompanying disease require more complex solutions than what are currently available.⁶⁻⁷ The aptitude of high-throughput screening to push the boundaries of drug discovery has been established, however this platform requires access to a more diverse array of small molecules to reach its full potential. Most candidates currently available for screening lack the three-dimensional architecture required for complex biological interactions, and without rapid and modular access to such structures, a wealth of biological potential remains unexplored.^{1, 3, 8-10}

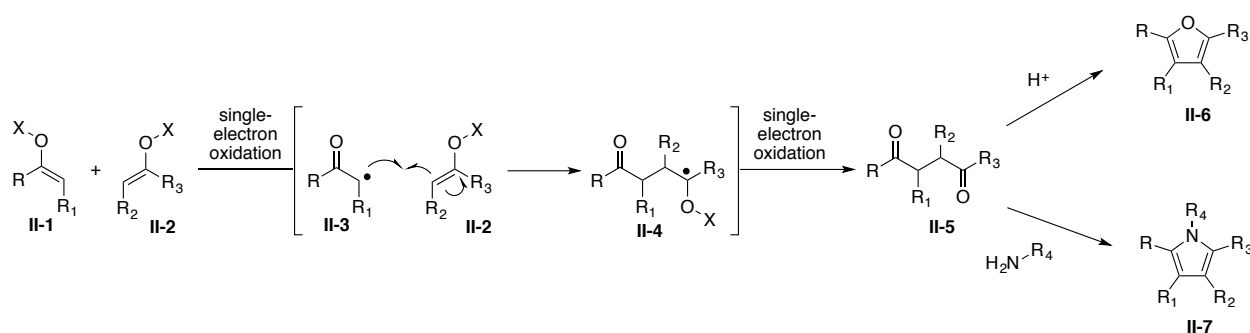
In response to this demand for more architecturally-complex structures modeled after those in nature that may be better equipped to address biological challenges, novel synthetic methods to efficiently access these scaffolds must be established. This chapter will discuss the development of such a strategy, allowing for the rapid and convergent construction of three-dimensionally complex fused polycyclic scaffolds prevalent within numerous bioactive natural product families.

2.2 Oxidative enolate coupling as a powerful tool

The development of strategies to assemble complex core structures in a convergent manner is particularly valuable for the modular synthesis of varied structures, and is an important feature for drug discovery. Within this context, oxidative enolate coupling has emerged as a powerful transformation for the rapid generation of complexity. The union of two fragments (i.e. **II-1** and **II-2**) by forging a new carbon-carbon bond under oxidative conditions to produce 1,4-diketone

products (**II-5**) is an inherently convergent and efficient approach to complex structures (Scheme 2.1).¹⁹⁵⁻¹⁹⁶ The single-electron oxidation of an enolate species results in a radical intermediate (**II-3**) that can combine with another enolate through a carbon–carbon bond forming event to produce another radical (**II-4**). A second single-electron oxidation results in a cation which is relieved by hydrolysis, leading to the diketone product **II-5**. The potential for the key bond formation to set vicinal stereocenters within the produced 1,4-diketone (**II-5**) enhances the level of complexity that is accessible through this reactivity.

Scheme 2.1 Oxidative enolate coupling

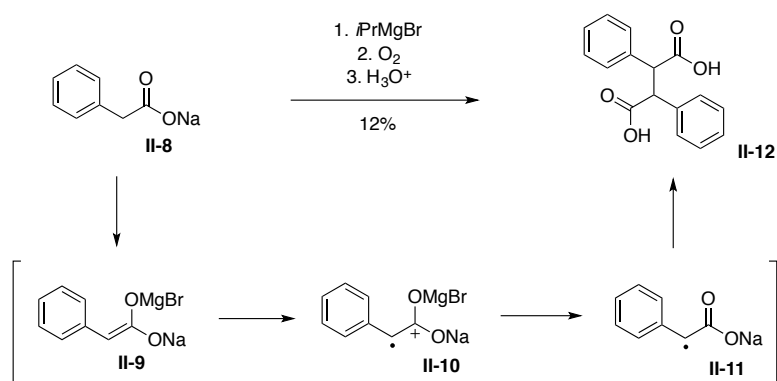


Moreover, this enabled access to the 1,4-diketone motif is significant, as the dissonant relationship between the two carbonyl groups makes this scaffold challenging to synthesize through classic methods (i.e. Michael addition). The value of a synthetic approach to 1,4-diketones is displayed through their ability to provide direct access to structures prevalent in bioactive molecules such as furans (**II-6**) and pyrroles (**II-7**), as well as indirect access to many other structures of interest. The power of this versatile reactivity has been demonstrated through the successful employment of oxidative coupling in natural product synthesis.¹⁹⁷⁻²⁰⁵

2.2.1 Coupling of metal enolates

Ivanoff and Spasoff reported the first instance of oxidative enolate coupling in 1935, demonstrating that the enolate of phenyl acetic acid underwent oxidative dimerization when exposed to dioxygen (Scheme 2.2).²⁰⁶ Enolate **II-9** was oxidized to radical cation intermediate **II-10** in the presence of dioxygen, and subsequent hydrolysis to radical **II-11** then enabled the ensuing radical recombination to form dimerized product **II-12**.

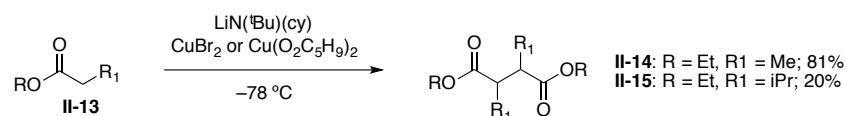
Scheme 2.2 Ivanoff's preliminary oxidative coupling report



This first example of oxidative coupling was plagued by low yields and undesired byproduct formation, and it wasn't until the 1970s when this transformation was rendered synthetically useful. In 1971, Rathke and Lindert disclosed the dimerization of ester enolates (derived from **II-13**, Scheme 2.3) in the presence of copper(II) bromide or copper(II) valerate to form dialkyl succinate esters (**II-14** and **II-15**).²⁰⁷ They generally isolated a mixture of stereoisomers, and showed that as the steric congestion adjacent to the carbonyl increased, the coupling yield decreased and unreacted starting material was recovered. For example, as shown in Scheme 2.3, when the size of R1 was increased from a methyl group to an isopropyl group, the yield diminished from 81% to 20%. This was the first time that a metal oxidant was shown to be capable of

promoting the coupling process, but these early observations demonstrated three of the key persisting challenges to oxidative coupling: accomplishing the cross-coupling of two different enolate species, coupling in sterically-hindered environments, and achieving stereocontrol.

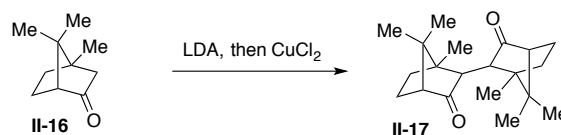
Scheme 2.3 Rathke's oxidative coupling



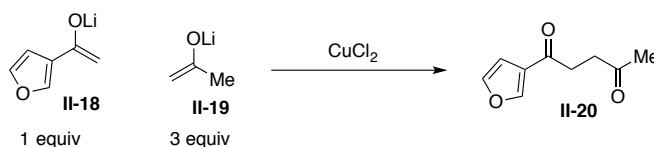
In the mid-to-late 1970s, Saegusa and coworkers established a method to couple various ketones in the presence of LDA and copper(II) chloride to form 1,4-diketones in good yields (Scheme 2.4a).²⁰⁸⁻²⁰⁹ Notably, they were able to forge the new carbon–carbon bond in sterically congested environments, such as for the production of **II-17**. They also showed the ability of their method to couple the lithium enolates of two different ketone species (i.e. **II-18** and **II-19**) to provide cross-coupled products (**II-20**), but this required a three-fold excess of one coupling partner (Scheme 2.4b). Over the years, the coupling of enolates has been accomplished with a variety of oxidants, such as Cu(OTf)₂,²¹⁰ FeCl₃,²¹¹ I₂,²¹²⁻²¹³ TiCl₄,²¹³⁻²¹⁴ and AgCl.²¹⁵

Scheme 2.4 Saegusa's oxidative coupling

a. Dimerization of ketone-derived enolates

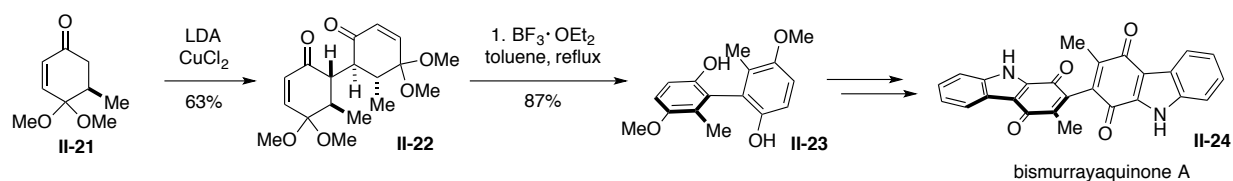


b. Cross-coupling of ketone-derived enolates



The Thomson group employed this type of chemistry and reported the successful dimerization of cyclic enones (i.e. **II-21**, Scheme 2.5) upon treatment with LDA and copper(II) chloride to form a linked bicycle (**II-22**) which could be aromatized with complete stereochemical transfer to produce a biaryl species (**II-23**).²¹⁶ This method was later applied by the group to the total synthesis of carbazole alkaloid bismurrayaquinone A **II-24** (Scheme 2.5).²¹⁷

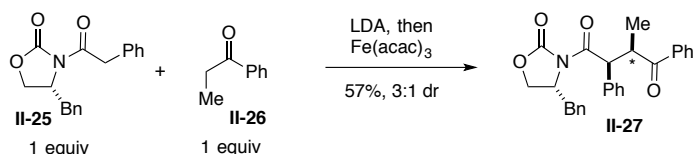
Scheme 2.5 Thomson's biaryl synthesis



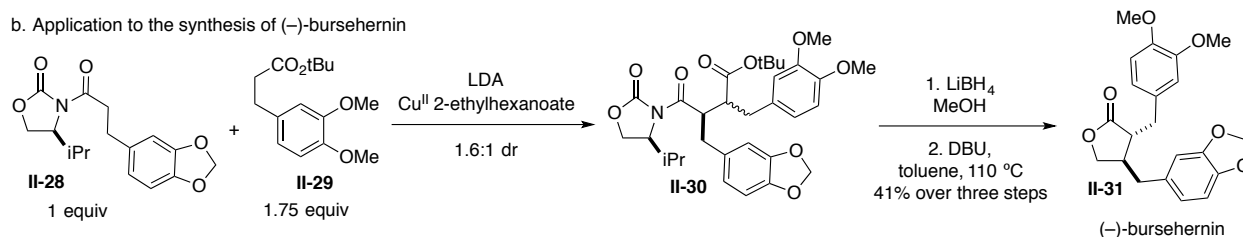
In 2006, Baran and coworkers disclosed the successful cross-coupling of the lithium enolate of an imide (**II-25**) with that of a ketone, ester, or lactone (**II-26**) in the presence of copper(II) or iron(III) oxidants, presenting a significant contribution to the field (Scheme 2.6a).^{199, 218} By taking advantage of the differences in oxidation potential of the coupling partners, this cross-coupling was achieved with equal stoichiometries of each coupling partner for the first time.

Scheme 2.6 Baran's cross-coupling with equal stoichiometries of coupling partners

a. Cross-coupling of amide- and ketone-derived enolates



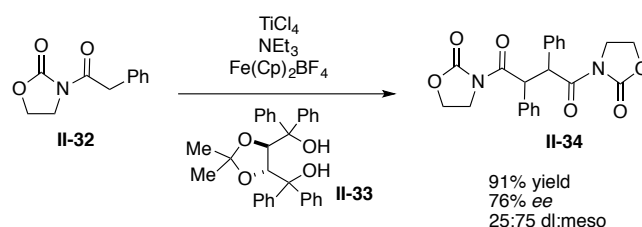
b. Application to the synthesis of (-)-bursehernin



Furthermore, the use of Evans oxazolidinones in the coupling enabled the preparation of enantioenriched 1,4-diketones (**II-27**). This strategy was applied to the enantioselective synthesis of (–)-bursehernin **II-31**, and although the coupling of **II-28** and **II-29** required a 1.75-fold excess of ester **II-29** and only provided a 1.6:1 mixture of diastereomers, the subsequent reduction and base-mediated lactonization sequence led to epimerization to the favored trans-relationship and exclusive production of **II-31** (Scheme 2.6b).

An early report by Nguyen and Schäfer in 2001 exhibited the potential for the asymmetric oxidative enolate dimerization of an oxazolidinone (**II-32**) with stoichiometric amounts of both $\text{Fe}(\text{Cp})_2\text{BF}_4$ oxidant and chiral additive **II-33**.²¹⁹ With the most successful example shown in Scheme 2.7, the reported dimerization proceeded in good yield but with modest enantio- and diastereoselectivities. Nevertheless, this report served as inspiration for enantioselective coupling.

Scheme 2.7 Schäfer's enantioselective dimerization

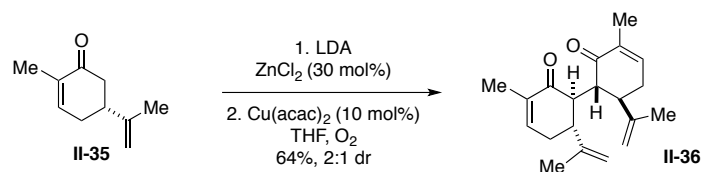


In 2011, Flowers and Casey thoroughly investigated the mechanism for the cross-coupling of ketone-derived lithium enolates in equal stoichiometries and determined that the formation of cross-coupled products was attributed to the preferential aggregation pattern of lithium enolates.²²⁰ Their ^7Li NMR spectroscopy studies exhibited a preference for an equimolar mixture of different ketone-derived lithium enolates to form heteroaggregates over homoaggregates, and this difference in accumulation was translated to the difference in formation of cross-coupled products over dimerized products. Mechanistically, this work presented a view of what occurs in these

reactions that had previously not been considered, however predicting the way that different substrates will aggregate is a major challenge.

Finally, in 2012 Daugulis and coworkers reported the dimerization of lithium enolates with substoichiometric amounts of a copper oxidant for the first time, utilizing oxygen as the terminal oxidant.²²¹ As shown in a representative example in Scheme 2.8, the lithium enolates (derived from ketones such as **II-35**) were stabilized in the reaction conditions with an electrophilic zinc salt, allowing for catalytic copper(II) acetylacetonate to deliver the coupled products (i.e **II-36**) under 1 atm of oxygen. Because oxidative coupling transformations up to this point required the stoichiometric addition of oxidants, this disclosure represented a significant contribution that may shape the direction of future advancements in the field.

Scheme 2.8 Daugulis's catalytic oxidative coupling



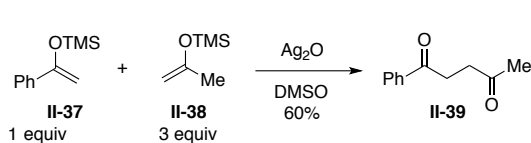
2.2.2 Coupling of enol silanes

In addition to metal enolates, enol silanes have also been successfully implemented in oxidative coupling. In 1975, Saegusa and coworkers demonstrated the ability to oxidatively couple silyl enol ether species in the presence of Ag₂O (Scheme 2.9a).²²² The study reported successful dimerizations as well as a few cross-coupling transformations. Similar to many of the previously discussed metal enolate studies, a three-fold excess of one coupling partner was required to accomplish the cross-coupling. In 1977, Tokuno and coworkers reported the use of Cu(OTf)₂ and Cu₂O for the dimerization of an enol silane.²¹⁰ As shown in Scheme 2.9b, in 1989, Ruzziconi

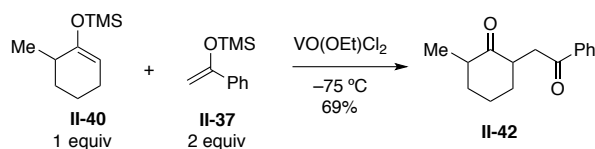
reported the cross-coupling of two enol silanes promoted by single-electron oxidant cerium(IV) ammonium nitrate (CAN).²²³⁻²²⁴ They demonstrated that under their reaction conditions, a 5- to 10-fold excess of one coupling partner was required to minimize undesired dimerization. In 1992, Ohshiro and coworkers established the ability for a pentavalent vanadium complex to serve as a single-electron oxidant for the coupling of two different enol silane species, as shown in Scheme 2.9c.²²⁵ This process also required the use of a two-fold excess of one coupling partner to access the cross-coupled product. Later, Livinghouse and Ryter,²²⁶ and more recently, Hirao and coworkers,²²⁷ also used a vanadium complex to promote the oxidative bond formation between silyl enol ethers. As shown in a representative example in Scheme 2.9d, Hirao and coworkers were able to expand upon Ohshiro's work, employing the vanadium complex to achieve the cross-coupling of boron enolates (**II-43**) and enol silanes (**II-37**) in a 1:1 ratio to form unsymmetrical 1,4-diketones (**II-44**).

Scheme 2.9 Coupling of enol silanes

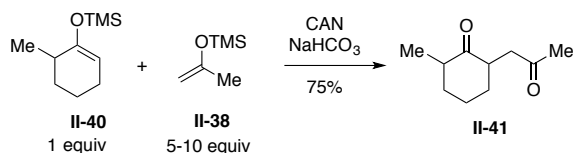
a. Saegusa's coupling of enol silanes



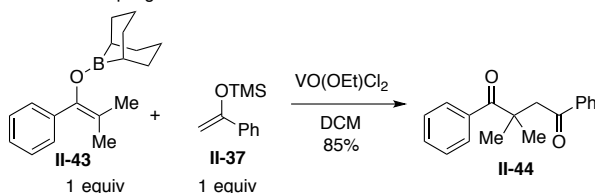
c. Ohshiro's coupling with vanadium



b. Ruzziconi's coupling of enol silanes



d. Hirao's coupling with vanadium



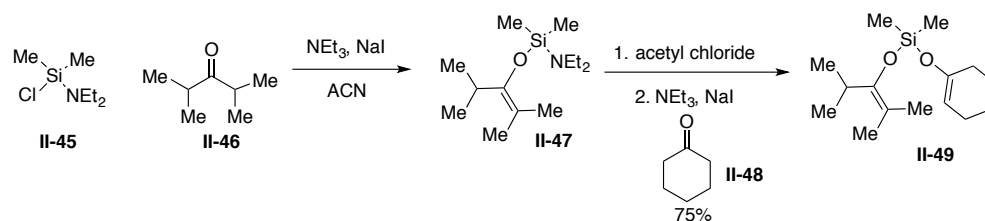
2.2.2.1 Coupling of silyl bis-enol ether intermediates

Though many methods for oxidative coupling have been developed in a variety of contexts, there remain key challenges associated with the reaction. For example, the cross-coupling of two

different species with similar oxidation potential without requiring a large excess of one coupling partner remains a challenge, an issue which significantly dampens the utility of oxidative coupling in complex molecule synthesis. Additionally, achieving the desired carbon–carbon bond formation with high levels of stereocontrol remains challenging. And lastly, forging a new bond in a sterically demanding environment is an ongoing obstacle.

Powerful in their ability to address these challenges, silyl bis-enol ether species have emerged as versatile intermediates for facilitating oxidative coupling transformations. The synthesis of these species was first reported by Rathke and Weipert in 1991 (Scheme 2.10), and although they did not demonstrate any utility of these intermediates at the time, their method to prepare unsymmetrical silyl bis-enol ethers proved useful to research groups in later years.²²⁸ The three-step sequence was initiated with the generation of an intermediate amino silane species (**II-47**) from one coupling partner (**II-46**), and then following regeneration of the silyl halide with acetyl chloride, the enolate of the second coupling partner (**II-48**) could be attached to deliver unsymmetrical **II-49**.

Scheme 2.10 Rathke’s unsymmetrical silyl bis-enol ether formation

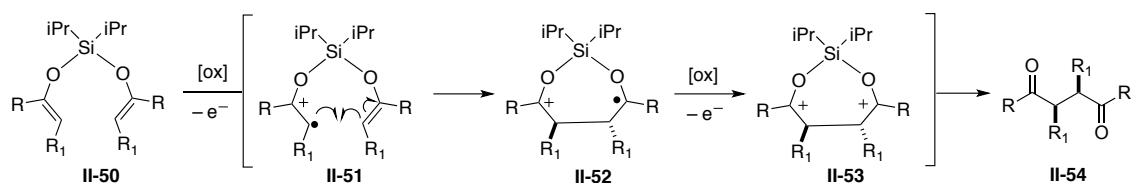


In 1998, Schmittl and coworkers were the first to display the potential for silyl bis-enol ethers in the context of oxidative coupling, demonstrating their successful coupling in the presence of numerous oxidants.²²⁹⁻²³⁰ As shown in Scheme 2.11a, when treated with two equivalents of an oxidant, silyl bis-enol ether **II-50** can undergo single-electron transfer to produce intermediate

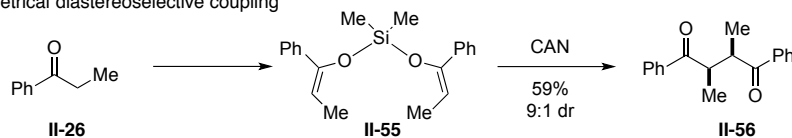
radical cation species **II-51**, which can forge a new carbon–carbon bond in combination with the enolate of the other coupling partner to form intermediate **II-52**. A second single-electron oxidation of this intermediate results in bis(cation) species **II-53**, which upon hydrolysis of the silicon tether, provides the ultimate coupled 1,4-diketone product **II-54**. Although Schmittel and coworkers only reported the synthesis of four different diketones, they showed that silyl bis-enol ethers not only underwent oxidative coupling in good yields, but also proceeded with diastereocontrol, one of the known challenges of oxidative coupling transformations to this point. As shown in Scheme 2.11b, in the presence of single-electron oxidant cerium(IV) ammonium nitrate (CAN), ketone **II-26** was oxidatively dimerized through symmetrical silyl bis-enol ether **II-55** to form 1,4-diketone **II-56** in 59% and 9:1 dr. Excitingly, the group displayed the ability to effectively cross-couple two ketone species **II-26** and **II-57** through unsymmetrical silyl bis-enol ether **II-58** to deliver the 1,4-diketone **II-59**, addressing another key challenge to oxidative coupling transformations (Scheme 2.11c).

Scheme 2.11 Schmittel's silyl bis-enol ether coupling

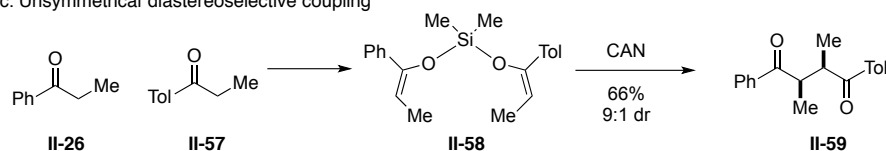
a. Concept of silyl bis-enol ether coupling



b. Symmetrical diastereoselective coupling



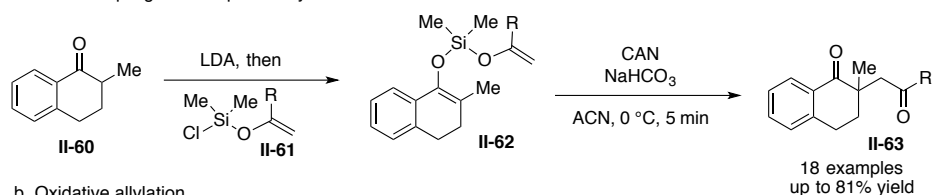
c. Unsymmetrical diastereoselective coupling



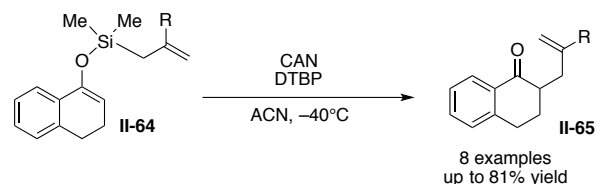
The Thomson lab has provided significant contributions to this area, demonstrating the ability for silyl bis-enol ethers to combat many of the challenges associated with oxidative coupling and rendering the reaction valuable to the synthesis of complex molecules. In 2007, the group first reported the use of silyl bis-enol ethers for the successful cross-coupling of 2-methyl tetralone **II-60** with various acyclic ketone coupling partners to form unsymmetrical 1,4-diketones (**II-63**, Scheme 2.12a).²³¹ They prepared the required unsymmetrical silyl bis-enol ethers (**II-62**) with modified Rathke conditions through the three-step protocol with initial generation of an amino silane (Scheme 2.10). CAN was discovered to be the stoichiometric oxidant of choice for this transformation, enabling the facile cross-coupling of two ketone coupling partners in a roughly 1:1 ratio while preparing a quaternary center through the carbon–carbon bond formation.

Scheme 2.12 Thomson's oxidative coupling methods development

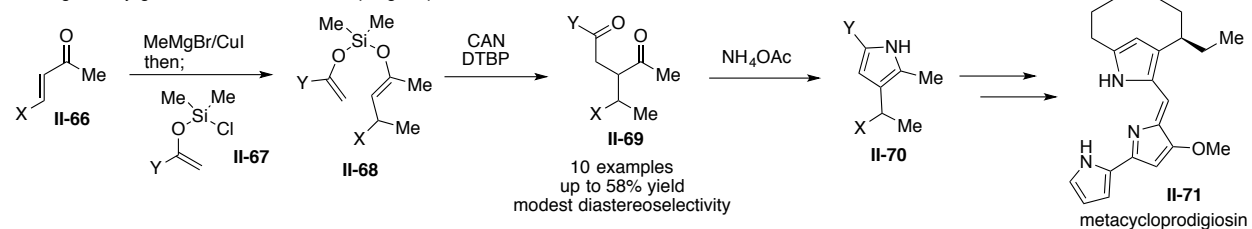
a. Cross-coupling to form quaternary stereocenters



b. Oxidative allylation



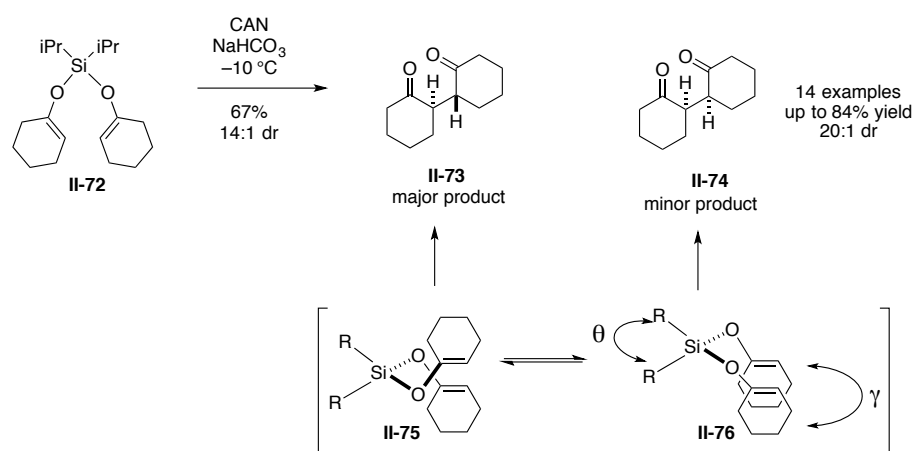
c. Merged conjugate addition–oxidative coupling sequence



With a similar strategy, the group demonstrated the successful oxidative allylation of ketones through silicon tethered intermediates (Scheme 2.12b).²³² Furthermore, the group developed a merged conjugate addition–oxidative coupling sequence that enabled the total synthesis of metacycloprodigiosin **II-71** and prodigiosin R1 (Scheme 2.12c).²³³ In this method, unsymmetrical silyl bis-enol ethers (**II-68**) were formed by trapping the conjugate addition product of **II-66** with an enol silyl halide (**II-67**). This intermediate then underwent oxidative coupling to form the unsymmetrical 1,4-diketones (**II-69**) in good yields and modest diastereoselectivities (~2:1 dr). In this developed methodology, the 1,4-diketones were then smoothly converted to the pyrrole species (**II-70**) through a Paal-Knorr reaction, which could be further elaborated to two prodigiosin natural products. This direct method was employed for the group’s second generation synthesis of metacycloprodigiosin **II-71**.²³⁴

In their quest to provide access to more three-dimensionally complex structures, the group demonstrated the ability for silyl bis-enol ethers (**II-72**) to facilitate the coupling of two cyclic ketone species to deliver linked bicyclic 1,4-diketones (**II-73**) with high levels of diastereocontrol (Scheme 2.13).²³⁵

Scheme 2.13 Thomson’s diastereoselective coupling of cyclic ketones

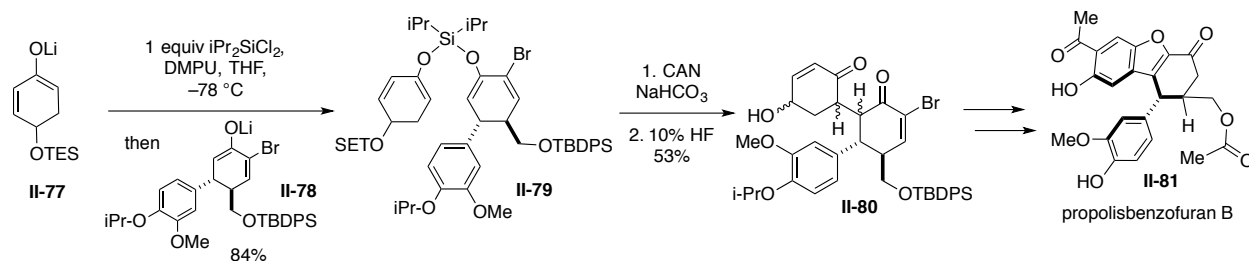


They performed dimerizations and cross-couplings via silyl bis-enol ether intermediates, accessing the unsymmetrical variants through the modified Rathke three-step protocol as mentioned earlier (Scheme 2.10). The proposed model for the observed stereoselectivity is shown in Scheme 2.13, where a conformational bias of the silyl bis-enol ether leads to selective formation of major product **II-73**. Of the possible conformations, **II-75** is favored because the cyclic coupling partners are held in an orientation that minimizes destabilizing interactions between the two rings. On the other hand, in conformation **II-76**, the cyclic coupling partners are held such that they are experiencing destabilizing ring–ring interactions. The group further probed this selectivity and discovered that increasing the size of the alkyl groups on the silicon tether (R) led to enhanced selectivity for the major product **II-73**. This observation is presumably attributed to a Thorpe-Ingold effect where the increased size of the alkyl groups on silicon (R) leads to greater repulsion and thus a larger angle between them (θ), which in turn compresses the angle between the two cyclic coupling partners (γ). This increased proximity of the two coupling partners exaggerates the destabilizing interactions within the minor conformation **II-76**, leading to the diminished production of minor product **II-74**.

This silyl bis-enol ether-facilitated coupling of cyclic ketones was successfully applied to the total synthesis of propolisbenzofuran B **II-81**, as shown in Scheme 2.14.²³⁶ In this synthesis, the unsymmetrical silyl bis-enol ether **II-79** was not prepared through the group's previously employed three-step procedure, but rather upon slow, controlled addition of the enolate of one coupling partner (**II-77**) to one equivalent of diisopropyldichlorosilane in the presence of DMPU at low temperatures, followed by the controlled addition of the enolate of the other coupling partner (**II-78**). This strategy to streamline the preparation of unsymmetrical silyl bis-enol ethers will be

discussed later in the chapter. These disclosures collectively establish the ability for silyl bis-enol ethers to facilitate challenging oxidative coupling transformations, elevating the utility of this reaction to complex molecule synthesis.

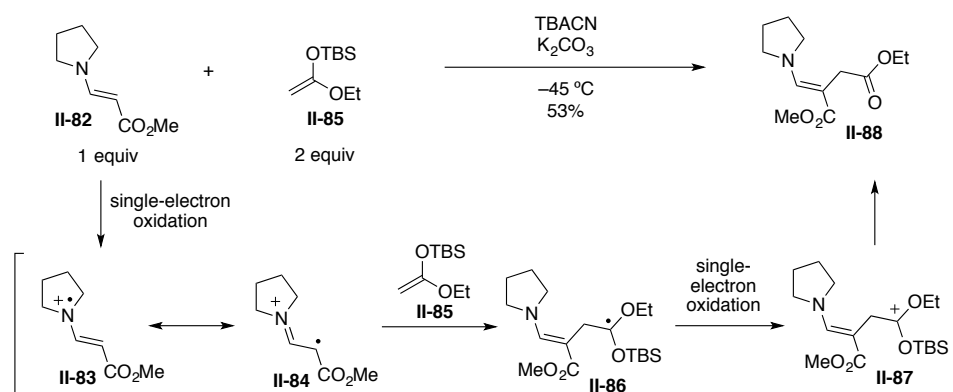
Scheme 2.14 Thomson's synthesis of propolisbenzofuran B



2.2.3 Coupling of enamines

In 1992, Narasaka and coworkers reported a method for the cross-coupling of enamines and enol silanes.²³⁷ As shown in Scheme 2.15, when enamine **II-82** was treated with single-electron oxidant tetrabutylammonium cerium(IV) nitrate (TBACN), it was oxidized to an enamine radical cation intermediate (**II-83** \leftrightarrow **II-84**) that could combine with the enol silane coupling partner **II-85** to forge the carbon–carbon bond and provide α -siloxy radical **II-86**.

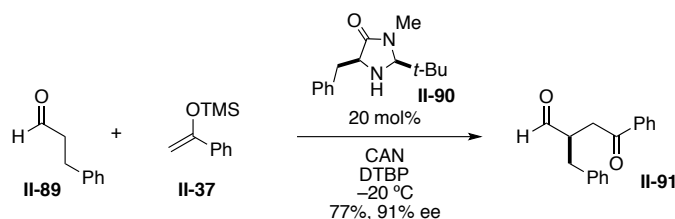
Scheme 2.15 Narasaka's early contribution



A subsequent single-electron oxidation from a second equivalent of TBACN resulted in the cation species **II-87** that was relieved upon hydrolysis of the silane, providing coupled product **II-88**. Although this method required a two-fold excess of the enol silane coupling partner, the concept set the stage for some further developments in future years.

In 2007, MacMillan and coworkers employed their singly occupied molecular orbital catalysis platform (SOMO) in the context of oxidative coupling to provide the first enantioselective variant of this transformation.²³⁸⁻²⁴¹ The general concept of this work follows that of the Narasaka disclosure but with incorporation of enamine organocatalysis, allowing for asymmetric induction. Condensation of an aldehyde species with a chiral amine catalyst produces an enamine intermediate that undergoes the previously described oxidation–combination–oxidation–hydrolysis sequence. As shown in the representative example in Scheme 2.16, in the presence of an imidazolidinone organocatalyst **II-90**, single-electron oxidant CAN, and di-*tert*-butylpyridine, aldehydes (**II-89**) could be successfully coupled with enol silanes (**II-37**) in equal stoichiometries and in enantioselective fashion to form 1,4-dicarbonyls (**II-91**).

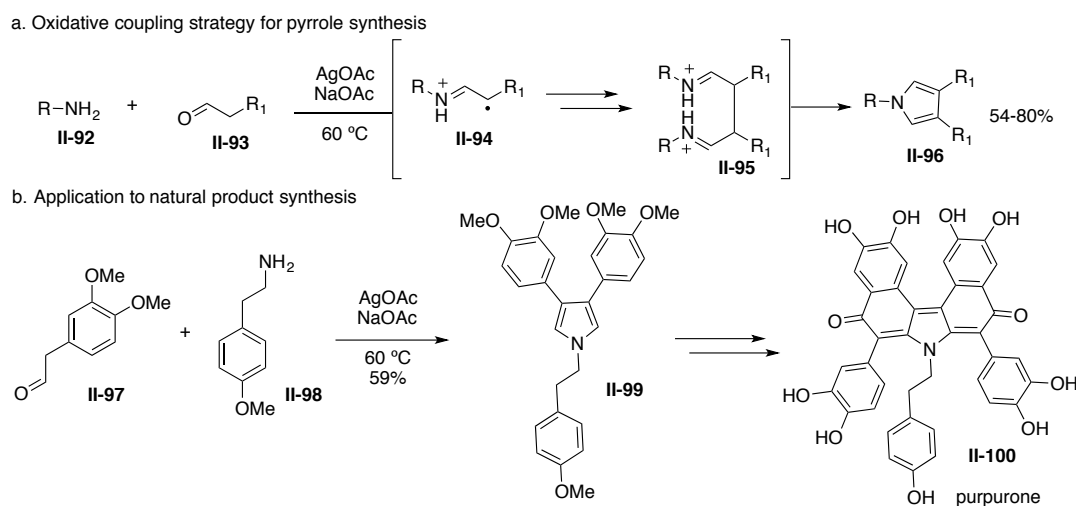
Scheme 2.16 MacMillan’s application of SOMO catalysis



In 2010, Jia and coworkers employed this general enamine approach to oxidative coupling for ultimate access to symmetrical pyrroles.²⁴² Various amine (**II-92**) and aldehyde (**II-93**) coupling partners condensed to form an enamine, which underwent a similar process as previously described except with a dimerization coupling event rather than the cross-coupling shown in

previous examples. This sequence led to a 1,4-diimine species (**II-95**) which aromatized to deliver pyrrole **II-96** (Scheme 2.17a). With this strategy, they successfully completed the synthesis of ATP-citrate lyase inhibitor purpurone (**II-100**, Scheme 2.17b), as well as other similar natural products.²⁴³

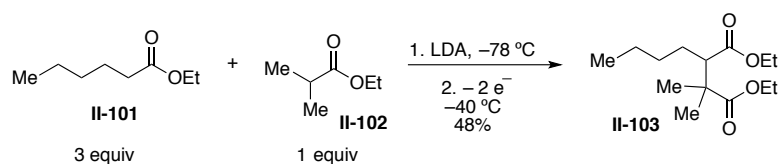
Scheme 2.17 Jia's pyrrole synthesis



2.2.4 Electrochemical oxidative coupling

As early as the 1970s, research groups have explored the oxidative coupling of lithium enolate species employing electrochemistry. Itoh and coworkers reported the successful electrochemical oxidative coupling of ester-derived lithium enolates (Scheme 2.18).²⁴⁴ They were successful in the dimerization of these species, and reported one cross-coupled example, however similar to work with metal oxidants, this required a three-fold excess of one coupling partner.

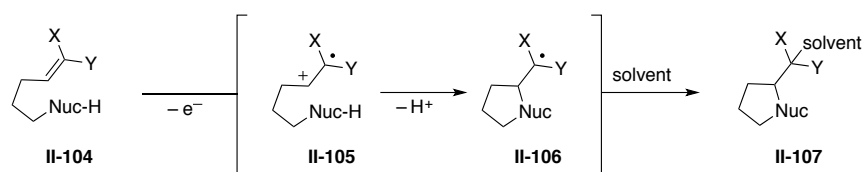
Scheme 2.18 Itoh's electrochemical coupling



As shown in Scheme 2.18, following preparation of the lithium enolates of esters **II-101** and **II-102**, electrolysis at low temperatures afforded the coupled product **II-103** in 48% yield.

Moeller and coworkers have successfully employed electrochemistry for a thorough investigation of intramolecular coupling reactions of radical cation species generated from electron-rich olefins, a strategy that he has recently reviewed.²⁴⁵ As shown in Scheme 2.19, the general approach that his group has developed involves the anodic oxidation of the electron-rich alkene within **II-104** to generate a radical cation species **II-105**. When the molecule contains a nucleophile, it can trap the cation in a cyclization event to form cyclic radical **II-106**, which can be quenched by solvent. These anodic cyclization reactions have been applied to the synthesis of various molecules, as discussed in the cited publication, and this work has demonstrated the great potential for electrochemical oxidations to promote the rapid construction of complexity.

Scheme 2.19 Moeller's electrochemical coupling strategy



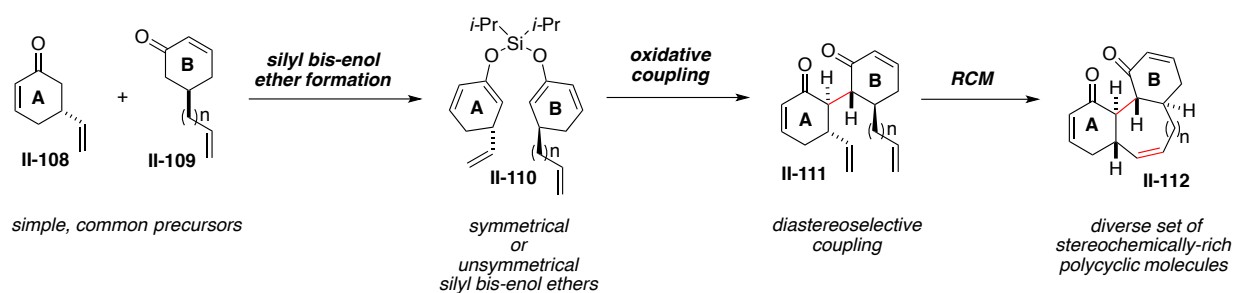
2.3 Development of a strategy for the construction of fused polycycles

With the wealth of promising research on oxidative coupling, and the Thomson group's extensive knowledge of the transformation, we imagined that this enabling reactivity could serve as the foundation for a convergent strategy to access polycyclic scaffolds. As discussed in Section 2.2.2.1, the Thomson group has demonstrated the utility of silyl bis-enol ethers in oxidative coupling to deliver complex structures in a convergent manner. Particularly with respect to the study revealing the diastereoselective coupling of cyclic ketones to form bicyclic 1,4-diketones

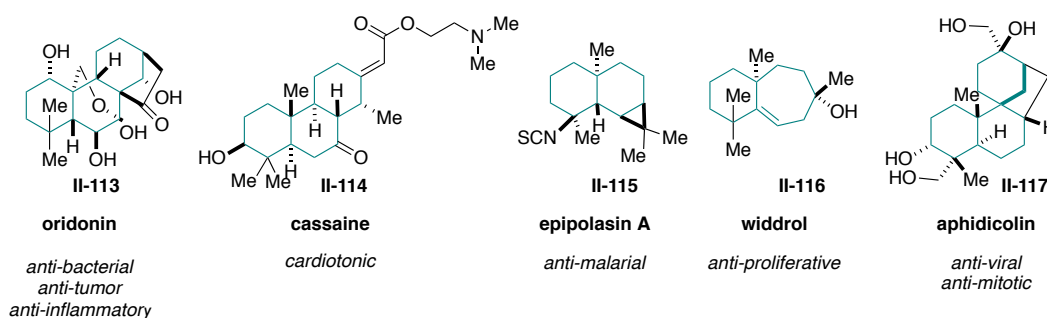
with stereocontrol (Scheme 2.13), we imagined that we could extend this reactivity to access a suite of fused polycyclic scaffolds from simple precursors. The general approach is shown in Scheme 2.20a, employing a diastereoselective oxidative coupling–ring-closing metathesis sequence to deliver fused carbocycles with three-dimensional complexity in just three steps from simple ketone substrates. We imagined that the coupling of two cyclic enones equipped with an olefin appendage (i.e. **II-108** and **II-109**) through a silyl bis-enol ether (**II-110**) would yield bicyclic intermediates (**II-111**) with stereocontrol, where the olefin substituents would then be poised to undergo a subsequent ring-closing metathesis to forge the fused tricyclic system with four contiguous stereocenters (**II-112**). This “couple and close” strategy could be categorized alongside the convergent fragment coupling approaches to provide tethered cyclic species that can be converted to polycyclic scaffolds, as discussed in Section 1.4.3.

Scheme 2.20 General couple and close strategy

a. General strategy for the convergent construction of fused polycycles



b. Representative bioactive natural products with potentially accessible core structures

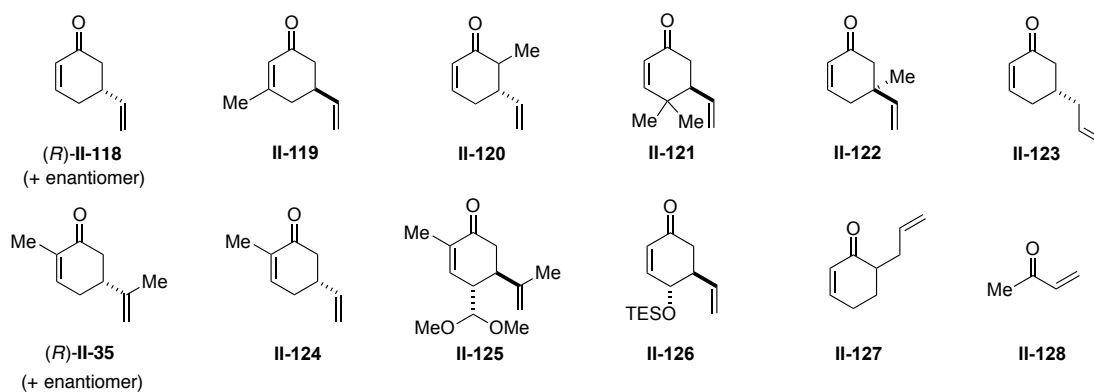


By simply engaging different starting materials, this strategy would deliver an array of polycyclic structures varying in substitution pattern and ring size. This modular approach exploiting two sequential powerful carbon–carbon bond forming reactions could provide rapid access to the core structures of a variety of natural product families with a wealth of biological activity, with some representative examples depicted in Scheme 2.20b.

2.4 Substrate preparation

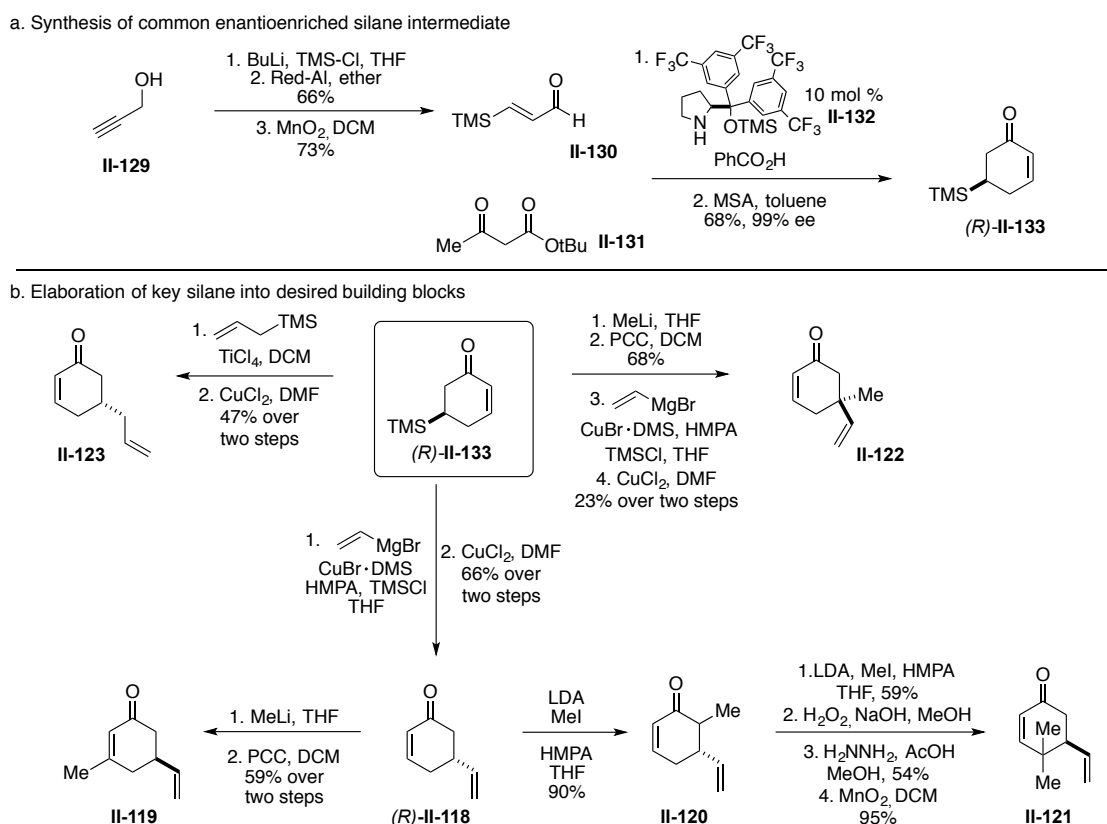
At the onset, we wished to synthesize a suite of cyclic building blocks which could be united through the designed approach in any number of combinations to provide an array of carbocyclic structures. We strategically elected to employ starting materials bearing enone functionality, as the unsaturation inherently allowed for regioselective enolate generation in the formation of the key silyl bis-enol ether intermediates (i.e. **II-110**). It was crucial for the success of the selective oxidative coupling that these starting substrates be prepared in enantiopure form, as racemic material would surely lead to mixtures of diastereomers. With these concerns in mind, a suite of building blocks was prepared for implementation in the strategy (Figure 2.1).

Figure 2.1 Suite of enone substrates



We imagined that known compound (*5R*)-trimethylsilylcyclohexenone **II-133**, readily prepared in enantiopure form by Jørgensen and coworkers through an organocatalytic Robinson annulation between (*E*)-3-trimethylsilyl-2-propenal **II-130** and *tert*-butyl acetoacetate **II-131** (Scheme 2.21a),²⁴⁶ could serve as a valuable common intermediate from which enones **II-118–II-123** could be assembled (Scheme 2.21b).^{247–249}

Scheme 2.21 Synthesis of substrates **II-118–II-123**

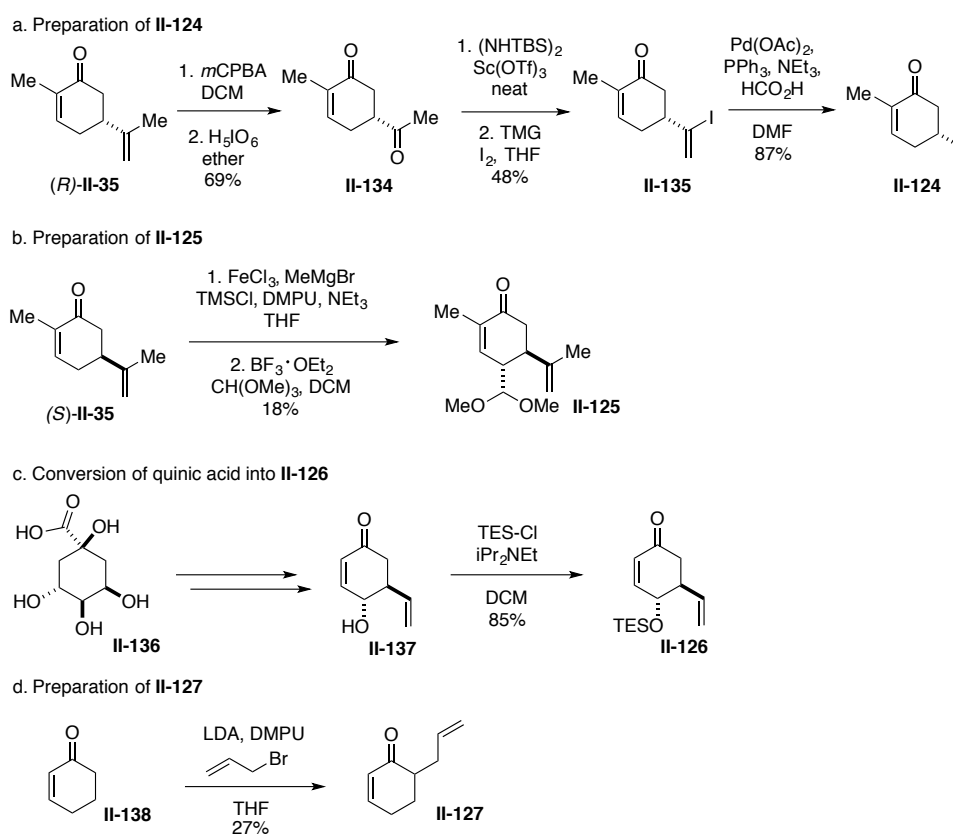


Through a simple vinyl conjugate addition to **II-133** followed by copper chloride-mediated elimination of the silane, parent vinyl substrate **II-118** was readily prepared. This intermediate could be converted to the 3-substituted variant **II-119** via a methyl lithium addition followed by a 1,3-oxidative transposition. Parent compound **II-118** could also be used to access α -methyl substrate **II-120** from a simple alkylation, and this compound could be converted to 4,4-*gem*-

dimethyl substrate **II-121** through a subsequent α -methylation, followed by epoxidation, Wharton transposition, and oxidation to the enone. Silane **II-133** could also be used to deliver allyl substituted **II-123** through a Sakurai reaction followed by copper chloride-mediated silane elimination. Alternatively, silane **II-133** was converted to substrate **II-122** containing a β -quaternary center, through a methyllithium addition to the ketone and 1,3-oxidative transposition, followed by a vinyl cuprate addition and copper chloride-mediated silane-eliminating sequence.

In addition to the key silane intermediate **II-133**, we imagined that commercially available (*R*)- and (*S*)-carvone (**II-35**) would not only be useful as substrates themselves but could also be further elaborated to produce desired enone building blocks (Scheme 2.22).

Scheme 2.22 Production of substrates **II-124–II-127**



For example, 2-substituted substrate **II-124** could be produced from (*R*)-carvone **II-35** through an epoxidation of the pendant olefin and subsequent oxidative cleavage to provide ketone **II-134**, followed by conversion to vinyl iodide **II-135** employing hydrazone chemistry developed in the Myers laboratory, which was converted to the target substrate with a palladium-mediated displacement (Scheme 2.22a).²⁵⁰⁻²⁵¹ (*S*)-carvone (*S*)-**II-35** was converted to 4-acetal-substituted enone **II-125** employing known conditions to generate the extended linear enolate and trapping with trimethyl orthoformate (Scheme 2.22b).²⁵² Commercially available (–)-quinic acid **II-136** was transformed to enone **II-137** according to Ventura and coworkers,²⁵³ which was protected as the triethyl silyl ether to produce substrate **II-126** (Scheme 2.22c). As shown in Scheme 2.22d, an allylation of cyclohexenone provided **II-127**.²⁵⁴ Finally, we envisioned that acyclic methylvinyl ketone **II-128** could be instrumental to the structural diversification of accessible scaffolds.

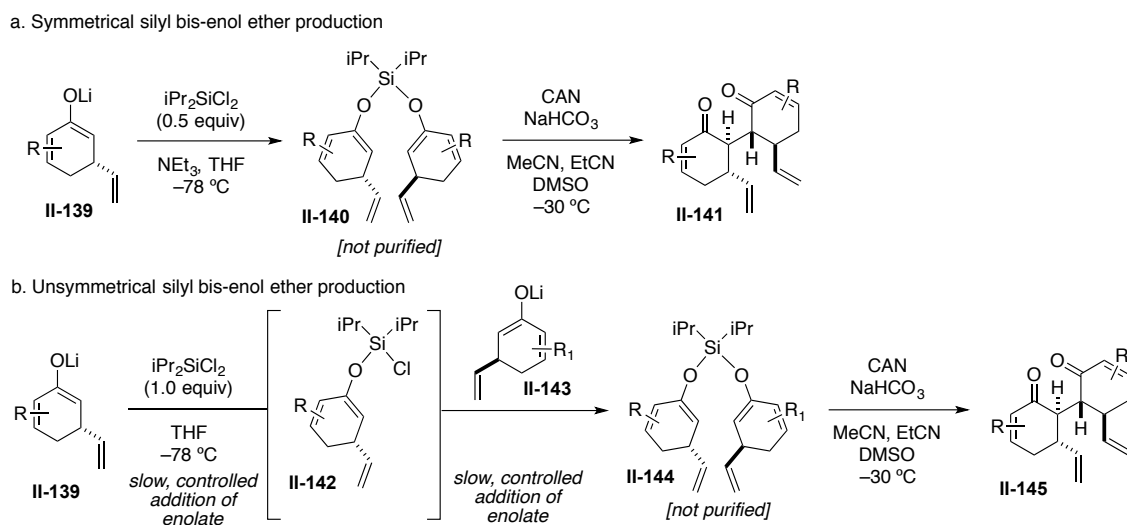
2.5 Realization of the couple and close strategy

2.5.1 Optimization of the process

With an array of enone building blocks in hand, we wished to explore the potential of the approach to unite these fragments and form a variety of phenanthrene-type core structures. As is depicted in Scheme 2.23a, and fully detailed within the Experimental Section (2.9), the preparation of the symmetrical silyl bis-enol ether intermediates (**II-140**) proceeded by the addition of the lithium enolate of the cyclic starting material (**II-139**) to 0.5 equivalents of $i\text{Pr}_2\text{SiCl}_2$ at $-78\text{ }^\circ\text{C}$. As shown in Scheme 2.23b, in order to access the unsymmetrical silyl bis-enol ethers (**II-144**), the lithium enolate of one coupling partner (**II-139**) was added in a slow and controlled manner to 1.0 equivalent of $i\text{Pr}_2\text{SiCl}_2$ at $-78\text{ }^\circ\text{C}$, providing intermittent chlorosilane **II-142**, followed by the slow addition of the second lithium enolate (**II-143**). Because the addition of a second enolate to the

intermittent monochloro enol silane species **II-142** is slower than the first addition to dichlorodiisopropylsilane, this protocol allows for the production of unsymmetrical silyl bis-enol ethers while minimizing symmetrical species.

Scheme 2.23 Silyl bis-enol ether preparation



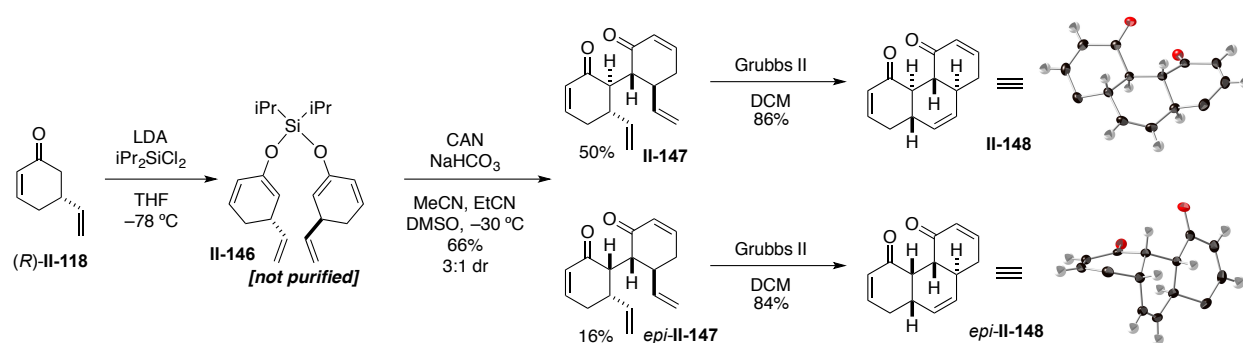
This streamlined process for unsymmetrical silyl bis-enol ether production was discovered to be most effective for these substrates without the inclusion of any additive, such as NEt_3 or DMPU. Direct subjecting of the unpurified silyl bis-enol ether intermediates to the subsequent coupling conditions was determined to be the optimal process for these substrates, employing 2.2 equivalents of single-electron oxidant CAN in the presence of 4.4 equivalents of sodium bicarbonate in a mixture of acetonitrile (ACN), propionitrile (EtCN), and DMSO at -30°C . As previous studies had illuminated, EtCN better enabled the solubility of the nonpolar silyl bis-enol ether for facile addition to the coupling reaction. In addition to formation of the desired coupled 1,4-diketone, hydrolysis of the silyl bis-enol ether to the starting enone substrates was shown to be a major reaction pathway under these conditions, particularly for substrates with greater steric congestion. Reducing the reaction temperature to -30°C (from the previously reported -10°C)

aided in diminishing this pathway but did not completely arrest the hydrolysis. Employment of organic bases such as 2,6-di-*tert*-butylpyridine, as opposed to the inorganic sodium bicarbonate, did not present any enhancement in yield. Additionally, other oxidants, such as $\text{Cu}(\text{OTf})_2$ and Cu_2O presented elevated hydrolysis compared to CAN. As the reaction takes place very quickly (~5 minutes) it was challenging to completely remedy this undesired hydrolysis, and the optimal conditions as described above were accepted. The ring-closing metathesis to fashion the final ring of the fused system was best achieved using 10 mol % Grubbs II in dichloromethane, providing superior conversion than Hoveyda-Grubbs II. This could be conducted smoothly at room temperature for the less sterically-hindered substrates, but required an elevation of temperature to 40 °C for the formation of trisubstituted olefins and larger rings (see Experimental Section 2.9).

2.5.2 Scaffolds constructed through the developed strategy

Initial proof of concept experiments focused on the preparation of the “parent” symmetrical system originating from the dimerization of enone **II-118**. As shown in Scheme 2.24, this vinyl enone underwent the oxidative coupling to provide a 3:1 mixture of coupled diastereomers in 66% overall yield (**II-147** and *epi*-**II-147**).

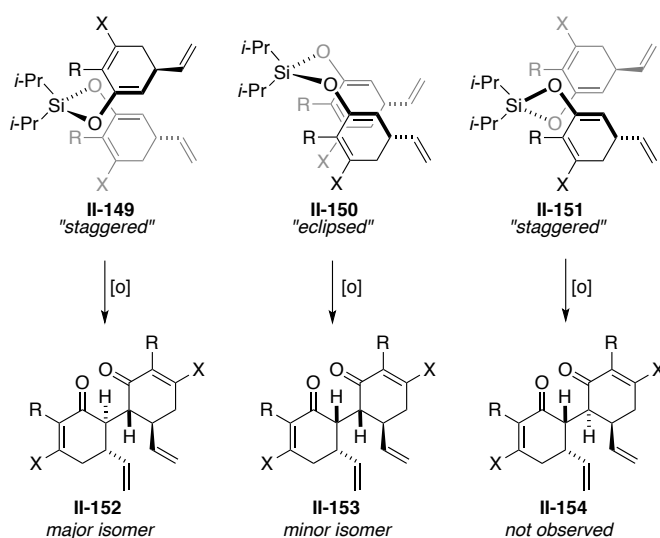
Scheme 2.24 Initial couple and close result



These diastereomers were readily separable by column chromatography, and were each independently subjected to the subsequent ring-closing metathesis, the products of which were both amenable to X-ray crystallography to determine the absolute structures. The major diastereomer from the coupling (**II-147**) underwent ring closure in 86% yield to fashion **II-148**, exhibiting the *trans-anti-trans* geometry about the ring junctions. Thus, fused tricyclic scaffold **II-148** was accessed from enone **II-118** in 43% yield over the three steps. The minor diastereomer (*epi-II-147*) underwent ring-closing in 84% to deliver *epi-II-148*, displaying the *cis-syn-trans* stereochemistry.

The demonstrated coupling preference for the *trans-anti-trans* geometry, as was indicated by simplified C2-symmetric NMR spectra and confirmed by X-ray analysis, is consistent with the stereochemical model previously developed within the group for the coupling of similar cyclic ketone substrates (see Scheme 2.13).²³⁵ As shown in Figure 2.2, this stereoselectivity is dictated by the conformational preference of the silicon tethered intermediate.

Figure 2.2 Model for coupling stereoselectivity



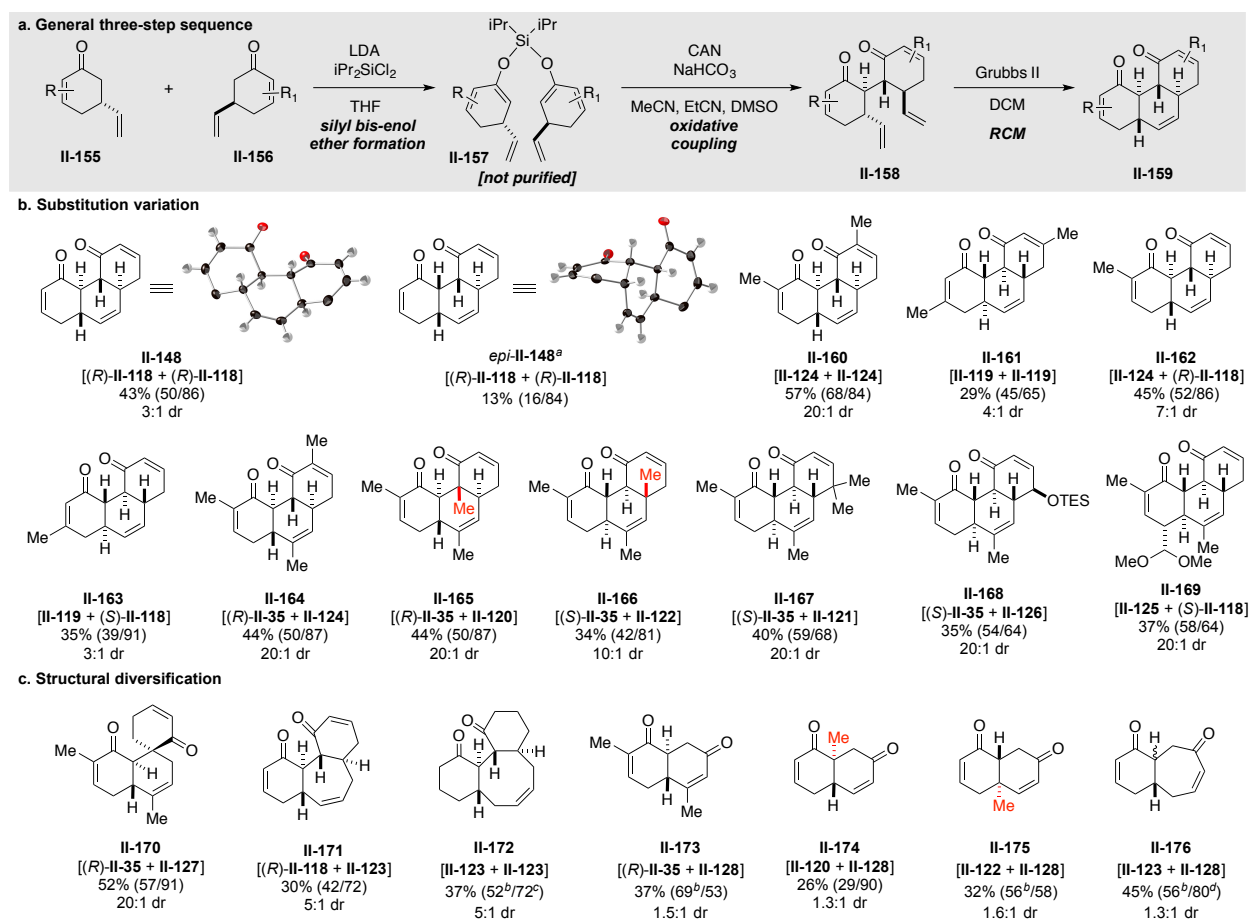
The “staggered” conformation **II-149**, leading to the major coupled product **II-152** (and then to closed product **II-148**), is preferred because the tether is orienting the cyclic substrates in such a way that minimizes destabilizing eclipsing interactions between the rings themselves, as well as allowing the new carbon–carbon bond to be formed opposite both β -substituents. In contrast, the “eclipsed” conformation **II-150**, which leads to the minor coupled product **II-153** (and then to *epi*-**II-148**), is disfavored because it experiences destabilizing interactions between the two ring fragments, as well as necessitating the bond formation to occur across the face of one β -substituent. The last conformation **II-151**, the product of which is not observed, is the highest in energy as it would require the new carbon–carbon bond to form across the face of both β -substituents.

With the established stereochemistry for the three-step process, a variety of fused tricyclic scaffolds were prepared from this sequence and are displayed in Figure 2.3, with the three-step yields provided and the individual yields for the major diastereomer from the oxidative coupling (two steps from the cyclic enones) and ring-closing metathesis steps shown in parentheses. The diastereoselectivities presented below the yields refer to the oxidative coupling step.

In further investigation of symmetrical systems, a marked enhancement in coupling selectivity was observed for enones bearing substitution in the 2-position of the enone, demonstrated by the 20:1 ratio of diastereomers that resulted from the dimerization of **II-124** in the preparation of scaffold **II-160**. This can be rationalized with the model in Figure 2.2, comparing the two relevant conformations **II-149** and **II-150** when R = Me. The destabilizing interactions between the two methyl substituents are exaggerated within conformation **II-150** leading to the diminished production of the minor product **II-153**. Furthermore, the additional instability of conformation **II-150** may be the consequence of the methyl substituents interacting

with the silicon tether. However, this augmentation of selectivity is not translated to the coupling of **II-119** bearing substitution in the 3-position, as its dimerization in the sequence to form **II-161** provided a 4:1 dr similar to the parent vinyl substrate. This result is more challenging to explain with simple models, but it is possible that the reduced proximity of the methyl substituents to the reacting center when X = Me is enough to attenuate the augmentation in selectivity observed when R = Me. Alternatively, the reduced proximity between the 3-methyl substituents and the silicon tether diminishes the potential for negative interaction between these groups, and thus lessens the extent to which conformer **II-150** is disfavored when X = Me as compared to when R = Me.

Figure 2.3 Scaffolds prepared from the developed three-step strategy



The value of the silicon tether to the dimerization of enones was definitively established through its ability to augment coupling diastereoselectivity relative to non-tethered reactions. For example, the dimerization of enone **II-124** by treating the lithium enolate with FeCl₃ as reported by Frazier and Harlow,²¹¹ resulted in a 3:1 mixture of diastereomers, whereas the silicon-tethered approach produced the 1,4-diketone in an enhanced 20:1 diastereomeric ratio. The capacity of the silicon tether to both enhance stereoselectivity and control the cross-coupling of ketones in a 1:1 ratio allowed us to generate a suite of more complex phenanthrene-type scaffolds (**II-162–II-169**).

Submission of enones (*R*)-**II-35** and **II-124** to the three-step sequence smoothly provided structure **II-164**, demonstrating that the preparation of trisubstituted olefins was well tolerated through this ring-closing with a simple elevation of temperature to 40 °C. Further emphasizing the utility of the silyl bis-enol ether method, the coupling of these two enones provided the 1,4-diketone intermediate in 50% yield and 20:1 dr, whereas treatment of a 1:1 mixture of the corresponding lithium enolates with FeCl₃ generated a complex mixture of inseparable dimeric and cross-coupled products.

Oxidative coupling in sterically-demanding environments is known to be challenging, particularly for the formation of a new carbon–carbon bond that produces a quaternary center. As such, we were pleased that this method enabled the facile production of tricyclic structure **II-165** in 44% from enones (*R*)-**II-35** and **II-120**, setting an α -methyl quaternary center through the oxidative coupling. Moreover, this angular methyl substitution pattern is common to many terpene natural products, providing added value to the strategy's ability to prepare **II-165**. The approach also proved to be tolerant of preexisting quaternary centers, allowing the union of enone (*S*)-**II-35** with **II-122** to form scaffold **II-166** containing a quaternary center in the β -position. As

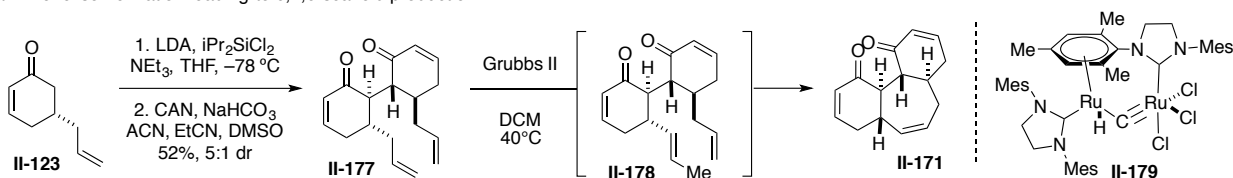
substitution in the 4-position is prevalent in numerous natural product families, we investigated the potential for our strategy to incorporate the ubiquitous 4,4-*gem*-dimethyl motif. The successful formation of scaffold **II-167** in 40% yield over three steps (20:1 dr) further supported the ability for the approach to withstand fairly sterically-congested environments. The ring-closing metathesis to access this structure did prove to be much more challenging due to the steric congestion, requiring elevated catalyst loading. The incorporation of alternative functional groups in the 4-position was successful by engaging enones (*S*)-**II-35** and **II-126** to access protected alcohol **II-168**, and employing enones **II-125** and (*S*)-**II-118** to deliver masked aldehyde **II-169**. Both of these functionalities could be efficiently unveiled, as detailed in the Experimental Section **2.9**.

In an effort to diversify the carbocyclic composition of the accessible scaffolds, we examined the preparation of structures outside of the 6,6,6-phenanthrene core. For example, by engaging (*R*)-**II-35** with enone **II-127** where the olefin-containing substituent was elongated to an allyl group and relocated to the α -position, spirocyclic scaffold **II-170** could be produced in 52% yield over three steps. The intermediate 1,4-diketone (generated in 20:1 dr) was amenable to X-ray analysis in order to definitively assign the stereochemical structure (see Experimental Section **2.9**). Alternatively, enone **II-123**, where the elongated allyl substituent was repositioned back to the usual β -position, could be united with parent enone (*R*)-**II-118** to achieve the 6,7,6-tricyclic core **II-171** in 30% yield over three steps. We imagined that this approach could be applied to access the 6,8,6-fused system as well through the dimerization and subsequent RCM of allyl-substituted enone **II-123**. Although the oxidative coupling of this substrate achieved **II-177** in 52% with 5:1 dr (Scheme 2.25a), the RCM of this material at room temperature solely resulted in

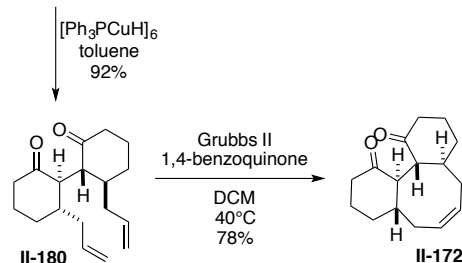
unchanged starting material. As shown in Scheme 2.25a, when this RCM was conducted at 40 °C, however, the previously intentionally isolated 6,7,6-fused product **II-171** was produced rather than the desired scaffold with the 8-membered center ring.

Scheme 2.25 Formation of the 6,8,6-fused system

a. Alkene isomerization leading to 6,7,6-scaffold production



b. Selective enone reduction allows for successful 6,8,6-ring closure



This result can be rationalized by the known propensity for alkene isomerization to occur under these ring-closing conditions (i.e. isomerization to **II-178**). As reported by Grubbs and coworkers, the Grubbs II catalyst can decompose to a ruthenium hydride species **II-179** that has been implicated in the promotion of this isomerization pathway.²⁵⁵⁻²⁵⁶ The group discovered additives to suppress this reactivity by scavenging the deleterious ruthenium hydride, and although inclusion of additive 1,4-benzoquinone successfully arrested production of the 6,7,6-product **II-171**, the formation of the desired 6,8,6-system was not achieved as only unchanged starting material was recovered. We imagined that the numerous sp²-hybridized atoms within the desired fused tricyclic product may cause a level of conformational strain that inhibits closure of the 8-membered ring. Thus, as shown in Scheme 2.25b, the enone functionality within the coupled product **II-177** was selectively reduced with Stryker's reagent to afford the saturated bicyclic intermediate **II-180**. To

our delight, this 1,4-diketone successfully underwent ring-closure to deliver the 6,8,6-core structure **II-172** in 78% yield with no observed alkene isomerization (37% over four steps from enone **II-123**).

Aside from the production of various tricyclic species, we imagined that by employing acyclic methylvinyl ketone **II-128** in the strategy, rapid access to bicyclic structures similar to the Wieland-Miescher ketone could be achieved. As discussed in Section 1.4, these types of intermediates have proven to be extremely useful for the synthesis of many natural products. The success of this aim was demonstrated through the union of (*R*)-**II-35** and methylvinyl ketone **II-128** to form **II-173** in good yields, however the oxidative coupling proceeded with greatly diminished levels of stereocontrol. Nevertheless, this approach could be engaged to access bicyclic species containing quaternary centers in the α -position (**II-174**) and β -position (**II-175**), as well as the ring-expanded 6,7-bicyclic system (**II-176**).

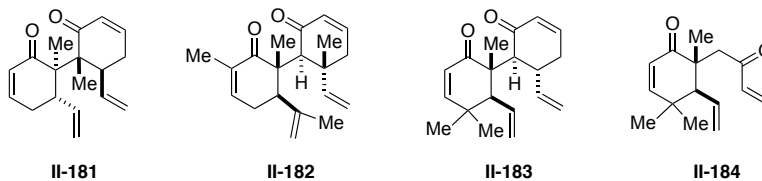
2.5.3 *Challenging systems for the strategy*

2.5.3.1 *Sterically-demanding oxidative coupling*

While the oxidative coupling of enones proved to be tolerant of a number of sterically-challenging substrates (Figure 2.3) the developed conditions were not conducive to the formation of other desired substitution patterns prevalent in nature (Figure 2.4). The attempted preparation of **II-181** through the dimerization of enone **II-120** led exclusively to aromatized products that displayed no ketones in the ^{13}C NMR spectrum of the crude material, and were difficult to separate and characterize. The oxidative coupling to produce **II-182** with two quaternary centers led to hydrolysis to the starting enones, and a complex mixture of products that could not be purified and characterized. Likewise, the attempted coupling to produce scaffolds containing both a *gem*-

dimethyl motif and an α -methyl quaternary center, such as **II-183** and **II-184**, resulted in significant hydrolysis as well as a complex mixture of compounds that could not be purified. However, one of the main products in both of these reactions was the same, and although it could not be purely isolated and characterized, this suggests a reaction pathway involving the *gem*-dimethyl-containing monomer. New coupling conditions must be investigated in order to access these desirable substitution patterns.

Figure 2.4 Inaccessible scaffolds due to unsuccessful oxidative coupling

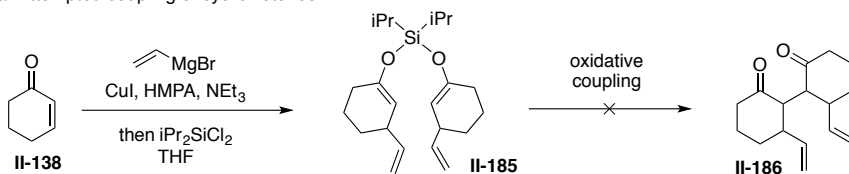


2.5.3.2 Saturated ketone coupling

Although the enone functionality within the starting substrates was valuable to enable selective enolate generation for silyl bis-enol ether production, initial experiments to probe the coupling of saturated analogues were explored. As shown in Scheme 2.26a, a vinyl conjugate addition to cyclohexenone **II-138** and trapping with 0.5 equivalents of dichlorodiisopropylsilane provided the racemic silyl bis-enol ether intermediate, which was subjected to a variety of oxidative coupling conditions. These initial experiments uncovered a potential conformational requirement for enone unsaturation to allow the coupling of compounds with substitution in the β -position. Rather than forming the desired carbon–carbon bond, each set of conditions shown in Scheme 2.26a provided a mixture of vinyl cyclohexanone, and the corresponding vinyl cyclohexenone material. The continued investigation of such saturated systems is required to better understand this apparent additional conformational challenge and how it may be remedied.

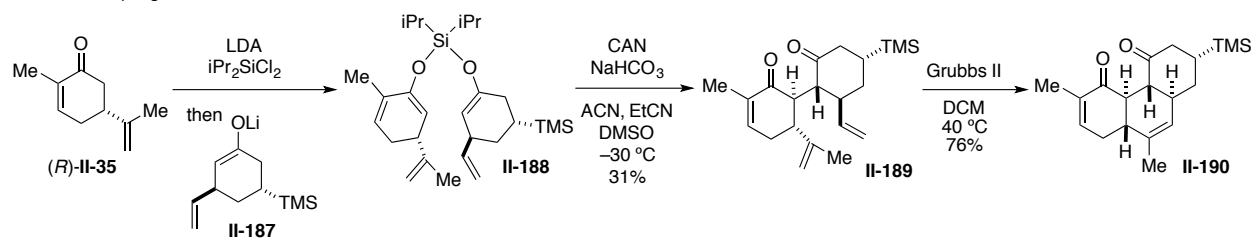
Scheme 2.26 Coupling of saturated systems

a. Attempted coupling of cyclic ketones



Entry	Conditions
1	CAN, NaHCO ₃ , ACN, EtCN, DMSO
2	CAN, NaHCO ₃ , ACN, EtCN
3	CAN, DTBP, ACN, EtCN, DMSO
4	Mn(hfac) ₃ , benzene
5	Cu(OTf) ₂ , Cu ₂ O, ACN, EtCN

b. Cross-coupling between enone **II-35** and an enantioenriched, saturated ketone



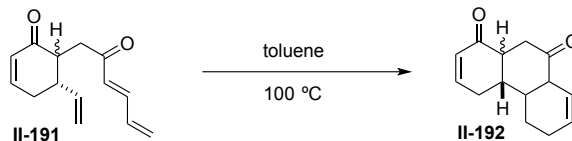
It was discovered, however, that the cross-coupling of unsymmetrical silyl bis-enol ether **II-188**, derived from carvone (*R*)-**II-35** and enantioenriched enolate **II-187**, provided the coupled product **II-189** in 31% yield employing the optimal coupling conditions developed for the strategy above (Scheme 2.26b). Although this half-saturated system resulted in significant hydrolysis to the individual starting enones, the coupled product was produced, albeit in a lower yield over the two steps than was typical for the coupling of two similar enones. This coupled product underwent successful ring-closing metathesis in 76% yield to form tricyclic compound **II-190**.

2.5.3.3 Alternative methods for ring closure

We imagined that the couple and close approach could be amenable to alternative closure opportunities outside of ring-closing metathesis. As shown in Scheme 2.27, initial efforts sought to access coupled product, **II-191**, which would be potentially poised to undergo an intramolecular

Diels–Alder cycloaddition to fashion the fused tricyclic ring system (**II-192**). Unfortunately, however, the electronic character of this particular system was not favorable enough to promote a thermal Diels–Alder reaction, providing unreacted starting material and decomposition after prolonged exposure to heat. The continued exploration of this approach certainly deserves further attention as an alternative means to construct fused polycyclic scaffolds employing an initial oxidative coupling.

Scheme 2.27 Attempted Diels–Alder to fashion the fused ring system

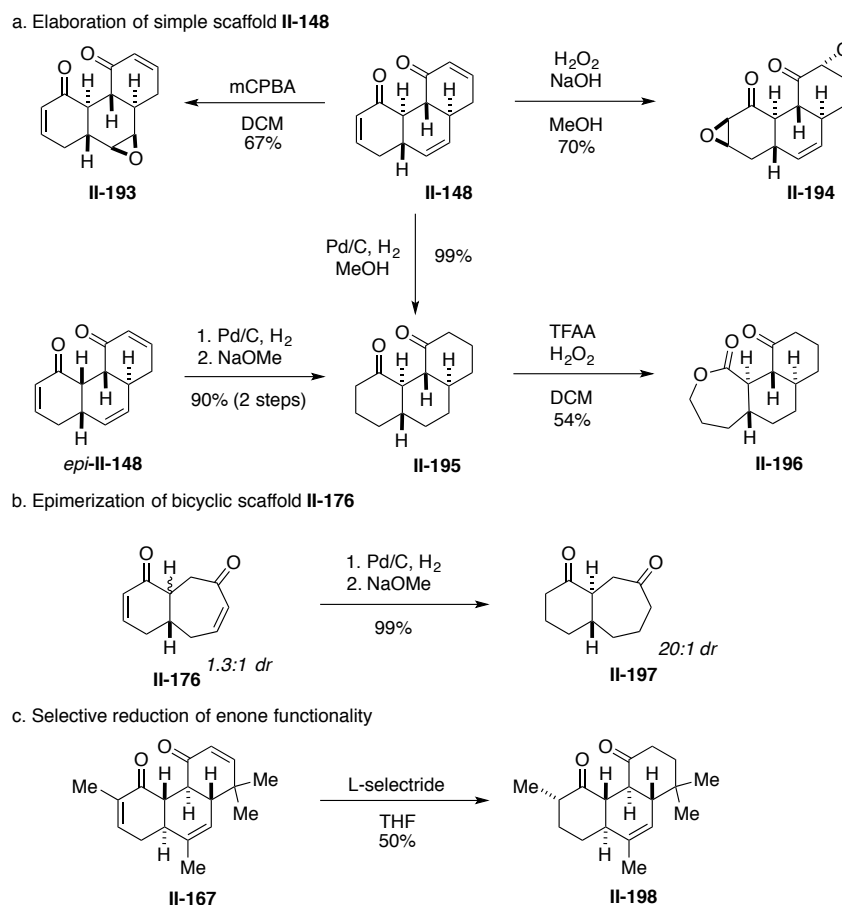


2.6 Selective functionalization of prepared substrates

We wished to further display the utility of the developed strategy to complex molecule synthesis by demonstrating selective manipulations of the prepared scaffolds. As shown in Scheme 2.28a, scaffold **II-148** underwent complementary epoxidation strategies, delivering monoepoxide **II-193** when treated with *m*CPBA, or bis(epoxide) **II-194** when exposed to nucleophilic epoxidation conditions with hydrogen peroxide and sodium hydroxide. A global hydrogenation of scaffold **II-148** resulted in saturated **II-195**, which underwent a Baeyer–Villiger reaction to form lactone **II-196**. Notably, it was discovered that the scaffold resulting from the minor diastereomer of the oxidative coupling reaction, *epi*-**II-148**, could be epimerized to the more thermodynamically favorable all-*trans* configuration (**II-195**) through an initial global hydrogenation and subsequent exposure to base. This epimerization protocol was successfully applied to the bicyclic scaffold **II-176**, converging on the *trans*-fused **II-197** (Scheme 2.28b). This valuable development

demonstrated that substrates exhibiting poor selectivity through the oxidative coupling can later be epimerized to furnish the all-*trans* products. Finally, selective reduction of the enone functionality within scaffold **II-167** was conducted without disturbing the isolated alkene upon treatment with L-selectride, delivering reduced scaffold **II-198** (Scheme 2.28c).

Scheme 2.28 Elaboration of prepared scaffolds

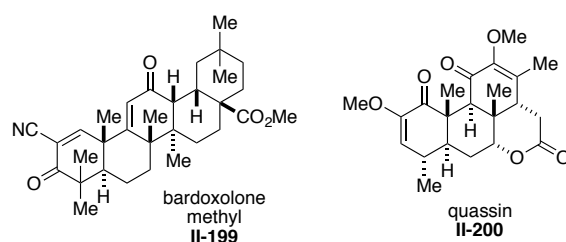


2.7 Investigation of the bioactivity of the prepared compounds

As an overarching goal for this project was to develop a convergent strategy to enable the increased availability of complex structures prevalent in bioactive natural products to supplement

drug discovery efforts, we wished to investigate the potential bioactivities of the prepared compounds. Our suite of compounds seemed to be structurally related to triterpenoid barboxolone methyl (**II-199**, Figure 2.5), which underwent a Phase 1 clinical trial as a potential therapeutic for solid tumors and lymphoma,²⁵⁷⁻²⁵⁸ and to quassin (**II-200**), which belongs to the quassinoid family of antineoplastic natural products.²⁵⁹

Figure 2.5 Anticancer compounds with similar carbocyclic cores containing enones



These structural similarities inspired us to investigate the potential anticancer activity of the compounds, screening a selection of scaffolds for activity against five tumor cell lines in collaboration with Dr. Irawati Kandela in the Developmental Therapeutics Core at Northwestern. As detailed in Table 2.1, cell viability studies were conducted at 1 mM concentrations against colon (HT29), prostate (PC-3), cervix (HeLa), breast (MDA-MB-231), and metastatic breast (MDA-MB-231-LM24) tumor cell lines.

The results establish a distinct difference in activity between those compounds containing enone functionality compared to their saturated counterparts (i.e. **II-148** vs. **II-195** and **II-167** vs. **II-198**). However, the IC_{50} values for two of the most active compounds, **II-170** and **II-167**, against MDA-MB-231 cells were 40.4 μ M and 185 μ M, respectively, demonstrating a relatively low activity. Moreover, a selection of the most active enone-containing compounds (**II-148**, **II-167**, **II-170**, and **II-193**) displayed the same activity against non-tumorigenic MCF10A cells as against

the tumor cells, showing no selectivity in their cytotoxic action. Notably, the bis(epoxide) **II-194** presented cytotoxic activity despite lacking the enone functionality present within the other active compounds, however the IC₅₀ value for this compound against MDA-MB-231-LM24 proved to be just 200 μ M. This bis(epoxide) **II-194**, however, did display a difference in activity between the tumor cell lines and the non-tumorigenic cell line, with a high IC₅₀ value of 3100 μ M against the “normal” MCF10A cells. These results established that certain prepared compounds possess some cytotoxic activity, but would require much optimization to obtain relevant levels of potency.

Table 2.1 Cell Assay Results

Compound	Percent Cell Viability of Treated Cell Lines at 1.0 mM					
	HT29	PC-3	HeLa	MDA-MB-231	MDA-MB-231-LM24	MCF10A
II-148	2	0	4	26	2	1
II-195	51	77	13	75	60	ND
II-160	1	72	46	69	67	ND
II-161	66	63	40	11	54	ND
II-165	1	1	0	0	0	ND
II-166	31	11	2	43	10	ND
II-167	0	0	0	0	0	4
II-198	64	77	41	53	55	ND
II-170	0	0	3	1	0	4
II-171	0	0	21	6	1	ND
II-174	0	1	0	2	16	ND
II-175	8	2	22	62	26	ND
II-193	0	0	2	26	3	5
II-194	1	1	0	25	0	70
DMSO	100	100	100	100	100	100

2.8 Conclusion

We have developed a convergent and modular strategy for the construction of fused polycyclic structures with three-dimensional complexity through a sequence of powerful carbon–

carbon bond forming reactions. The flexible approach enabled the preparation of several polycyclic scaffolds with facile variation of substitution pattern and structural composition. Selective manipulations of the prepared scaffolds demonstrated the value of this approach to complex molecule synthesis, and as such, exhibited the potential for the strategy to uncover novel compounds with desirable bioactivities.²⁶⁰

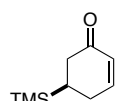
2.9 *Experimental Section*

2.9.1 *General information*

All reactions were carried out under a nitrogen atmosphere in flame-dried glassware with magnetic stirring unless otherwise stated. Methanol, THF, ether and DCM were purified by passage through a bed of activated alumina.²⁶¹ Reagents were purified prior to use unless otherwise stated following the guidelines of Armarego and Chai.²⁶² Purification of reaction products was carried out by flash chromatography using SiliCycle silica gel F60, 40-63 μm (230-400 mesh). Analytical thin layer chromatography was performed on EM Reagent 0.25 mm silica gel 60-F plates. Visualization was accomplished with UV light and *p*-anisaldehyde stain. Germanium ATR infrared spectra were recorded using a Bruker Tensor 37. ¹H-NMR spectra were recorded on a Varian Inova 500 (500 MHz), Agilent DD2 (500MHz), Agilent DD MR-400 (400MHz), or Bruker Advance III 500 (500 MHz) spectrometer and are reported in ppm using solvent as an internal standard (CDCl₃ at 7.26 ppm). Data are reported as (app = apparent, obs = obscured, s = singlet, d = doublet, t = triplet, q = quartet, p = pentet, h = hextet, sep = septet, o = octet, m = multiplet, b = broad; integration; coupling constant(s) in Hz. ¹³C-NMR spectra were recorded on a Bruker Advance III 500 spectrometer equipped with DCH CryoProbe, and are reported in ppm using solvent as an internal standard (CDCl₃ at 77.16 ppm, except where noted). Mass spectra data were

obtained on an Agilent 6210 Time-of-Flight LC/MS. All optical rotation measurements were obtained on a Rudolph Research Analytical Autopol IV, Serial #82239. X-ray data were collected on the Kappa Apex 2 diffractometer.

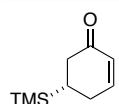
2.9.2 Starting material experimental procedures and characterization data



Compound (R)-II-133.

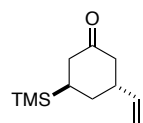
The common enantioenriched silane intermediate was prepared as reported by Jørgensen and coworkers.²⁴⁶ The proline-derived catalyst (*S*)- α,α -Bis[3,5-bis(trifluoromethyl)phenyl]-2-pyrrolidinemethanol trimethylsilyl ether **II-132** (1.74 g, 2.92 mmol, 10 mol %), PhCO₂H (0.360 g, 2.92 mmol, 10 mol %), and toluene (10 mL) were added to a flame-dried 250 mL round-bottom flask. **II-130** (3.75 g, 29.2 mmol, 1.0 equiv) in toluene (4 mL) was added via cannula (1 mL toluene rinse), followed by **II-131** (7.14 mL, 43.8 mmol, 1.5 equiv). The yellow reaction was allowed to stir at room temperature for 20 hours, after which toluene (97 mL) and methanesulfonic acid (0.664 mL, 10.2 mmol, 35 mol %) were added and the mixture heated to 90 °C for 40 minutes. The red-orange mixture was cooled to room temperature, diluted with water, and extracted with ether. The combined organic layers were dried over MgSO₄ and the solvent evaporated under reduced pressure. The crude orange oil was purified by flash chromatography on silica gel using a 5% ether/pentane to 20% ether pentane gradient, yielding a yellow oil (3.40 g, 20.0 mmol, 68%). This procedure was scalable to 12.5 g **S1** to provide a 59% yield. ¹H NMR (499 MHz, Chloroform-*d*) δ 7.03 (ddd, *J* = 10.1, 5.6, 2.4 Hz, 1H), 6.00 (ddt, *J* = 10.1, 2.6, 1.1 Hz, 1H), 2.43 (ddt, *J* = 16.5, 3.9, 1.3 Hz, 1H), 2.32 (dddd, *J* = 19.0, 5.8, 4.7, 1.3 Hz, 1H), 2.27 – 2.13 (m, 2H), 1.47 – 1.40 (m, 1H), 0.03 (s, 9H); ¹³C NMR (126 MHz, CDCl₃) δ 200.4,

151.7, 129.5, 38.7, 26.9, 23.3, -3.6. The ee was determined by HPLC to be 99%, as reported in the literature. All spectroscopic data for this compound agrees with previously reported values.²⁴⁶



Compound (S)-II-133.

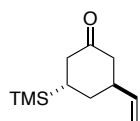
This compound was prepared as described for (*R*)-II-133 above, according to Jørgensen and coworkers, using the (*R*)-enantiomer of the catalyst. All spectroscopic data for this compound agrees with previously reported values.²⁴⁶



Compound (R)-II-201

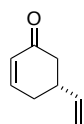
Freshly prepared and titrated vinyl Grignard (0.79 M, 16.5 mL, 13.0 mmol, 2.0 equiv) and THF (38 mL) were added to a flame-dried 100 mL round-bottom flask. The mixture was cooled to -78 °C, and CuBr•DMS (0.27 g, 1.3 mmol, 20 mol %) and HMPA (2.3 mL, 13.0 mmol, 2.0 equiv) were added. After stirring at this temperature for 1 hour, (*R*)-II-133 (1.1 g, 6.5 mmol, 1.0 equiv) in THF (1 mL) and TMS-Cl (2.5 mL, 19.5 mmol, 3.0 equiv) was added via cannula dropwise over 10 minutes (0.5 mL THF rinse). After 40 minutes, the reaction was warmed to room temperature. Upon observed consumption of starting material (~2 hours) the black reaction was quenched with 1 M HCl, allowing the mixture to stir for 10 minutes, after which it was extracted with ether. The combined organic layers were washed with brine, dried over MgSO₄, and the solvent evaporated under reduced pressure. The crude material was purified by flash chromatography using silica gel with a 5% ether/pentane to 10% ether/pentane gradient, yielding a yellow oil (1.0 g, 5.1 mmol, 78%): [α]_D = +90.3 (*c* 0.088, CHCl₃); IR (Germanium ATR): 2954, 1710, 1249, 838 cm⁻¹; ¹H NMR (500 MHz, Chloroform-*d*) δ 5.78 (ddd, *J* = 17.4, 10.7, 5.5 Hz, 1H), 5.10 (dt, *J* = 10.7, 1.5 Hz, 1H), 5.05 (dt, *J* = 17.4, 1.5 Hz, 1H), 2.99 (dtt, *J* = 7.7, 3.7, 1.8 Hz, 1H), 2.57 – 2.42 (m, 2H), 2.28 (ddt, *J* = 14.3, 3.7, 1.8 Hz, 1H), 2.10 (td, *J* = 14.3, 13.3, 0.9 Hz,

1H), 1.87 – 1.68 (m, 2H), 1.29 (ddt, $J = 13.3, 12.1, 4.0$ Hz, 1H), -0.00 (s, 9H); ^{13}C NMR (126 MHz, CDCl_3) δ 212.2, 140.5, 115.8, 45.0, 42.3, 41.0, 30.7, 21.7, -3.5 ; HRMS (ESI): Exact mass calc'd for $\text{C}_{11}\text{H}_{21}\text{OSi}$ $[\text{M}+\text{H}]^+$, 197.1362. Found 197.1355. All spectroscopic data for this compound agrees with previously reported values.²⁶³



Compound (S)-II-201.

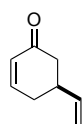
This compound was prepared using the same procedure as for the preparation of (*R*)-**II-201** detailed above. (*S*)-**II-133** (3.05 g, 18.1 mmol) was converted to (*S*)-**II-201** (1.93 g, 9.83 mmol, 55% yield). All NMR, IR, and HRMS data is identical to (*R*)-**II-201**. $[\alpha]_{\text{D}} = -83.5$ (c 0.62, CHCl_3).



Compound (R)-II-118.

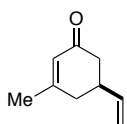
Copper-mediated elimination of the silane was achieved with conditions reported by Corey and coworkers.²⁴⁷ CuCl_2 (2.1 g, 15.3 mmol, 3.0 equiv) was added to a flame-dried 100 mL round-bottom flask outfitted with a reflux condenser. (*R*)-**II-201** (1.0 g, 5.0 mmol, 1.0 equiv) in DMF (35 mL, with an additional 3 mL rinse) was added via cannula and the reaction was heated to 55 °C for 2 hours. The green reaction was cooled to room temperature, diluted with water, and extracted with pentane twice and 5% ether/pentane once. The combined organic layers were dried over MgSO_4 and the solvent removed under reduced pressure carefully due to the volatility of the product. The crude material was purified by flash chromatography with silica gel using 20% ether/pentane, yielding a yellow oil (522 mg, 4.3 mmol, 85%): $[\alpha]_{\text{D}} = -47.6$ (c 0.32, CHCl_3); IR (Germanium ATR): 3081, 2886, 1677, 1642, 1388, 918 cm^{-1} ; ^1H NMR (500 MHz, Chloroform-*d*) δ 6.97 (ddd, $J = 10.1, 5.5, 2.8$ Hz, 1H), 6.13 – 5.97 (m, 1H), 5.83 (ddd, $J = 17.0, 10.4, 6.4$ Hz, 1H), 5.15 – 4.98 (m, 2H), 2.81 (dddd, $J = 15.0, 10.3, 7.4, 4.6$ Hz, 1H), 2.57 (dd, $J = 16.3, 4.1$ Hz, 1H),

2.54 – 2.46 (m, 1H), 2.31 (dd, $J = 16.2, 12.3$ Hz, 1H), 2.24 (ddt, $J = 18.7, 9.9, 2.7$ Hz, 1H); ^{13}C NMR (126 MHz, CDCl_3) δ 199.2, 149.3, 140.3, 130.0, 114.8, 43.6, 38.8, 31.8; HRMS (ESI): Exact mass calc'd for $\text{C}_8\text{H}_{11}\text{O}$ $[\text{M}+\text{H}]^+$, 123.0810. Found 123.0801. The ee was determined to be 99% by HPLC on a Chiralpak-As-H column running 2% iPrOH in hexanes with a flow rate of 1.0 mL/min All spectroscopic data for this compound agrees with previously reported values.²⁶³



Compound (S)-II-118.

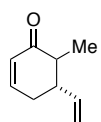
This compound was prepared using the same procedure as for the preparation of (*R*)-**II-118**. (*S*)-**II-201** (1.9 g, 9.7 mmol) was converted to (*S*)-**II-118** (541.7 mg, 4.43 mmol, 46%). All NMR, IR, and HRMS data is identical to (*R*)-**II-118**. $[\alpha]_{\text{D}} = +41.4$ (c 0.38, CHCl_3).



Compound II-119.

(*R*)-**II-118** (400 mg, 3.27 mmol, 1.0 equiv) was diluted with THF (6.5 mL, 0.5M) in a flame-dried 25 mL round-bottom flask. The solution was cooled to -78 °C and a solution of MeLi (1.6 M, 3.1 mL, 4.90 mmol, 1.5 equiv) was added dropwise. The reaction was warmed to 0 °C and then slowly allowed to warm to room temperature in the ice bath. After observed consumption of the starting material by TLC (2.5 hours), the yellow mixture was quenched with water, and extracted with ether. The combined organic layers were washed with brine, dried over MgSO_4 and the solvent evaporated under reduced pressure. The crude material was used directly in the next reaction. To a flame-dried 25 mL round-bottom flask was added PCC (1.4 g, 6.54 mmol, 2.0 equiv), DCM (13 mL), and 0.3 g silica gel. The crude alcohol in DCM (1 mL) was added via cannula at room temperature (0.3 mL DCM rinse). The solution turned dark brown upon addition. Following the observed consumption of starting material by TLC (3 hours), the brown mixture was filtered through a mixture of Celite and silica gel with 50% ether/pentane and the solvent

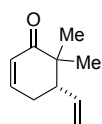
evaporated under reduced pressure carefully due to the volatility of the product. The crude material was purified by flash chromatography on silica gel with 10% to 15% ether/pentane to yield a slight yellow oil (264 mg, 1.94 mmol, 59% over two steps): $[\alpha]_D = +60.7$ (c 0.6, CHCl_3); IR (Germanium ATR): 3081, 2979, 1664, 1380, 912 cm^{-1} ; ^1H NMR (400 MHz, Chloroform- d) δ 5.93 – 5.87 (m, 1H), 5.82 (ddd, $J = 17.1, 10.4, 6.4$ Hz, 1H), 5.12 – 5.02 (m, 2H), 2.84 – 2.71 (m, 1H), 2.54 – 2.45 (m, 1H), 2.37 (dd, $J = 18.1, 4.8$ Hz, 1H), 2.28 – 2.16 (m, 2H), 1.98 (d, $J = 1.4$ Hz, 3H); ^{13}C NMR (126 MHz, CDCl_3) δ 199.1, 161.4, 140.4, 126.7, 114.7, 76.9, 42.6, 38.7, 37.0; HRMS (ESI): Exact mass calc'd for $\text{C}_9\text{H}_{13}\text{O}$ $[\text{M}+\text{H}]^+$, 137.0966. Found 137.0959.



Compound II-120.

A solution of LDA was prepared by adding diisopropylamine (0.169 mL, 1.2 mmol, 1.4 equiv) and THF (4 mL) to a flame-dried 25 mL round-bottom flask. The solution was cooled to -78 °C and $n\text{-BuLi}$ (1.9 M, 0.56 mL, 1.1 mmol, 1.3 equiv) was added. After 10 minutes at this temperature, (*R*)-**II-118** (100 mg, 0.82 mmol, 1.0 equiv) in THF (0.8 mL) was added via cannula (0.2 mL THF rinse). This mixture stirred for 30 minutes before adding Me-I (0.10 mL, 1.6 mmol, 2.0 equiv). This resulting mixture was allowed to stir at -78 °C for 40 minutes before adding HMPA (0.47 mL, 2.7 mmol, 3.3 equiv). The reaction was kept at this temperature for 2 hours before warming to room temperature. Upon the observed consumption of starting material by TLC (after 1 h at room temperature), the yellow reaction was quenched with saturated NH_4Cl solution and extracted with ether. The combined organic layers were dried over MgSO_4 and the solvent evaporated under reduced pressure carefully due to volatility of the product. The crude material was purified by flash chromatography on silica gel with 15% ether/pentanes, yielding a yellow oil as a mixture of diastereomers. This lack of selectivity is insignificant for our purposes, as formation

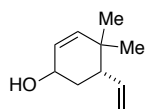
of the silyl bis-enol ether destroys the stereochemistry at that alpha position (101 mg, 0.74 mmol, 90%, the ^1H NMR spectrum shows minor impurities from grease, but due to the volatility of the compound, it was not purified further): IR (Germanium ATR): 2928, 1678, 1389, 916 cm^{-1} ; ^1H NMR (499 MHz, Chloroform-*d*) δ 6.94 – 6.86 (m, 2H), 6.06 – 5.97 (m, 2H), 5.76 (dddd, $J = 21.7$, 17.8, 10.3, 7.7 Hz, 2H), 5.15 – 5.04 (m, 4H), 2.85 (s, 1H), 2.62 – 2.50 (m, 2H), 2.49 – 2.38 (m, 3H), 2.38 – 2.30 (m, 1H), 2.30 – 2.22 (m, 1H), 1.12 (d, $J = 6.7$ Hz, 3H), 1.05 (d, $J = 7.1$ Hz, 3H); ^{13}C NMR (126 MHz, CDCl_3) δ 202.5, 201.3, 148.1, 147.9, 140.3, 137.6, 129.5, 129.1, 116.7, 116.2, 46.8, 46.2, 45.5, 43.4, 32.4, 29.5, 12.9, 11.5; HRMS (ESI): Exact mass calc'd for $\text{C}_9\text{H}_{13}\text{O}$ $[\text{M}+\text{H}]^+$, 137.0966. Found 137.0957.



Compound II-202.

A solution of LDA was prepared by adding diisopropylamine (0.108 mL, 0.77 mmol, 1.4 equiv) and THF (2.5 mL) to a flame-dried 10 mL round-bottom flask. The solution was cooled to -78 $^{\circ}\text{C}$ and *n*-BuLi (2.24 M, 0.32 mL, 0.72 mmol, 1.3 equiv) was added. After 10 minutes at this temperature, **II-120** (75 mg, 0.55 mmol, 1.0 equiv) in THF (0.5 mL) was added via cannula (0.4 mL THF rinse). This mixture stirred for 50 minutes before adding Me-I (69 μL , 1.1 mmol, 2.0 equiv). This resulting mixture was allowed to stir at -78 $^{\circ}\text{C}$ for 40 minutes before adding HMPA (0.32 mL, 1.8 mmol, 3.3 equiv). The reaction slowly warmed to room temperature overnight. The orange reaction was quenched with saturated NH_4Cl solution and extracted with ether. The combined organic layers were dried over MgSO_4 and the solvent evaporated under reduced pressure carefully due to volatility of the product. The crude material was purified by flash chromatography on silica gel with 5% ether/pentanes, yielding a yellow oil (49 mg, 0.33 mmol, 59%): $[\alpha]_{\text{D}} = -50.7$ (*c* 0.70, CHCl_3); IR (Germanium ATR): 2969, 1707, 1676, 1388, 916 cm^{-1} ; ^1H

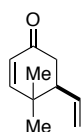
NMR (500 MHz, Chloroform-*d*) δ 6.85 (ddd, $J = 10.1, 4.8, 3.2$ Hz, 1H), 5.96 (ddd, $J = 10.1, 2.4, 1.7$ Hz, 1H), 5.84 (ddd, $J = 16.6, 10.8, 8.5$ Hz, 1H), 5.14 – 5.08 (m, 2H), 2.57 – 2.48 (m, 1H), 2.45 – 2.32 (m, 2H), 1.13 (s, 3H), 1.00 (s, 3H); ^{13}C NMR (126 MHz, CDCl_3) δ 204.4, 147.3, 137.4, 128.3, 117.3, 49.0, 44.8, 29.6, 22.7, 19.4; HRMS (ESI): Exact mass calc'd for $\text{C}_{10}\text{H}_{15}\text{O}$ $[\text{M}+\text{H}]^+$, 151.1123. Found 151.1115.



Compound II-203.

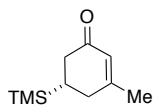
II-202 (327 mg, 2.17 mmol, 1.0 equiv) was added to a 50 mL round-bottom flask and diluted with MeOH (21 mL). The solution was cooled to 0 °C and aqueous NaOH (1 M, 0.65 mL, 0.65 mmol, 0.3 equiv) was added dropwise, followed by the slower dropwise addition of 30 wt% H_2O_2 (0.32 mL, 2.8 mmol, 1.3 equiv), and the reaction slowly warmed to room temperature. Upon observed consumption of the starting material by TLC (2 hours), the reaction was poured into saturated Na_2SO_3 and extracted with DCM. The combined organic layers were dried over MgSO_4 and the solvent evaporated under reduced pressure. The crude epoxide was taken directly on to the next reaction by diluting the material with MeOH (20 mL) in a flame-dried 50 mL round-bottom flask. The solution was cooled to 0 °C and $\text{NH}_2\text{NH}_2 \cdot \text{H}_2\text{O}$ (0.21 mL, 6.7 mmol, 3.1 equiv) was added. The reaction stirred for 15 minutes before adding AcOH (0.25 mL, 4.3 mmol, 2.0 equiv). The reaction was warmed to room temperature. Upon observed consumption of the starting material by TLC (6 hours), the yellow reaction was poured into saturated NaHCO_3 and extracted with DCM. The combined organic layers were washed with brine, dried over MgSO_4 , and the solvent evaporated under reduced pressure. The crude material was purified by flash chromatography with silica gel using a 10% ether/pentane to 30% ether/pentane solvent gradient (177 mg, 1.16 mmol, 54% over two steps): $[\alpha]_{\text{D}} = +65.8$ (c 0.36, CHCl_3); IR (Germanium ATR):

3347, 3015, 2934, 1039, 910 cm^{-1} ; ^1H NMR (500 MHz, Chloroform-*d*) δ 5.85 – 5.75 (m, 1H), 5.69 (ddt, $J = 9.9, 4.6, 1.3$ Hz, 1H), 5.62 (dt, $J = 9.9, 1.0$ Hz, 1H), 5.10 – 5.07 (m, 1H), 5.05 (d, $J = 1.3$ Hz, 1H), 4.18 (dt, $J = 6.8, 3.4$ Hz, 1H), 2.29 (ddd, $J = 12.0, 8.3, 3.7$ Hz, 1H), 1.85 – 1.70 (m, 2H), 1.02 (d, $J = 1.0$ Hz, 3H), 0.82 (d, $J = 1.0$ Hz, 3H); ^{13}C NMR (126 MHz, CDCl_3) δ 142.8, 139.4, 125.1, 115.8, 64.1, 43.6, 35.0, 33.9, 28.6, 22.0; HRMS (EI): Exact mass calc'd for $\text{C}_{10}\text{H}_{16}\text{O}$ $[\text{M}]^+$, 152.1201. Found 152.1227.



Compound II-121.

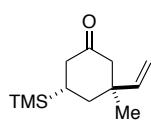
II-203 (175 mg, 1.1 mmol, 1.0 equiv) was diluted in DCM (2.5 mL, 0.5 M) in a flame-dried 10 mL round-bottom flask. MnO_2 (0.99 g, 11.5 mmol, 10 equiv) was added at room temperature and the reaction stirred overnight. The black mixture was filtered through Celite with 50% ether/pentane and the solvent carefully evaporated under reduced pressure, yielding pure yellow oil product (158 mg, 1.05 mmol, 95%): $[\alpha]_{\text{D}} = +16.9$ (c 0.49, CHCl_3); IR (Germanium ATR): 2960, 1684, 1268, 920 cm^{-1} ; ^1H NMR (499 MHz, Chloroform-*d*) δ 6.67 (dd, $J = 10.1, 1.3$ Hz, 1H), 5.87 (d, $J = 10.1$ Hz, 1H), 5.85 – 5.75 (m, 1H), 5.14 (d, $J = 10.4$ Hz, 1H), 5.09 (d, $J = 17.1$ Hz, 1H), 2.57 (dt, $J = 13.0, 6.9$ Hz, 1H), 2.50 – 2.37 (m, 2H), 1.16 (d, $J = 1.3$ Hz, 3H), 1.03 (d, $J = 1.3$ Hz, 3H); ^{13}C NMR (126 MHz, CDCl_3) δ 199.6, 160.6, 137.2, 126.7, 117.2, 48.5, 39.7, 36.0, 27.9, 21.2; HRMS (ESI): Exact mass calc'd for $\text{C}_{10}\text{H}_{15}\text{O}$ $[\text{M}+\text{H}]^+$, 151.1123. Found 151.1120.



Compound II-204.

(R)-II-133 (1.0 g, 5.9 mmol, 1.0 equiv) and THF (12 mL, 0.5M) were added to a flame-dried 50 mL round-bottom flask. The flask was cooled to -78 $^{\circ}\text{C}$, and a solution of MeLi (1.6 M, 5.6 mL, 8.9 mmol, 1.5 equiv) was added dropwise. The reaction was warmed to 0 $^{\circ}\text{C}$ and

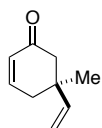
then slowly to room temperature. Upon observed consumption of starting material by TLC (2h), the mixture was quenched with water and extracted with ether. The combined organic layers were dried over MgSO₄ and the solvent evaporated under reduced pressure. The crude material was taken on to the next reaction. To a flame-dried 50 mL round-bottom flask was added PCC (2.5 g, 11.8 mmol, 2.0 equiv), DCM (25 mL), and 0.5 g silica gel. The crude material was diluted in DCM (2 mL) and added via cannula to the reaction flask at room temperature (0.5 mL DCM rinse). Following observed consumption of starting material by TLC (1.5 hours), the black mixture was filtered through a mixture of Celite and silica gel with 50% ether/pentane. The crude material was purified by flash chromatography with silica gel using 10% ether/pentane (0.73 g, 4.0 mmol, 68% over two steps): [α]_D = +67.6 (*c* 0.054, CHCl₃); IR (Germanium ATR): 2952, 1668, 1630, 1251, 833 cm⁻¹; ¹H NMR (499 MHz, Chloroform-*d*) δ 5.86 (s, 1H), 2.40 – 2.32 (m, 1H), 2.17 (d, *J* = 8.1 Hz, 2H), 2.10 (dd, *J* = 16.3, 14.6 Hz, 1H), 1.95 (d, *J* = 1.3 Hz, 3H), 1.44 – 1.33 (m, 1H), 0.03 (d, *J* = 1.0 Hz, 9H); ¹³C NMR (126 MHz, CDCl₃) δ 200.3, 163.5, 126.4, 37.8, 32.2, 24.4, 23.1, –3.6; HRMS (ESI): Exact mass calc'd for C₁₀H₁₉OSi [M+H]⁺, 183.1205. Found 183.1195.



Compound II-205.

LiCl (34 mg, 0.796 mmol, 20 mol %) and CuI (76 mg, 0.398 mmol, 10 mol %) were added to a flame-dried 50 mL round-bottom flask, cooled to 0 °C, and **II-204** (0.726 g, 3.98 mmol, 1.0 equiv) in THF (5 mL) was added (1 mL THF rinse). The solution was further diluted with THF (18 mL), and then TMS-Cl (0.56 mL, 4.38 mmol, 1.1 equiv) was added. The mixture stirred for 20 minutes at 0 °C before adding freshly prepared and titrated vinylmagnesium bromide solution (0.93 M, 5.2 mL, 4.78 mmol, 1.2 equiv) dropwise over 20 minutes. Upon observed consumption of the starting material by TLC (2 hours), the black reaction was quenched with saturated NH₄Cl,

and extracted with ether. The combined organic layers were washed three times with 1M HCl before drying over MgSO₄ and removing the solvent under reduced pressure. The crude material was purified by flash chromatography with silica gel using 5% ether/pentane (509 mg, 2.42 mmol, 61%): [α]_D = -41.0 (*c* 0.30, CHCl₃); IR (Germanium ATR): 2954, 1709, 1247, 839 cm⁻¹; ¹H NMR (500 MHz, Chloroform-*d*) δ 5.60 (dd, *J* = 17.6, 10.9 Hz, 1H), 5.06 (d, *J* = 10.9 Hz, 1H), 4.99 (d, *J* = 17.6 Hz, 1H), 2.51 (dt, *J* = 14.2, 2.5 Hz, 1H), 2.27 – 2.15 (m, 2H), 1.96 (t, *J* = 14.2 Hz, 1H), 1.63 (dq, *J* = 13.8, 2.5 Hz, 1H), 1.57 – 1.41 (m, 1H), 1.18 (tt, *J* = 13.8, 3.4 Hz, 1H), 1.11 (s, 3H), -0.01 (d, *J* = 0.8 Hz, 9H); ¹³C NMR (126 MHz, CDCl₃) δ 212.1, 144.8, 114.5, 51.2, 43.9, 41.6, 38.6, 30.5, 22.2, -3.6; HRMS (ESI): Exact mass calc'd for C₁₂H₂₃OSi [M+H]⁺, 211.1518. Found 211.1506.

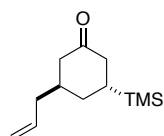


Compound II-122.

CuCl₂ (0.60 g, 3.84 mmol, 3.0 equiv) was added to a flame-dried 25 mL round-bottom flask. DMF (8 mL) was added to the flask. **II-205** (270 mg, 1.28 mmol, 1.0 equiv) in DMF (1 mL, with an additional 0.8 mL DMF rinse) was added and the reaction heated to 65 °C overnight. The green reaction was diluted with water and extracted twice with pentane and once with 5% ether/pentane. The combined organic layers were dried over MgSO₄ and the solvent removed under reduced pressure carefully due to the volatility of the product. The crude material was purified by flash chromatography with silica gel using 10% ether/pentane, yielding a yellow oil (55.4 mg, 0.41 mmol, 38% unoptimized): [α]_D = +37.0 (*c* 0.60, CHCl₃); IR (Germanium ATR): 2924, 1680, 1388, 914 cm⁻¹; ¹H NMR (400 MHz, Chloroform-*d*) δ 6.86 (dt, *J* = 10.1, 4.1 Hz, 1H), 6.03 (dt, *J* = 10.1, 2.1 Hz, 1H), 5.78 (dd, *J* = 17.4, 10.8 Hz, 1H), 5.07 – 4.92 (m, 2H), 2.55 – 2.25

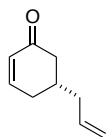
(m, 4H), 1.14 (s, 3H); ^{13}C NMR (126 MHz, CDCl_3) δ 199.2, 147.8, 145.0, 129.6, 112.6, 49.3, 39.7, 38.1, 26.7; HRMS (ESI): Exact mass calc'd for $\text{C}_9\text{H}_{12}\text{ONa}$ $[\text{M}+\text{Na}]^+$, 159.0786. Found 159.0775.

It should be noted that unreacted starting material was reisolated, as well as chlorinated products that could be converted back to starting material upon treatment with Zn and AcOH.

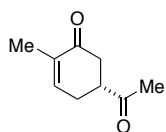


Compound II-206.

The Hosomi-Sakurai reaction was achieved using conditions reported by Takei and coworkers.²⁴⁹ (*R*)-**II-133** (300 mg, 1.78 mmol, 1.0 equiv) and DCM (8.9 mL, 0.2 M) were added to a flame-dried 25 mL round-bottom flask. The solution was cooled to -78 °C, and allyl trimethylsilane (0.42 mL, 2.67 mmol, 1.5 equiv) was added. Then, TiCl_4 (1 M, 2.14 mL, 2.14 mmol, 1.2 equiv) was added to the reaction slowly. After 30 minutes, the starting material was consumed as observed by TLC, and water was added to the reaction at -78 °C and the cold bath removed. The mixture was extracted with DCM and the combined organic layers dried over MgSO_4 and solvent evaporated under reduced pressure. The crude material was purified by flash chromatography with silica gel using 5% ether/pentane, yielding a yellow oil (240 mg, 1.14 mmol, 64%, ^1H NMR shows very minor impurities but the material was taken forward to the next reaction): $[\alpha]_{\text{D}} = +95.2$ (*c* 0.05, CHCl_3); IR (Germanium ATR): 2953, 1710, 1641, 1249, 841 cm^{-1} ; ^1H NMR (500 MHz, Chloroform-*d*) δ 5.70 (ddt, $J = 17.2, 10.4, 7.1$ Hz, 1H), 5.11 – 4.96 (m, 2H), 2.48 (ddd, $J = 13.7, 5.6, 1.0$ Hz, 1H), 2.32 – 2.19 (m, 3H), 2.17 – 2.00 (m, 3H), 1.72 – 1.66 (m, 2H), 1.27 (dddd, $J = 12.9, 9.3, 6.8, 4.3$ Hz, 1H), -0.01 (s, 9H); ^{13}C NMR (126 MHz, CDCl_3) δ 212.9, 136.4, 116.8, 46.5, 42.3, 37.7, 37.6, 29.5, 21.5, -3.4 ; HRMS (ESI): Exact mass calc'd for $\text{C}_{12}\text{H}_{22}\text{OSiNa}$ $[\text{M}+\text{Na}]^+$, 233.1338. Found 233.1328.

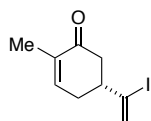
**Compound II-123.**

CuCl_2 (600 mg, 4.17 mmol, 3.0 equiv) was added to a flame-dried 25 mL round-bottom flask. **II-206** (292 mg, 1.39 mmol, 1.0 equiv) in DMF (9 mL, with an additional 1.7 mL DMF rinse) was added via cannula and the reaction was heated to 55 °C for two hours. The green reaction was cooled to room temperature, diluted with water and extracted with pentane two times and 5% ether/pentane one time. The combined organic layers were dried over MgSO_4 and the solvent removed under reduced pressure carefully due to the volatility of the product. The crude material was purified by flash chromatography with silica gel using 10% ether/pentane, yielding a yellow oil (138 mg, 1.01 mmol, 73%): $[\alpha]_D = -59.4$ (c 0.43, CHCl_3); IR (Germanium ATR): 3076, 2908, 1681, 1641, 1388, 916 cm^{-1} ; ^1H NMR (500 MHz, Chloroform- d) δ 6.96 (ddd, $J = 10.0, 5.6, 2.6$ Hz, 1H), 6.02 (dt, $J = 10.0, 2.6, 1.2$ Hz, 1H), 5.75 (ddt, $J = 16.0, 10.7, 6.9$ Hz, 1H), 5.17 – 4.96 (m, 2H), 2.53 (ddd, $J = 14.7, 3.0, 1.8$ Hz, 1H), 2.44 (dtd, $J = 18.5, 5.6, 3.8, 1.8$ Hz, 1H), 2.22 – 2.12 (m, 4H), 2.13 – 2.03 (m, 1H); ^{13}C NMR (126 MHz, CDCl_3) δ 199.9, 149.8, 135.4, 130.0, 117.4, 44.2, 40.1, 35.0, 31.9; HRMS (ESI): Exact mass calc'd for $\text{C}_9\text{H}_{13}\text{O}$ $[\text{M}+\text{H}]^+$, 137.0966. Found 137.0961.

**Compound II-134.**

This compound was prepared as reported by Miftakhov and coworkers.²⁵⁰ (*R*)-carvone (**(R)-II-35**) (3.0 g, 20.0 mmol, 1.0 equiv) and DCM (200 mL, 0.1 M) were added to an oven-dried 500 mL round-bottom flask. The solution was cooled to 0 °C before adding *m*CPBA (5.2 g, 30.0 mmol, 1.5 equiv) in three portions. Upon observed consumption of the starting material by TLC (after 5 hours), the reaction was quenched with saturated NaHCO_3 and extracted with DCM. The combined organic layers were washed with brine, dried over MgSO_4 , and the solvent

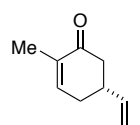
evaporated under reduced pressure. The crude epoxide was taken on to the next reaction, where it was diluted in ether (500 mL), cooled to 0 °C, and H₅IO₆ (7.3 g, 32.0 mmol, 1.6 equiv) was added in three portions. The reaction was left to stir overnight, after which it was diluted with saturated NaHCO₃ and extracted with ether. The combined organic layers were washed with brine, dried with MgSO₄, and the solvent evaporated under reduced pressure. The crude material was purified using flash chromatography on silica gel using 20% to 50% ether/pentanes yielding a yellow oil (2.1 g, 13.8 mmol, 69% over two steps): ¹H NMR (500 MHz, Chloroform-*d*) δ 6.70 (ddq, *J* = 4.8, 3.0, 1.5 Hz, 1H), 3.10 (dddd, *J* = 12.1, 9.5, 5.4, 4.2 Hz, 1H), 2.69 (ddd, *J* = 16.4, 4.2, 1.1 Hz, 1H), 2.58 – 2.45 (m, 3H), 2.19 (s, 3H), 1.78 (q, *J* = 1.8 Hz, 3H); ¹³C NMR (126 MHz, CDCl₃) δ 208.0, 197.6, 142.8, 136.0, 48.3, 39.6, 28.0, 27.6, 15.9; HRMS (ESI): Exact mass calc'd for C₉H₁₃O₂ [M+H]⁺, 153.0916. Found 153.0910. All spectroscopic data for this compound agrees with previously reported values.²⁵⁰



Compound II-135.

This vinyl iodide was prepared employing chemistry developed in the Myers laboratory.²⁵¹ Sc(OTf)₃ (2 mg, 0.004 mmol, 1.0 mol %) was added to a flame-dried 50 mL conical flask, and was purged with N₂ for 10 minutes. The flask was cooled to 0 °C and (TBSNH)₂ (10.3 g, 39.4 mmol, 1.0 equiv), which was prepared as described by Myers et al. in the same report, was added via syringe. **II-134** (6.0 g, 39.4 mmol) was added via syringe over 15 minutes. The solution gradually warmed to room temperature, and monitored by taking NMR aliquots. After all of the starting material had been consumed (after 3 hours), the yellow hydrazone was placed carefully on the vacuum manifold for one hour at room temperature, and then heated to 35 °C under high vacuum overnight. The crude material was used directly in the next reaction. I₂ (50 g, 197 mmol,

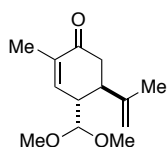
5.0 equiv) and THF (200 mL) were added to an oven-dried 1 L round-bottom flask. The mixture was cooled to 0 °C and placed under a box with the hood lights off. Tetramethylguanidine (99 mL, 788 mmol, 20 equiv) was cannulated to the flask. The crude material (11.0 g, 39.4 mmol, 1.0 equiv) in THF (50 mL) was cannulated to the flask in the dark over 2 hours. After 15 minutes following the completed addition of the starting material, the reaction was quenched with saturated NaS₂O₃, extracted with ether, and the combined organic layers washed with saturated NaS₂O₃, 1 M HCl, and saturated NaHCO₃. The combined organic layers were dried over MgSO₄, and the solvent evaporated under reduced pressure. The crude orange oil was purified by flash chromatography on silica gel using a pentane to 5% ether/pentane solvent gradient (4.95 g, 18.9 mmol, 48% over two steps, ¹H NMR shows very minor impurities, but the material was not purified further and taken on to the next reaction): [α]_D = +0.6 (*c* 0.23, CHCl₃); IR (Germanium ATR): 2921, 1672, 1365, 902 cm⁻¹; ¹H NMR (499 MHz, Chloroform-*d*) δ 6.72 (ddd, *J* = 4.9, 3.1, 1.5 Hz, 1H), 6.19 (t, *J* = 1.4 Hz, 1H), 5.82 (d, *J* = 1.9 Hz, 1H), 2.70 – 2.53 (m, 2H), 2.53 – 2.38 (m, 3H), 1.79 (p, *J* = 2.0 Hz, 3H); ¹³C NMR (126 MHz, CDCl₃) δ 197.9, 143.3, 135.9, 125.8, 116.4, 48.2, 44.4, 32.8, 15.8; HRMS (GC-TOF): Exact mass calc'd for C₇H₉I [M-CH₂CO]⁺, 219.9749. Found 219.9749.



Compound II-124.

II-135 (388 mg, 1.48 mmol, 1.0 equiv) and DMF (4.4 mL, 0.34M) were added to a flame-dried 10 mL round-bottom flask outfitted with a reflux condenser. Pd(OAc)₂ (7.0 mg, 0.03 mmol, 2.0 mol %), PPh₃ (20 mg, 0.07 mmol, 5.0 mol %), NEt₃ (0.66 mL, 4.74 mmol, 3.2 equiv), and formic acid (56 μL, 1.48 mmol, 1.0 equiv) were added sequentially and the reaction was heated to 60 °C. Upon observed consumption of the starting material by TLC after 1.5 hours, the dark red

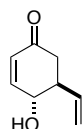
reaction was cooled to room temperature, diluted with water, and extracted with pentanes. The combined organic layers were washed with brine, dried over MgSO_4 , and the solvent evaporated under reduced pressure carefully due to the volatility of the product. The crude material was purified by flash chromatography on silica gel using 5% ether/pentane to yield a light yellow oil (175 mg, 1.28 mmol, 87%): $[\alpha]_D = -58.0$ (c 0.54, CHCl_3); IR (Germanium ATR): 2923, 1672, 1642, 1365, 910 cm^{-1} ; ^1H NMR (400 MHz, Chloroform- d) δ 6.72 (ddq, $J = 5.7, 2.9, 1.4$ Hz, 1H), 5.82 (dddd, $J = 16.9, 10.4, 6.4, 1.1$ Hz, 1H), 5.12 – 4.96 (m, 2H), 2.86 – 2.67 (m, 1H), 2.58 (ddt, $J = 16.2, 4.1, 1.3$ Hz, 1H), 2.45 (dddt, $J = 18.4, 7.3, 4.3, 1.4$ Hz, 1H), 2.38 – 2.14 (m, 2H), 1.78 (dq, $J = 2.6, 1.3$ Hz, 3H); ^{13}C NMR (126 MHz, CDCl_3) δ 199.4, 144.3, 140.6, 135.9, 114.5, 43.7, 39.3, 32.1, 15.9; HRMS (ESI): Exact mass calc'd for $\text{C}_9\text{H}_{13}\text{O}$ $[\text{M}+\text{H}]^+$, 137.0966. Found 137.0957.



Compound II-125.

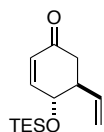
This compound was prepared from *S*-carvone following a procedure reported by Inoue and coworkers.²⁵² FeCl_3 (325 mg, 2.0 mmol, 3 mol %) was added to a flame-dried flask and diluted with THF (120 mL). The mixture was cooled to -20 $^\circ\text{C}$, and MeMgBr (3.0 M, 49.0 mL, 147 mmol, 2.2 equiv) was added over 2 hours. Then, a solution of (*S*)-carvone ((*S*)-**II-35**), (10.0 g, 66.6 mmol, 1.0 equiv) in THF (38 mL) was added over 1.5 hours (2 mL THF rinse). The reaction stirred at -20 $^\circ\text{C}$ for 1.5 hours, after which it was warmed to 0 $^\circ\text{C}$, and TMS-Cl (11.8 mL, 93.2 mmol, 1.4 equiv), DMPU (9.6 mL, 80.0 mmol, 1.2 equiv), and NEt_3 (12.1 mL, 86.6 mmol, 1.3 equiv) were added successively. The reaction was warmed to room temperature and stirred overnight. The black mixture was then cooled to 0 $^\circ\text{C}$, and quenched with pH 7 buffer. The mixture was filtered through Celite with EtOAc, extracted with EtOAc, and dried over MgSO_4 . The crude material was purified by flash chromatography on silica gel using 5% EtOAc/hexane. This product

was then diluted with DCM (133 mL) and CH(OMe)₃ (8.0 mL, 73.3 mmol, 1.1 equiv), cooled to -50 °C, and BF₃•OEt₂ (8.3 mL, 67.3 mmol, 1.01 equiv) was added. The mixture stirred at -50 °C for 2.5 hours, after which the bright orange reaction was poured into saturated NaHCO₃ at 0 °C. The mixture was extracted with DCM, and dried over MgSO₄. The crude material was purified by flash chromatography on silica gel with 20% ether/pentane (2.67 g, 11.9 mmol, 18% yield of major diastereomer over two steps): ¹H NMR (500 MHz, Benzene-*d*₆) δ 6.86 (dt, *J* = 3.1, 1.6 Hz, 1H), 4.69 (s, 1H), 4.67 (s, 1H), 4.05 (dd, *J* = 3.3, 1.1 Hz, 1H), 3.12 (d, *J* = 1.1 Hz, 3H), 3.05 (d, *J* = 1.6 Hz, 3H), 2.72 (ddd, *J* = 13.5, 9.9, 4.2 Hz, 1H), 2.43 (tdd, *J* = 13.1, 4.8, 2.3 Hz, 2H), 2.18 (ddd, *J* = 16.1, 12.7, 1.0 Hz, 1H), 1.85 (p, *J* = 2.6 Hz, 3H), 1.41 (s, 3H); ¹³C NMR (126 MHz, C₆D₆) δ 197.3, 145.6, 143.3, 136.0, 112.9, 105.9, 56.2, 55.2, 45.0, 43.5, 42.8, 19.2, 16.1. All spectroscopic data for this compound agrees with previously reported values.²⁵²



Compound II-137.

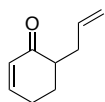
This compound was prepared from quinic acid **II-136** as detailed by Ventura et al.²⁵³ ¹H NMR (500 MHz, Chloroform-*d*) δ 6.93 (dd, *J* = 10.2, 1.9 Hz, 1H), 5.98 (ddd, *J* = 10.2, 2.3, 1.3 Hz, 1H), 5.79 (ddd, *J* = 17.2, 10.4, 8.1 Hz, 1H), 5.31 – 5.19 (m, 2H), 4.36 – 4.25 (m, 1H), 2.72 (dtd, *J* = 13.1, 8.7, 4.1 Hz, 1H), 2.57 (ddd, *J* = 16.7, 4.1, 1.3 Hz, 1H), 2.34 (dd, *J* = 16.7, 13.4 Hz, 1H); ¹³C NMR (126 MHz, CDCl₃) δ 197.9, 152.1, 137.3, 129.1, 118.8, 70.3, 49.2, 41.4. All spectroscopic data for this compound, as well as for all compounds leading to **II-137**, agrees with the reported values.²⁵³



Compound II-126.

II-137 (75 mg, 0.54 mmol) was diluted in DCM (2 mL, 0.27 M). TES-Cl (0.10 mL, 0.60 mmol, 1.1 equiv) was added to the flask. The mixture was cooled to 0 °C before adding Hünig's

base (0.24 mL, 1.36 mmol, 2.5 equiv) dropwise. The reaction slowly warmed to room temperature overnight. The yellow reaction was then poured into pH 7 buffer and extracted with DCM. The combined organic extracts were dried over Na₂SO₄. The crude material was purified by flash chromatography on silica gel with 10% ether/pentane (116.2 mg, 0.46 mmol, 85%): [α]_D = -111.2 (*c* 2.48, CHCl₃); IR (Germanium ATR): 2955, 2912, 2877, 1691, 1100, 894, 742 cm⁻¹; ¹H NMR (500 MHz, Chloroform-*d*) δ 6.78 (dd, *J* = 10.2, 2.1 Hz, 1H), 5.94 (ddd, *J* = 10.2, 2.0, 1.2 Hz, 1H), 5.85 (ddd, *J* = 17.4, 10.5, 7.1 Hz, 1H), 5.15 – 5.14 (m, 1H), 5.12 (dt, *J* = 10.2, 1.2 Hz, 1H), 4.28 (dt, *J* = 8.7, 2.1 Hz, 1H), 2.75 (dddd, *J* = 12.4, 9.7, 6.5, 3.1, 2.0 Hz, 1H), 2.59 (ddd, *J* = 16.5, 4.1, 1.2 Hz, 1H), 2.33 (dd, *J* = 16.6, 12.6 Hz, 1H), 0.98 (t, *J* = 7.9 Hz, 9H), 0.65 (q, *J* = 8.1 Hz, 6H); ¹³C NMR (126 MHz, CDCl₃) δ 198.5, 153.4, 138.0, 128.7, 116.7, 71.4, 48.2, 41.0, 6.9, 5.1; HRMS (ESI): Exact mass calc'd for C₁₄H₂₄O₂SiNa [M+Na]⁺, 275.1443. Found 275.1445



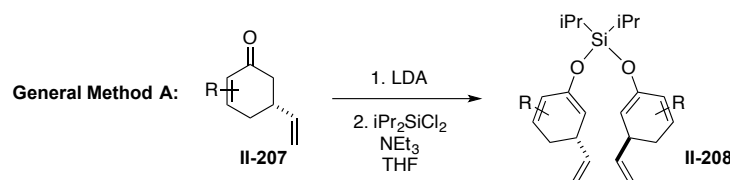
Compound II-127.

A solution of LDA was prepared by adding diisopropylamine (1.02 mL, 7.3 mmol, 1.4 equiv) and THF (21 mL) to a flame-dried 50 mL round-bottom flask. The solution was cooled to -78 °C and freshly titrated *n*-BuLi added (2.13 M, 3.2 mL, 6.8 mmol, 1.3 equiv). After stirring for 10 minutes at this temperature, cyclohexenone **II-138** (500 mg, 5.2 mmol, 1.0 equiv) in THF (4 mL, with an additional 1 mL THF rinse) was added. This solution stirred for 30 minutes before DMPU (1.33 mL, 10.4 mmol, 2.0 equiv) was added. The resulting solution stirred for another 50 minutes before allyl bromide (1.9 mL, 15.6 mmol, 3.0 equiv) was added dropwise. The solution slowly warmed to room temperature. Upon observed consumption of the starting material by TLC (3 hours), the orange reaction was quenched with saturated NH₄Cl, and extracted with ether. The combined organic layers were dried over MgSO₄ and the solvent evaporated under reduced

pressure carefully due to the volatility of the product. The crude material was purified by flash chromatography on silica gel using 5% ether/pentane (191.2 mg, 1.40 mmol, 27% unoptimized): ^1H NMR (499 MHz, Chloroform-*d*) δ 6.94 (dddd, $J = 10.2, 4.4, 3.2, 1.0$ Hz, 1H), 6.00 (ddd, $J = 10.0, 2.4, 1.6$ Hz, 1H), 5.78 (dddd, $J = 16.8, 10.1, 7.8, 6.3$ Hz, 1H), 5.15 – 4.93 (m, 2H), 2.70 – 2.55 (m, 1H), 2.47 – 2.29 (m, 3H), 2.21 – 2.03 (m, 2H), 1.73 (dddd, $J = 13.6, 11.5, 9.0, 5.7$ Hz, 1H); ^{13}C NMR (126 MHz, CDCl_3) δ 201.1, 149.9, 136.3, 129.7, 116.9, 46.3, 33.8, 27.5, 25.4. All spectroscopic data for this compound agrees with previously reported values.²⁵⁴

2.9.3 Oxidative coupling experimental procedures and characterization data

Scheme 2.29 General method A for synthesis of symmetrical silyl bis-enol ethers

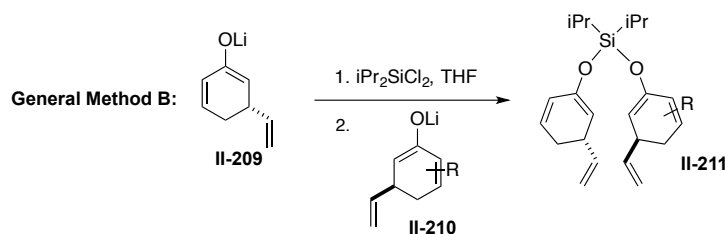


General Method A:

To a flame dried conical flask was added freshly distilled diisopropylamine (1.2 equiv) and THF (0.17 M). The flask was cooled to -78 °C, and *n*-BuLi (freshly titrated, 1.1 equiv) was added. After 10 minutes, enone **II-207** (1.0 equiv) in THF (0.4 M) was added (0.3 mL rinse). The solution stirred at this temperature for 30 minutes before adding $\text{iPr}_2\text{SiCl}_2$ (freshly distilled, 0.5 equiv) and NEt_3 (freshly distilled, 0.5 equiv) in rapid succession. The mixture stirred at -78 °C for 30 minutes before warming to room temperature. Upon observed consumption of the starting material by TLC (ranging from 1-3 hours), the orange reaction was quenched with pH 7 buffer and extracted with pentanes. The combined organic layers were dried over MgSO_4 , and concentrated under reduced

pressure. The crude material (**II-208**) was placed on the vacuum manifold overnight and was then used directly in the subsequent oxidative coupling reaction.

Scheme 2.30 General method B for synthesis of unsymmetrical silyl bis-enol ethers



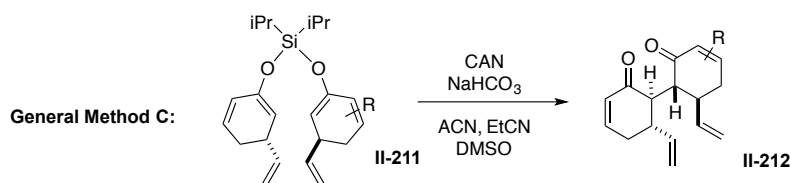
General Method B:

To a flame dried conical flask was added freshly distilled diisopropylamine (1.2 equiv) and THF (0.72 M with respect to **II-209**). The flask was cooled to $-78\text{ }^\circ\text{C}$, and *n*-BuLi (freshly titrated, 1.1 equiv) added. After 10 minutes, enone **II-209** (1.0 equiv) in THF (1.7 M with respect to **II-209**) was added (with an additional 0.2 mL rinse). The solution stirred for 30 minutes before very slowly adding it via cannula to a flask containing $i\text{Pr}_2\text{SiCl}_2$ (freshly distilled, 1.0 equiv) and THF (0.25 M with respect to **II-209**), also at $-78\text{ }^\circ\text{C}$, dropwise in a controlled manner, over at least 1 hour (with an additional 0.2 mL THF rinse). Meanwhile, LDA was prepared exactly as above in a separate conical flask. After 10 minutes, enone **II-210** (1.0 equiv) in THF (1.7 M with respect to **II-209**) was added to the LDA (with an additional 0.2 mL rinse). This solution stirred for 30 minutes before adding it slowly to the reaction flask via cannula over 1 hour (about 40 minutes following the completion of the first enolate addition, with an additional 0.2 mL THF rinse). The mixture stirred at $-78\text{ }^\circ\text{C}$ for 45 min and then was warmed to room temperature. Upon observed consumption of the starting materials by TLC (ranging from 1-3 hours), the orange reaction was quenched with pH 7 buffer and extracted with pentanes. The combined organic layers were dried over MgSO_4 ,

and concentrated under reduced pressure. The crude material (**II-211**) was placed on the vacuum manifold overnight and was used directly in the subsequent oxidative coupling reaction.

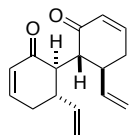
Note: The formation of the silyl bis-enol ether is more successful when the more hindered enone is added to the silane first. All enones to form cross-coupled products described below are listed in order of addition in the silyl bis-enol ether formation.

Scheme 2.31 General method C for the oxidative coupling of silyl bis-enol ethers

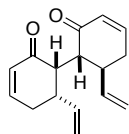


General Method C:

To a flame dried round bottom flask was added CAN (2.2 equiv), NaHCO₃ (4.4 equiv), ACN (distilled and dried over activated sieves, 0.03 M), and DMSO (2.0 equiv) The mixture was cooled to -30 °C and stirred vigorously while silyl bis-enol ether **II-211** in EtCN (distilled and dried over activated sieves, 0.2 M) was added (with an additional 0.2 mL rinse) via cannula. Upon observed consumption of the starting material by TLC (5-15 min), the orange mixture was diluted with saturated NaHCO₃ solution, extracted with CHCl₃. The combined organic layers were dried over MgSO₄ filtered through Celite with EtOAc, and concentrated under reduced pressure. The crude material was purified by flash chromatography on silica gel using 5-10% EtOAc/hexane to yield 1,4-diketone product **II-212**.

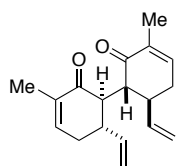
**Compound II-147.**

Enone (*R*)-**II-118** (100 mg, 0.82 mmol) was converted to the silyl bis-enol ether according to General Method A, which was then subjected to oxidative conditions via General Method C to afford the crude 1,4-diketone as a 3:1 mixture of diastereomers that were separated by flash chromatography (major product exhibits C2 symmetry: 48.4 mg, 0.20 mmol, 50% yield over two steps; total coupled yield: 65.2 mg, 0.27 mmol, 66%): IR (Germanium ATR): 2923, 1728, 1671, 1387, 812 cm^{-1} ; ^1H NMR (500 MHz, Chloroform-*d*) δ 6.89 (ddd, $J = 10.0, 6.0, 2.4$ Hz, 1H), 6.02 (ddd, $J = 10.0, 2.8, 1.0$ Hz, 1H), 5.61 (dt, $J = 17.1, 9.8$ Hz, 1H), 5.13 – 5.03 (m, 2H), 3.23 (s, 1H), 2.81 (broad s, 1H), 2.37 (dt, $J = 18.6, 5.4$ Hz, 1H), 2.27 (ddt, $J = 18.7, 11.3, 2.6$ Hz, 1H); ^{13}C NMR (126 MHz, CDCl_3) δ 199.5, 148.0, 140.8, 130.2, 117.2, 50.2, 44.5, 33.4; HRMS (ESI): Exact mass calc'd for $\text{C}_{16}\text{H}_{19}\text{O}_2$ $[\text{M}+\text{H}]^+$, 243.1385. Found 243.1383.

**Compound *epi*-II-147.**

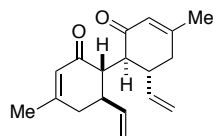
From the above reaction to form **II-147**, the minor diastereomer, *epi*-**II-147**, was cleanly isolated (16.8 mg, 0.07 mmol, 16%) $[\alpha]_{\text{D}} = -128.4$ (c 0.39, CHCl_3); IR (Germanium ATR): 3075, 2924, 1668, 1386, 911 cm^{-1} ; ^1H NMR (500 MHz, Chloroform-*d*) δ 6.91 – 6.84 (m, 1H), 6.81 (ddd, $J = 10.1, 5.0, 3.2$ Hz, 1H), 6.19 (dt, $J = 10.2, 1.8$ Hz, 1H), 5.93 (dt, $J = 10.3, 2.1$ Hz, 1H), 5.90 (dt, $J = 17.0, 10.0$ Hz, 1H), 5.76 (ddd, $J = 17.1, 10.2, 8.5$ Hz, 1H), 5.19 (dt, $J = 17.0, 1.2$ Hz, 1H), 5.11 (dd, $J = 10.2, 1.2$ Hz, 1H), 4.96 (dd, $J = 17.1, 1.7$ Hz, 1H), 4.90 (dd, $J = 10.0, 1.7$ Hz, 1H), 3.23 (dd, $J = 10.0, 6.0$ Hz, 1H), 2.92 (qd, $J = 8.7, 4.9$ Hz, 1H), 2.85 (dq, $J = 9.1, 4.6$ Hz, 1H), 2.68 (dd, $J = 6.0, 4.9$ Hz, 1H), 2.59 (ddt, $J = 18.5, 5.4, 2.8$ Hz, 1H), 2.51 (dtd, $J = 19.1, 5.0, 1.6$ Hz, 1H), 2.43 – 2.35 (m, 1H), 2.31 (ddt, $J = 19.1, 8.3, 2.8$ Hz, 1H); ^{13}C NMR (126 MHz, CDCl_3)

δ 198.3, 198.1, 147.0, 146.3, 139.5, 139.2, 130.5, 130.1, 116.6, 115.7, 50.5, 49.2, 41.1, 40.9, 32.2, 31.6; HRMS (ESI): Exact mass calc'd for $C_{16}H_{19}O_2$ $[M+H]^+$, 243.1385. Found 243.1378.



Compound II-160a.

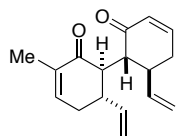
Enone **II-124** (100 mg, 0.734 mmol) was converted to the silyl bis-enol ether according to General Method A, which was then subjected to oxidative conditions via General Method C to afford the C₂-symmetric 1,4-diketone **II-160a** as a 20:1 mixture of diastereomers that was purified by flash chromatography (68 mg, 0.25 mmol, 68% yield over two steps): IR (Germanium ATR): 3076, 2922, 1659, 1366, 917 cm^{-1} ; 1H NMR (500 MHz, Chloroform-*d*) δ 6.64 (dt, $J = 6.2, 1.9$ Hz, 1H), 5.58 (dt, $J = 17.0, 9.8$ Hz, 1H), 5.07 (dd, $J = 17.0, 1.8$ Hz, 1H), 5.04 – 4.99 (m, 1H), 3.21 (s, 1H), 2.84 – 2.52 (broad m, 1H), 2.31 (dt, $J = 18.0, 5.5$ Hz, 1H), 2.21 (ddt, $J = 18.0, 11.3, 2.6$ Hz, 1H), 1.75 (t, $J = 2.6, 1.9$ Hz, 3H); ^{13}C NMR (126 MHz, $CDCl_3$) δ 199.8, 142.7, 141.2, 135.9, 116.8, 50.8, 45.0, 33.2, 16.2; HRMS (ESI): Exact mass calc'd for $C_{18}H_{23}O_2$ $[M+H]^+$, 271.1698. Found 271.1691.



Compound II-161a:

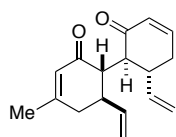
Enone **II-119** (110 mg, 0.808 mmol) was converted to the silyl bis-enol ether according to General Method A, which was then subjected to oxidative conditions via General Method C to afford the crude 1,4-diketone **II-161a** as a 4:1 mixture of diastereomers that were separated by flash chromatography (major diastereomer exhibits C₂ symmetry: 49.0 mg, 0.18 mmol, 45% yield over two steps; total coupled yield: 62.2 mg, 0.23 mmol, 57% over two steps): IR (Germanium ATR): 2926, 1732, 1659, 1379, 884 cm^{-1} ; 1H NMR (499 MHz, Chloroform-*d*) δ 5.87 (s, 1H), 5.60 (dt, $J = 17.0, 9.8$ Hz, 1H), 5.12 – 4.98 (m, 2H), 3.21 (s, 1H), 2.65 (broad s, 1H), 2.34 – 2.15 (m, 2H), 1.93 (s, 3H); ^{13}C NMR (126 MHz, $CDCl_3$) δ 199.5, 159.7, 141.1, 127.0, 117.0,

48.9, 44.3, 38.6, 24.2; HRMS (ESI): Exact mass calc'd for C₁₈H₂₃O₂ [M+H]⁺, 271.1698. Found 271.1697.



Compound II-162a.

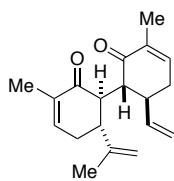
Enones **II-124** (85.0 mg, 0.62 mmol) and (*R*)-**II-118** (76.0 mg, 0.62 mmol) were converted to the silyl bis-enol ether according to General Method B, which was then subjected to oxidative conditions via General Method C to afford the crude 1,4-diketone **II-162a** as a 7:1 mixture of diastereomers that were separated by flash chromatography (major diastereomer: 82.5 mg, 0.32 mmol, 52% yield over two steps; total coupled yield: 95.1 mg, 0.37 mmol, 60% over two steps): [α]_D = +24.3 (*c* 1.06, CHCl₃); IR (Germanium ATR): 2922, 1661, 1387, 917 cm⁻¹; ¹H NMR (500 MHz, Chloroform-*d*) δ 6.88 (ddd, *J* = 10.1, 6.0, 2.3 Hz, 1H), 6.65 (dt, *J* = 6.2, 1.8 Hz, 1H), 6.01 (dd, *J* = 10.1, 2.9 Hz, 1H), 5.61 (t, *J* = 9.8 Hz, 1H), 5.57 (t, *J* = 9.8 Hz, 1H), 5.09 (dd, *J* = 6.2, 1.7 Hz, 1H), 5.08 – 5.01 (m, 3H), 3.22 (s, 2H), 2.87 – 2.58 (broad m, 2H), 2.47 – 2.10 (m, 4H), 1.73 (q, *J* = 1.8 Hz, 3H); ¹³C NMR (126 MHz, CDCl₃) δ 199.7, 199.7, 147.8, 143.0, 141.1, 140.9, 135.8, 130.3, 117.1, 117.0, 50.5, 50.4, 45.0, 44.6, 33.3, 33.3, 16.2; HRMS (ESI): Exact mass calc'd for C₁₇H₂₁O₂ [M+H]⁺, 257.1542. Found 257.1531.



Compound II-163a.

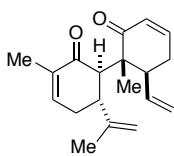
Enones (*S*)-**II-118** (82.0 mg, 0.67 mmol) and **II-119** (91.0 mg, 0.67 mmol) were converted to the silyl bis-enol ether according to General Method B, which was then subjected to oxidative conditions via General Method C to afford the crude 1,4-diketone **II-163a** as a 3:1 mixture of diastereomers that were separated by flash chromatography (major diastereomer: 67.0 mg, 0.26 mmol, 39% yield over two steps; total coupled yield: 89.8 mg, 0.35 mmol, 52% over two steps): [α]_D = +8.1 (*c* 1.06, CHCl₃); IR (Germanium ATR): 3075, 2916, 1656, 1380, 917 cm⁻¹; ¹H

NMR (500 MHz, Chloroform-*d*) δ 6.88 (ddd, $J = 10.0, 6.0, 2.4$ Hz, 1H), 6.01 (dd, $J = 10.0, 2.8$ Hz, 1H), 5.87 (q, $J = 1.4$ Hz, 1H), 5.60 (dtd, $J = 17.1, 9.8, 1.7$ Hz, 2H), 5.10 (d, $J = 1.6$ Hz, 1H), 5.07 (d, $J = 1.6$ Hz, 1H), 5.06 – 5.02 (m, 2H), 3.24 (d, $J = 22.7$ Hz, 2H), 2.99 – 2.50 (broad m, 2H), 2.36 (dt, $J = 18.5, 5.5$ Hz, 1H), 2.32 – 2.18 (m, 3H), 1.93 (s, 3H); ^{13}C NMR (126 MHz, CDCl_3) δ 199.7, 199.2, 159.8, 147.9, 141.0, 140.9, 130.2, 127.0, 117.1, 117.1, 50.0, 49.1, 44.5, 44.4, 38.6, 33.4, 24.2; HRMS (ESI): Exact mass calc'd for $\text{C}_{17}\text{H}_{21}\text{O}_2$ $[\text{M}+\text{H}]^+$, 257.1542. Found 257.1539.



Compound II-164a:

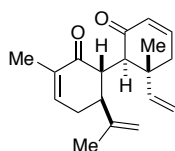
Enones (*R*)-**II-35** (24.8 mg, 0.165 mmol) and **II-124** (22.5 mg, 0.165 mmol) were converted to the silyl bis-enol ether according to General Method B, which was then subjected to oxidative conditions via General Method C to afford the 1,4-diketone **II-164a** as a 20:1 mixture of diastereomers that was purified by flash chromatography (23.5 mg, 0.083 mmol, 50% yield over two steps): $[\alpha]_{\text{D}} = -17.6$ (c 0.19, CHCl_3); IR (Germanium ATR): 2922, 1659, 1366, 903 cm^{-1} ; ^1H NMR (500 MHz, Chloroform-*d*) δ 6.69 – 6.65 (m, 1H), 6.63 (dt, $J = 6.1, 1.9$ Hz, 1H), 5.59 (dt, $J = 17.1, 9.8$ Hz, 1H), 5.15 – 5.05 (m, 2H), 4.82 (d, $J = 1.3$ Hz, 2H), 3.46 (td, $J = 12.3, 4.8$ Hz, 1H), 3.41 – 3.29 (m, 1H), 2.63 (dd, $J = 14.7, 10.9$ Hz, 1H), 2.43 – 2.14 (m, 5H), 1.75 (ddt, $J = 3.9, 2.7, 1.3$ Hz, 6H), 1.69 – 1.62 (m, 3H); ^{13}C NMR (126 MHz, CDCl_3) δ 200.4, 199.7, 145.8, 143.1, 142.4, 140.9, 136.0, 135.7, 117.3, 114.6, 50.8, 49.3, 33.1, 31.7, 18.7, 18.7, 16.2, 16.2, 16.2; HRMS (ESI): Exact mass calc'd for $\text{C}_{19}\text{H}_{25}\text{O}_2$ $[\text{M}+\text{H}]^+$, 285.1855. Found 285.1853.



Compound II-165a:

Enones (*R*)-**II-35** (93.0 mg, 0.62 mmol) and **II-120** (85.0 mg, 0.62 mmol) were converted to the silyl bis-enol ether according to General Method B, which was then subjected to oxidative conditions via General Method C to afford 1,4-diketone **II-165a** as a

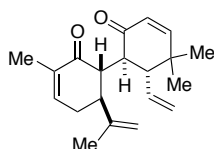
20:1 mixture of diastereomers that was purified by flash chromatography (88.0 mg, 0.31 mmol, 50% yield over two steps): $[\alpha]_D = -7.3$ (c 1.40, CHCl_3); IR (Germanium ATR): 3033, 2922, 1655, 1379, 916 cm^{-1} ; ^1H NMR (500 MHz, Chloroform- d) δ 6.70 (dt, $J = 10.1, 4.0$ Hz, 1H), 6.59 (tq, $J = 4.2, 1.4$ Hz, 1H), 6.01 (dt, $J = 10.1, 2.1$ Hz, 1H), 5.77 (dt, $J = 16.9, 9.8$ Hz, 1H), 5.15 (dd, $J = 16.9, 1.8$ Hz, 1H), 5.12 (dd, $J = 10.2, 1.8$ Hz, 1H), 4.76 (s, 1H), 4.74 (p, $J = 1.5$ Hz, 1H), 3.31 (ddd, $J = 9.5, 6.6, 5.2$ Hz, 1H), 3.13 (q, $J = 6.1$ Hz, 1H), 2.93 (d, $J = 5.9$ Hz, 1H), 2.60 – 2.47 (m, 2H), 2.32 – 2.21 (m, 2H), 1.74 (q, $J = 1.9$ Hz, 3H), 1.73 – 1.71 (m, 3H), 1.09 (s, 3H); ^{13}C NMR (126 MHz, CDCl_3) δ 203.5, 200.7, 149.5, 144.4, 142.4, 137.8, 136.7, 129.4, 118.3, 111.9, 53.1, 52.7, 47.6, 43.3, 31.1, 30.1, 21.1, 16.5, 16.4; HRMS (ESI): Exact mass calc'd for $\text{C}_{19}\text{H}_{25}\text{O}_2$ $[\text{M}+\text{H}]^+$, 285.1855. Found 285.1855.



Compound II-166a:

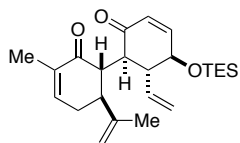
Enones (*S*)-**II-35** (56.0 mg, 0.37 mmol) and **II-122** (50.0 mg, 0.37 mmol) were converted to the silyl bis-enol ether according to General Method B, which was subjected to oxidative conditions via General Method C to afford the crude 1,4-diketone **II-166a** as a 10:1 mixture of diastereomers that were separated by flash chromatography (major diastereomer: 44.6 mg, 0.16 mmol, 42% yield over two steps, total coupled yield: 49.2 mg, 0.17 mmol, 47% over two steps): $[\alpha]_D = -62.9$ (c 0.17, CHCl_3); IR (Germanium ATR): 2924, 1698, 1641, 1279, 849 cm^{-1} ; ^1H NMR (500 MHz, Chloroform- d) δ 6.80 (ddd, $J = 10.1, 6.4, 2.4$ Hz, 1H), 6.63 (ddd, $J = 6.2, 2.6, 1.4$ Hz, 1H), 6.07 (dd, $J = 10.1, 2.9$ Hz, 1H), 5.70 (dd, $J = 17.3, 10.8$ Hz, 1H), 5.12 – 5.10 (m, 1H), 5.08 (dd, $J = 9.7, 1.0$ Hz, 1H), 4.89 (p, $J = 1.7$ Hz, 1H), 4.84 – 4.82 (m, 1H), 3.23 (td, $J = 12.1, 4.7$ Hz, 1H), 2.61 (s, 1H), 2.46 – 2.35 (m, 3H), 2.32 – 2.23 (m, 1H), 2.14 (dd, $J = 18.1, 6.4$ Hz, 1H), 1.77 (dt, $J = 2.7, 1.3$ Hz, 3H), 1.68 (t, $J = 1.1$ Hz, 3H), 1.20 (s, 3H); ^{13}C NMR (126 MHz, CDCl_3)

δ 199.3, 198.1, 147.5, 146.0, 146.0, 142.1, 136.0, 130.4, 115.4, 114.0, 54.9, 50.4, 49.2, 44.2, 40.5, 31.2, 19.7, 19.2, 16.6; HRMS (ESI): Exact mass calc'd for $C_{19}H_{25}O_2$ $[M+H]^+$, 285.1855. Found 285.1853.



Compound II-167a:

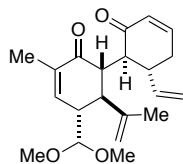
Enones (*S*)-**II-35** (62.0 mg, 0.41 mmol) and **II-121** (62.0 mg, 0.41 mmol) were converted to the silyl bis-enol ether according to General Method B, which was then subjected to oxidative conditions via General Method C to afford 1,4-diketone **II-167a** as a 20:1 mixture of diastereomers that was purified by flash chromatography (71.9 mg, 0.24 mmol, 59% yield over two steps): $[\alpha]_D^{25} = +24.7$ (*c* 1.10, $CHCl_3$); IR (Germanium ATR): 2962, 1662, 1376, 1364, 921, 894 cm^{-1} ; 1H NMR (500 MHz, Chloroform-*d*) δ 6.68 – 6.61 (m, 1H), 6.56 (d, *J* = 10.1 Hz, 1H), 5.82 (d, *J* = 10.0 Hz, 1H), 5.53 (dt, *J* = 17.1, 10.3 Hz, 1H), 5.20 (d, *J* = 10.1 Hz, 1H), 5.13 – 5.05 (m, 1H), 4.83 (t, *J* = 4.2 Hz, 2H), 3.49 (td, *J* = 12.6, 4.8 Hz, 1H), 3.17 (t, *J* = 11.5 Hz, 1H), 2.55 (d, *J* = 13.0 Hz, 1H), 2.49 (d, *J* = 12.6 Hz, 1H), 2.40 – 2.20 (m, 2H), 1.75 – 1.71 (m, 3H), 1.65 (s, 3H), 1.07 (s, 3H), 0.99 (s, 3H); ^{13}C NMR (126 MHz, $CDCl_3$) δ 200.4, 200.0, 158.4, 145.7, 143.3, 136.9, 135.6, 126.9, 120.1, 114.6, 53.8, 49.7, 48.9, 45.6, 36.3, 31.7, 28.6, 20.7, 18.7, 16.0; HRMS (ESI): Exact mass calc'd for $C_{20}H_{27}O_2$ $[M+H]^+$, 299.2011. Found 299.2014.



Compound II-168a.

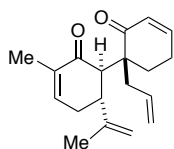
Enones (*S*)-**II-35** (120.2 mg, 0.80 mmol) and **II-126** (201.9 mg, 0.80 mmol) were converted to the silyl bis-enol ether according to General Method B, which was then subjected to oxidative conditions via General Method C to afford 1,4-diketone **II-168a** as a 20:1 mixture of diastereomers that was purified by flash chromatography (171.6 mg, 0.43 mmol, 54% over two steps): $[\alpha]_D^{25} = -62.8$ (*c* 1.69, $CHCl_3$); IR (Germanium ATR): 2954, 2913, 2876, 1666,

1381, 1087, 843, 725 cm^{-1} ; ^1H NMR (500 MHz, Chloroform-*d*) δ 6.71 (dd, $J = 10.3, 1.7$ Hz, 1H), 6.69 – 6.63 (m, 1H), 5.90 (dd, $J = 10.2, 2.3$ Hz, 1H), 5.45 (dt, $J = 16.9, 10.0$ Hz, 1H), 5.24 – 5.12 (m, 2H), 4.83 (s, 2H), 4.28 (dt, $J = 9.7, 2.1$ Hz, 1H), 3.48 (s, 1H), 3.35 (s, 1H), 2.66 – 2.55 (m, 1H), 2.41 – 2.19 (m, 3H), 1.74 (d, $J = 2.4$ Hz, 3H), 1.66 (s, 3H), 0.95 (t, $J = 7.9$ Hz, 9H), 0.61 (q, $J = 8.1$ Hz, 6H); ^{13}C NMR (126 MHz, CDCl_3) δ 199.9, 198.9, 152.3, 145.6, 143.3, 138.2, 135.6, 128.7, 120.4, 114.8, 71.5, 55.0, 49.5, 48.6, 47.9, 31.7, 18.8, 16.1, 7.0, 5.2; HRMS (ESI): Exact mass calc'd for $\text{C}_{24}\text{H}_{36}\text{O}_3\text{SiNa}$ $[\text{M}+\text{Na}]^+$, 423.2331. Found 423.2340.



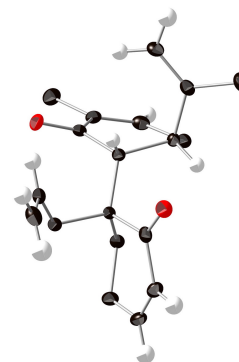
Compound II-169a.

Enones **II-125** (184 mg, 0.82 mmol) and (*S*)-**II-118** (100 mg, 0.82 mmol) were converted to the silyl bis-enol ether according to General Method B, which was then subjected to oxidative conditions via General Method C to afford 1,4-diketone **II-169a** as a 20:1 mixture of diastereomers that was purified by flash chromatography (163.0 mg, 0.473 mmol, 58% yield over two steps): $[\alpha]_{\text{D}} = -47.0$ (c 1.41, CHCl_3); IR (Germanium ATR): 2925, 1663, 1383, 1138, 1061, 752 cm^{-1} ; ^1H NMR (500 MHz, Chloroform-*d*) δ 6.89 – 6.78 (m, 2H), 5.98 (dd, $J = 10.1, 2.8$ Hz, 1H), 5.63 – 5.49 (m, 1H), 5.09 (dd, $J = 14.3, 8.3$ Hz, 2H), 4.94 (s, 1H), 4.88 (d, $J = 2.2$ Hz, 1H), 4.18 (d, $J = 2.7$ Hz, 1H), 3.52 – 3.32 (m, 8H), 2.66 (dq, $J = 11.5, 2.6$ Hz, 1H), 2.59 (d, $J = 12.9$ Hz, 1H), 2.38 (dt, $J = 18.6, 5.5$ Hz, 1H), 2.31 – 2.14 (m, 2H), 1.81 – 1.70 (m, 3H), 1.66 (s, 3H); ^{13}C NMR (126 MHz, CDCl_3) δ 199.8, 199.2, 147.2, 143.3, 142.5, 140.6, 135.9, 130.5, 117.7, 116.9, 106.1, 57.3, 56.2, 50.5, 50.2, 48.6, 45.3, 44.1, 33.1, 18.5, 16.1; HRMS (ESI): Exact mass calc'd for $\text{C}_{21}\text{H}_{29}\text{O}_4$ $[\text{M}+\text{H}]^+$, 345.2066. Found 345.2063.

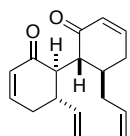


Compound II-170a.

Enones (*R*)-**II-35** (75 mg, 0.50 mmol) and **II-127** (68 mg, 0.50 mmol) were converted to the silyl bis-enol ether according to General Method B, which was then subjected to oxidative conditions via General Method C to afford 1,4-diketone **II-170a** as a 20:1 mixture of diastereomers that was purified by flash chromatography (80.5 mg, 0.28 mmol, 57% yield). While most coupled products were oils, for **II-170a**, solid crystals suitable for x-ray crystallography were obtained by slow diffusion of hexane in ethyl acetate. $[\alpha]_D = -47.4$ (c 1.24, CHCl_3); IR (Germanium ATR): 3075, 2922, 1657, 1431, 909 cm^{-1} ; ^1H NMR (500 MHz, $\text{Chloroform-}d$) δ 6.78 (dt, $J = 10.1, 3.9$ Hz, 1H), 6.55 (ddt, $J = 4.7, 3.1, 1.4$ Hz, 1H), 5.96 (dt, $J = 10.1, 2.0$ Hz, 1H), 5.75 (dddd, $J = 16.5, 11.0, 8.2, 6.1$ Hz, 1H), 5.05 (d, $J = 1.3$ Hz, 1H), 5.03 – 4.99 (m, 1H), 4.69 (p, $J = 1.5$ Hz, 1H), 4.66 (d, $J = 1.3$ Hz, 1H), 2.94 (d, $J = 2.1$ Hz, 1H), 2.86 (dd, $J = 7.4, 2.1$ Hz, 1H), 2.66 (ddt, $J = 20.6, 7.4, 2.8$ Hz, 1H), 2.60 (ddt, $J = 14.0, 6.1, 1.5$ Hz, 1H), 2.36 – 2.28 (m, 3H), 2.28 – 2.15 (m, 2H), 1.98 (dt, $J = 14.2, 6.2$ Hz, 1H), 1.76 (q, $J = 1.8$ Hz, 3H), 1.70 – 1.66 (m, 3H); ^{13}C NMR (126 MHz, CDCl_3) δ 200.4, 200.0, 149.0, 147.3, 142.5, 136.8, 134.2, 129.8, 118.6, 111.6, 52.4, 52.1, 41.4, 38.1, 29.6, 29.5, 23.2, 21.2, 16.5; HRMS (ESI): Exact mass calc'd for $\text{C}_{19}\text{H}_{25}\text{O}_2$ $[\text{M}+\text{H}]^+$, 285.1855. Found 285.1852.



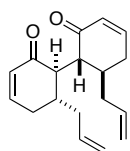
X-ray structure



Compound II-171a.

Enones **II-123** (91.0 mg, 0.66 mmol) and (*R*)-**II-118** (82.0 mg, 0.66 mmol) were converted to the silyl bis-enol ether according to General Method B, which was then subjected to oxidative conditions via General Method C to afford the crude 1,4-diketone **II-171a** as a 5:1 mixture of diastereomers that were separated by flash chromatography. The major NMR of the

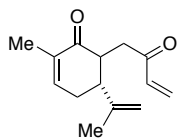
major diastereomer shows a small amount of **II-177** which could not be separated, however both compounds converge to the coupled product **II-171** in the RCM (major diastereomer: 70.8 mg, 0.28 mmol, 42% over two steps; total coupled yield: 86.2 mg, 0.34 mmol, 51% over two steps): $[\alpha]_D = -5.4$ (c 1.20, CHCl_3); IR (Germanium ATR): 3075, 2924, 1663, 1625, 1388, 915 cm^{-1} ; ^1H NMR (500 MHz, Chloroform- d) δ 7.00 – 6.83 (m, 2H), 6.05 (dddd, $J = 9.9, 5.3, 2.8, 1.0$ Hz, 1H), 6.02 – 5.98 (m, 1H), 5.78 – 5.68 (m, 1H), 5.68 – 5.58 (m, 1H), 5.14 – 4.99 (m, 4H), 3.15 (s, 1H), 2.99 (d, $J = 10.7$ Hz, 1H), 2.92 – 2.76 (m, 1H), 2.70 – 2.56 (m, 1H), 2.56 – 2.36 (m, 2H), 2.32 (ddt, $J = 18.7, 11.1, 2.7$ Hz, 1H), 2.27 – 2.14 (m, 1H), 2.09 (tdt, $J = 18.9, 11.3, 2.7$ Hz, 1H), 1.97 (dq, $J = 14.1, 8.4$ Hz, 1H); ^{13}C NMR (126 MHz, CDCl_3) δ 200.2, 199.5, 148.6, 148.1, 140.7, 135.6, 130.1, 129.9, 117.5, 117.2, 51.0, 49.1, 44.3, 38.5, 36.8, 33.3, 32.0; HRMS (ESI): Exact mass calc'd for $\text{C}_{17}\text{H}_{21}\text{O}_2$ $[\text{M}+\text{H}]^+$, 257.1542. Found 257.1538.



Compound II-177.

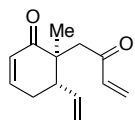
Enone **II-123**, (100 mg, 0.73 mmol) was converted to the silyl bis-enol ether according to General Method A, which was then subjected to oxidative conditions via General Method C to afford C2-symmetric 1,4-diketone **II-177** as a 5:1 mixture of diastereomers that could not be separated by flash chromatography (51.5 mg, 0.19 mmol, 52% yield over two steps, as a mixture of diastereomers): IR (Germanium ATR): 2923, 1663, 1640, 1388, 911 cm^{-1} ; ^1H NMR (500 MHz, Chloroform- d) δ 6.93 (ddd, $J = 10.0, 5.8, 2.6$ Hz, 1H), 6.04 (ddd, $J = 10.0, 2.9, 1.0$ Hz, 1H), 5.71 (dddd, $J = 16.6, 10.4, 8.1, 6.1$ Hz, 1H), 5.12 – 4.99 (m, 2H), 2.98 (d, $J = 10.8$ Hz, 1H), 2.56 – 2.48 (m, 1H), 2.48 – 2.38 (m, 1H), 2.18 (dddd, $J = 13.5, 5.5, 3.8, 1.7$ Hz, 1H), 2.10 (ddt, $J = 18.6, 9.9, 2.7$ Hz, 1H), 1.96 (dt, $J = 14.1, 8.7$ Hz, 1H); ^{13}C NMR (126 MHz, CDCl_3) δ 200.1,

148.5, 135.7, 129.7, 117.5, 50.2, 38.7, 36.6, 31.3; HRMS (ESI): Exact mass calc'd for $C_{18}H_{22}O_2Na$ $[M+Na]^+$, 293.1518. Found 293.1513.



Compound II-173a.

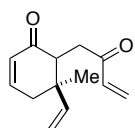
Enones (*R*)-**II-35** (157.7 mg, 1.05 mmol) and methylvinyl ketone **II-128** (73.6 mg, 85.2 μ L, 1.05 mmol) were converted to the silyl bis-enol ether according to General Method B, which was then subjected to oxidative conditions via General Method C to afford 1,4-diketone **II-173a** as a 1.5:1 mixture of diastereomers that could not be separated by flash chromatography (157 mg, 0.72 mmol, 69% yield over two steps, as a mixture of diastereomers): IR (Germanium ATR): 2922, 1665, 1614, 1400, 896 cm^{-1} ; 1H NMR (499 MHz, Chloroform-*d*) δ 6.71 (dt, $J = 5.9, 1.9$ Hz, 1H), 6.61 (d, $J = 4.0$ Hz, 1H), 6.41 (ddd, $J = 17.6, 14.9, 10.6$ Hz, 2H), 6.26 (t, $J = 1.2$ Hz, 1H), 6.23 (d, $J = 1.2$ Hz, 1H), 5.82 (ddd, $J = 10.6, 8.5, 1.1$ Hz, 2H), 4.84 – 4.78 (m, 3H), 4.58 (dd, $J = 1.7, 0.9$ Hz, 1H), 3.38 (q, $J = 6.1$ Hz, 1H), 3.17 (dd, $J = 17.3, 6.4$ Hz, 1H), 3.11 (ddd, $J = 13.3, 7.9, 3.2$ Hz, 1H), 2.98 – 2.89 (m, 2H), 2.81 – 2.68 (m, 2H), 2.55 – 2.47 (m, 2H), 2.47 – 2.44 (m, 1H), 2.38 (dddd, $J = 19.2, 5.1, 3.5, 1.7$ Hz, 1H), 2.34 – 2.26 (m, 1H), 1.77 (ddt, $J = 6.3, 2.7, 1.4$ Hz, 6H), 1.69 (t, $J = 1.0$ Hz, 3H), 1.61 (dd, $J = 1.5, 0.7$ Hz, 3H); ^{13}C NMR (126 MHz, $CDCl_3$) δ 200.2, 200.1, 199.3, 199.3, 145.5, 145.0, 143.8, 142.4, 136.9, 136.8, 135.3, 134.9, 128.3, 127.8, 114.3, 113.8, 48.7, 46.5, 45.6, 45.1, 37.4, 36.9, 31.5, 30.2, 22.2, 18.3, 16.2, 16.1; HRMS (ESI): Exact mass calc'd for $C_{14}H_{19}O_2$ $[M+H]^+$, 219.1385. Found 219.1389.



Compound II-174a.

Enones **II-120** (75.0 mg, 0.55 mmol) methylvinyl ketone **II-128** (39.0 mg, 0.55 mmol) were converted to the silyl bis-enol ether according to General Method B, which was then subjected to oxidative conditions via General Method C to afford 1,4-diketone **II-174a** and *epi*-**II-**

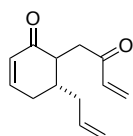
174a as a 1.3:1 mixture of diastereomers that were separated by flash chromatography. The stereochemistry of this major product was elucidated by NMR studies of the corresponding closed product **II-174** (major diastereomer: 32.7 mg, 0.16 mmol, 29% yield over two steps; total coupled yield: 56.6 mg, 0.28 mmol, 51% over two steps): $[\alpha]_D = -16.6$ (c 0.77, CHCl_3); IR (Germanium ATR): 2933, 1671, 1633, 1389, 921 cm^{-1} ; ^1H NMR (499 MHz, Chloroform- d) δ 6.90 (ddd, $J = 10.1, 5.6, 2.5$ Hz, 1H), 6.31 (dd, $J = 17.6, 10.5$ Hz, 1H), 6.19 (dd, $J = 17.6, 1.2$ Hz, 1H), 6.05 (ddd, $J = 10.1, 2.9, 1.2$ Hz, 1H), 5.82 – 5.70 (m, 1H), 5.76 (dd, $J = 10.5, 1.2$ Hz, 1H), 5.10 (dd, $J = 10.3, 1.8$ Hz, 1H), 5.02 (ddd, $J = 17.0, 1.8, 0.9$ Hz, 1H), 3.37 – 3.27 (m, 1H), 3.21 (d, $J = 18.0$ Hz, 1H), 2.73 (d, $J = 18.0$ Hz, 1H), 2.39 (ddt, $J = 19.2, 11.0, 2.6$ Hz, 1H), 2.35 – 2.28 (m, 1H), 1.03 (s, 3H); ^{13}C NMR (126 MHz, CDCl_3) δ 202.4, 198.2, 147.5, 137.2, 136.7, 128.6, 127.8, 118.2, 46.8, 45.0, 43.5, 29.1, 18.3; HRMS (ESI): Exact mass calc'd for $\text{C}_{13}\text{H}_{17}\text{O}_2$ $[\text{M}+\text{H}]^+$, 205.1229. Found 205.1210.



Compound II-175a.

Enones **II-122** (90.0 mg, 0.66 mmol) and methylvinyl ketone **II-128** (46.0 mg, 0.66mmol) were converted to the silyl bis-enol ether according to General Method B, which was then subjected to oxidative conditions via General Method C to afford 1,4-diketone **II-175a** as a 1.6:1 mixture of diastereomers that could not be separated by flash chromatography (76.1 mg, 0.37 mmol, 56% yield over two steps, as a mixture of diastereomers): IR (Germanium ATR): 2971, 1674, 1641, 1387, 1279, 851 cm^{-1} ; ^1H NMR (499 MHz, Chloroform- d) δ 6.81 (ddt, $J = 10.1, 5.9, 2.1$ Hz, 2H), 6.42 (ddd, $J = 17.6, 10.6, 5.8$ Hz, 2H), 6.26 (ddd, $J = 17.6, 7.2, 1.0$ Hz, 2H), 6.09 – 6.00 (m, 2H), 5.88 – 5.74 (m, 4H), 5.12 – 4.96 (m, 4H), 3.36 (dd, $J = 8.6, 3.1$ Hz, 1H), 3.31 (dd, $J = 7.0, 4.3$ Hz, 1H), 3.19 (dd, $J = 17.4, 7.0$ Hz, 1H), 3.08 (dd, $J = 17.2, 8.6$ Hz, 1H), 2.62 (ddt, $J =$

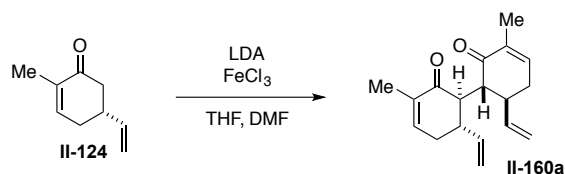
24.3, 18.9, 2.8 Hz, 2H), 2.41 – 2.38 (m, 1H), 2.35 (td, $J = 5.6, 4.9, 3.7$ Hz, 1H), 2.25 (dd, $J = 17.2, 3.0$ Hz, 1H), 2.17 (dd, $J = 19.0, 5.9$ Hz, 1H), 1.14 (s, 3H), 1.01 (s, 3H); ^{13}C NMR (126 MHz, CDCl_3) δ 199.3, 199.2, 199.1, 199.0, 146.6, 146.5, 145.6, 140.1, 136.7, 136.7, 129.2, 128.9, 128.1, 127.9, 115.2, 113.9, 52.3, 51.1, 43.6, 43.2, 40.4, 40.0, 34.6, 34.4, 25.7, 16.7; HRMS (ESI): Exact mass calc'd for $\text{C}_{13}\text{H}_{17}\text{O}_2$ $[\text{M}+\text{H}]^+$, 205.1229. Found 205.1224.



Compound II-176a.

Enones **II-123** (91.0 mg, 0.67 mmol) and methylvinyl ketone **II-128** (47.0 mg, 0.67mmol) were converted to the silyl bis-enol ether according to General Method B, which was then subjected to oxidative conditions via General Method C to afford 1,4-diketone **II-176a** as a 1.3:1 mixture of diastereomers that could not be separated by flash chromatography (76.0 mg, 0.37 mmol, 56% yield over two steps, as a mixture of diastereomers): IR (Germanium ATR): 3076, 2922, 1673, 1641, 1390, 917 cm^{-1} ; ^1H NMR (500 MHz, Chloroform-*d*) δ 6.98 – 6.89 (m, 1H), 6.79 (dddd, $J = 9.7, 5.6, 2.6, 1.2$ Hz, 1H), 6.43 (ddd, $J = 17.7, 10.6, 1.4$ Hz, 2H), 6.28 (ddd, $J = 17.7, 10.4, 1.0$ Hz, 2H), 6.03 (dtd, $J = 10.1, 3.0, 1.1$ Hz, 2H), 5.86 (ddd, $J = 11.9, 10.5, 1.0$ Hz, 2H), 5.79 – 5.58 (m, 2H), 5.12 – 4.93 (m, 4H), 3.41 (td, $J = 6.3, 4.3$ Hz, 1H), 3.28 (dd, $J = 17.2, 6.9$ Hz, 1H), 3.14 (dd, $J = 17.3, 5.7$ Hz, 1H), 2.89 (dt, $J = 11.2, 5.4$ Hz, 1H), 2.74 (dd, $J = 17.3, 5.2$ Hz, 1H), 2.61 (ddt, $J = 19.3, 5.6, 2.9$ Hz, 1H), 2.51 – 2.38 (m, 4H), 2.35 – 2.26 (m, 1H), 2.26 – 2.19 (m, 1H), 2.18 – 2.00 (m, 3H), 1.93 (ddd, $J = 14.2, 10.9, 8.4$ Hz, 1H); ^{13}C NMR (126 MHz, CDCl_3) δ 199.9, 199.5, 198.9, 198.9, 149.0, 147.1, 136.7, 136.6, 136.6, 135.1, 129.6, 129.1, 128.5, 128.2, 117.8, 117.2, 48.3, 47.2, 38.4, 38.0, 38.0, 36.8, 36.6, 32.0, 31.6, 30.1; HRMS (ESI): Exact mass calc'd for $\text{C}_{13}\text{H}_{17}\text{O}_2$ $[\text{M}+\text{H}]^+$, 205.1229. Found 205.1212.

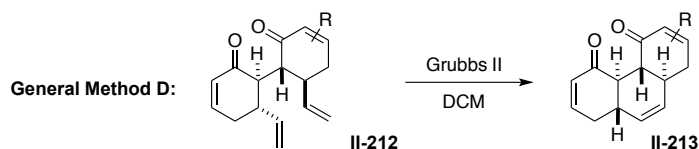
Scheme 2.32 Oxidative coupling control experiment without the silicon tether



This oxidative coupling procedure was carried under conditions developed by Frazier and Harlow.²¹¹ A solution of LDA was prepared by adding freshly distilled diisopropylamine (68 μL , 0.48 mmol, 1.3 equiv) to a flame dried round-bottom flask and diluting with THF (0.4 mL). The solution was cooled to $-78\text{ }^\circ\text{C}$, and n-BuLi (0.23 mL, 1.99 M, 0.45 mmol, 1.2 equiv) was added. After 10 minutes at this temperature, enone **II-124** (50 mg, 0.37 mmol) in THF (0.4 mL) was added via cannula (with an additional 0.1 mL THF rinse). The reaction stirred at this temperature for 30 minutes before adding FeCl_3 (80 mg, 0.49 mmol, 1.3 equiv) in DMF (0.4 mL) via cannula (with an additional 0.1 mL DMF rinse). The reaction warmed to room temperature. After stirring for 15 hours, the reaction was quenched with 1 M HCl and extracted with 10% ether/pentane. The combined organic layers were dried over MgSO_4 . The diastereoselectivity of the reaction was determined from the crude ^1H NMR spectrum to be 3:1 **II-160a** to the minor diastereomer. The crude material was purified by flash chromatography on silica gel with 5% EtOAc/hexanes (23.8 mg major product **II-160a**, 0.088 mmol, 48%; 8.1 mg minor diastereomer, 0.03 mmol, 16%; 31.9 mg total, 0.12 mmol, 64% combined yield). This result is compared to the observed 20:1 diastereoselectivity and 68% yield over two steps when employing the designed silicon tether approach.

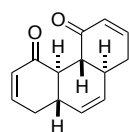
2.9.4 Ring-closing metathesis experimental procedures and characterization data

Scheme 2.33 General method D for the ring-closing metathesis of coupled products



General Method D:

To a flame-dried flask was added Grubbs II from the glove box (10 mol %). **II-212** in DCM (0.05 M) was added to the flask via cannula and the reaction stirred at room temperature under N₂. Where noted below, when forming a trisubstituted olefin or a larger, more challenging ring system through the RCM, the reaction was heated to reflux at 40 °C. Upon observed consumption of the starting material by TLC (5-15h), DMSO (10 μL) was added, and the mixture stirred for 2h-12h. The solvent was evaporated, and the crude material was purified by flash chromatography on silica gel with 20% EtOAc/hexanes to yield couple and close product **II-213**.



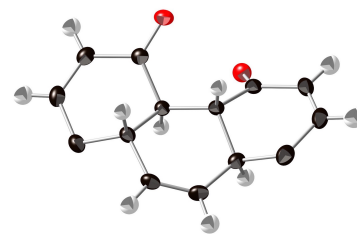
Compound II-148.

Coupled product **II-147** (105.5 mg, 0.44 mmol) was submitted to ring-closing metathesis conditions according to General Method D to afford **II-148** (81.4 mg, 0.38 mmol, 86% yield). Solid crystals for X-ray crystallography were obtained by slow evaporation of ethyl acetate.

IR (Germanium ATR): 3028, 2876, 1685, 1378, 793 cm⁻¹; ¹H NMR

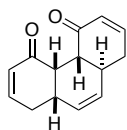
(499 MHz, Chloroform-*d*) δ 6.79 (ddd, *J* = 10.1, 5.2, 2.3 Hz, 1H), 6.08

(ddd, *J* = 10.1, 3.2, 0.9 Hz, 1H), 5.56 (d, *J* = 0.8 Hz, 1H), 2.74 – 2.69 (m, 1H), 2.61 – 2.47 (m, 2H), 2.26 (dddd, *J* = 18.4, 11.1, 3.2, 2.2 Hz, 1H). ¹³C NMR (126 MHz, CDCl₃) δ 199.7, 145.4,



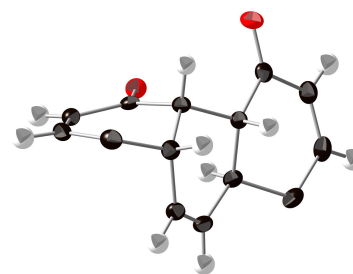
X-ray structure

130.7, 128.9, 46.7, 38.8, 34.3; HRMS (ESI): Exact mass calc'd for $C_{14}H_{15}O_2$ $[M+H]^+$, 215.1072. Found 215.1070.

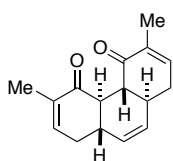


Compound *epi*-II-148.

Coupled product *epi*-II-147 (24.6 mg, 0.100 mmol) was submitted to ring-closing metathesis conditions according to General Method D to afford *epi*-II-148 (17.9 mg, 0.084 mmol, 84% yield). Solid crystals for X-ray crystallography were obtained by slow evaporation of ethyl acetate. $[\alpha]_D = -2.2$ (c 0.56, $CHCl_3$); IR (Germanium ATR): 3015, 2918, 1670, 1390, 867 cm^{-1} ; 1H NMR (500 MHz, Chloroform- d) δ 6.97 (ddd, $J = 10.2, 6.1, 2.1$ Hz, 1H), 6.72 (ddd, $J = 10.1, 5.9, 2.4$ Hz, 1H), 6.16 (dd, $J = 10.1, 2.8$ Hz, 1H), 5.93 (dd, $J = 10.1, 3.0$ Hz, 1H), 5.62 (dt, $J = 9.9, 2.5$ Hz, 1H), 5.48 (dq, $J = 9.9, 2.9, 1.5$ Hz, 1H), 3.59 (dd, $J = 5.4, 2.5$ Hz, 1H), 3.14 – 3.05 (m, 1H), 2.93 – 2.77 (m, 2H), 2.51 (ddd, $J = 18.2, 6.2, 4.3$ Hz, 1H), 2.41 (dd, $J = 19.2, 5.6$ Hz, 1H), 2.20 – 2.04 (m, 2H); ^{13}C NMR (126 MHz, $CDCl_3$) δ 197.7, 197.4, 148.2, 145.8, 132.4, 131.1, 130.4, 129.5, 51.2, 43.5, 36.6, 34.2, 32.5, 31.6; HRMS (ESI): Exact mass calc'd for $C_{14}H_{15}O_2$ $[M+H]^+$, 215.1072. Found 215.1070.

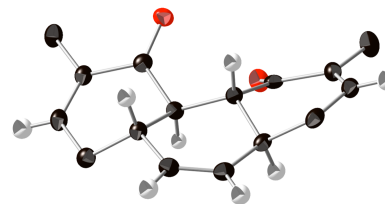


X-ray structure



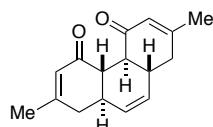
Compound II-160.

Coupled product II-160a (20.0 mg, 0.074 mmol) was submitted to ring-closing metathesis conditions according to General Method D to afford II-160 (15.1 mg, 0.062 mmol, 84% yield). Solid crystals for X-ray crystallography were obtained by slow evaporation of ethyl acetate. IR (Germanium ATR): 3019, 2920, 1677, 1690, 1357, 908 cm^{-1} ; 1H NMR (500 MHz, Chloroform- d) δ 6.50 (qd, $J = 3.4,$



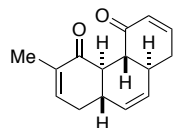
X-ray structure

2.9, 1.4 Hz, 1H), 5.52 (s, 1H), 2.68 – 2.61 (m, 1H), 2.56 – 2.38 (m, 2H), 2.21 (ddt, $J = 18.1, 11.1, 2.6$ Hz, 1H), 1.83 (dt, $J = 2.6, 1.4$ Hz, 3H); ^{13}C NMR (126 MHz, CDCl_3) δ 200.8, 139.8, 137.0, 129.1, 46.7, 39.0, 34.2, 16.1. HRMS (ESI): Exact mass calc'd for $\text{C}_{16}\text{H}_{19}\text{O}_2$ $[\text{M}+\text{H}]^+$, 243.1385. Found 243.1375.



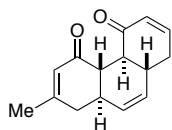
Compound II-161.

Coupled product **II-161a** (16.8 mg, 0.062 mmol) was submitted to ring-closing metathesis conditions according to General Method D to afford **II-161** (9.7 mg, 0.040 mmol, 65% yield): IR (Germanium ATR): 2914, 1676, 1627, 1379, 834 cm^{-1} ; ^1H NMR (500 MHz, Chloroform-*d*) δ 5.91 (dd, $J = 2.7, 1.4$ Hz, 1H), 5.54 (s, 1H), 2.67 – 2.55 (m, 1H), 2.51 (td, $J = 10.6, 8.5, 3.8$ Hz, 1H), 2.37 (dd, $J = 17.9, 3.8$ Hz, 1H), 2.25 (ddt, $J = 17.8, 11.2, 2.7, 1.4$ Hz, 1H), 1.93 (d, $J = 1.4$ Hz, 3H); ^{13}C NMR (126 MHz, CDCl_3) δ 199.4, 156.8, 129.0, 127.3, 46.2, 39.4, 38.5, 23.6; HRMS (ESI): Exact mass calc'd for $\text{C}_{16}\text{H}_{19}\text{O}_2$ $[\text{M}+\text{H}]^+$, 243.1385. Found 243.1374.

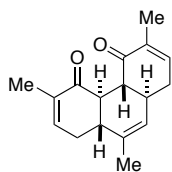


Compound II-162.

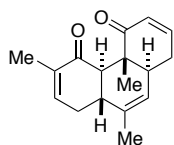
Coupled product **II-162a** (15.0 mg, 0.059 mmol) was submitted to ring-closing metathesis conditions according to General Method D to afford **II-162** (11.5 mg, 0.050 mmol, 86% yield): $[\alpha]_{\text{D}} = -615.6$ (*c* 0.39, CHCl_3); IR (Germanium ATR): 2920, 1681, 1352, 1041 cm^{-1} ; ^1H NMR (500 MHz, Chloroform-*d*) δ 6.78 (ddd, $J = 10.1, 5.3, 2.2$ Hz, 1H), 6.51 (dt, $J = 5.3, 1.9$ Hz, 1H), 6.07 (dd, $J = 10.1, 3.0$ Hz, 1H), 5.55 – 5.53 (m, 2H), 2.72 (t, $J = 12.1, 10.6$ Hz, 1H), 2.64 (t, $J = 12.1, 10.6$ Hz, 1H), 2.60 – 2.41 (m, 4H), 2.31 – 2.16 (m, 2H), 1.83 (dt, $J = 2.8, 1.5$ Hz, 3H); ^{13}C NMR (126 MHz, CDCl_3) δ 200.5, 200.0, 145.3, 139.9, 136.9, 130.7, 129.3, 128.7, 47.0, 46.5, 39.0, 38.9, 34.4, 34.2, 16.1; HRMS (ESI): Exact mass calc'd for $\text{C}_{15}\text{H}_{17}\text{O}_2$ $[\text{M}+\text{H}]^+$, 229.1229. Found 229.1215.

**Compound II-163.**

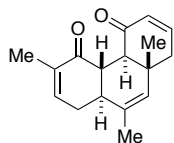
Coupled product **II-163a** (11.7 mg, 0.046 mmol) was submitted to ring-closing metathesis conditions according to General Method D to afford **II-163** (9.5 mg, 0.042 mmol, 91% yield): $[\alpha]_D = +582.4$ (*c* 0.22, CHCl₃); IR (Germanium ATR): 2874, 1678, 1630, 1294, 821 cm⁻¹; ¹H NMR (500 MHz, Chloroform-*d*) δ 6.78 (ddd, *J* = 10.1, 5.4, 2.2 Hz, 1H), 6.08 (dd, *J* = 10.1, 3.0 Hz, 1H), 5.91 (dd, *J* = 2.6, 1.5 Hz, 1H), 5.65 – 5.49 (m, 2H), 2.76 – 2.44 (m, 5H), 2.38 (dd, *J* = 18.0, 4.0 Hz, 1H), 2.26 (ddt, *J* = 18.3, 11.1, 2.6 Hz, 2H), 2.00 – 1.88 (m, 3H); ¹³C NMR (126 MHz, CDCl₃) δ 199.9, 199.3, 157.0, 145.2, 130.8, 129.0, 128.9, 127.2, 46.9, 46.1, 39.4, 39.0, 38.3, 34.3, 23.7; HRMS (ESI): Exact mass calc'd for C₁₅H₁₇O₂ [M+H]⁺, 229.1229. Found 229.1217.

**Compound II-164.**

Coupled product **II-164a** (11.5 mg, 0.040 mmol) was submitted to ring-closing metathesis conditions according to General Method D with elevated temperature, refluxing at 40 °C, to afford **II-164** (9.0 mg, 0.035 mmol, 87% yield): $[\alpha]_D = -488.1$ (*c* 0.31, CHCl₃); IR (Germanium ATR): 2920, 1639, 1677, 1366, 863 cm⁻¹; ¹H NMR (499 MHz, Chloroform-*d*) δ 6.53 (dq, *J* = 5.7, 1.8 Hz, 1H), 6.50 (dq, *J* = 5.1, 1.6 Hz, 1H), 5.25 (q, *J* = 1.8 Hz, 1H), 2.73 – 2.57 (m, 3H), 2.50 – 2.32 (m, 3H), 2.16 (dddt, *J* = 20.5, 16.1, 11.1, 2.5 Hz, 2H), 1.84 (dt, *J* = 2.8, 1.5 Hz, 3H), 1.82 (dt, *J* = 2.6, 1.4 Hz, 3H), 1.68 (dt, *J* = 2.5, 1.3 Hz, 3H); ¹³C NMR (126 MHz, CDCl₃) δ 201.1, 201.1, 140.1, 139.9, 136.8, 136.8, 134.5, 124.9, 47.4, 46.6, 42.0, 38.6, 34.5, 32.4, 20.1, 16.1, 16.0; HRMS (ESI): Exact mass calc'd for C₁₇H₂₁O₂ [M+H]⁺, 257.1542. Found 257.1532.

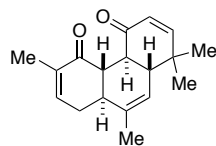
**Compound II-165.**

Coupled product **II-165a** (30.0 mg, 0.105 mmol) was submitted to ring-closing metathesis conditions according to General Method D with elevated temperature, refluxing at 40 °C, to afford **II-165** (23.5 mg, 0.092 mmol, 87% yield): $[\alpha]_D = -93.3$ (*c* 0.41, CHCl₃); IR (Germanium ATR): 2923, 1672, 1380, 910 cm⁻¹; ¹H NMR (500 MHz, Chloroform-*d*) δ 6.60 (dt, *J* = 10.2, 3.8 Hz, 1H), 6.52 (dq, *J* = 5.7, 1.7 Hz, 1H), 5.92 (dt, *J* = 10.2, 2.0 Hz, 1H), 5.11 (h, *J* = 1.5 Hz, 1H), 2.73 – 2.62 (m, 1H), 2.65 (d, *J* = 12.7 Hz, 1H), 2.58 (tq, *J* = 8.2, 2.6 Hz, 1H), 2.46 – 2.36 (m, 1H), 2.26 (dd, *J* = 3.4, 2.3 Hz, 1H), 2.24 (dd, *J* = 3.8, 2.1 Hz, 1H), 2.16 – 2.04 (m, 1H), 1.82 (dt, *J* = 2.8, 1.5 Hz, 3H), 1.69 (dt, *J* = 2.6, 1.2 Hz, 3H), 1.27 (s, 3H); ¹³C NMR (126 MHz, CDCl₃) δ 203.5, 199.3, 143.4, 139.5, 137.2, 134.8, 128.7, 123.3, 52.1, 45.0, 42.3, 40.6, 32.3, 29.8, 20.1, 16.2, 9.9; HRMS (ESI): Exact mass calc'd for C₁₇H₂₁O₂ [M+H]⁺, 257.1542. Found 257.1536.

**Compound II-166.**

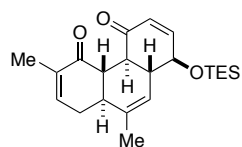
Coupled product **II-166a** (27.0 mg, 0.095 mmol) was submitted to ring-closing metathesis conditions according to General Method D with elevated temperature, refluxing at 40 °C, to afford **II-166** (19.8 mg, 0.077 mmol, 81% yield): $[\alpha]_D = +531.9$ (*c* 0.68, CHCl₃); IR (Germanium ATR): 2962, 1683, 1375, 722 cm⁻¹; ¹H NMR (500 MHz, Chloroform-*d*) δ 6.63 (ddd, *J* = 10.1, 5.5, 2.2 Hz, 1H), 6.52 (dq, *J* = 5.4, 1.8 Hz, 1H), 6.08 (dd, *J* = 10.1, 3.1 Hz, 1H), 5.29 – 5.23 (m, 1H), 2.89 (d, *J* = 11.3 Hz, 1H), 2.73 (dd, *J* = 12.5, 11.2 Hz, 1H), 2.63 (dddd, *J* = 18.0, 5.6, 3.9, 1.6 Hz, 1H), 2.45 (dt, *J* = 18.5, 2.8 Hz, 1H), 2.36 – 2.27 (m, 1H), 2.18 (ddd, *J* = 18.8, 5.6, 0.9 Hz, 1H), 2.12 (ddt, *J* = 16.0, 11.1, 2.5 Hz, 1H), 1.82 (dt, *J* = 2.8, 1.4 Hz, 3H), 1.65 (t, *J* = 1.3 Hz, 3H), 0.87 (s, 3H); ¹³C NMR (126 MHz, CDCl₃) δ 201.0, 199.9, 143.4, 139.9, 136.9, 131.8,

131.4, 131.1, 50.2, 44.9, 42.6, 41.3, 38.8, 32.4, 21.8, 20.1, 15.9; HRMS (ESI): Exact mass calc'd for $C_{17}H_{21}O_2$ $[M+H]^+$, 257.1542. Found 257.1539.



Compound II-167.

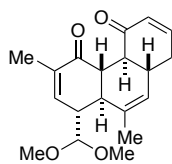
Coupled product **II-167a** (24.0 mg, 0.080 mmol) was submitted to ring-closing metathesis conditions according to General Method D with elevated temperature, refluxing at 40 °C. As the reaction was proceeding much more slowly than for less hindered substrates, an additional 10 mol % Grubbs II was added after refluxing for 24 hours, and an additional 5 mol % Grubbs II after another 24 hours. The reaction was worked up after a total of 72 hours to afford **II-167** (14.8 mg, 0.055 mmol, 68% yield; also reisolating unreacted SM): $[\alpha]_D = +288.2$ (*c* 0.40, $CHCl_3$); IR (Germanium ATR): 2923, 1686, 1371, 1083, 700 cm^{-1} ; 1H NMR (500 MHz, Chloroform-*d*) δ 6.54 (dt, $J = 5.5, 1.9$ Hz, 1H), 6.39 (d, $J = 10.1$ Hz, 1H), 5.88 (d, $J = 10.1$ Hz, 1H), 5.40 (q, $J = 1.8$ Hz, 1H), 2.86 (dd, $J = 12.6, 10.9$ Hz, 1H), 2.73 – 2.61 (m, 2H), 2.40 – 2.32 (m, 2H), 2.12 (ddq, $J = 18.1, 11.0, 2.5$ Hz, 1H), 1.84 (dt, $J = 2.9, 1.5$ Hz, 3H), 1.72 (p, $J = 1.2$ Hz, 3H), 1.18 (s, 3H), 1.03 (s, 3H); ^{13}C NMR (126 MHz, $CDCl_3$) δ 201.1, 201.0, 156.1, 139.9, 136.8, 135.7, 126.7, 121.2, 47.2, 46.6, 41.5, 41.3, 37.9, 32.3, 27.6, 20.5, 19.6, 16.0; HRMS (ESI): Exact mass calc'd for $C_{18}H_{23}O_2$ $[M+H]^+$, 271.1698. Found 271.1696.



Compound II-168.

Coupled product **II-168a**, (80.1 mg, 0.20 mmol) was submitted to ring-closing metathesis conditions according to General Method D with elevated temperature, refluxing at 40 °C. Just as with the reaction to form compound **II-167**, this reaction was proceeding much more slowly than for less hindered substrates, so an additional 10 mol % Grubbs II was added after refluxing for 24 hours, and an additional 5 mol % Grubbs II added after 48 hours. The reaction

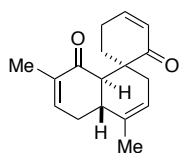
was worked up after a total of 72 hours to afford **II-168** (46.9 mg, 0.13 mmol, 64%): $[\alpha]_D = +261.8$ (*c* 1.23, CHCl_3); IR (Germanium ATR): 2954, 2914, 2876, 1687, 1348, 1078, 835, 731 cm^{-1} ; ^1H NMR (500 MHz, Chloroform-*d*) δ 6.60 (dd, $J = 10.3, 1.8$ Hz, 1H), 6.54 (dt, $J = 5.7, 1.9$ Hz, 1H), 5.99 (dd, $J = 10.3, 2.3$ Hz, 1H), 5.64 (d, $J = 2.0$ Hz, 1H), 4.27 (dt, $J = 9.3, 2.1$ Hz, 1H), 2.73 – 2.61 (m, 3H), 2.48 (ddd, $J = 11.7, 6.5, 2.3$ Hz, 1H), 2.37 – 2.29 (m, 1H), 2.12 (ddt, $J = 18.2, 11.2, 2.5$ Hz, 1H), 1.83 (dt, $J = 3.1, 1.5$ Hz, 3H), 1.70 (dt, $J = 2.7, 1.3$ Hz, 3H), 1.00 (t, $J = 8.0$ Hz, 9H), 0.68 (q, $J = 8.0$ Hz, 6H); ^{13}C NMR (126 MHz, CDCl_3) δ 200.5, 199.5, 149.9, 140.1, 136.6, 135.1, 129.4, 121.1, 73.7, 47.8, 47.0, 45.0, 41.4, 32.2, 20.3, 15.9, 7.0, 5.1; HRMS (ESI): Exact mass calc'd for $\text{C}_{22}\text{H}_{32}\text{O}_3\text{SiNa}$ $[\text{M}+\text{Na}]^+$, 395.2018. Found 395.2026.



Compound II-169.

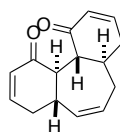
Coupled product **II-169a** (52.0 mg, 0.15 mmol) was submitted to ring-closing metathesis conditions according to General Method D with elevated temperature, refluxing at 40 °C. Just as with the reactions to form compounds **II-167** and **II-168**, the reaction was proceeding much more slowly than for less hindered substrates, so an additional 10 mol % Grubbs II was added after refluxing for 24 hours. The reaction was worked up after a total of 65 hours to afford **II-169** (30.6 mg, 0.097 mmol, 64%): $[\alpha]_D = +298.5$ (*c* 0.95, CHCl_3); IR (Germanium ATR): 2922, 1684, 1378, 1119, 1059, 751 cm^{-1} ; ^1H NMR (499 MHz, Chloroform-*d*) δ 6.75 (ddd, $J = 10.2, 5.2, 2.2$ Hz, 1H), 6.71 – 6.63 (m, 1H), 6.02 (dd, $J = 10.1, 3.0$ Hz, 1H), 5.34 (q, $J = 1.8$ Hz, 1H), 4.74 (d, $J = 2.7$ Hz, 1H), 3.48 (s, 3H), 3.39 (s, 3H), 2.82 – 2.72 (m, 2H), 2.67 (t, $J = 11.7$ Hz, 1H), 2.55 (t, $J = 11.3$ Hz, 1H), 2.46 (dq, $J = 14.2, 4.5$ Hz, 2H), 2.19 (ddt, $J = 19.2, 11.8, 2.7$ Hz, 1H), 1.86 (p, $J = 1.7$ Hz, 6H); ^{13}C NMR (126 MHz, CDCl_3) δ 201.1, 200.1, 145.3,

139.1, 137.5, 134.3, 130.5, 128.3, 106.5, 56.8, 56.3, 48.6, 47.1, 46.8, 43.0, 38.1, 34.4, 24.9, 15.9;
 HRMS (ESI): Exact mass calc'd for C₁₉H₂₄O₄Na [M+Na]⁺, 339.1572. Found 339.1569.



Compound II-170.

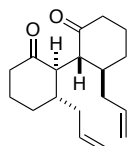
Coupled product **II-170a** (30.0 mg, 0.100 mmol) was submitted to ring-closing metathesis conditions according to General Method D with elevated temperature, refluxing at 40 °C, to afford **II-170** (23.4 mg, 0.091 mmol, 91% yield): [α]_D = -42.3 (*c* 1.04, CHCl₃); IR (Germanium ATR): 2920, 1668, 1381, 728 cm⁻¹; ¹H NMR (500 MHz, Chloroform-*d*) δ 6.81 (ddt, *J* = 9.7, 5.9, 1.8 Hz, 1H), 6.65 (dt, *J* = 6.0, 1.8 Hz, 1H), 5.89 (dd, *J* = 10.1, 2.9 Hz, 1H), 5.33 – 5.22 (m, 1H), 3.28 (t, *J* = 12.4 Hz, 1H), 3.08 (td, *J* = 12.6, 5.6 Hz, 1H), 2.72 (dddd, *J* = 18.2, 5.7, 3.9, 1.5 Hz, 1H), 2.53 – 2.40 (m, 2H), 2.30 (dt, *J* = 19.3, 5.8, 1.5 Hz, 1H), 2.21 (d, *J* = 12.3 Hz, 1H), 2.15 (dq, *J* = 18.2, 2.8 Hz, 1H), 2.01 (ddt, *J* = 18.3, 11.6, 2.5 Hz, 1H), 1.75 (dt, *J* = 2.6, 1.4 Hz, 3H), 1.72 – 1.66 (m, 3H), 1.42 (ddt, *J* = 12.9, 5.1, 1.6 Hz, 1H); ¹³C NMR (126 MHz, CDCl₃) δ 201.9, 200.2, 146.9, 142.3, 136.3, 135.2, 129.0, 117.6, 56.9, 42.4, 41.6, 36.1, 33.1, 32.5, 22.9, 20.5, 16.0; HRMS (ESI): Exact mass calc'd for C₁₇H₂₁O₂ [M+H]⁺, 257.1542. Found 257.1534.



Compound II-171.

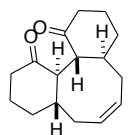
Coupled product **II-171a** (19.0 mg, 0.074 mmol) was submitted to ring-closing metathesis conditions according to General Method D with elevated temperature, refluxing at 40 °C, to afford **II-171** (12.2 mg, 0.053 mmol, 72% yield): [α]_D = -254.9 (*c* 0.34, CHCl₃); IR (Germanium ATR): 3028, 2905, 1668, 1384, 795 cm⁻¹; ¹H NMR (500 MHz, Chloroform-*d*) δ 6.85 (ddd, *J* = 10.0, 4.9, 3.8 Hz, 1H), 6.77 (ddd, *J* = 9.9, 5.5, 2.4 Hz, 1H), 6.08 – 5.99 (m, 2H), 5.96 (dddd, *J* = 10.4, 8.4, 6.1, 2.2 Hz, 1H), 5.42 (dddd, *J* = 10.3, 3.6, 2.2, 1.0 Hz, 1H), 3.18 (dd, *J* =

12.9, 8.8 Hz, 1H), 3.07 – 2.95 (m, 2H), 2.59 – 2.50 (m, 2H), 2.44 – 2.21 (m, 3H), 1.99 – 1.85 (m, 2H); ^{13}C NMR (126 MHz, CDCl_3) δ 200.8, 200.2, 146.6, 145.9, 134.4, 132.5, 129.8, 129.5, 53.9, 45.9, 39.6, 37.0, 36.8, 35.1, 33.3; HRMS (ESI): Exact mass calc'd for $\text{C}_{15}\text{H}_{17}\text{O}_2$ $[\text{M}+\text{H}]^+$, 229.1229. Found 229.1215.



Compound II-180.

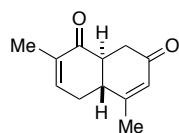
Stryker's reagent (200.0 mg, 0.10 mmol, 0.8 equiv) was added to a flame-dried round bottom flask from the glovebox. The flask was cooled to 0 °C, and benzene (3 mL) that had been sparged with argon for 2 hours was added. **II-177** (35.0 mg, 0.13 mmol) in benzene (1 mL, with an additional 0.3 mL rinse) was added. The reaction was warmed to room temperature after 15 minutes and stirred overnight, after which the mixture was filtered through Celite with ether and concentrated. The crude material was purified by flash chromatography on silica gel with 5% EtOAc/hexane (32.2 mg, 0.12 mmol, 92% yield): IR (Germanium ATR): 2934, 1694, 1640, 1446, 995, 910 cm^{-1} ; ^1H NMR (500 MHz, Chloroform-*d*) δ 5.81 – 5.68 (m, 1H), 5.10 – 4.98 (m, 2H), 2.55 – 2.41 (m, 1H), 2.35 (d, $J = 9.9$ Hz, 1H), 2.28 – 2.10 (m, 3H), 2.04 – 1.86 (m, 3H), 1.80 (dq, $J = 16.9, 8.7, 7.8, 4.6$ Hz, 1H), 1.31 (dtd, $J = 13.3, 11.3, 3.0$ Hz, 1H); ^{13}C NMR (126 MHz, CDCl_3) δ 211.6, 136.2, 117.1, 54.2, 41.6, 40.6, 39.3, 30.5, 23.6; HRMS (ESI): Exact mass calc'd for $\text{C}_{18}\text{H}_{26}\text{O}_2\text{Na}$ $[\text{M}+\text{Na}]^+$, 297.1831. Found 297.1829.



Compound II-172.

Grubbs II (2.2 mg, 0.0026 mmol, 10 mol %) was added to a flame-dried round-bottom flask in the glove box. 1,4-benzoquinone (1.0 mg, 0.009 mmol, 35 mol %) was added and the flask was purged with N_2 for 2 minutes. DCM (1 mL) was added to the mixture. Compound **II-180** (7.0 mg, 0.026 mmol) in DCM (0.7 mL) was added to the flask (with an additional 0.3 mL DCM rinse)

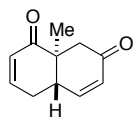
at room temperature, and the reaction was heated to 40 °C. Upon observed consumption of the starting material by TLC (5.25h), the reaction was cooled to room temperature and DMSO (10 μ L) was added. After stirring at room temperature for 2h, the solvent was evaporated. The crude material was purified by flash chromatography on silica gel with 10% EtOAc/hexane to afford **II-172** (4.9 mg, 0.020 mmol, 78% yield): IR (Germanium ATR): 2932, 1695, 1457, 1262, 909, 730 cm^{-1} ; ^1H NMR (499 MHz, Chloroform-*d*) δ 5.52 (t, $J = 3.5$ Hz, 1H), 2.48 (d, $J = 15.7$ Hz, 1H), 2.37 – 2.26 (m, 2H), 2.21 – 2.10 (m, 2H), 2.00 – 1.92 (m, 1H), 1.86 (q, $J = 13.2$ Hz, 1H), 1.71 (d, $J = 13.7$ Hz, 1H), 1.56 – 1.47 (m, 2H); ^{13}C NMR (126 MHz, CDCl_3) δ 212.4, 128.5, 52.0, 42.0, 40.6, 35.4, 30.8, 24.1; HRMS (ESI): Exact mass calc'd for $\text{C}_{32}\text{H}_{45}\text{O}_4$ $[\text{2M}+\text{H}]^+$, 493.3318. Found 493.3311.



Compound II-173.

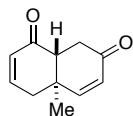
Coupled product **II-173a** (40.0 mg, 0.183 mmol, 1.5:1 mixture of diastereomers) was submitted to ring-closing metathesis conditions according to General Method D with elevated temperature, refluxing at 40 °C, to afford **II-173** as a 1.5:1 mixture of diastereomers that could be separated by flash chromatography (major diastereomer: 18.6 mg, 0.098 mmol, 53% yield; total yield: 34.4 mg, 0.180 mmol, 98%): $[\alpha]_D = -271.4$ (c 0.10, CHCl_3); IR (Germanium ATR): 2922, 1661, 1379, 879 cm^{-1} ; ^1H NMR (499 MHz, Chloroform-*d*) δ 6.76 (ddq, $J = 4.7, 2.9, 1.3$ Hz, 1H), 5.91 (t, $J = 1.3$ Hz, 1H), 3.01 (dt, $J = 11.7, 4.9$ Hz, 1H), 2.92 (dt, $J = 9.8, 5.1$ Hz, 1H), 2.72 – 2.57 (m, 2H), 2.50 – 2.39 (m, 2H), 1.99 (d, $J = 1.3$ Hz, 3H), 1.81 (q, $J = 1.3$ Hz, 3H); ^{13}C NMR (126 MHz, CDCl_3) δ 198.6, 196.6, 162.2, 142.6, 135.7, 127.5, 46.0, 39.7, 35.5, 27.3, 22.8, 16.1; HRMS (ESI): Exact mass calc'd for $\text{C}_{12}\text{H}_{15}\text{O}_2$ $[\text{M}+\text{H}]^+$, 191.1072. Found 191.1051. HSQC data revealed that the protons at 3.01 ppm and 2.92 ppm are the protons at the ring junctions (only one proton

on each carbon). 1D-NOE experiments individually irradiating each of these protons did not display a NOE interaction between them, indicating a *trans*-relationship.



Compound II-174.

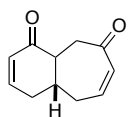
Coupled product **II-174a** (14.0 mg, 0.069 mmol) was submitted to ring-closing metathesis conditions according to General Method D to afford **II-174** (10.9 mg, 0.062 mmol, 90% yield): $[\alpha]_D = -61.8$ (*c* 0.063, CHCl_3); IR (Germanium ATR): 2975, 1669, 1392, 824 cm^{-1} ; ^1H NMR (500 MHz, Chloroform-*d*) δ 6.94 (ddd, $J = 10.1, 5.7, 2.1$ Hz, 1H), 6.62 (dd, $J = 10.0, 2.0$ Hz, 1H), 6.08 (ddd, $J = 10.0, 3.1, 1.2$ Hz, 1H), 6.03 (ddd, $J = 10.1, 2.9, 1.1$ Hz, 1H), 3.06 (dddd, $J = 12.3, 5.0, 3.1, 2.0$ Hz, 1H), 2.81 (dt, $J = 16.8, 0.9$ Hz, 1H), 2.59 (dddt, $J = 19.1, 5.7, 4.8, 1.0$ Hz, 1H), 2.48 – 2.33 (m, 2H), 1.09 (d, $J = 1.0$ Hz, 3H); ^{13}C NMR (126 MHz, CDCl_3) δ 201.4, 198.2, 148.3, 146.9, 130.0, 128.3, 47.3, 45.8, 41.0, 28.2, 15.4; HRMS (ESI): Exact mass calc'd for $\text{C}_{11}\text{H}_{13}\text{O}_2$ $[\text{M}+\text{H}]^+$, 177.0916. Found 177.0911. HSQC data revealed the proton at 3.06 ppm to be the one at the ring fusion (only one proton on that carbon). 1D-NOE experiments irradiating the methyl peak at 1.09 ppm did not display a NOE interaction between this proton at 3.06 ppm, indicating a *trans*-relationship.



Compound II-175.

Coupled product **II-175a** (25.0 mg, 0.12 mmol, 1.6:1 mixture of diastereomers) was submitted to ring-closing metathesis conditions according to General Method D with elevated temperature, refluxing at 40 $^\circ\text{C}$, to afford **II-175** as a 1.6:1 mixture of diastereomers that could be separated by flash chromatography (major: 12.3 mg, 0.070 mmol, 58% yield; total yield: 19.8 mg, 0.11 mmol, 94%): $[\alpha]_D = +237.2$ (*c* 0.34, CHCl_3); IR (Germanium ATR): 2967, 1670, 1387, 1244, 817 cm^{-1} ; ^1H NMR (500 MHz, Chloroform-*d*) δ 6.87 (ddd, $J = 10.2, 5.8, 2.3$ Hz, 1H), 6.73 (d, $J =$

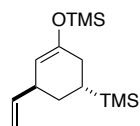
10.0 Hz, 1H), 6.12 (dd, $J = 10.2, 3.1$ Hz, 1H), 5.94 (dd, $J = 10.0, 1.0$ Hz, 1H), 3.04 (dd, $J = 13.5, 4.2$ Hz, 1H), 2.81 (dd, $J = 18.1, 4.2$ Hz, 1H), 2.58 (dt, $J = 18.5, 2.9$ Hz, 1H), 2.53 – 2.41 (m, 2H), 1.12 (s, 3H); ^{13}C NMR (126 MHz, CDCl_3) δ 198.2, 197.5, 156.0, 145.7, 129.6, 127.9, 51.7, 39.0, 38.9, 33.4, 17.7; HRMS (ESI): Exact mass calc'd for $\text{C}_{11}\text{H}_{13}\text{O}_2$ $[\text{M}+\text{H}]^+$, 177.0916. Found 177.0911. HSQC data revealed the proton at 3.04 ppm to be the one at the ring junction (only one proton on that carbon). 1D-NOE experiments irradiating the methyl peak at 1.12 ppm did not display a NOE interaction between this proton at 3.04 ppm, indicating a *trans*-relationship.



Compound II-176.

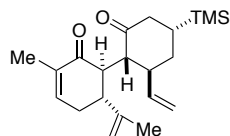
Coupled product **II-176a** (24.0 mg, 0.117 mmol, 1.3:1 mixture of diastereomers) was submitted to ring-closing metathesis conditions according to General Method D with elevated temperature, refluxing at 40 °C, to afford **II-176** as a 1.3:1 mixture of diastereomers that could not be separated by flash chromatography (16.5 mg, 0.094 mmol, 80% yield as a mixture of inseparable diastereomers): IR (Germanium ATR): 2920, 1667, 1388, 825 cm^{-1} ; ^1H NMR (500 MHz, Chloroform-*d*) δ 6.98 – 6.86 (m, 2H), 6.62 (ddd, $J = 11.6, 6.9, 5.7$ Hz, 1H), 6.50 (ddd, $J = 11.6, 7.2, 4.1$ Hz, 1H), 6.08 (dddd, $J = 11.4, 5.6, 2.7, 1.2$ Hz, 3H), 6.02 (dd, $J = 12.0, 2.6$ Hz, 1H), 3.16 (ddd, $J = 15.6, 4.9, 1.0$ Hz, 1H), 3.04 – 2.94 (m, 2H), 2.83 (dd, $J = 15.6, 6.9$ Hz, 1H), 2.76 – 2.72 (m, 1H), 2.72 – 2.65 (m, 2H), 2.59 (dddd, $J = 13.2, 11.9, 6.1, 3.1$ Hz, 2H), 2.53 (ddt, $J = 9.2, 4.1, 2.4$ Hz, 1H), 2.50 – 2.39 (m, 3H), 2.37 (ddd, $J = 9.4, 4.4, 2.0$ Hz, 1H), 2.33 (td, $J = 4.2, 1.4$ Hz, 1H), 2.32 – 2.23 (m, 1H); ^{13}C NMR (126 MHz, CDCl_3) δ 202.1, 201.8, 198.9, 198.0, 148.2, 147.9, 143.3, 142.5, 134.3, 133.0, 129.7, 129.6, 48.5, 45.7, 42.3, 40.5, 40.3, 37.6, 34.8, 33.7, 33.7, 32.7; HRMS (ESI): Exact mass calc'd for $\text{C}_{11}\text{H}_{13}\text{O}_2$ $[\text{M}+\text{H}]^+$, 177.0916. Found 177.0888.

2.9.5 Challenging systems



Compound II-214.

LiCl (50.4 mg, 1.19 mmol, 20 mol %) and CuI (113 mg, 0.59 mmol, 10 mol %) were added to a flame-dried flask, cooled to 0 °C, and (*R*)-**II-133** (1 g, 5.94 mmol) in THF (30 mL, with an additional 5 mL rinse) was added. TMS-Cl (0.83 mL, 6.53 mmol, 1.1 equiv) was added and the mixture stirred for 15 minutes before adding freshly prepared vinyl Grignard (1.0 M, 7.13 mL, 7.13 mmol, 1.2 equiv) dropwise over 25 minutes. After stirring for 20 minutes, the black reaction was poured into pH 7 buffer and extracted with ether. The combined organic extracts were washed with brine, dried over MgSO₄ and the solvent evaporated under reduced pressure. The crude material was purified by flash chromatography on silica gel with 5% ether/pentane (0.88 g, 3.3 mmol, 55%). This material was then used in the coupling reaction below, first regenerating the lithium enolate with methyllithium.

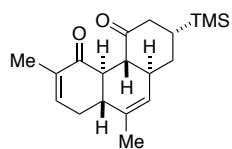


Compound II-189.

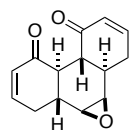
To a flame-dried round-bottom flask was added diisopropylamine (113 μL, 0.80 mmol, 1.2 equiv) and THF (0.8 mL). The mixture was cooled to -78 °C, and *n*-BuLi added (2.13 M, 0.35 mL, 0.74 mmol, 1.1 equiv). After 10 minutes at this temperature, carvone (*R*)-**II-35** (100 mg, 0.67 mmol) in THF (0.3 mL) was added and this solution stirred for 30 minutes before adding it in a slow and controlled manner over 45 minutes to a flame-dried flask containing iPr₂SiCl₂ (121 μL, 0.67 mmol, 1.0 equiv) and THF (2.7 mL), also at -78 °C (an additional 0.1 mL THF rinse). Meanwhile, the lithium enolate of **II-214** was prepared in a separate flask through the addition of MeLi (1.6 M, 0.46 mL, 0.74 mmol, 1.1 equiv) to **II-214** (180 mg, 0.67 mmol) in THF (0.8 mL) at -78 °C. This enolate (**II-187**) was added to the reaction flask after stirring for 25

minutes (37 minutes following the completion of the first enolate addition), over 45 minutes. Once the second enolate addition was complete, the mixture stirred at $-78\text{ }^{\circ}\text{C}$ for 15 minutes before warming to room temperature. After two hours, the solution was poured into pH 7 buffer and extracted with pentane. The combined organic extracts were dried over MgSO_4 , and the solvent evaporated under reduced pressure. The crude silyl bis-enol ether was placed on the vacuum manifold over night before using directly in the next reaction.

To a flame-dried flask was added CAN (0.81 g, 1.47 mmol, 2.2 equiv), NaHCO_3 (0.25 g, 2.95 mmol, 4.4 equiv), ACN (22 mL), and DMSO (95 μL , 1.34 mmol, 2.0 equiv). The mixture was cooled to $-30\text{ }^{\circ}\text{C}$, and the crude silyl bis-enol ether in EtCN (3 mL) was added via cannula to the vigorously stirring solution (an additional 0.4 mL EtCN rinse). After 3.3 hours, the orange heterogeneous reaction was poured into saturated NaHCO_3 solution and extracted with CHCl_3 . The combined organic extracts were dried over MgSO_4 before filtering through celite with EtOAc, and the solvent evaporated under reduced pressure. The crude material was purified by flash chromatography on silica gel with 5% EtOAc/hexanes (70.6 mg, 0.205 mmol, 31% yield): $[\alpha]_{\text{D}} = +38.7$ (*c* 1.35, CHCl_3); IR (Germanium ATR): 2953, 2856, 1709, 1668, 1250, 837 cm^{-1} ; ^1H NMR (500 MHz, Chloroform-*d*) δ 6.65 (ddt, $J = 5.8, 3.0, 1.4$ Hz, 1H), 5.57 (dt, $J = 17.1, 9.8$ Hz, 1H), 5.07 – 4.98 (m, 2H), 4.83 (d, $J = 1.7$ Hz, 2H), 3.32 (ddd, $J = 12.9, 11.3, 4.8$ Hz, 1H), 3.10 (dtd, $J = 11.2, 9.1, 6.7$ Hz, 1H), 2.56 (dd, $J = 12.7, 1.8$ Hz, 1H), 2.47 – 2.17 (m, 6H), 1.83 (ddd, $J = 14.1, 9.6, 6.8$ Hz, 1H), 1.75 (dt, $J = 2.6, 1.3$ Hz, 3H), 1.64 (d, $J = 1.3$ Hz, 3H), 1.62 – 1.54 (m, 1H), 0.01 (d, $J = 1.4$ Hz, 9H); ^{13}C NMR (126 MHz, CDCl_3) δ 213.8, 200.5, 145.7, 143.3, 141.7, 135.6, 116.0, 114.5, 50.6, 50.0, 48.4, 43.3, 40.4, 31.6, 30.4, 18.7, 18.3, 16.1, -3.3; LRMS (ESI): Exact mass calc'd for $\text{C}_{21}\text{H}_{33}\text{O}_5\text{Si}$ $[\text{M}+\text{H}]^+$, 345.2250. Found 345.32.

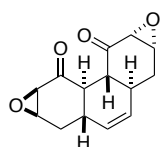
**Compound II-190.**

Grubbs II (9 mg, 0.010 mmol, 10 mol %) was added to a flame-dried round-bottom flask and diluted with DCM (1 mL). Coupled product **II-189** (34.5 mg, 0.10 mmol) in DCM (0.5 mL) was added to the flask (with an additional 0.5 mL rinse). The mixture was heated to 40 °C. Upon observed consumption of the starting material by TLC (5 hours), the reaction was cooled to room temperature and three drops of DMSO were added. After stirring over night, the solvent was removed, and the crude material was purified by flash chromatography on silica gel with 10% EtOAc/hexane (24.0 mg, 0.076 mmol, 76%): $[\alpha]_D = -343.2$ (c 1.04, CHCl_3); IR (Germanium ATR): 2949, 2860, 1715, 1683, 1251, 834 cm^{-1} ; ^1H NMR (500 MHz, Chloroform- d) δ 6.56 (dt, $J = 5.8, 1.8$ Hz, 1H), 5.28 (q, $J = 1.8$ Hz, 1H), 2.76 (dd, $J = 14.2, 8.3$ Hz, 1H), 2.71 – 2.57 (m, 3H), 2.42 – 2.29 (m, 2H), 2.21 – 2.05 (m, 2H), 1.92 (dt, $J = 13.6, 4.5$ Hz, 1H), 1.79 (dt, $J = 2.7, 1.4$ Hz, 3H), 1.73 (ddd, $J = 13.6, 12.2, 7.1$ Hz, 1H), 1.66 (dt, $J = 2.5, 1.3$ Hz, 3H), 1.61 – 1.54 (m, 1H), 0.00 (s, 9H); ^{13}C NMR (126 MHz, CDCl_3) δ 211.2, 200.4, 140.8, 136.3, 134.0, 126.3, 49.3, 47.9, 41.9, 41.2, 40.0, 32.4, 32.1, 23.7, 20.1, 15.9, -2.0; LRMS (ESI): Exact mass calc'd for $\text{C}_{19}\text{H}_{29}\text{O}_2\text{Si}$ $[\text{M}+\text{H}]^+$, 317.1937. Found 317.29.

2.9.6 Selective functionalization of prepared scaffolds**Compound II-193.**

Compound **II-148** (8.5 mg, 0.040 mmol) was diluted in DCM (1 mL) in a flame-dried round-bottom flask. NaHCO_3 (50.0 mg, 0.60 mmol, 15 equiv) was added at room temperature, followed by $m\text{CPBA}$ (18.0 mg, 0.10 mmol, 2.5 equiv). The solution stirred at room temperature until observed consumption of the starting material by TLC (2.5 h), after which it was diluted with saturated aqueous NaHCO_3 and extracted with DCM. The combined organic layers were washed

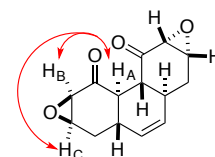
with brine, dried over MgSO_4 , and concentrated under reduced pressure. The crude material was purified by flash chromatography on silica gel with 30% EtOAc/hexanes to 50% EtOAc/hexanes gradient (6.2 mg, 0.027 mmol, 68% yield): $[\alpha]_D = -267.8$ (c 0.13, CHCl_3); IR (Germanium ATR): 2917, 1685, 1176, 793 cm^{-1} ; ^1H NMR (500 MHz, Chloroform- d) δ 6.86 – 6.71 (m, 2H), 6.06 (dtd, $J = 9.9, 4.1, 3.6, 2.0$ Hz, 2H), 3.22 (dd, $J = 3.9, 1.9$ Hz, 1H), 3.01 (d, $J = 3.8$ Hz, 1H), 2.75 – 2.66 (m, 1H), 2.66 – 2.51 (m, 3H), 2.51 – 2.40 (m, 2H), 2.29 (dtt, $J = 15.1, 6.6, 3.1$ Hz, 2H); ^{13}C NMR (126 MHz, CDCl_3) δ 199.7, 199.1, 145.0, 144.6, 130.7, 130.2, 56.3, 54.6, 46.2, 43.2, 38.3, 37.9, 32.8, 31.3; HRMS (ESI): Exact mass calc'd for $\text{C}_{14}\text{H}_{15}\text{O}_3$ $[\text{M}+\text{H}]^+$, 231.1021. Found 231.1017.



Compound II-194.

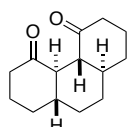
II-148 (12.0 mg, 0.056 mmol) was diluted in a flame-dried round bottom flask with MeOH (0.7 mL), and 30% H_2O_2 was added (35 μL , 0.30 mmol, 5.0 equiv) The mixture was cooled to 0 $^\circ\text{C}$, and aqueous NaOH (1M, 0.12 mL, 0.12 mmol, 2.0 equiv) was added. The reaction was warmed to room temperature. Upon observed consumption of starting material by TLC (2.5h), the reaction was poured into saturated aqueous $\text{Na}_2\text{S}_2\text{O}_3$ and extracted with ether. The combined organic layers were washed with brine, dried over MgSO_4 , and concentrated under reduced pressure. The crude material was purified by flash chromatography with 20% EtOAc/hexanes (9.6 mg, 0.039 mmol, 70% yield): IR (Germanium ATR): 2919, 2850, 1783, 1241,

733 cm^{-1} ; ^1H NMR (500 MHz, Chloroform- d) δ 5.42 (d, $J = 2.4$ Hz, 1H), 3.60 (q, $J = 3.9$ Hz, 1H), 3.38 – 3.28 (m, 1H), 2.98 (dd, $J = 8.8, 3.1$ Hz, 1H), 2.46



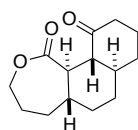
(s, 1H), 2.24 (dt, $J = 14.5, 5.0$ Hz, 1H), 1.90 (t, $J = 13.7$ Hz, 1H); ^{13}C NMR (126 MHz, CDCl_3) δ 205.9, 128.5, 58.4, 55.7, 42.4, 41.5, 30.0; HRMS (ESI): Exact mass calc'd for $\text{C}_{14}\text{H}_{14}\text{O}_4\text{Na}$ $[\text{M}+\text{Na}]^+$, 269.0790. Found 269.0770.

The ^1H NMR and ^{13}C NMR spectra are symmetrical, proving preservation of C_2 symmetry in the product. The epoxide stereochemistry was elucidated through COSY and NOESY NMR spectra, as each proton was assigned, and NOE interactions observed between proton H_A and protons H_B and H_C .



Compound II-195.

II-148 (46.0 mg, 0.21 mmol) was diluted in a flame-dried round bottom flask with MeOH (4 mL). Pd/C (22.8 mg, 0.021 mmol, 10 mol %) was added at room temperature. H_2 was bubbled through the solution for 1 minute, and then the reaction stirred under H_2 overnight. The reaction was then purged with N_2 for 10 minutes before filtering through Celite with EtOAc. The solvent was evaporated under reduced pressure, and the crude material was purified by flash chromatography with 20% EtOAc/hexanes (45.7 mg, 0.21 mmol, 99% yield): IR (Germanium ATR): 2922, 2851, 1709, 1447 cm^{-1} ; ^1H NMR (499 MHz, Chloroform-*d*) δ 2.56 – 2.48 (m, 1H), 2.47 – 2.41 (m, 1H), 2.35 (ddt, $J = 12.4, 4.2, 1.9$ Hz, 1H), 2.10 (dddt, $J = 12.8, 6.3, 4.3, 2.4$ Hz, 1H), 1.82 – 1.74 (m, 2H), 1.65 (qt, $J = 13.4, 4.2$ Hz, 1H), 1.54 – 1.44 (m, 1H), 1.40 (dtq, $J = 11.3, 8.5, 2.8$ Hz, 1H), 1.19 – 1.13 (m, 1H); ^{13}C NMR (126 MHz, CDCl_3) δ 211.4, 53.2, 44.8, 42.2, 33.2, 33.0, 27.8; HRMS (ESI): Exact mass calc'd for $\text{C}_{14}\text{H}_{20}\text{O}_2\text{Na}$ $[\text{M}+\text{Na}]^+$, 243.1361. Found 243.1354.

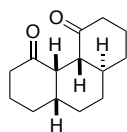
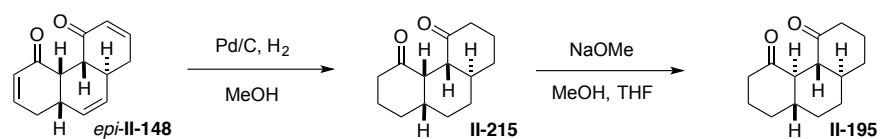


Compound II-196.

Trifluoroacetic acid was prepared by the addition of CHCl_3 (3 mL) and TFAA (445 μL , 3.2 mmol, 65 equiv) to a flame-dried round-bottom flask. The flask was cooled to 0°C and 30 wt% H_2O_2 (180 μL , 1.6 mmol, 32 equiv) was added to this solution dropwise. After five minutes, this solution was added dropwise over 15 minutes to another flame-dried round-bottom flask with **II-195** (10.0 mg, 0.045 mmol), CHCl_3 (1 mL), and Na_2HPO_4 (130 mg, 0.92 mmol, 18

equiv) at 0 °C. Upon observed consumption of the starting material by TLC (3h), the mixture was slowly poured into saturated aqueous NaHSO₃ and extracted twice with CHCl₃ and once with EtOAc. The combined organic layers were washed with brine, dried over MgSO₄, and concentrated under reduced pressure. The crude material was purified by flash chromatography on silica gel with 20% EtOAc/hexanes (5.8 mg, 0.025 mmol, 56% yield): $[\alpha]_D = -6.7$ (*c* 0.13, CHCl₃); IR (Germanium ATR): 2918, 2850, 1728, 1713, 1463 cm⁻¹; ¹H NMR (499 MHz, Chloroform-*d*) δ 4.40 (dd, *J* = 12.5, 10.4 Hz, 1H), 4.36 – 4.26 (m, 1H), 2.87 (ddd, *J* = 12.1, 10.5, 1.1 Hz, 1H), 2.75 (t, *J* = 10.8 Hz, 1H), 2.48 (tdd, *J* = 13.7, 6.3, 1.1 Hz, 1H), 2.38 (ddt, *J* = 13.1, 4.3, 2.2 Hz, 1H), 2.15 – 2.06 (m, 1H), 2.03 – 1.90 (m, 2H), 1.86 (dt, *J* = 13.6, 3.9 Hz, 2H), 1.82 – 1.71 (m, 2H), 1.71 – 1.61 (m, 1H), 1.47 (dtd, *J* = 15.3, 7.7, 3.8 Hz, 1H), 1.40 – 1.29 (m, 2H), 1.30 – 1.17 (m, 2H), 1.01 (tdd, *J* = 13.5, 11.5, 3.6 Hz, 1H); ¹³C NMR (126 MHz, CDCl₃) δ 211.4, 177.2, 68.1, 55.8, 43.2, 43.2, 42.0, 37.9, 35.3, 34.3, 33.1, 32.5, 28.4, 27.1; HRMS (ESI): Exact mass calc'd for C₁₄H₂₁O₃ [M+H]⁺, 237.1491. Found 237.1478.

Scheme 2.34 Epimerization of the minor stereochemistry to the major, all-*trans* **II-195**



Compound II-215.

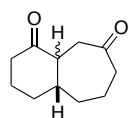
The same procedure was followed as for the formation of **compound II-195** above.

Compound *epi-II-148* (110.0 mg, 0.51 mmol) was diluted in a flame-dried flask with MeOH (9.6 mL). Pd/C (55.0 mg, 0.051 mmol, 10 mol %) was added at room temperature. H₂ was bubbled through solution for 1 minute, and then the reaction stirred under H₂ overnight. The reaction was then purged with N₂ for 10 minutes before filtering through Celite with EtOAc. The solvent was

evaporated under reduced pressure, yielding the clean hydrogenated product (101.5 mg, 0.46 mmol, 90%): $[\alpha]_D = -37.1$ (c 0.19, CHCl_3); IR (Germanium ATR): 2924, 2851, 1704, 1446, 1121 cm^{-1} ; ^1H NMR (500 MHz, Chloroform- d) δ 3.30 (t, $J = 4.4$ Hz, 1H), 2.52 (ddt, $J = 16.1, 4.8, 2.3$ Hz, 1H), 2.42 (td, $J = 13.4, 6.4$ Hz, 1H), 2.28 (ddt, $J = 13.3, 4.1, 2.2$ Hz, 1H), 2.19 (ddd, $J = 16.2, 12.7, 6.4$ Hz, 2H), 2.05 (qq, $J = 12.5, 5.0, 4.2$ Hz, 1H), 1.94 (tdd, $J = 14.2, 6.9, 3.8$ Hz, 3H), 1.89 – 1.76 (m, 4H), 1.72 – 1.61 (m, 2H), 1.45 – 1.35 (m, 1H), 1.25 (dtd, $J = 17.3, 13.3, 4.2$ Hz, 2H), 1.16 – 1.01 (m, 1H); ^{13}C NMR (126 MHz, CDCl_3) δ 210.3, 209.6, 55.6, 49.6, 42.6, 41.4, 40.5, 36.9, 34.1, 32.3, 31.0, 27.7, 23.9, 23.5; HRMS (ESI): Exact mass calc'd for $\text{C}_{14}\text{H}_{20}\text{O}_2\text{Na}$ $[\text{M}+\text{Na}]^+$, 243.1361. Found 243.1360.

*To epimerize to the all trans conformation **II-195**:*

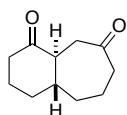
II-215 (135.0 mg, 0.61 mmol) was dissolved in THF (6 mL, 0.10 M). NaOMe (1.53 mL, 1 M in MeOH, 1.53 mmol, 2.5 equiv) was added at room temperature. After stirring for 50 minutes, the yellow mixture was quenched with saturated NH_4Cl and extracted with ether. The combined organic extracts were dried over MgSO_4 and the solvent evaporated under reduced pressure, yielding the cleanly epimerized material, **II-195** (134.8 mg, 0.61 mmol, quantitative yield).



Compound II-216.

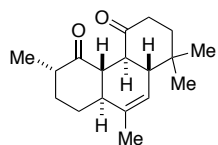
II-176, a 1.3:1 mixture of diastereomers, (5.0 mg, 0.03 mmol) was diluted in a flame-dried flask with MeOH (1 mL). Pd/C (3.2 mg, 0.003 mmol, 10 mol %) was added at room temperature. H_2 was bubbled through solution for 1 minute, and then the reaction stirred under H_2 overnight. The reaction was then purged with N_2 for 10 minutes before filtering through Celite with EtOAc. The solvent was evaporated under reduced pressure, yielding the clean hydrogenated product as a mixture of diastereomers (5.0 mg, 0.03 mmol, quantitative yield): ^1H NMR (500 MHz,

Chloroform-*d*) δ 2.98 – 2.92 (m, 1H), 2.88 (d, $J = 12.6$ Hz, 1H), 2.64 (t, $J = 12.1$ Hz, 1H), 2.56 (dt, $J = 17.7, 4.0$ Hz, 1H), 2.50 (dd, $J = 16.8, 6.5$ Hz, 1H), 2.36 (dddd, $J = 33.0, 22.8, 16.3, 11.9$ Hz, 6H), 2.23 (t, $J = 11.5$ Hz, 1H), 2.12 – 1.90 (m, 6H), 1.90 – 1.48 (m, 11H), 1.31 – 1.20 (m, 3H); ^{13}C NMR (126 MHz, CDCl_3) δ 214.3, 212.7, 211.4, 209.8, 53.6, 50.9, 49.1, 44.1, 44.0, 43.8, 42.2, 41.8, 41.5, 41.2, 36.7, 34.1, 32.4, 32.0, 26.4, 23.3, 22.6, 22.3.

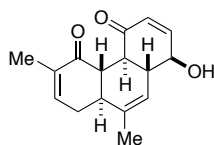


Compound II-197.

The same epimerization conditions were used as detailed above, converting the mixture of hydrogenated diastereomers into the *trans* product. **II-216** (5.0 mg, 0.03 mmol) was dissolved in THF (0.5 mL). NaOMe (75 μL , 1 M in MeOH, 0.08 mmol, 2.5 equiv) was added at room temperature. After stirring for 20 minutes, the yellow mixture was quenched with saturated NH_4Cl and extracted with ether. The combined organic extracts were dried over MgSO_4 and the solvent evaporated under reduced pressure, yielding a single diastereomer where the minor diastereomer had successfully epimerized to the major *trans*-product, **II-197** (5.0 mg, 0.03 mmol, quantitative yield): $[\alpha]_{\text{D}} = -15.4$ (c 0.23, CHCl_3); IR (Germanium ATR): 2918, 2849, 1701, 1462, 1091 cm^{-1} ; ^1H NMR (500 MHz, Chloroform-*d*) δ 2.88 (dd, $J = 12.7, 1.7$ Hz, 1H), 2.67 – 2.60 (m, 1H), 2.56 (dddd, $J = 17.6, 4.9, 3.2, 1.3$ Hz, 1H), 2.45 – 2.26 (m, 3H), 2.23 (tt, $J = 11.4, 1.4$ Hz, 1H), 2.07 (dtd, $J = 12.6, 6.2, 3.2$ Hz, 1H), 2.04 – 1.98 (m, 1H), 1.98 – 1.91 (m, 1H), 1.87 – 1.79 (m, 1H), 1.77 – 1.68 (m, 1H), 1.68 – 1.59 (m, 1H), 1.56 – 1.48 (m, 1H), 1.26 (d, $J = 9.9$ Hz, 2H); ^{13}C NMR (126 MHz, CDCl_3) δ 214.3, 209.8, 53.6, 49.1, 43.8, 41.8, 41.5, 36.7, 34.1, 26.4, 22.3; HRMS (EI): Exact mass calc'd for $\text{C}_{11}\text{H}_{16}\text{O}_2$ $[\text{M}]^+$, 180.1150. Found 180.1148.

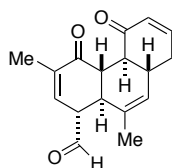
**Compound II-198.**

A solution of **II-167** (8.0 mg, 0.030 mmol) in THF (0.6 mL) was cooled to $-78\text{ }^{\circ}\text{C}$ and a solution of L-selectride was added dropwise (1 M, 90 μL , 0.088 mmol, 2.4 equiv). The reaction was maintained at this temperature, and upon observed consumption of the starting material by TLC, (2h) the gold reaction was warmed to $0\text{ }^{\circ}\text{C}$ and quenched with saturated NH_4Cl solution. The mixture was extracted with EtOAc, the combined organic extracts were dried over Na_2SO_4 , and the solvent evaporated under reduced pressure. The crude material was flashed with 2% EtOAc/hexanes (4.5 mg, 0.016, 54%): $[\alpha]_{\text{D}} = +197.6$ (c 0.20, CHCl_3); IR (Germanium ATR): 2963, 2929, 1719, 1690, 1373 cm^{-1} ; ^1H NMR (499 MHz, Chloroform- d) δ 5.35 (s, 1H), 2.82 (t, $J = 11.3$ Hz, 1H), 2.75 – 2.65 (m, 2H), 2.61 (t, $J = 11.1$ Hz, 1H), 2.28 – 2.19 (m, 2H), 2.19 – 2.10 (m, 1H), 2.06 – 1.95 (m, 2H), 1.84 – 1.78 (m, 1H), 1.70 (s, 3H), 1.69 – 1.58 (m, 1H), 1.44 (t, $J = 11.7$ Hz, 1H), 1.38 – 1.28 (m, 1H), 1.03 (d, $J = 3.6$ Hz, 9H); ^{13}C NMR (126 MHz, CDCl_3) δ 212.6, 211.9, 136.7, 122.5, 52.3, 51.6, 47.3, 46.0, 45.1, 43.1, 39.3, 37.2, 33.9, 29.7, 28.6, 21.4, 19.7, 14.4; HRMS (ESI): Exact mass calc'd for $\text{C}_{18}\text{H}_{26}\text{O}_2\text{Na}$ $[\text{M}+\text{Na}]^+$, 297.1831. Found 297.1831.

**Compound II-217.**

To a solution of **II-168** (14.7 mg, 0.039 mmol) in THF (0.5 mL) at $0\text{ }^{\circ}\text{C}$ was added a solution of 1 M TBAF in THF dropwise (50 μL , 0.05 mmol, 1.3 equiv). Upon observed consumption of starting material by TLC (40 min), the reaction was filtered through silica gel with EtOAc and the solvent evaporated under reduced pressure. The crude material was purified by flash chromatography on silica gel with 30% to 50% EtOAc/hexanes (9.3 mg, 0.036 mmol, 91%): $[\alpha]_{\text{D}} = +499.1$ (c 0.39, CHCl_3); IR (Germanium ATR): 3435, 2922, 2855, 1679, 1372, 1052, 806 cm^{-1} ; ^1H NMR (500 MHz, Chloroform- d) δ 6.70 (dd, $J = 10.2, 2.0$ Hz, 1H), 6.55 (dt, $J = 5.7, 1.8$

Hz, 1H), 6.04 (dd, $J = 10.2, 2.4$ Hz, 1H), 5.73 (q, $J = 1.9$ Hz, 1H), 4.27 (dt, $J = 9.6, 2.2$ Hz, 1H), 2.74 – 2.63 (m, 3H), 2.43 (tdd, $J = 11.6, 4.5, 2.3$ Hz, 1H), 2.35 (td, $J = 11.7, 11.1, 5.9$ Hz, 1H), 2.14 (ddq, $J = 18.5, 10.9, 2.5$ Hz, 1H), 1.97 (d, $J = 15.9$ Hz, 1H), 1.83 (dt, $J = 2.9, 1.5$ Hz, 3H), 1.72 (q, $J = 1.6$ Hz, 3H); ^{13}C NMR (126 MHz, CDCl_3) δ 200.5, 199.5, 148.8, 140.3, 136.6, 135.8, 130.1, 120.3, 73.1, 47.7, 47.0, 45.0, 41.4, 32.2, 20.3, 15.9; HRMS (ESI): Exact mass calc'd for $\text{C}_{16}\text{H}_{18}\text{O}_3\text{Na}$ $[\text{M}+\text{Na}]^+$, 281.1154. Found 281.1159.



Compound II-218.

To a solution of **II-169** (10.0 mg, 0.031 mmol) in acetone (0.5 mL) was added I_2 (~1 mg) at room temperature. The brown reaction stirred at room temperature for 20 minutes before quenching with saturated $\text{Na}_2\text{S}_2\text{O}_3$. The mixture was extracted with DCM, the combined organic extracts were dried over Na_2SO_4 , and the solvent evaporated under reduced pressure. The crude material was purified by flash chromatography on silica gel with 20% EtOAc/hexanes (7.8 mg, 0.029 mmol, 93%): $[\alpha]_{\text{D}} = +260.7$ (c 0.31, CHCl_3); IR (Germanium ATR): 3026, 2920, 2825, 1724, 1685, 1378, 1042, 749 cm^{-1} ; ^1H NMR (500 MHz, Chloroform- d) δ 9.59 (d, $J = 3.7$ Hz, 1H), 6.80 (ddd, $J = 10.1, 5.2, 2.2$ Hz, 1H), 6.06 (dd, $J = 10.1, 3.0$ Hz, 1H), 6.01 (dq, $J = 3.3, 1.7$ Hz, 1H), 5.34 (q, $J = 1.8$ Hz, 1H), 3.35 (ddt, $J = 9.9, 3.6, 2.4$ Hz, 1H), 2.96 – 2.89 (m, 1H), 2.82 (dd, $J = 12.6, 10.8$ Hz, 1H), 2.75 (dd, $J = 12.3, 10.8$ Hz, 1H), 2.55 – 2.45 (m, 2H), 2.24 (ddt, $J = 19.3, 12.0, 2.5$ Hz, 1H), 1.94 – 1.89 (m, 3H), 1.61 (dt, $J = 2.6, 1.4$ Hz, 3H); ^{13}C NMR (126 MHz, CDCl_3) δ 200.0, 199.5, 199.5, 145.8, 141.3, 133.2, 132.2, 130.5, 126.8, 57.1, 46.7, 44.6, 40.4, 38.3, 34.3, 23.3, 16.3; HRMS (ESI): Exact mass calc'd for $\text{C}_{17}\text{H}_{18}\text{O}_3\text{Na}$ $[\text{M}+\text{Na}]^+$, 293.1154. Found 293.1159.

2.9.7 Cell viability assays

2.9.7.1 Cell line growth conditions

Cell lines PC-3, HT29, HeLa, and MDA-MB-231 were cultured in RPMI1640 with 10% FBS media. Cell line MDA-MB-231-LM24 was cultured in DMEM with 400 $\mu\text{g}/\text{mL}$ geneticin.

Normal breast cell line MCF10A was cultured in DMEM/F12 with 5% horse serum, 20 ng/mL EGF, 0.5 mg/mL hydrocortisone, 100 ng/mL cholera toxin, 10 $\mu\text{g}/\text{mL}$ insulin, and 1% pen/strep.

2.9.7.2 Cell viability experiments at 1 mM

PC-3, HT29, HeLa, and MDA-MB-231, and MDA-MB-231-LM24 cells were plated in 96-well black plates at a density of 20,000 cells per well (based on NCI recommendation for adherent cells) in 90 μL volume of 5% FBS RPMI1640 complete media with 50 $\mu\text{g}/\text{mL}$ gentamicin and incubated at 37 °C overnight. Each compound was diluted in RPMI1640 complete media supplemented with 5% FBS and 50 $\mu\text{g}/\text{mL}$ of gentamycin, and 10 μL of this solution was added to each well to give a final concentration of 1 mM (1% overall DMSO, N=4 wells).

Normal breast cells (MCF10A) were plated in 96-well black plates at a density of 20,000 cells per well (based on the NCI recommendation for adherent cells) in 90 μL volume of DMEM/F12 with 2% horse serum, 0.5 $\mu\text{g}/\text{mL}$ hydrocortisone, 100 ng/mL cholera toxin, 10 $\mu\text{g}/\text{mL}$ insulin, and 1% pen/strep, and incubated at 37 °C overnight. The compounds were diluted in the media specified above, and 10 μL of this solution was added to each well to give a final concentration of 1 mM (1% overall DMSO, N=4 wells). Cells treated with media containing 1% DMSO were used as a negative control.

48 hours following treatment, cell proliferation was evaluated using the CellTiter-GLO Luminescent Cell Viability Assay (Promega, Madison, WI). Plates were allowed to equilibrate to

room temperature for 20 minutes, and 100 μ L of CellTiter-GLO reagent was added to all wells. The plates were shaken for 2 minutes and incubated at room temperature for 10 minutes. Luminescence was measured using a Synergy H1-M microplate reader (BioTek Instruments, Inc.).

2.9.7.3 IC50 experiments

The compound was diluted in RPMI1640 complete media supplemented with 5% FBS and 50 μ g/mL of gentamycin, and 10 μ L of this solution was added to each well to give a final concentration of 0.00001-1 mM (N=4 wells). DMSO was held constant at 1%, for all dose points.

48 hours following treatment, cell proliferation was evaluated using the CellTiter-GLO Luminescent Cell Viability Assay (Promega, Madison, WI). Plates were allowed to equilibrate to room temperature for 20 minutes, and 100 μ L of CellTiter-GLO reagent was added to all wells. The plates were shaken for 2 minutes and incubated at room temperature for 10 minutes. Luminescence was measured using a Synergy H1-M microplate reader (BioTek Instruments, Inc.). The IC50 value was determined by Prism GraphPad Software.

Chapter 3

Application of the Developed “Couple and Close” Strategy to the Synthesis of Antimalarial
Diterpene (+)-7,20-Diisocyanoadociane

Portions of this chapter appear in the following publication:

Emily E. Robinson and Regan J. Thomson, A Strategy for the Convergent and Stereoselective
Assembly of Polycyclic Molecules. *J. Am. Chem. Soc.* **2018**, *140*, 1956–1965.

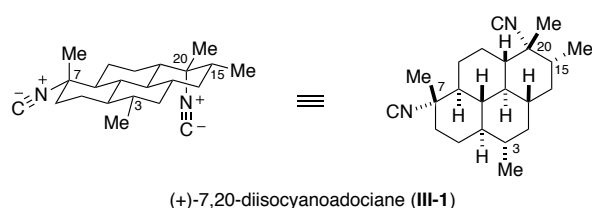
3 Chapter 3

3.1 Introduction

The development of novel synthetic methods and approaches enables strategic innovation for the construction of complex natural products with desirable properties for further investigation. Complex structures from nature with inherently selective and potent bioactivities serve as unlimited inspiration for effective therapeutics and as a testing ground for novel synthetic methods and strategies. The continued synthetic innovation by combining strategy and methods development is invaluable to the exploration of these great sources for advanced bioactivity.

This chapter will discuss the application of the developed “couple and close” strategy for the construction of fused polycyclic structures (Chapter 2) to the synthesis of marine diterpenoid (+)-7,20-diisocyanoadociane (DICA, **III-1**, Figure 3.1). This unique strategic development enabled the synthesis of this intricate natural product, demonstrating the ability to employ the approach in complex molecule synthesis in order to facilitate further investigations of bioactive compounds.

Figure 3.1 Diterpene 7,20-diisocyanoadociane **III-1**



3.2 Isocyanoterpenes

3.2.1 Structure of isocyanoterpenes

Isocyanoterpenes (ICTs) are a class of over 130 terpene natural products isolated from marine organisms that contain nitrogenous functionality (i.e. isonitrile, isocyanate, formamide, and

isothiocyanate) which imparts an array of biological activity among the family. These compounds have been of interest to chemists and biologists alike due to their noteworthy biological properties, complex chemical structures, and unique nitrogen-containing functionality suggesting interesting biosynthetic pathways. As such, they have been central to many investigations and reviewed in different capacities over the years.²⁶⁴⁻²⁷⁰

Within this class of molecules exists a wide assortment of structures with varied carbocyclic composition (Figure 3.2), all of which contain a dense array of stereocenters and are equipped with nitrogenous functionality.

Figure 3.2 Various ICT carbocyclic scaffolds

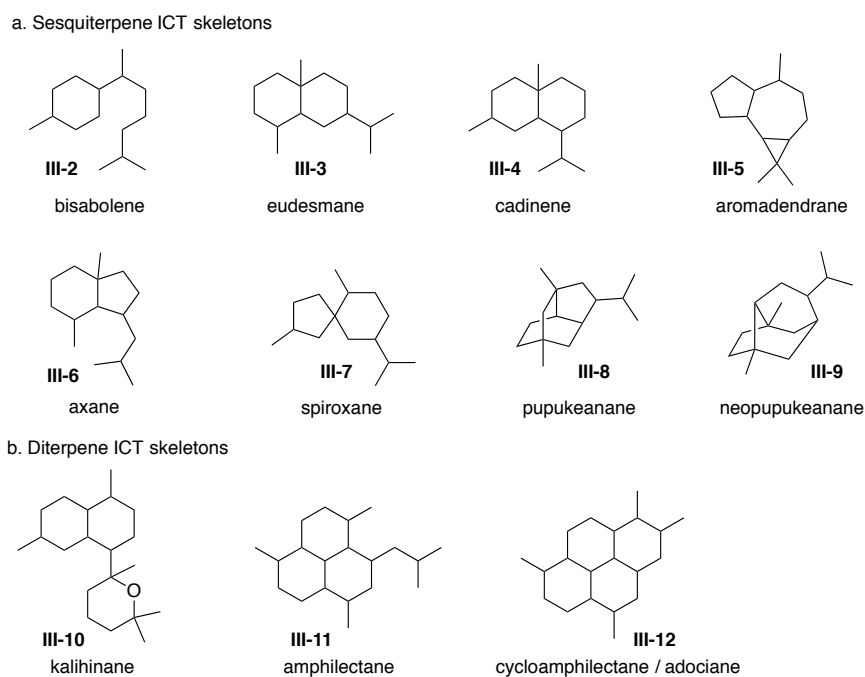


Figure 3.2a depicts representative sesquiterpene carbon skeletons, demonstrating a vast diversity from the monocyclic bisabolene core (**III-2**) to the bicyclic cores of varying ring size and fusion (**III-3–III-7**), to the tricyclic pupukeananes (**III-8** and **III-9**). Figure 3.2b exhibits representative

diterpenoid scaffolds, showing the tricyclic kalihinane (**III-10**) and amphilectane cores (**III-11**), as well as the tetracyclic cycloamphilectane, or adociane, scaffold (**III-12**). The perhydropyrene core of the cycloamphilectane family (**III-12**) will be the main focus of the discussion herein. Isolated in 1976 from the *Cymbastela hooperi* species of *Adocia* sponges on the Great Barrier Reef near Townsville, Australia, 7,20-diisocyanoadociane (**III-1**, Figure 3.1) was the first isocyanoterpene to be isolated containing a perhydropyrene core.²⁷¹ The unique structure boasts all-*trans* stereochemistry about the ring junctions with two equatorial methyl substituents at C3 and C15. One of the molecule's most intriguing and challenging structural features lies in the two isonitrile substituents at C7 and C20, occupying the equatorial and axial positions, respectively.

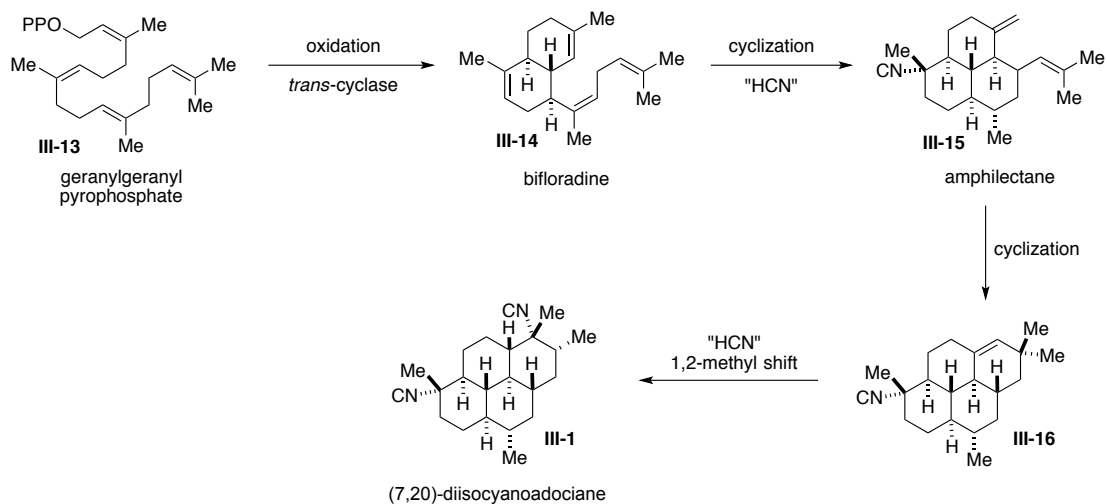
3.2.2 Biosynthesis of diterpenoid isonitriles

3.2.2.1 Construction of the carbocyclic core

The biosynthesis of terpenes has been heavily investigated and as such, the construction of the core structures of many ICTs is well understood, with the introduction of the nitrogen-containing functionality following the production of the carbocyclic scaffold.²⁶⁷ Diterpenes are derived from geranylgeranyl pyrophosphate **III-13**, and as shown in Scheme 3.1, upon oxidation and enzyme-facilitated cyclization of **III-13**, bicyclic bifloradine intermediate **III-14** can be produced bearing the *trans*-relationship as shown, or the *cis*-relationship, depending on the enzyme. This is a key intermediate for the biosynthesis of a variety of structurally distinct ICTs, but with respect to the biosynthesis of DICA **III-1**, a subsequent cyclization and hydroisocyanation event, which will be discussed in more detail later in the section, delivers the tricyclic amphilectane **III-15**. Following the cyclization of **III-15** to produce tetracyclic cycloamphilectane **III-16**,

another hydroisocyanation with accompanying 1,2-methyl shift is required for the conversion to DICA **III-1**, although the exact process by which this occurs has not been yet proven.²⁶⁷

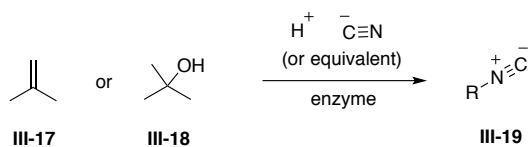
Scheme 3.1 Proposed biosynthesis of diisocyanoadociane **III-1**



3.2.2.2 Incorporation of nitrogen-containing functionality

Nature's integration of the nitrogen-containing functionality to this class of molecules has been of great interest to the scientific community. It was originally hypothesized that the addition of ammonia to a carbenium ion would result in an amine that could be alkylated and subsequently dehydrated to the isocyanide.²⁷² However, it is now widely accepted that either unsaturation within the terpene structures can undergo a hydroisocyanation with inorganic cyanide, or the corresponding alcohol can be ionized and trapped by a cyanide ion (Scheme 3.2).^{266, 270}

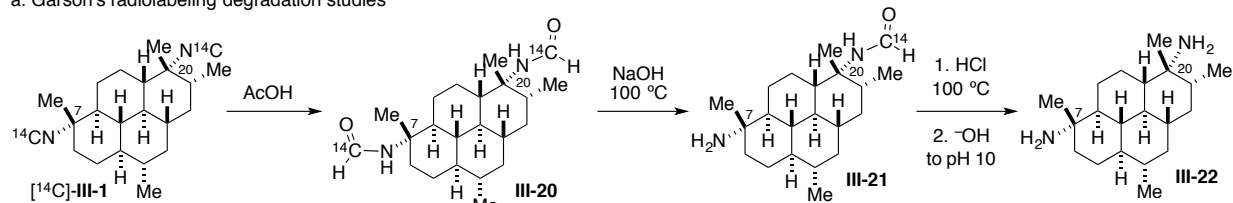
Scheme 3.2 Proposed isocyanide incorporation



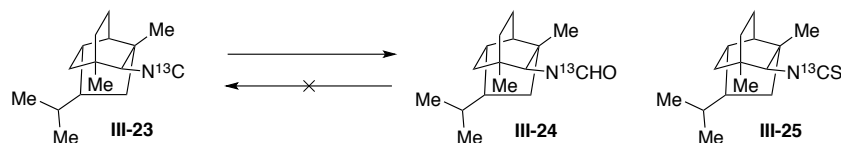
Garson and coworkers demonstrated for the first time in the late 1980s that the isocyanide substituents of 7,20-diisocyanoadociane **III-1** were indeed derived from inorganic cyanide, as experiments incorporating [^{14}C]-cyanide into the sponge species led to the production of radioactive [^{14}C]-**III-1**.²⁷²⁻²⁷³ As shown in Scheme 3.3a, it was proven that the isonitrile functionality was responsible for this radioactivity through a series of hydrolyses. The first hydrolysis product, bis(formamide) **III-20**, preserved 96% of the radioactivity of the bis(isonitrile) [^{14}C]-**III-1**; the subsequent monoformamide intermediate **III-21** retained 49% of the radioactivity; and finally, the bis(amine) species **III-22** only maintained 1.5–3.7% of the radioactivity, resulting from slight amide impurities. These studies have led to the understanding of how the common isonitrile functionality is naturally inserted into these molecules, and as ICTs are often isolated alongside the corresponding isothiocyanates, formamides, and amines, many research groups have investigated the biological process for the incorporation of these alternative functionalities.

Scheme 3.3 Origin of isonitrile, formamide, and isothiocyanate functionalities

a. Garson's radiolabeling degradation studies



b. Scheuer's demonstration of isonitrile conversion



For example, Scheuer and Hagadone demonstrated the potential for the isonitrile within 2-isocyanopopukeanane **III-23** to be converted to formamide **III-24** and isothiocyanate **III-25** functionalities through [^{13}C]-labeling experiments, showing that the reverse reactions converting

the isothiocyanate or formamide into the isonitrile did not occur (Scheme 3.3b).²⁷⁴ Later, Garson and coworkers established cyanide to be a common precursor to isonitrile, isothiocyanate, and the less common thiocyanate-containing molecules, indicating the ability for marine sponges to interconvert cyanide and thiocyanate at the inorganic level.^{266-267, 275-276}

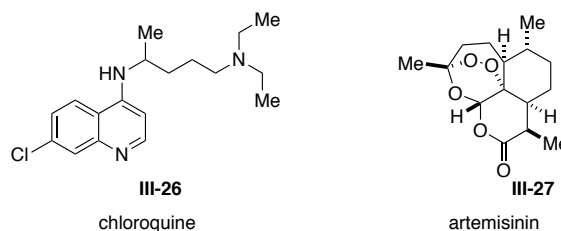
3.2.3 *Bioactivity of isocyanoterpenes*

Marine ICTs have been investigated for a variety of biological activities. In general, the family displays only weak cytotoxic activity in mammalian cells, and demonstrates low toxicity.²⁷⁰ The kalihinol family of diterpenes have exhibited some antibacterial activity, and some amphilectane diterpenes have revealed anti-inflammatory activity.²⁷⁰

However, this class of compounds is known for their potent and selective antimalarial activity, serving as lead compounds for novel malaria therapeutics development. Malaria is a devastating disease transmitted by mosquitos that affected 91 countries in 2016, with the large majority of cases occurring in sub-Saharan Africa.²⁷⁷ According to the World Health Organization's most recent annual report, roughly 216 million cases of malaria occurred in 2016, 99% of which can be attributed to the most common malaria parasite, *Plasmodium falciparum*, and 445,000 of which resulted in death.²⁷⁷ The major challenges confronting the elimination of this disease include a general lack of sufficient funding, the prevalence of the disease in conflict-containing areas, and the development of resistance of mosquitos to insecticides and the parasite to current therapeutics. While impressive effort and funds have been supplied since 2000 to discover novel treatments and create distribution programs for less economically fortunate areas, the discovery of novel therapeutics to combat the increasing resistance to available medicines is of ever-growing importance.²⁷⁷

The need for architecturally complex structures to enhance the selective action of available drugs is represented in the history of malaria therapeutics. Early drugs, such as chloroquine (**III-26**, Figure 3.3) are flat, composed of a quinoline ring system with only one sp^3 -center, however developing resistance to this compound led to a shift to topologically complex artemisinin-based treatments (**III-27**), with seven chiral centers and four fused rings.²⁷⁸ Adverse effects have been reported far less frequently with artemisinin-based treatments than for chloroquine, implicating structural sophistication in the selective action leading to less off-target effects.²⁷⁹⁻²⁸⁰ As the compound has saved millions of lives, the 2015 Nobel Prize in Physiology or Medicine was awarded to Professor Youyou Tu for her role in its discovery.²⁸¹ Unfortunately, however, it too is beginning to suffer from growing resistance, driving the critical demand for the development of new chemotypes for supplementary therapeutics.²⁷⁸

Figure 3.3 Common malaria therapeutics



3.2.3.1 Mechanism of antimalarial activity

Marine isocyanoterpenes have displayed potent antimalarial activities, and as such, have sparked an interest from the chemical and biological communities. Although the antimalarial action of marine ICTs is complicated and not fully understood, the isonitrile functionality is proposed to bind to iron porphyrins, forming a complex that inhibits the transformation of heme into β -hematin, disrupting a process that is necessary for parasite survival. These compounds also inhibit the peroxide- and glutathione-facilitated destruction of heme. The resulting buildup of toxic

heme substances is responsible for destroying the parasitic membrane and proteins.^{267, 282} This inhibition of heme detoxification is the process by which quinoline antimalarial therapeutics have been known to derive their activity.²⁸³ However, it has been recently revealed that these quinoline-based compounds may have additional productive targets in addition to binding heme that add to the desired activity, and as such, continued research in this area is required to better understand the complete process and provide an informed path forward for optimal therapeutic development.²⁸⁴

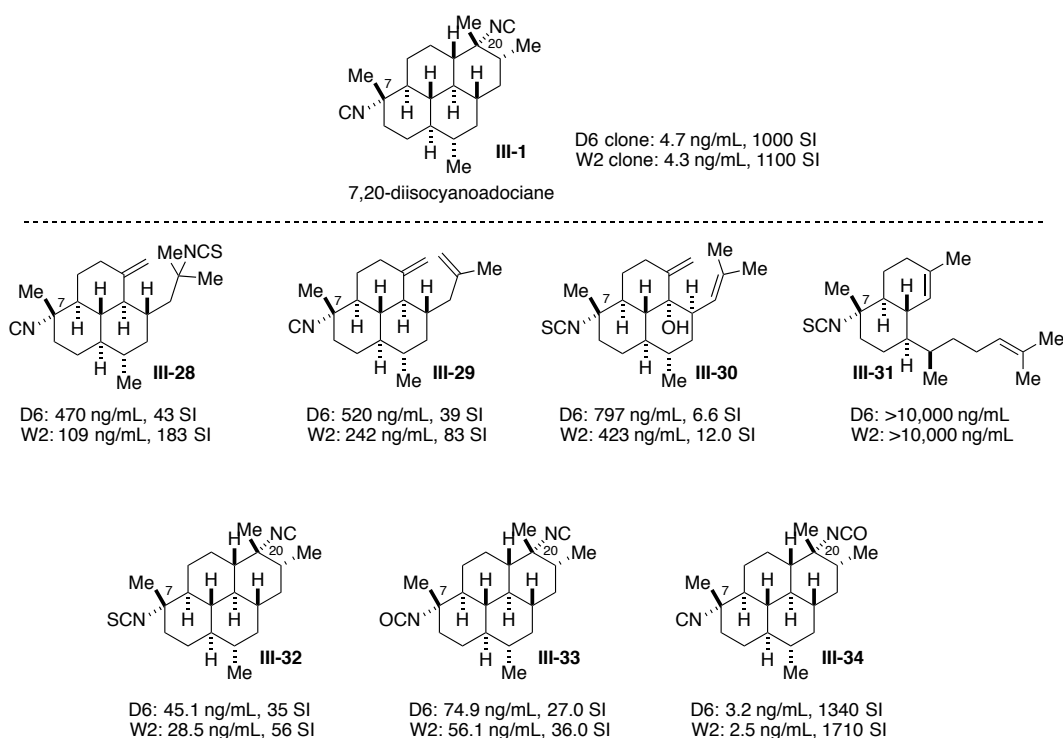
3.2.3.2 *Structural-activity relationship studies*

In addition to the isonitrile functionality, compound structure and orientation of distal stereocenters have been shown to affect bioactivity.²⁷⁰ Wright and König published an extensive study of the antimalarial activity of a number of natural nitrogenous compounds.²⁸⁵ A selection of 21 structurally distinct compounds isolated from marine sponges *Cymbastela hooperi* and *Laurencia papillosa*, a few of which are shown in Figure 3.4, were examined against two clones of *Plasmodium falciparum* (D6 and W2) as well as the mammalian KB cell line in order to probe the selectivity of action.

Their results revealed (7,20)-diisocyanoadociane **III-1** to be at the top of its class, exhibiting both potent and selective antimalarial activity with an IC₅₀ value down to 4.7 nM against *Plasmodium falciparum* D6 clones and a selectivity index (SI) of 1000 against normal mammalian cells. As the family's gold standard, the steric and electronic properties of all other natural compounds were compared to that of **III-1** to identify potential structural sources or obstructions of activity. The alteration of the steric environment around C20 by disrupting the tetracyclic framework of **III-1** diminished activity due to the proposed unfavorable steric environment of the

side chain, as α -substituted amphilectanes (**III-28** and **III-29**) as well as β -substituted amphilectanes (i.e. **III-30**) provided greatly decreased activity and selectivity. Similarly, bicyclic **III-31** displayed no antimalarial activity against either parasite clone. It is noted that the electronic properties of these natural compounds at C20 is also varied, and for **III-30** and **III-31**, the electronic environment at C7 is also altered, and thus it is difficult to ascertain which change led to the observed reduction of activity.

Figure 3.4 Antimalarial activity of nitrogenous terpene natural products



The generation of molecular electrostatic potential maps (MEPs) revealed that compounds most closely mimicking the negative potential spatial regions of diisocyanoadociane **III-1** showed more activity than those with greatly differing MEPs. The activity correlations were most notable in compounds with similar lobes of electron density associated with the isonitrile functionality, which was expected as they are implicated in the mechanism of bioactivity, and therefore positions

C7 and C20 were the sites of particular interest. Investigations of the natural compounds containing the tetracyclic framework demonstrated that preservation of isonitrile electron density at C7 was best for activity, as compounds containing increased electron density at this position, with the isonitrile replaced by an isothiocyanate (**III-32**) or an isocyanate (**III-33**) substituent led to a large decrease in activity and selectivity. Interestingly, an increase in the electron density with an isocyanate substituent at C20, while the C7 isonitrile remains in tact (**III-34**), maintained effective levels of potency and selectivity. König and coworkers published a subsequent study employing molecular modeling in conjunction with observed activity to determine that for optimal binding to heme, leading to the desired antimalarial activity by inhibiting heme detoxification, a rigid carbocyclic backbone composed of at least three rings with an axial isonitrile moiety at C7 is required.²⁸³

These investigations into the structural-activity relationship of marine ICT natural products established an elementary understanding of the factors that generally maintain or diminish the activity of DICA **III-1**, providing a broad picture of structural requirements for activity. However, the conclusions from these studies are limited by the use of only natural samples, as a greater number of structural permutations were unavailable. Moreover, the complex results from some of these studies suggest that another mechanism aside from the isonitrile binding of heme and resulting detoxification may be at play. Many unanswered questions remain about the mechanism or mechanisms of action, and how structural features affect these pathways.

3.3 Previous syntheses of 7,20-diisocyanoadociane

In addition to its desirable antimalarial activity, DICA **III-1** has been of significant interest to the synthetic community due to its complex carbocyclic structure, as has been demonstrated

over the years by the six successful syntheses of **III-1**.^{260, 286-290} The molecule continues to serve as an interesting structural target, as the three most recent syntheses have been disclosed within the past two years. The differing strategies that have emerged to build the three-dimensionally complex architecture highlight how the same structure can inspire such varied synthetic approaches. This variety of strategies emphasizes the challenge associated with the rapid and convergent synthesis of complex polycyclic core structures.

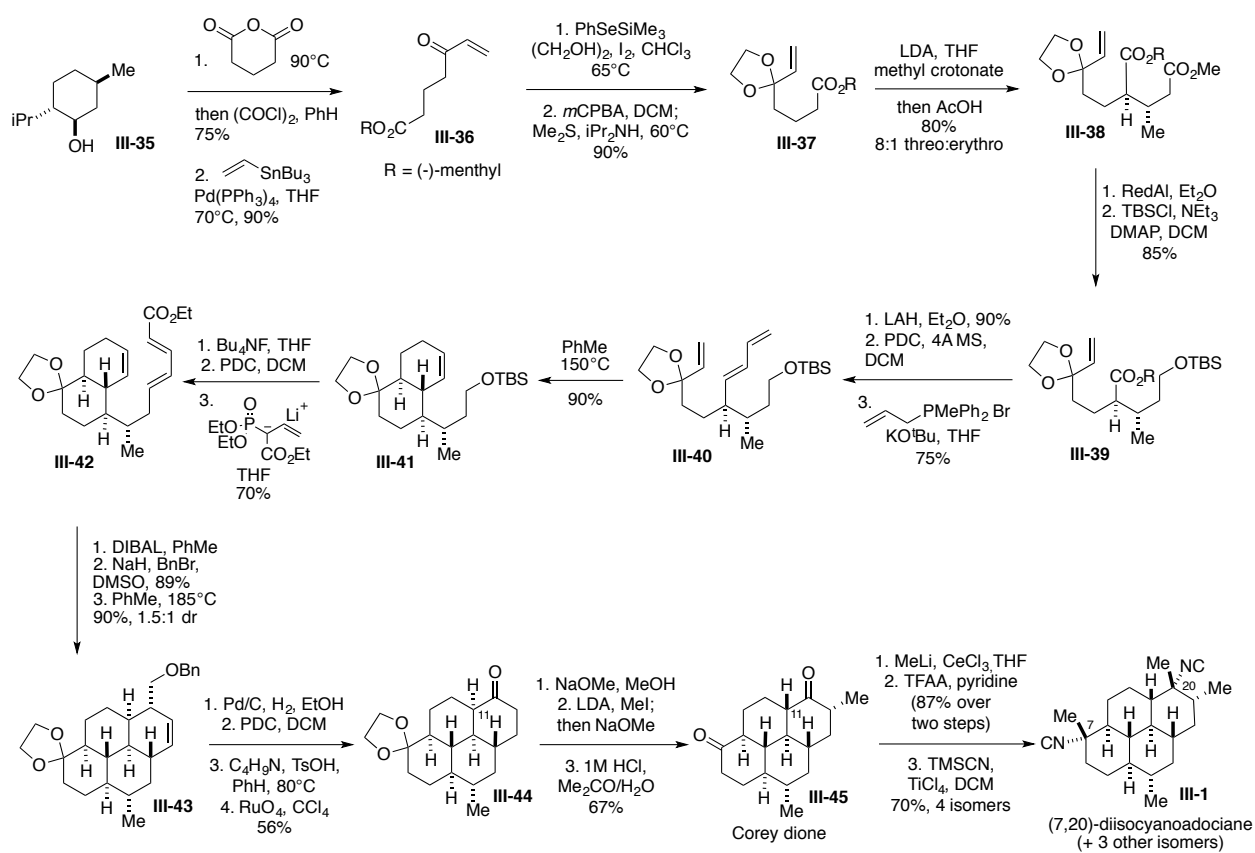
3.3.1 Corey's synthesis

The first successful synthesis of DICA **III-1** was achieved by Corey and Magriotis in 1987 in 29 steps.²⁸⁶ The group accomplished two olefination–intramolecular Diels–Alder sequences to build the tetracyclic core structure of the natural product, highlighting the power of intramolecular Diels–Alder reactions to rapidly build carbocyclic complexity.

As shown in Scheme 3.4, the synthesis began from the addition of chiral auxiliary (–)-menthol **III-35** to glutaric anhydride and subsequent conversion of the resulting carboxylic acid to the acid chloride to allow for a Stille coupling with tributyl(vinyl)tin, delivering enone **III-36**. Upon treatment with TMS phenyl selenide, ethylene glycol, and I₂, **III-36** was converted to a phenylseleno ketal intermediate, which was subsequently oxidized to the selenoxide with *m*CPBA, and eliminated to form ketal **III-37**. The authors noted that this two-step protocol was required because standard acid-catalyzed direct ketalization proved to be unsuccessful. Ketal **III-37** was transformed to diester **III-38** through an enantioselective and diastereoselective Michael addition to methyl crotonate (8:1 threo:erythro). Treatment with RedAl selectively reduced the less hindered ester, and subsequent protection of the resulting alcohol yielded ester **III-39**. Reduction of the ester with lithium aluminum hydride led to an intermediate primary alcohol which was

oxidized to the aldehyde with pyridinium dichromate, and a subsequent Wittig olefination afforded *trans*-diene **III-40**. This diene underwent the first intramolecular Diels–Alder cycloaddition upon heating to 150 °C to present *trans*-decalin species **III-41** selectively. The acetal was discovered to be necessary, as this transformation with the unprotected ketone exclusively provided the *cis*-decalin system. To set the stage for the second olefination–Diels–Alder sequence, the silyl ether within **III-41** was deprotected to the alcohol and subsequently oxidized to the aldehyde with pyridinium dichromate. The desired olefination was achieved using Horner–Wadsworth–Emmons conditions, providing the (*E,E*)-diene **III-42**.

Scheme 3.4 Corey's synthesis



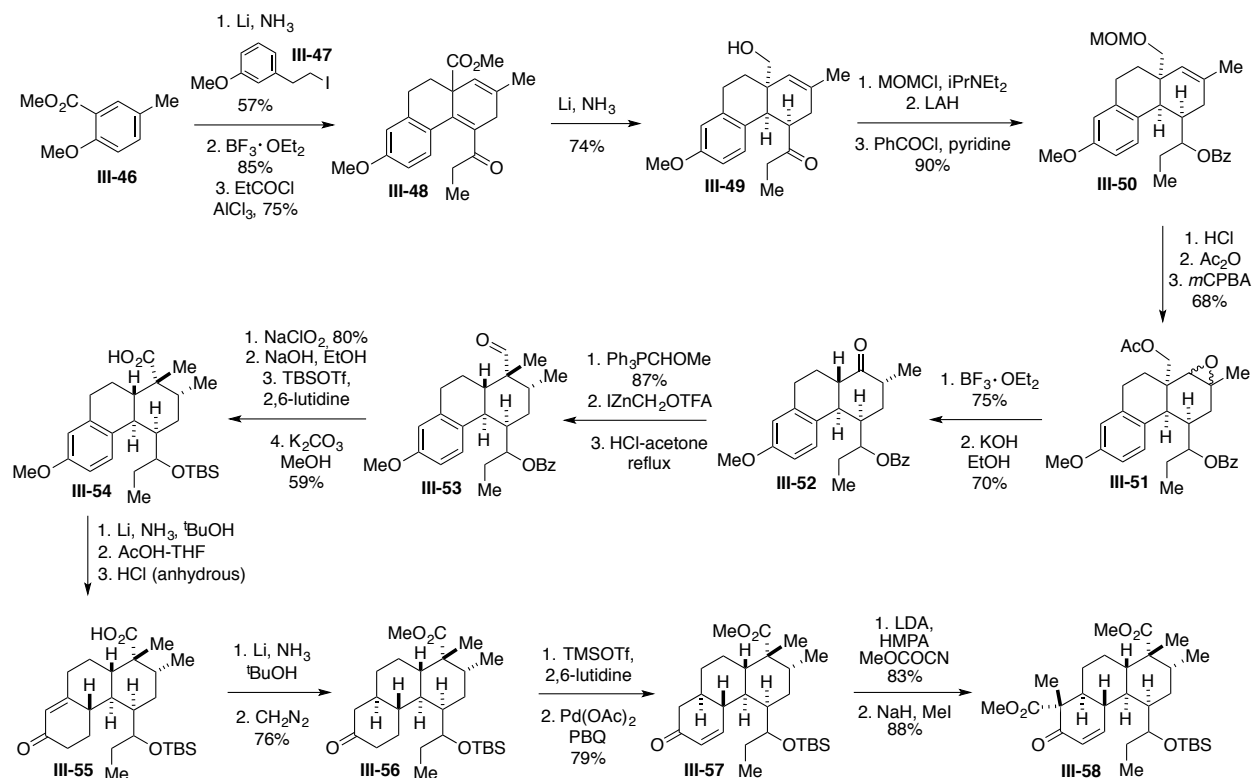
Subsequent DIBAL reduction of the ester and protection of the resulting alcohol gave a benzyl ether intermediate which underwent the second intramolecular Diels–Alder reaction upon heating to 185 °C, providing tetracyclic product **III-43** as a 1.5:1 mixture of diastereomers. This mixture would prove to be inconsequential, as epimerization later in the synthesis was possible. Upon treatment with Pd/C and H₂, the alkene of **III-43** was hydrogenated and the primary alcohol unveiled, which was then oxidized to the aldehyde with pyridinium dichromate. This aldehyde intermediate was refluxed with pyrrolidine and tosic acid in benzene to give an enamine which was oxidatively cleaved at the alkene with ruthenium tetroxide to deliver **III-44**. To achieve the all *trans*-carbocyclic core, it was necessary at this stage to epimerize the C11 position using sodium methoxide. A subsequent α -methylation upon exposure to LDA and methyl iodide resulted in a mixture of axial and equatorial α -methyl ketones, but again, treatment of this mixture with sodium methoxide provided smooth epimerization to the desired equatorial α -methyl ketone. The ketal was removed upon treatment with HCl in acetone to afford the key tetracyclic diketone intermediate **III-45**, known as the “Corey dione,” which has been the target of three formal syntheses to date.^{260, 288-289} To access the natural product, diketone **III-45** was treated with methyllithium and cerium chloride to selectively access the diaxial diol, which was converted to the bis(trifluoroacetate) upon exposure to trifluoroacetic anhydride and pyridine. In the final step, the unselective installation of the isonitrile functionality by trifluoroacetate displacement with TMSCN in the presence of titanium tetrachloride resulted in a mixture of four diastereomeric isonitriles, two of which were separable using thin-layer chromatography, and the other two were isolated by HPLC. This allowed for the assignment of the absolute stereochemistry of the natural compound **III-1**.

3.3.2 Mander's synthesis

In 2006, Mander and Fairweather completed a successful 42-step formal synthesis of racemic DICA **III-1**.²⁸⁷ The strategy features multiple key Birch reductions, a late-stage Michael addition to fashion the fourth ring of the system, and a double Curtius rearrangement to install the isonitrile functionality with stereocontrol.

The synthesis began with a Birch reduction of **III-46** and subsequent in situ alkylation with iodide **III-47** (Scheme 3.5). A Lewis acid-mediated cyclization, followed by an acylation catalyzed by aluminum trichloride at cold temperatures provided tricyclic ester **III-48**. Upon treatment with lithium metal in ammonia, this intermediate was reduced to *cis*-fused hydroxy ketone **III-49**. Protection of the primary alcohol, followed by reduction of the carbonyl and subsequent benzoate protection of the resulting secondary alcohol afforded **III-50** as a single diastereomer. As the desired epoxidation of **III-50** was hindered by the MOM protecting group, it was replaced with an acetate protecting group, which allowed for the epoxidation with *m*CPBA to yield **III-51** as a mixture of epimers. Upon exposure to $\text{BF}_3 \cdot \text{OEt}_2$, epoxide **III-51** successfully rearranged to the α -methyl ketone, providing a mixture of diastereomers. Fortunately, this mixture proved to be inconsequential because the hydrolysis of the acetate group and subsequent retro-aldol transformation to remove the substituent under basic conditions led to simultaneous epimerization of the α -methyl substituent to the desired more thermodynamically favorable equatorial position, providing **III-52** as a single diastereomer. A Wittig olefination of the ketone provided an intermediate vinyl methyl ether which was hydrolyzed to unveil the aldehyde, however the desired subsequent α -alkylation to access aldehyde **III-53** proved to be unsuccessful. As a clever solution, the vinyl methyl ether Wittig product underwent a Simmons–Smith cyclopropanation, which was

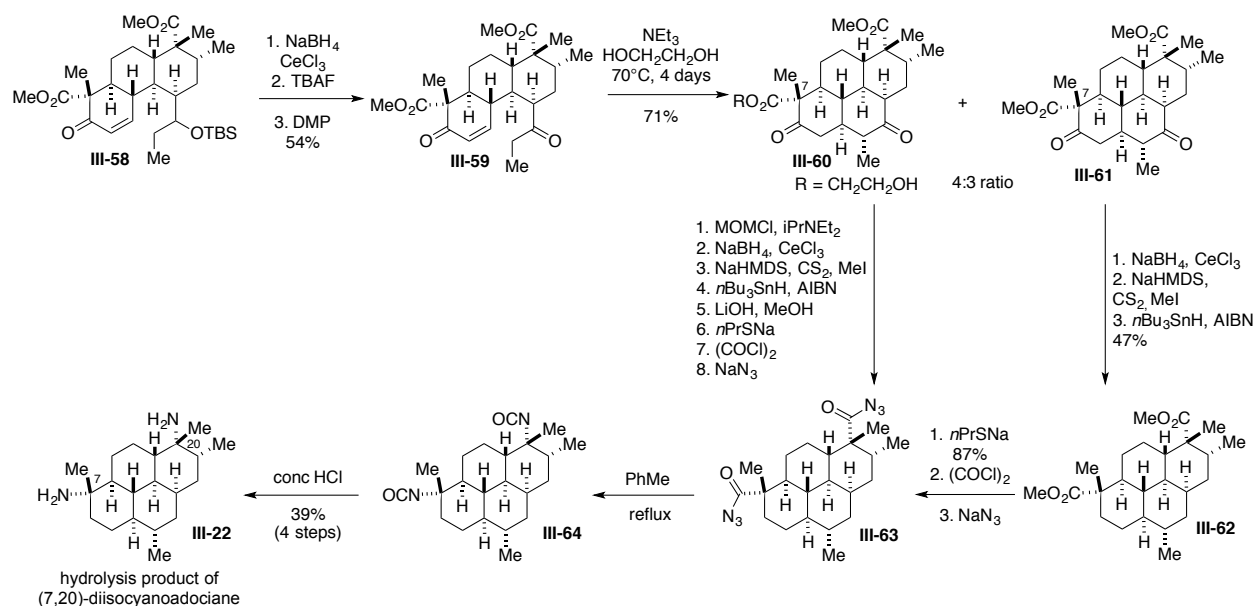
Scheme 3.5 Mander's synthesis



relaxed in acid to promote ring-opening to the desired aldehyde **III-53**. NMR experiments at this point confirmed that the methylenation had occurred on the less hindered *exo*-face, providing the correct diastereomer. Aldehyde **III-53** was oxidized to the acid, and the benzoate group was removed and replaced as a TBS ether to afford **III-54**. A subsequent Birch reduction of the aromatic ring, acetic acid-mediated hydrolysis, and acid-promoted isomerization of the alkene delivered enone **III-55**. The isomeric enone **III-57** was prepared by an initial reduction of **III-55** in the presence of lithium metal and ammonia and subsequent esterification of the acid with diazomethane to give ketone **III-56**, which underwent a Saegusa oxidation. Acylation of **III-57** in the presence of methyl cyanofornate and subsequent α -methylation gave enone **III-58**.

To set the stage for the key late-stage Michael addition, it was first necessary that the protected alcohol within **III-58** be converted to the ketone. The group hypothesized that upon removal of the TBS protecting group, however, the resulting alcohol would rapidly cyclize onto the enone, thus the enone carbonyl was first reduced with sodium borohydrate in the presence of cerium chloride (Scheme 3.6). Deprotection of the TBS group followed by a double Dess–Martin periodinane-mediated oxidation provided diketone **III-59**.

Scheme 3.6 Completion of Mander's formal synthesis



However, the cyclizing Michael addition proved to be challenging and required much optimization. Ultimately, the successful transformation was achieved with inspiration from conditions employed for a difficult Michael reaction in Corey's synthesis of longifolene,²⁹¹ heating diketone **III-59** in ethylene glycol and triethylamine for four days to provide tetracyclic products **III-60** and **III-61** in a 4:3 ratio. Unfortunately, ethylene glycol was the only successful solvent for the transformation, but also provided a significant amount of trans-esterified product at C7, **III-60**. The desired diketone **III-61** was reduced to the diol and converted to the dioxanthate, which

then underwent a Barton-McCombie deoxygenation to form tetracyclic intermediate **III-62**. Conversion of bis(ester) **III-62** to the bis(acid chloride) was achieved upon treatment with sodium propanethiolate followed by oxalyl chloride, and subsequent transformation to the diacyl azide **III-63** was accomplished with sodium azide. The undesired byproduct from the Michael reaction **III-60** could also converge on the key late-stage diacyl azide **III-63** through a series of eight transformations. A final Curtius rearrangement was performed by refluxing **III-63** in toluene to achieve the bis(isocyanate) **III-64**. The formal synthesis was then completed when this intermediate **III-64** was hydrolyzed in concentrated HCl to give the diamine **III-22**, which was found to be identical to samples from the hydrolysis of the natural DICA **III-1** (Scheme 3.3).

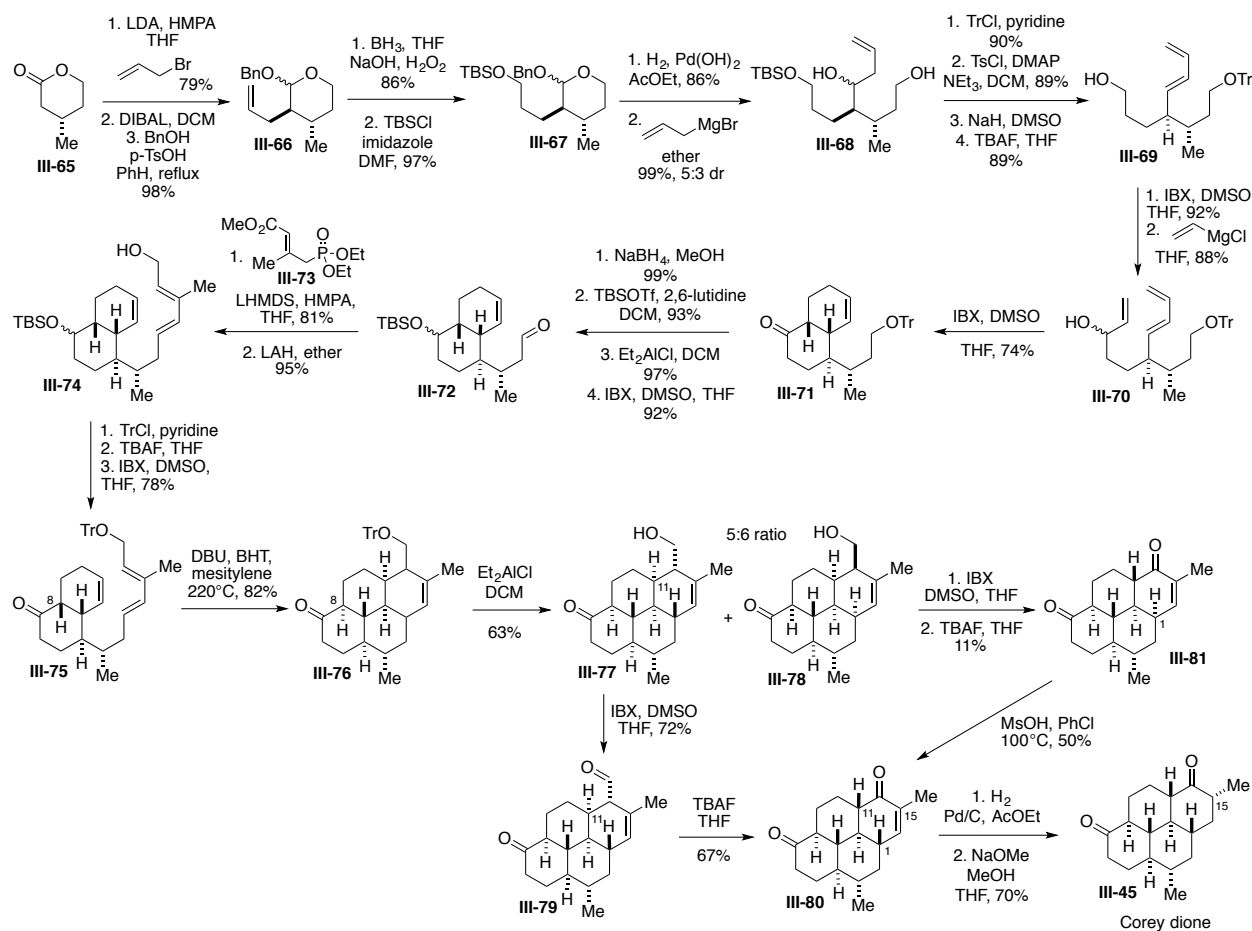
3.3.3 *Miyaoka's synthesis*

In 2011, Miyaoka and coworkers published a 29-step formal synthesis of DICA **III-1**, targeting Corey's late-stage dione intermediate **III-45** as their formal endpoint.²⁸⁸ The strategy bears much resemblance to the Corey strategy, employing a key olefination and two intramolecular Diels–Alder reactions to fashion the carbocyclic core structure.

As shown in Scheme 3.7, the synthesis began with enantioenriched lactone **III-65**, affecting a stereoselective α -allylation, followed by a reduction of the ketone with DIBAL, and subsequent protection of the resulting alcohol as the benzyl ether to afford **III-66**. A hydroboration/oxidation of the alkene and protection of the resulting alcohol delivered **III-67**. The benzyl protecting group was removed upon treatment with Pearlman's catalyst in the presence of hydrogen, and the intermediate hemiacetal was treated with allyl Grignard to produce diol **III-68** as a 5:3 mixture of diastereomers. The primary alcohol was then selectively protected as the triphenylmethyl ether, and the remaining secondary alcohol was converted to the tosylate and then

eliminated in the presence of sodium hydride in DMSO, providing the (*E*)-diene. Finally, deprotection of the silyl protecting group provided alcohol **III-69**. The free alcohol was oxidized in the presence of IBX, and a vinyl Grignard addition into the resulting aldehyde delivered alcohol **III-70**. Upon treatment with IBX, the allylic alcohol was oxidized to the enone which underwent a Diels–Alder cycloaddition, yielding *cis*-decalin **III-71** as the only product. The ketone within **III-71** was then reduced to the alcohol with sodium borohydride, yielding a mixture of diastereomers that were protected as the TBS ether. The triphenylmethyl ether protecting group

Scheme 3.7 Miyaoka's synthesis



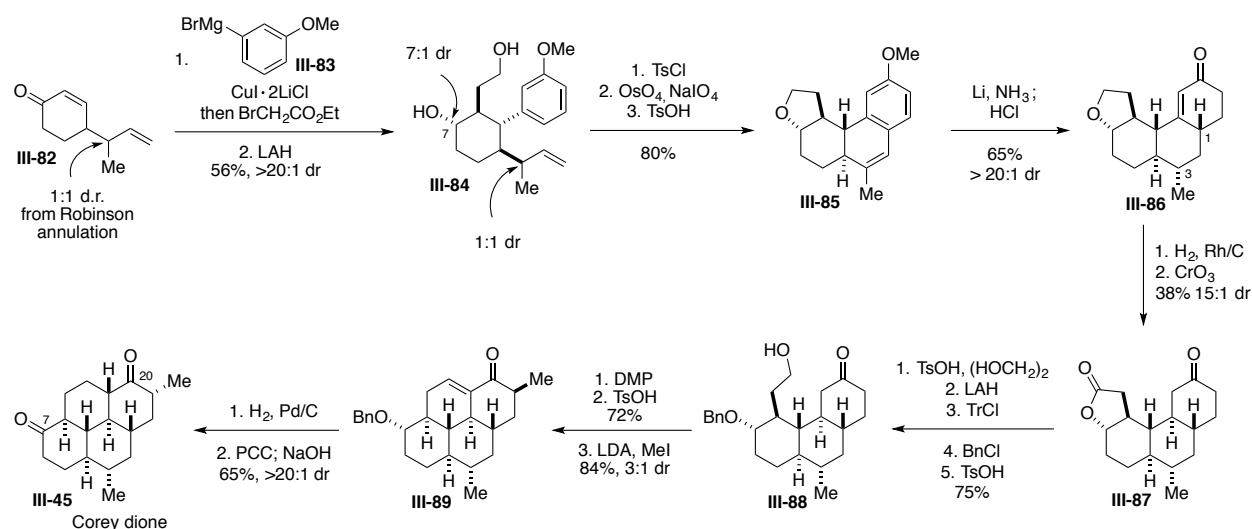
was removed in the presence of diethylaluminum chloride to provide the primary alcohol which was oxidized to aldehyde **III-72** with IBX. This aldehyde underwent a Horner–Wadsworth–Emmons olefination with **III-73** to give the (*E,E*)-unsaturated ester, which was then reduced with lithium aluminum hydride to produce allylic alcohol **III-74**. The alcohol was protected as a triphenylmethyl ether, the silicon protecting group removed with TBAF, and the resulting secondary alcohol oxidized to the ketone with IBX to yield **III-75**. When treated with DBU and BHT in mesitylene at 220 °C, this ketone **III-75** underwent a key isomerization at the C8 position with accompanying intramolecular Diels–Alder reaction to afford tetracyclic **III-76** as a 5:6 mixture of diastereomers (*exo:endo*). To enable purification of the diastereomers, the triphenylmethyl protecting group was removed with diethylaluminum chloride to afford the separable alcohols **III-77** (*exo*-adduct) and **III-78** (*endo*-adduct) that were each taken forward to converge on the desired target Corey’s intermediate **III-45**. The *exo*-adduct **III-77** was oxidized to aldehyde **III-79** with IBX, which was subsequently deformylated and epimerized at the C11 position in the presence of TBAF to afford **III-80**. Alternatively, the *endo*-adduct **III-78** was first similarly oxidized to the aldehyde with IBX and deformylated with TBAF to achieve intermediate **III-81**. The required epimerization at the C1 position was accomplished in the presence of methanesulfonic acid in chlorobenzene at 100 °C to converge on intermediate **III-80**. The enone of this tetracycle **III-80** was then hydrogenated with palladium on carbon and hydrogen to achieve the saturated diketone, which underwent a base-mediated epimerization at C15, thus accessing their formal target, Corey’s dione **III-45**.

3.3.4 Vanderwal's synthesis

Diisocyanoadociane **III-1** continues to be of interest to the synthetic community, as three research groups have published novel syntheses of the molecule with different strategies since 2016. Vanderwal and Roosen designed a 21-step synthesis formally targeting Corey's intermediate **III-45** in an efficient manner, featuring a Friedel-Crafts cyclodehydration and key stereoselective reductions.²⁸⁹

As shown in Scheme 3.8, the racemic synthesis began with cyclohexenone **III-82**, accessed from a Robinson annulation of 3-methyl-4-pentenal and methylvinyl ketone. Conjugate addition of the cuprate of aryl nucleophile **III-83** and enolate alkylation afforded an intermediate ketone with high diastereoselectivity, setting the three stereocenters in a *trans*-relationship. Reduction of the ketone with lithium aluminum hydride afforded diol **III-84** as a 7:1 mixture of diastereomers. As this C7 position eventually contains the ketone within target **III-45**, this selectivity was inconsequential. Dual protection of both alcohols through generation of a tetrahydrofuran ring was achieved due to the observed tendency of the diol to cyclize. This allowed for an oxidative cleavage of the pendant alkene with osmium tetroxide, and subsequent cyclodehydration in the presence of toluenesulfonic acid to provide tetracyclic **III-85**. Enone **III-86** was achieved in gram quantities by employing a Birch reduction and subsequent acid-mediated hydrolysis and isomerization of the alkene to the enone, successfully installing the two new stereocenters at C1 and C3 with complete control. Reduction of this intermediate **III-86** to the desired *trans*-product required some optimization. Although similar ring systems have been shown in the literature to produce the *trans*-ring junction with dissolving metal conditions, this resulted in predominantly the *cis*-ring-fused product (2:1 dr). Other alkali-metal and homogenous hydride reagents (i.e Na, K, Karstedt's

Scheme 3.8 Vanderwal's synthesis

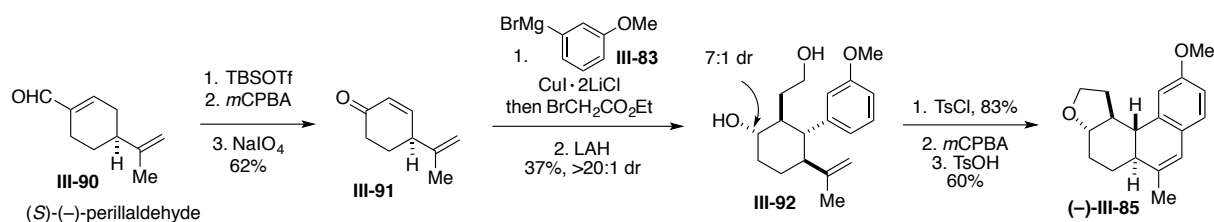


catalyst, *t*BuCu/DIBAL) gave similar undesirable selectivities. On the other hand, the group found that heterogeneous reductants favored production of the desired *trans*-product, and a screen of catalysts showed Rh/C in the presence of hydrogen to provide a high level of *trans*-selectivity (15:1 dr). As the opening of the tetrahydrofuran ring within the reduced product of **III-86** in the presence of a Lewis acid proved to be unsuccessful, it was oxidized to lactone **III-87** in the presence of Fieser's reagent. The ketone within **III-87** was then protected as the acetal to enable the lactone opening in the presence of lithium aluminum hydride. The resulting primary alcohol was selectively protected as a triphenylmethyl ether, and the secondary alcohol subsequently protected as a benzyl ether. Deprotection of the primary alcohol upon treatment with toluenesulfonic acid resulted in alcohol **III-88**, which was oxidized to the aldehyde to allow for the acid-mediated intramolecular aldol condensation. Subsequent alkylation of the ketone delivered α -methyl-substituted **III-89** as a mixture of diastereomers, which was treated with palladium on carbon and hydrogen to simultaneously hydrogenate the enone unsaturation and deprotect the benzyl protecting group. The resulting alcohol was then oxidized to the ketone, and

the mixture of diastereomers was easily epimerized in the presence of base to afford the thermodynamically favored all-*trans* Corey dione **III-45** as the formal endpoint of the synthesis.

In order to access enantiopure **III-45**, the group had intended to render the first Robinson annulation enantioselective with the use of a chiral organocatalyst, however they were unable to discover conditions that allowed for the aldol condensation to occur without loss of enantiopurity. Therefore, they redesigned the beginning of the synthesis using readily available chiral (–)-perillaldehyde **III-90** to introduce the desired asymmetry (Scheme 3.9). They accessed cyclohexenone **III-91** in three steps from **III-90**, and then successfully achieved the same conjugate addition/alkylation cascade as had been developed for their racemic synthesis to install the three all-*trans* stereocenters, followed by reduction with lithium aluminum hydride to provide **III-92**. Again, similar to their racemic synthetic route, generation of the tetrahydrofuran ring was accomplished upon treatment of **III-92** with TsCl. Subsequent exposure of this intermediate to *m*CPBA generated the epoxide, which was refluxed in acid to form (–)-**III-85** through a rearrangement to the aldehyde and subsequent ring closure and dehydration. This enantiopure tetracycle (–)-**III-85** was an intermediate in the developed racemic synthesis, thus allowing for extrapolation to access the enantiopure target, Corey dione **III-45**. The Vanderwal route to Corey's intermediate only required 10 purifications, and demonstrated the utility of a chiral-pool approach to rapidly generate enantiopure material in complex molecule synthesis.

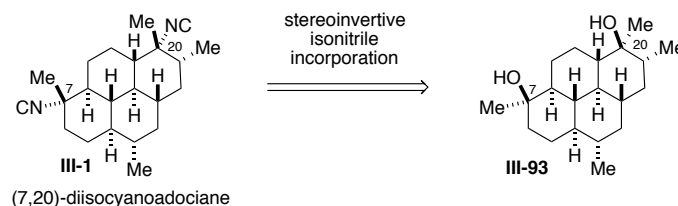
Scheme 3.9 Enantioselective synthesis with chiral pool materials



3.3.5 Shenvi's synthesis

In 2016, Shenvi and coworkers designed a concise, 17-step synthesis of DICA **III-1** that cleverly introduced the isonitrile functionality with stereocontrol, which had been a challenge to previous syntheses due to difficulty differentiating between the isonitrile at C7 occupying the equatorial position, and the isonitrile at C20 occupying the axial position. The group elegantly employed chemistry that they had previously developed to convert a *tert*-alkyl trifluoroacetate to an isonitrile with stereoinversion in the presence of $\text{Sc}(\text{OTf})_3$ and TMSCN .²⁹² As shown in Figure 3.5, this required their overall strategy to differentiate the C7 and C20 positions throughout the synthesis to arrive at tetracycle **III-93** with an axial alcohol at C7 and an equatorial alcohol at C20.

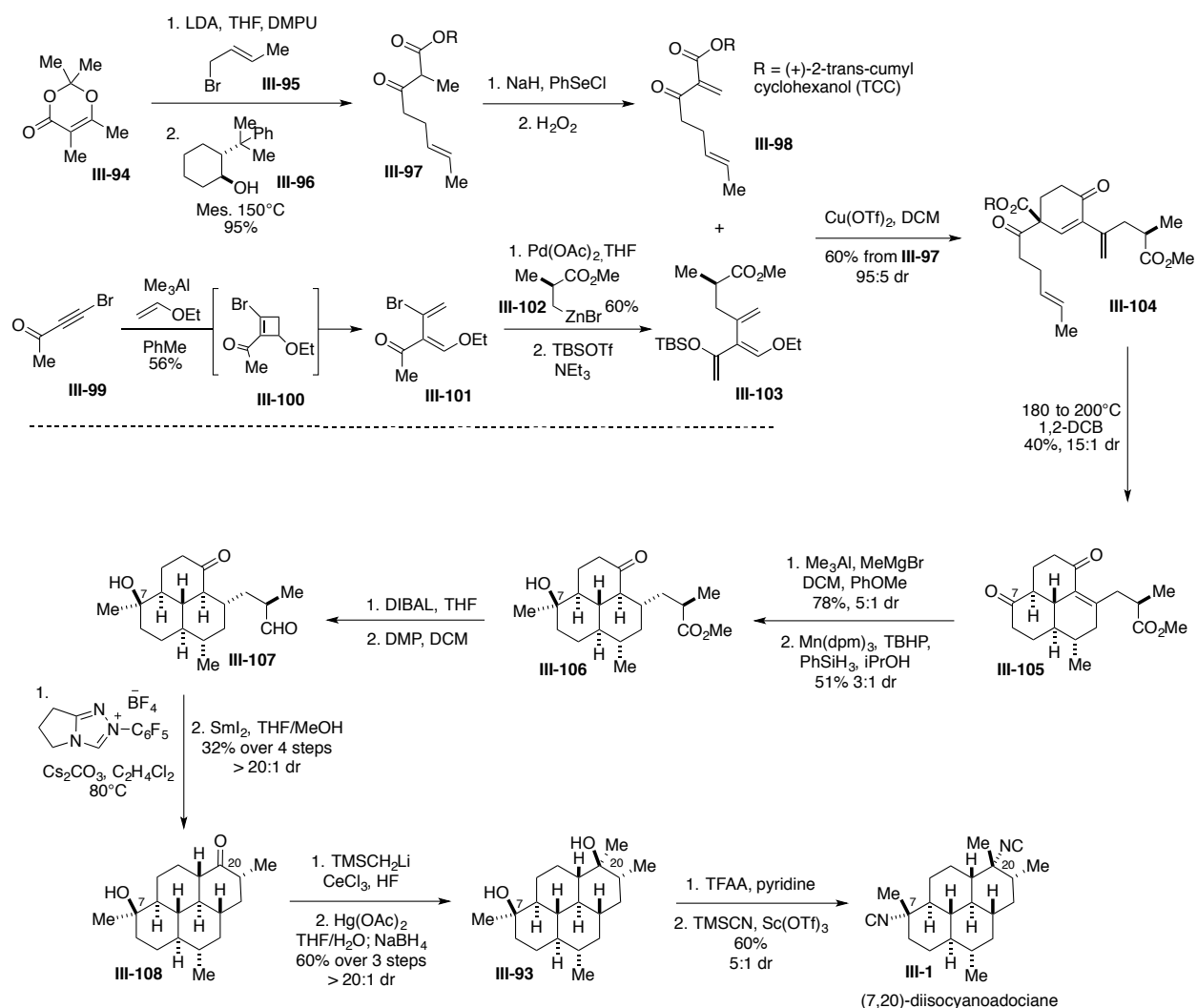
Figure 3.5 Shenvi's late-stage strategy for selective isonitrile installation



The carbocyclic core construction featured two Diels–Alder cycloadditions and an N-heterocyclic carbene-mediated cyclization. Successful execution of this selective synthesis enabled further investigation of the compound's mechanism of action against malaria parasites, an activity that has been of wide interest to the scientific community, but one that remains poorly understood because of the lack of access to sufficient material (see Section 3.2.3.1).²⁹⁰

As shown in Scheme 3.10, the synthesis began by constructing dienophile **III-98** and diene **III-103**, which were to be united in a Diels–Alder reaction. Dienophile **III-98** was prepared as a single enantiomer from dioxenone **III-94**, which underwent crotylation, acyl ketene formation and addition of chiral auxiliary **III-96**, and finally a selenium-mediated elimination. Dendralene

Scheme 3.10 Shenvi's synthesis



III-101 was prepared from bromoalkyne **III-99** through a [2+2] cycloaddition/retroelectrocyclization tandem with ethyl vinyl ether in the presence of Lewis acid trimethylaluminum, which proceeded through cyclobutene **III-100**. This intermediate **III-101** underwent a palladium-catalyzed coupling with commercially available zinc bromide **III-102**, and subsequent enol silane formation to deliver the desired diene **III-103** for the Diels–Alder reaction. The crude solutions of both dienophile **III-98** and diene **III-103** were treated with copper(II) triflate at $-78\text{ }^{\circ}\text{C}$, promoting the desired Diels–Alder cycloaddition and silyl ether elimination to

produce **III-104** as a 95:5 mixture of diastereomers. This intermediate underwent a subsequent Diels–Alder reaction and auxiliary removal by a heteroretroene/decarboxylation sequence when heated to 200 °C to provide **III-105**. As the group’s overall strategy was rooted in the differentiation of the final isonitrile substituents, they sought to selectively achieve a methyl addition into the ketone at the C7 position of **III-105** while leaving the enone in tact. This proved to be more difficult than the group had hoped, however it was eventually discovered that treatment of **III-105** with tetramethylaluminum magnesium bromide and anisole gave the axial alcohol at the C7 position without reacting with the enone carbonyl. Attempts to stereoselectively hydrogenate the alkene employing palladium, platinum, or rhodium catalysts were unsuccessful because the strain associated with the alkene led to deconjugation and unselective hydrogenation. Fortunately, the group had previously developed hydrogen atom transfer hydrogenation conditions, using a manganese catalyst in the presence of *tert*-butyl hydrogen peroxide, phenyl silane, and isopropanol, to provide thermodynamically favored axial hydride delivery to other systems.²⁹³ These conditions successfully eliminated undesired isomerization and produced **III-106** as the major diastereomer (3:1 dr). The ester within **III-106** was reduced in the presence of DIBAL and the resulting alcohol oxidized to yield aldehyde **III-107**. N-heterocyclic carbene-mediated cyclization produced the tetracyclic intermediate, which was deoxygenated with samarium diiodide to yield ketone **III-108**. At this point, with the C7 axial alcohol in place, the strategy required a methyl addition into the ketone at C20 to give the equatorial alcohol at that position, which would enable the application of their stereoinvertive isonitrile installation to access the desired stereochemistry of the natural product **III-1**.²⁹² With this goal, the group employed Yamamoto’s MAD reagent, which had successfully provided the desired equatorial alcohol in

model systems, however this reagent only provided the axial alcohol in the presence of organolithium, organomagnesium, and organocerium nucleophiles. The solution to this challenge resulted from an initial methylenation of the C20 ketone within **III-108**, followed by an oxymercuration, which delivered diol **III-93** with the desired equatorial alcohol at C20. Late-stage installation of the isonitrile functionality employing their previously developed conditions by conversion of the diol **III-93** to the bis(trifluoroacetate) and subsequent solvolysis in the presence of Sc(OTf)₃ and TMSCN delivered DICA **III-1** as a 5:1 mixture of diastereomers.

Shenvi's robust synthesis enabled biological investigations that led to interesting insights into the antimalarial mechanism of action of DICA. While it had been demonstrated previously that DICA binds to heme in blood-stage parasites, preventing its crystallization to β -hematin, which is necessary for *P. falciparum* survival (Section 3.2.3.1), these studies demonstrated that the compound was still active against liver-stage parasites, which do not require the protective crystallization of heme to survive. This activity suggests that another mechanism may also be at play, and provides more insight into the interesting and sought after bioactivity of these ICTs.

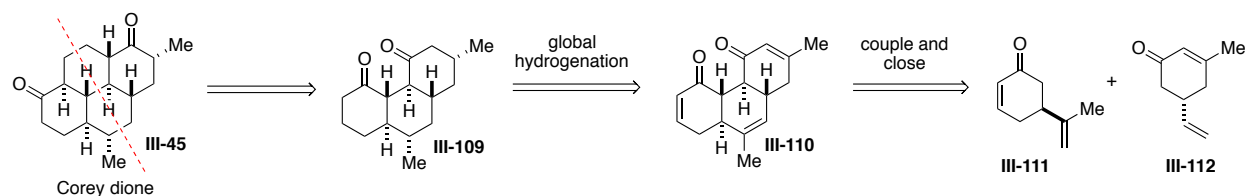
3.4 Implementation of the couple and close strategy to DICA

3.4.1 General strategy

The all-*trans* perhydrophenanthrene core of DICA **III-1** mapped nicely onto the *trans-anti-trans* phenanthrene-type core structures that were readily accessible through the developed oxidative coupling–ring-closing metathesis strategy, as detailed in Chapter 2. With this realization, we selected the marine diterpenoid as the first natural product target with which to apply the approach, reasoning that we could efficiently access the late-stage Corey dione **III-45** (Scheme 3.11). We envisioned that the couple and close strategy would enable us to take advantage of the

pseudo-symmetry within the Corey dione **III-45** and retrosynthetically dissect the structure down the middle. In this way, the synthetic strategy would provide highly convergent access to much of the target's carbocyclic core, and allow for an efficient, symmetry-exploiting end game to furnish the final ring in the tetracyclic structure. Therefore, we targeted diketone **III-109** as the key intermediate from which the Corey dione could be accessed through the appendage of a suitable two-carbon bridge to install the fourth ring. This central diketone intermediate could result from the global hydrogenation with axial hydrogen delivery of unsaturated tricyclic species **III-110**, which is simply the product of the three-step couple and close sequence from simple enantioenriched starting materials **III-111** and **III-112**.

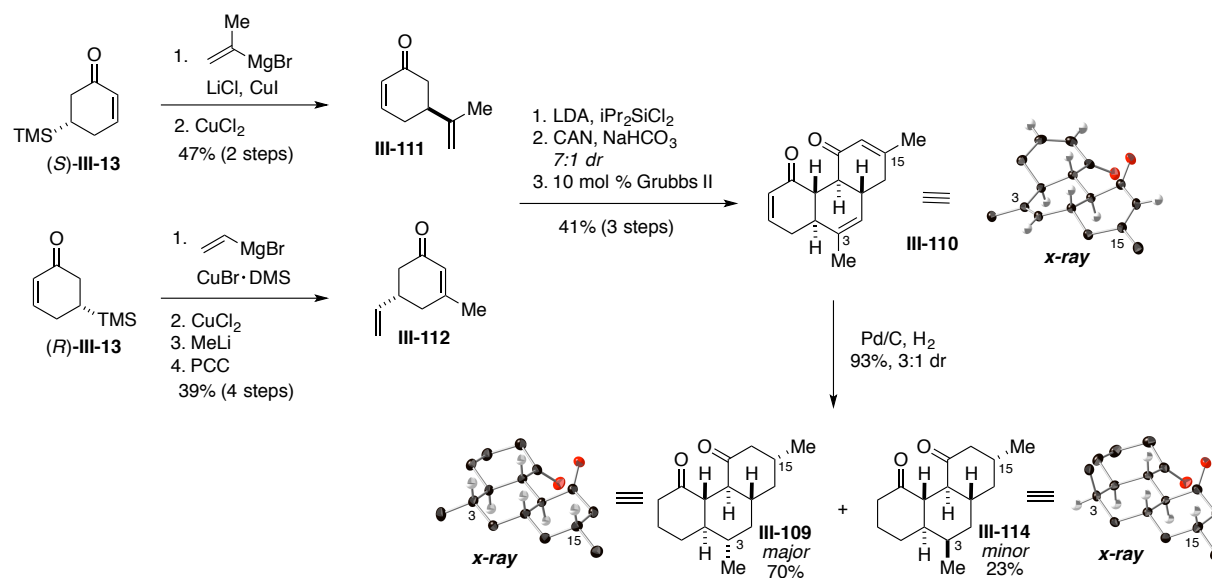
Scheme 3.11 General strategy to access Corey's intermediate **III-45**



As shown in Scheme 3.12, implementation of this strategy proceeded smoothly, starting from key enantioenriched β -silane cyclohexenones (*S*)-**III-113** and (*R*)-**III-113**, which were synthesized as described in Chapter 2 from an organocatalytic Robinson annulation between *tert*-butyl acetoacetate and (*E*)-3-trimethylsilyl-2-propenal.²⁴⁶ Enone **III-111** was accessed in 47% yield over two steps from (*S*)-**III-113** through a conjugate addition of isopropenyl Grignard followed by a copper(II) chloride-mediated elimination of the silane. On the other hand, (*R*)-**III-113** was converted to enone **III-112** through a vinyl cuprate addition and copper(II) chloride-promoted elimination of the silane, followed by a 1,2-methyl addition and PCC-mediated oxidative transposition. These two coupling partners were subjected to the three-step couple and close

strategy, producing tricyclic diketone **III-110** in 41% yield. This compound was amenable to X-ray analysis, confirming the desired all-*trans* stereochemistry about the ring junctions. To access the required stereochemistry at the C3 and C15 positions within the natural product where both methyl substituents occupy the equatorial position, it was required that the ensuing hydrogenation of **III-110** proceed with axial delivery of the hydrogen atoms.

Scheme 3.12 Access to the key diketone intermediate **III-109**



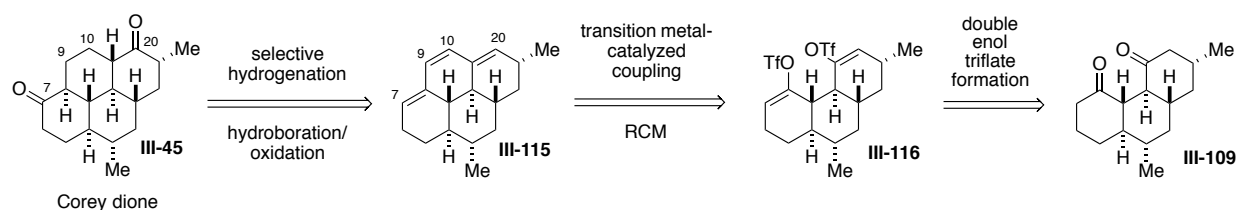
Upon treatment with palladium on carbon and hydrogen, a 3:1 mixture of stereoisomers was obtained in 93% yield. Although the products were inseparable by normal column chromatography, preparative HPLC enabled their isolation. The crystalline nature of each isomer allowed for X-ray analysis, confirming that major isomer **III-109** contained the desired equatorial methyl substitution at both C3 and C15, while the minor isomer **III-114** demonstrated that the loss in selectivity arose from promiscuity at the C3 position. Employment of other catalysts for this transformation did not result in any enhancement of selectivity. For example, Adam's catalyst in the presence of hydrogen failed to achieve a facile global hydrogenation, resulting in a mixture of

semi-hydrogenated products. We were aware that Shenvi and coworkers had reported hydrogen atom transfer conditions selective for the production of thermodynamically favored products,²⁹³ however application of these conditions to this system provided a more complex mixture of diastereomers than what was observed upon exposure to palladium on carbon and hydrogen.

3.4.2 Initial late-stage strategy

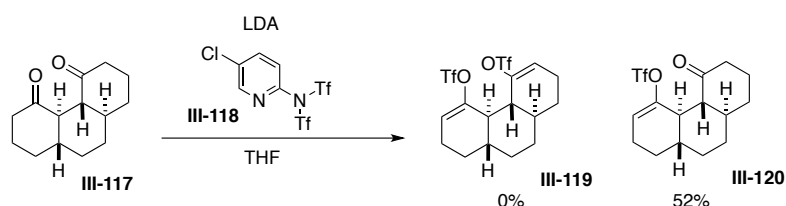
With a suitable strategy to access the key diketone intermediate **III-109**, rapidly constructing the majority of the target molecule's core structure, we shifted our attention to the closure of the fourth and final ring of the system. As shown in Scheme 3.13, we imagined that the tetracyclic Corey dione **III-45** could be accomplished from tetracyclic triene **III-115** through a selective hydrogenation of the disubstituted olefin over the trisubstituted alkenes,²⁹⁴⁻²⁹⁷ followed by a hydroboration/oxidation sequence to install the ketone functionality at C7 and C20. We envisioned that tetracyclic triene **III-115** could be accessed from bis(enol triflate) **III-116** through a double transition metal-catalyzed coupling of a vinyl group to install the required C9 and C10 carbons, followed by a ring-closing metathesis to close the fourth ring. We imagined that the coupling of alternative alkyl groups may be investigated for the C9 and C10 installation should the double vinyl coupling be unsuccessful. Finally, **III-116** could be rapidly accessed from key diketone intermediate **III-109** through a double enol triflate formation.

Scheme 3.13 Initial late-stage strategy



With this strategy in mind, we initiated its execution on a model system lacking the peripheral methyl substituents due to the ease of preparation and analysis afforded by its C2-symmetry. Thus, as shown in Scheme 3.14, the conversion of symmetrical diketone **III-117** to the desired bis(triflate) **III-119** was investigated. Unfortunately, all attempts to access the bis(triflate) species employing standard hard enolization conditions provided only the monotriflate species **III-120**, with the most effective conditions of LDA and Comins' reagent **III-118** shown. Even full conversion to this monotriflate compound was difficult to achieve, resulting in significant amounts of reisolated starting material. Alteration of the triflating source to *N*-phenyl-triflimide only returned unchanged starting diketone **III-117**. Sequential additions of base and Comins' reagent **III-118** were successful in driving the reaction further to the monotriflate **III-120**, but this approach remained unable to deliver any of the desired bis(triflate) **III-119**. Additionally, resubjection of the isolated monotriflate **III-120** to these conditions only resulted in unchanged starting material.

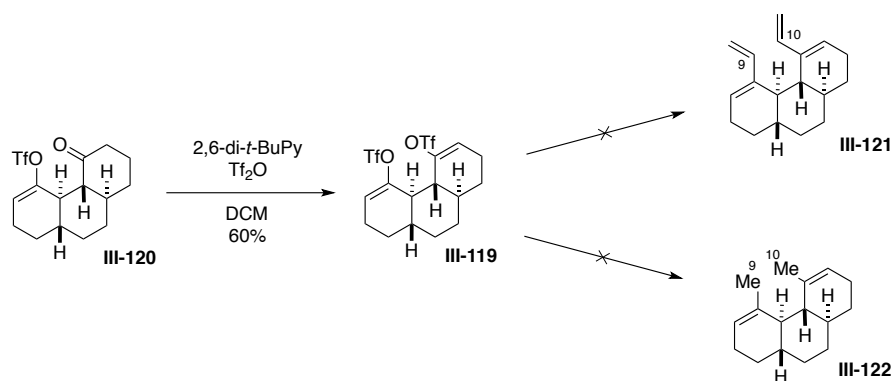
Scheme 3.14 Attempts to form bis(triflate) **III-119**



Although hard enolization conditions were unsuccessful in the delivery of the desired bis(triflate) species, interestingly, exposure of monotriflate **III-120** to soft enolization conditions such as 2,6-di-*tert*-butylpyridine in the presence of triflic anhydride, provided the bis(triflate) **III-119** in 60% yield (Scheme 3.15). When diketone **III-117** was treated with these conditions directly, no production of monotriflate **III-120** or bis(triflate) **III-119** was observed. This bis(triflate) **III-**

119, however, proved to be unproductive under transition metal-catalyzed conditions to couple two suitable alkyl groups that would serve as the C9 and C10 carbons in the target molecule (Scheme 3.15). The double vinyl Stille coupling under a variety of conditions did not achieve the desired product **III-121**, either providing unreacted starting material or resulting in decomposition. Attempted conversion of bis(triflate) **III-119** to bis(vinyl methyl) species **III-122** with methyllithium and copper(I) iodide returned unreacted starting material. Similarly, methyl Grignard in the presence of NiCl₂(dppp), methyl boronic acid in the presence of Ph(CN)₂PdCl₂, dimethyl zinc in the presence of Pd(PPh₃)₄, and tetramethyl tin in the presence of Pd(PPh₃)₄ all provided reisolated starting material **III-119**. These conditions were simultaneously employed on a model decalone-derived vinyl triflate system, demonstrating successful cross-coupling and confirming that the reactivity of the real compound was the root of the failed transformation.

Scheme 3.15 Access to bis(triflate) **III-119** and attempted manipulations



3.4.3 Strategic departure from symmetry

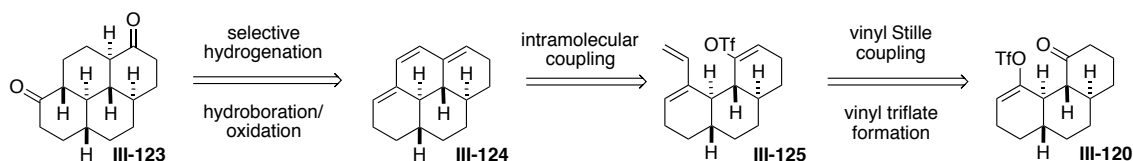
With the observed challenges associated with the reactivity of the bis(triflate) (**III-119**), we imagined that the monotriflate species (**III-120**) may be a useful intermediate with which to construct the desired two-carbon bridge of the fourth ring in the carbocyclic core, although this

approach was less ideal as it would remove the efficiency that could be achieved by exploiting the natural pseudo-symmetry of the molecule.

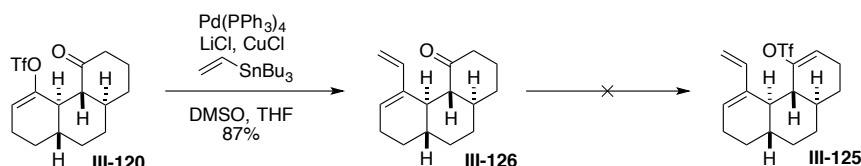
In the first approach, as shown in Scheme 3.16a on the model system, we imagined that the tetracyclic core **III-123** could be achieved from triene **III-124** through a selective hydrogenation and hydroboration/oxidation sequence, as described previously. This time, however, we proposed that this tetracycle **III-124** could be obtained from diene **III-125** through a ring-closing intramolecular transition metal-catalyzed coupling. This intermediate could arise from the monotriflate **III-120** through a vinyl Stille coupling followed by conversion of the other ketone to the vinyl triflate. In the forward sense, as shown in Scheme 3.16b, monotriflate **III-120** successfully underwent a vinyl Stille coupling to produce diene **III-126**. The ketone within **III-126**, however, could not be converted to the vinyl triflate **III-125**. Treatment with LDA and Comins' reagent, conditions successful for the formation of the monotriflate **III-120**, resulted in unchanged starting material. After successive additions of these reagents, only starting material remained, and started to decompose over time. Alteration of the base to KHMDS also provided unchanged starting material.

Scheme 3.16 First strategy from monotriflate **III-120**

a. Retrosynthetic strategy



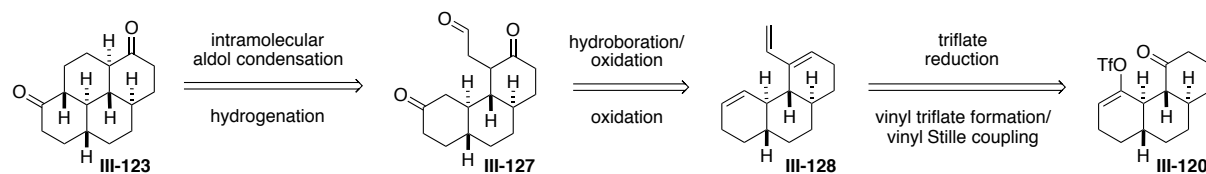
b. Synthetic results



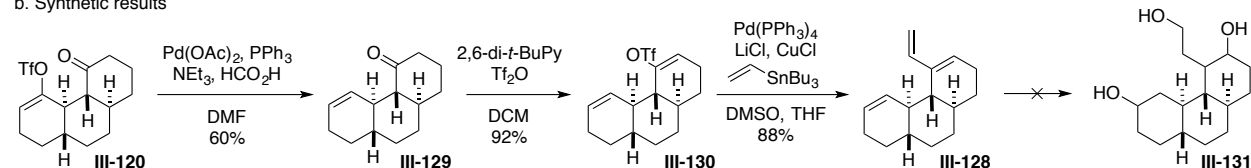
We then turned our attention to the potential application of an intramolecular aldol condensation to fashion the fourth ring within **III-123**, thus targeting tricyclic tricarbonyl **III-127**, as shown in Scheme 3.17a. We did recognize the potential for this structure to undergo a competing aldol condensation with the alternate ketone to form the undesired five-membered ring, but nevertheless, we imagined that this intermediate could be accessed from triene **III-128** through a triple hydroboration/oxidation and subsequent oxidation sequence. Triene **III-128** could be obtained from the monotriflate **III-120** through a transition metal-catalyzed triflate reduction followed by vinyl triflate formation of the remaining ketone and subsequent vinyl Stille coupling.

Scheme 3.17 Second strategy from monotriflate **III-120**

a. Retrosynthetic strategy



b. Synthetic results



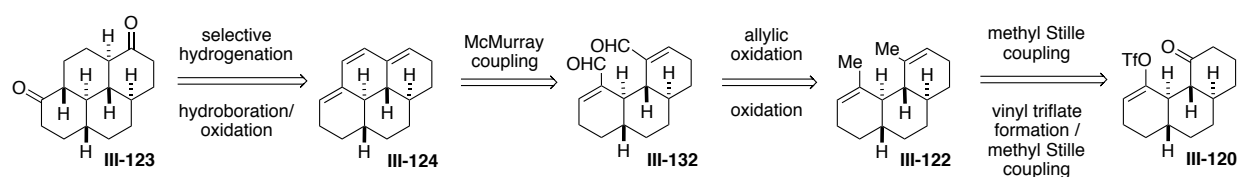
In the forward sense, as shown in Scheme 3.17b, a palladium-catalyzed reduction of the monotriflate **III-120** produced alkene **III-129**, which was readily converted to the vinyl triflate **III-130** in 92% yield upon exposure to 2,6-di-*tert*-butylpyridine and triflic anhydride. The successful Stille coupling with tributyl(vinyl)tin smoothly delivered triene **III-128** in 88% yield, however all attempts to perform a triple hydroboration of this compound resulted in a complex mixture of indiscernible products. To ensure that the employed conditions were generally

successful, these hydroborations were simultaneously conducted on a model decalin diene system, providing successful double hydroboration diol products.

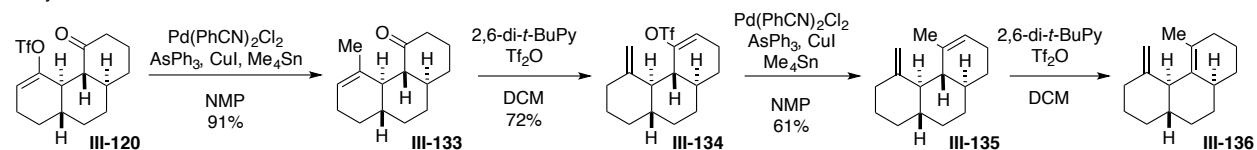
In the third designed approach, as shown in Scheme 3.18a, we envisioned that tetracyclic dione **III-123** could be accessed in the same manner as detailed previously from tetracyclic triene **III-124**. In this case, we imagined that this intermediate could be accessed from bis(aldehyde) **III-132** through a McMurray reaction, which in turn could arrive from tricyclic **III-122** through a double allylic oxidation and subsequent oxidation sequence. Because the bis(triflate) **III-119** was unsuccessful in the attempted double palladium-catalyzed methyl installation to afford **III-122** (Scheme 3.15), we imagined that this bis(methyl) tricycle **III-122** could be accessed in a stepwise manner from monotriflate **III-120** through an initial methyl Stille coupling, followed by vinyl triflate formation of the remaining ketone and subsequent methyl Stille coupling.

Scheme 3.18 Third strategy from monotriflate **III-120**

a. Retrosynthetic strategy



b. Synthetic results



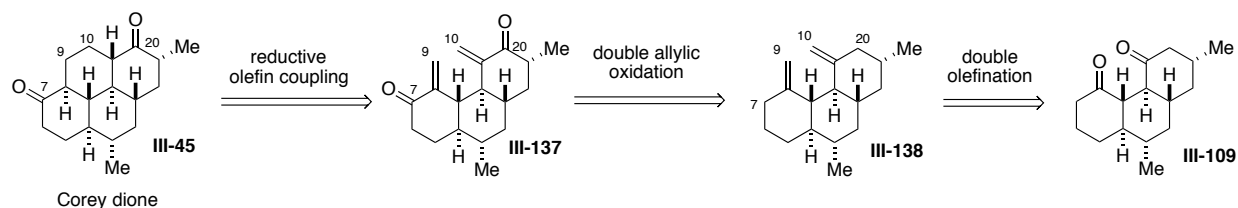
In the forward sense, as shown in Scheme 3.18b, monotriflate **III-120** was smoothly converted to vinyl methyl **III-133** in 91% yield. Interestingly, upon exposure to 2,6-di-*tert*-butylpyridine and triflic anhydride, the vinyl triflate formation proceeded along with a simultaneous alkene isomerization to the exocyclic olefin **III-134**. This result, in conjunction with

the difficulty in forming and further manipulating bis(triflate) **III-119**, highlighted the instability associated with certain unsaturation within the rigid fused ring system. We imagined that with **III-134** in hand, we could repeat the two-step process to install the second methyl substituent and then isomerize to the bis(exocyclic olefin). Thus, the methyl coupling of this compound provided **III-135**, however subsequent treatment with 2,6-di-*tert*-butylpyridine and triflic anhydride with the intention to promote isomerization to the exocyclic olefin provided instead isomerized **III-136**.

3.4.4 Strategic return to symmetry

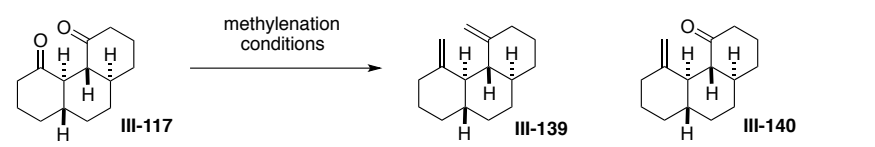
It was clear to us at this point that the unsaturation within the rigid ring system was leading to challenging reactivity or undesired isomerization to relieve the apparently high levels of ring strain present. The unexpected access to the exocyclic olefin within **III-134** (Scheme 3.18b) provided inspiration to target the bis(exocyclic alkene) in a direct manner from the key diketone intermediate. As shown in Scheme 3.19 on the real DICA system, we imagined that tetracyclic Corey dione **III-45** could be accessed from a central tricyclic bis(enone) **III-137** through a reductive olefin coupling. We surmised that due to the inherent proximity of the exocyclic alkene substituents, if a radical could be generated at the C9 or C10 position, the desired C9–C10 bond would readily form to fashion the fourth and final ring of the system. This bis(enone) **III-137** could be accessed from a double allylic oxidation of bis(olefin) **III-138**, which could be efficiently obtained from a double olefination of the key diketone **III-109**.

Scheme 3.19 Revised strategy returning to symmetry



Implementation of this strategy on the symmetrical model system began with investigations into the double olefination of diketone **III-117**. As shown in Table 3.1, this transformation, analogous to the triflate formation as discussed above, also proved to be difficult to achieve, often producing only the monoolefin **III-140**. With a variety of known methylenation conditions, an assortment of experiments were conducted.

Table 3.1 Olefination of diketone **III-117**



The reaction scheme shows the conversion of diketone **III-117** to bis(olefin) **III-139** and monoolefin **III-140** under various methylenation conditions. The starting material **III-117** is a bicyclic diketone. The products are **III-139** (bis(olefin)) and **III-140** (monoolefin).

Entry	Conditions	Temperature	Result
1	TMS(CH ₂)MgCl, then AcOH	RT, then 65 °C	exclusive production of III-140
2	Tebbe reagent, pyridine	-55 °C	exclusive production of III-140
3	Petasis reagent	65 °C	N/R
4	Zn powder, Br ₂ CH ₂ , TiCl ₄	5 °C	N/R
5	KO ^t Bu, Ph ₃ PMeBr	RT	N/R
6	KO ^t Bu, Ph ₃ PMeBr	70 °C	exclusive production of III-140
7	KO ^t Bu, Ph ₃ PMeBr	80 °C	production of III-140 and III-139

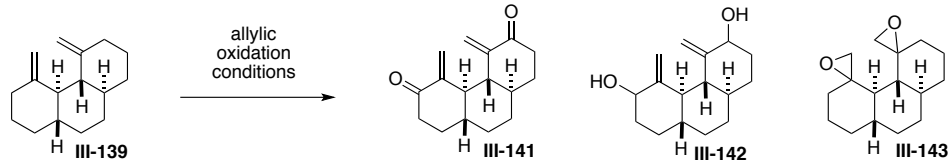
Petersen olefination conditions (entry 1) were successful in production of monoolefin **III-140**, but were not able to achieve any desired bis(olefin) species **III-139**. Subsequent resubjection of the isolated monoolefin **III-140** to these Petersen conditions, including experiments with additive cerium(III) chloride, solely resulted in unchanged starting material. Organometallic reagents such as Tebbe's reagent or the Petasis reagent are known to be successful for the methylenation of hindered ketones, however treatment of diketone **III-117** with Tebbe's reagent only produced monoolefin **III-140** (entry 2), and refluxing in Petasis reagent resulted in unchanged starting diketone (entry 3). Similarly, Lombardo methylenation conditions (entry 4) did not alter the

starting diketone. Wittig olefination conditions at room temperature provided unchanged starting diketone (entry 5), and raising the temperature to 70 °C exclusively generated the monoolefin **III-140** with no bis(olefin) **III-139** production (entry 6). However, upon sublimation of the potassium *tert*-butoxide and a slight elevation of the reaction temperature to 80 °C, the first observation of the bis(olefin) **III-139** was established (entry 7). As detailed in the Experimental Section 3.6, this unoptimized reaction employed 2.2 equivalents of base and 2.4 equivalents of the phosphonium reagent, providing a mixture of monoolefin **III-140** (39%), and bis(olefin) **III-139** (46%). These conditions were further optimized on the real DICA system, as will be detailed below.

With the bis(olefin) **III-139** in hand, we turned our attention to the double allylic oxidation required to provide the key late-stage bis(enone). As shown in Table 3.2, initial investigations sought to access this bis(enone) **III-141** directly. Treatment of bis(olefin) **III-139** with known allylic oxidant CrO₃•3,5-dimethylpyrazole (CrO₃•DMP) did not provide the desired bis(enone) **III-141**, but rather bis(epoxide) **III-143** (entry 1). Other known conditions for this direct transformation employing IBX and diphenyl diselenide at 80 °C resulted in unchanged starting material (entry 2). An elevation of temperature to 115 °C with these reagents provided a very complex mixture of products, with the bis(epoxide) **III-143** as the major component (entry 3). Thus, we turned our attention to a two-step approach, first achieving the allylic oxidation to diol **III-142**, followed by a subsequent oxidation to the enone. Treatment of bis(olefin) **III-139** with selenium dioxide, *tert*-butyl hydrogen peroxide, and salicylic acid at room temperature provided unchanged starting material (entry 4). Exposure of bis(olefin) **III-139** to selenium dioxide in methanol and dichloromethane at 65 °C delivered a mixture of desired symmetrical and unsymmetrical diol diastereomers **III-142**, but did not achieve completion, with the isolation of

monoalcohol intermediates (entry 5). The same reagents in ethanol and dichloromethane at an increased temperature of 78 °C enabled the reaction to proceed to completion, isolating 69% of the desired mixture of diastereomeric diols **III-142** (entry 6). Disappointingly, an attempt to oxidize this mixture (**III-142**) to the bis(enone) **III-141** with manganese dioxide resulted in only unchanged starting material (entry 7). When treated with Dess-Martin periodinane at room temperature, however, the mixture of diols (**III-142**) successfully converged on the desired bis(enone) **III-141** in 89% yield.

Table 3.2 Double allylic oxidation of bis(olefin) **III-139**

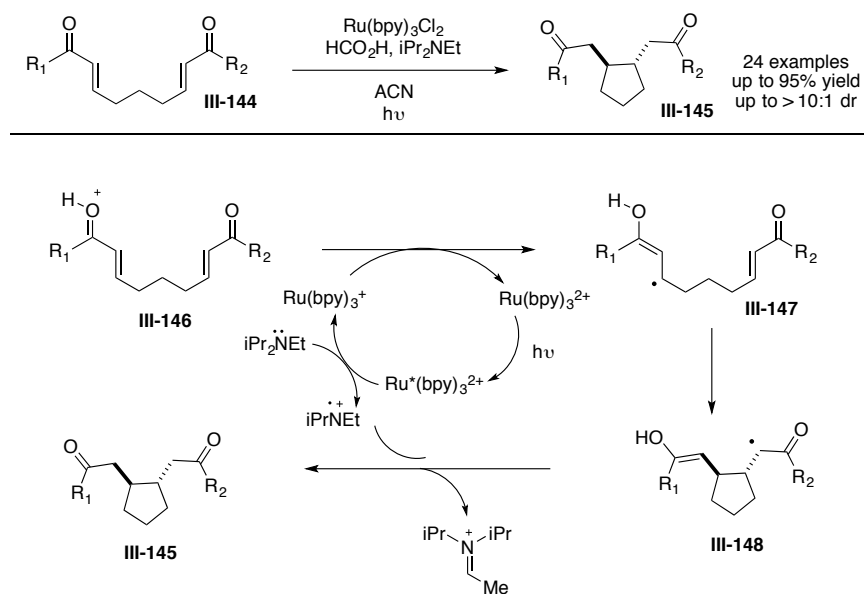


	<i>Entry</i>	<i>Conditions</i>	<i>Temperature</i>	<i>Result</i>
a. One-step oxidation	1	CrO ₃ ·DMP	-20 °C	bis(epoxide) III-143
	2	IBX, (PhSe) ₂ , benzene, pyridine	80 °C	N/R
	3	IBX, (PhSe) ₂ , dichlorobenzene, pyridine	115 °C	complex mixture some production of III-143
b. Two-step oxidation	4	SeO ₂ , ^t BuOOH, salicylic acid, DCM	RT	N/R
	5	SeO ₂ , MeOH, DCM	65 °C	mixture of symmetrical and unsymmetrical diols III-142 - did not go to completion
	6	SeO ₂ , EtOH, DCM	78 °C	69% mixture of symmetrical and unsymmetrical diols III-142
	7	MnO ₂	RT	N/R
	8	DMP	RT	89% III-141

With the desired bis(enone) **III-141** in hand, we wished to generate a radical at the terminal position of the enone, with the hope that it would promote rapid ring closure onto the other enone. Although the use of single-electron reductants was a possibility (i.e. samarium diiodide²⁹⁸), we

imagined that this substrate would be a suitable candidate for the application of conditions developed by Yoon and coworkers for the photocatalytic reductive cyclization of enones.²⁹⁹ As shown in Scheme 3.20, this disclosure allowed for the formation of a variety of cyclized products (**III-145**) from bis(enone) species such as **III-144** in good yields and selectivities. The authors propose that under irradiation with a fluorescent bulb, the ruthenium catalyst is excited to the photoexcited state which is reduced by Hünig's base to form the Ru^+ species that delivers an electron to the protonated starting substrate (**III-146**). This radical delivery produces intermediate radical **III-147**, as well as regenerating the initial Ru^{2+} catalyst. The radical intermediate is then poised to undergo a 5-*exo*-trig cyclization to generate radical **III-148**, and a subsequent hydrogen atom transfer from the oxidized Hünig's base species delivers the cyclized product **III-145**.

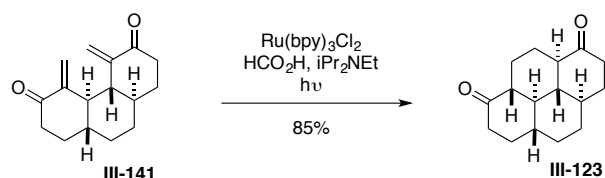
Scheme 3.20 Yoon's reductive cyclization of enones



We imagined that the mild nature of these conditions lent themselves nicely to facile application to complex molecule synthesis, and that specifically within the context of our strategy to access Corey dione **III-45**, they had the potential to generate a radical in the desired position of

the bis(enone) system. To our delight, when bis(enone) **III-141** was subjected to the conditions exactly as described by Yoon and coworkers, the desired tetracyclic diketone **III-123** was smoothly delivered in 85% yield with no required optimization, producing a single symmetrical stereoisomer (Scheme 3.21).

Scheme 3.21 Successful reductive ring closure

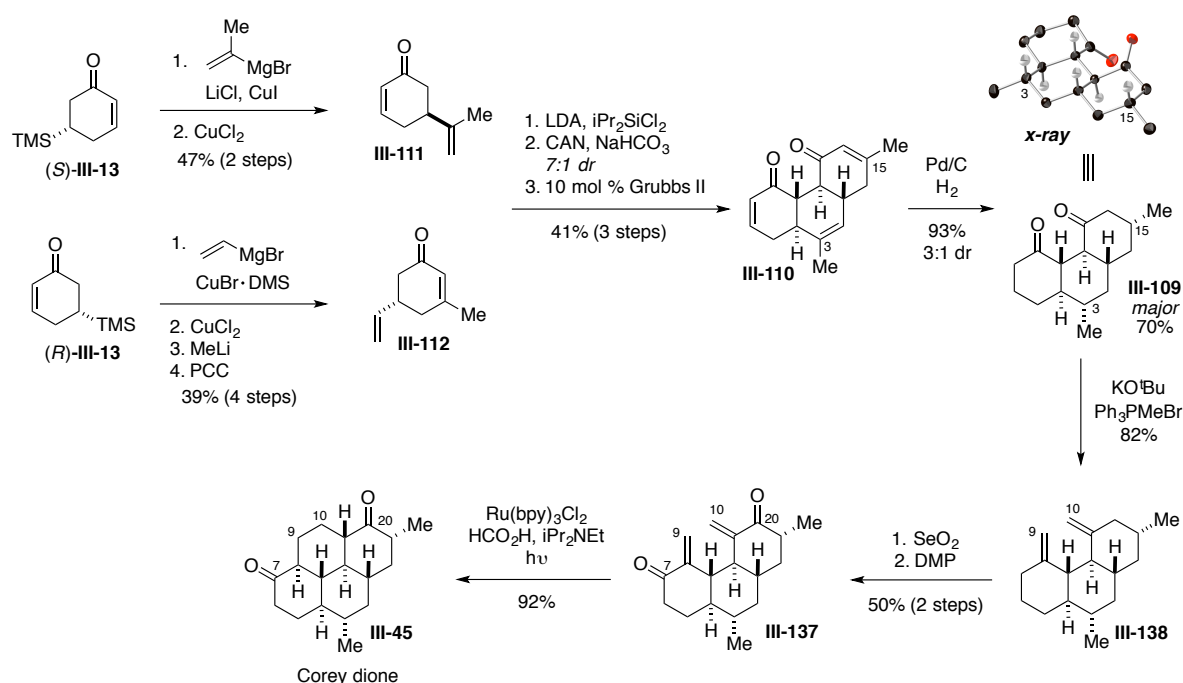


3.4.5 Successful synthesis of Corey dione

Having successfully accessed the symmetrical, demethylated version of the Corey dione (**III-123**), we sought to implement the sequence and optimize the conditions on the real DICA system to access Corey dione **III-45** (Scheme 3.22). The ideal route to diketone **III-109** was previously discussed, and the ensuing double olefination of this central intermediate was optimized, discovering that an increase in the equivalents of base and phosphonium reagents to 3.6 and 3.7, respectively, allowed for complete conversion to the bis(olefin) **III-138** in 82% yield. The two-step double allylic oxidation was operationally simplified to proceed without purification of the intermediate mixture of diol diastereomers, but rather a simple removal of the solvent, followed by dilution with dichloromethane and addition of Dess-Martin periodinane provided a 50% yield of bis(enone) **III-137** over two steps. The final reductive enone coupling proceeded without optimization to deliver the target Corey dione **III-45** in 92% yield. Axial protonation for the generation of the all-*trans* carbocyclic scaffold is certainly favored thermodynamically, a fact that previous syntheses have exploited with base-mediated epimerizations,^{286, 288-289} but it is also

likely favored kinetically due to the strain imparted by the rigid fused system for equatorial delivery, as has been observed for similar cyclohexanone and decalone systems.³⁰⁰⁻³⁰¹ This concluded our synthesis of Corey dione **III-45** in 12 steps from (*R*)-**III-113** in 4.2% overall yield (or 2.4% yield from commercially available (*E*)-3-(trimethylsilyl)prop-2-en-1-ol), thus completing a 17-step formal synthesis of (+)-7,20-diisocyanoadociane **III-1**.²⁶⁰

Scheme 3.22 Successful synthesis of Corey dione **III-45**



3.5 Conclusion

The isocyanoterpene family of natural products have been of interest to chemists and biologists for their complex chemical structures and promising biological activities. As the leader of the family in antimalarial activity, 7,20-diisocyanoadociane **III-1** has been the center of many scientific investigations. Six successful syntheses of DICA have been completed by different research groups, each providing a unique synthetic approach to construct the complex core

structure. We have successfully applied the developed couple and close strategy to the formal synthesis of DICA, demonstrating a novel approach to build the core scaffold compared to the previous syntheses. The implementation of our general strategy allowed for much of the carbocyclic core to be convergently assembled, and enabled the natural pseudo-symmetry of the molecule to amplify the efficiency of the final stages of the synthesis.²⁶⁰

3.6 Experimental Section

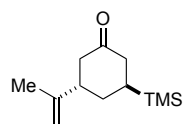
3.6.1 General information

All reactions were carried out under a nitrogen atmosphere in flame-dried glassware with magnetic stirring unless otherwise stated. Methanol, THF, ether and DCM were purified by passage through a bed of activated alumina.²⁶¹ Reagents were purified prior to use unless otherwise stated following the guidelines of Armarego and Chai.²⁶² Purification of reaction products was carried out by flash chromatography using SiliCycle silica gel F60, 40-63 μm (230-400 mesh). Analytical thin layer chromatography was performed on EM Reagent 0.25 mm silica gel 60-F plates. Visualization was accomplished with UV light and *p*-anisaldehyde stain. Germanium ATR infrared spectra were recorded using a Bruker Tensor 37. ¹H-NMR spectra were recorded on a Varian Inova 500 (500 MHz), Agilent DD2 (500MHz), Agilent DD MR-400 (400MHz), or Bruker Advance III 500 (500 MHz) spectrometer and are reported in ppm using solvent as an internal standard (CDCl₃ at 7.26 ppm). Data are reported as (app = apparent, obs = obscured, s = singlet, d = doublet, t = triplet, q = quartet, p = pentet, h = hextet, sep = septet, o = octet, m = multiplet, b = broad; integration; coupling constant(s) in Hz. ¹³C-NMR spectra were recorded on a Bruker Advance III 500 spectrometer equipped with DCH CryoProbe, and are reported in ppm using solvent as an internal standard (CDCl₃ at 77.16 ppm, except where noted). Mass spectra data were

obtained on an Agilent 6210 Time-of-Flight LC/MS. All optical rotation measurements were obtained on a Rudolph Research Analytical Autopol IV, Serial #82239. X-ray data were collected on the Kappa Apex 2 diffractometer.

3.6.2 Construction of the key diketone intermediate III-109

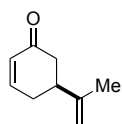
3.6.2.1 Starting material synthesis from common enantioenriched silane intermediates



Compound III-149.

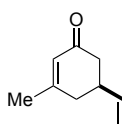
LiCl (95 mg, 2.13 mmol, 20 mol %) and CuI (0.20 g, 1.06 mmol, 10 mol %) were added to a flame-dried round-bottom flask. The flask was cooled to 0 °C, and (*S*)-**III-113** (1.79 g, 10.6 mmol, 1.0 equiv) in THF (50 mL) was added via cannula (12 mL THF rinse). TMS-Cl (1.5 mL, 11.7 mmol, 1.1 equiv) was added, and the mixture stirred for 25 minutes. The freshly prepared and titrated isopropenyl Grignard solution, (0.62 M, 20.7 mL, 12.8 mmol, 1.2 equiv) was added dropwise via syringe over 30 minutes and the reaction allowed to slowly warm to room temperature. Upon observed consumption of the starting material by TLC (1.5h), the black reaction was quenched with saturated NH₄Cl solution and extracted with ether. The combined organic extracts were washed twice with 3 M HCl and once with brine, then dried over MgSO₄, and concentrated under reduced pressure. The crude material was purified by flash chromatography on silica gel with 5% ether/pentane. (1.45 g, 6.89 mmol, 65% yield): $[\alpha]_D = -56.3$ (*c* 0.12, CHCl₃); IR (Germanium ATR): 2953, 1713, 1249, 839 cm⁻¹; ¹H NMR (499 MHz, Chloroform-*d*) δ 4.90 (d, *J* = 1.7 Hz, 1H), 4.72 (d, *J* = 1.7 Hz, 1H), 2.81 (s, 1H), 2.64 – 2.55 (m, 1H), 2.46 (ddd, *J* = 15.0, 6.0, 1.0 Hz, 1H), 2.35 – 2.26 (m, 1H), 2.08 (ddd, *J* = 14.8, 12.9, 1.1 Hz, 1H), 1.94 – 1.84 (m, 1H), 1.75 – 1.66 (m, 4H), 1.17 (tt, *J* = 12.6, 3.8 Hz, 1H), 0.00 (d, *J* = 0.6 Hz, 9H); ¹³C NMR (126 MHz,

CDCl₃) δ 212.5, 146.5, 112.8, 45.2, 43.5, 42.2, 28.6, 22.1, 20.7, -3.4; HRMS (ESI): Exact mass calc'd for C₁₂H₂₂OSiNa [M+Na]⁺, 233.1338. Found 233.1328.



Compound III-111.

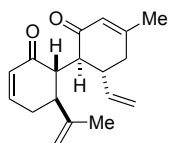
CuCl₂ (2.7 g, 20.0 mmol, 3.0 equiv) was added to a flame-dried round-bottom flask. **III-149** (1.4 g, 6.65 mmol, 1.0 equiv) in DMF (48 mL, with an additional 3 mL DMF rinse) was added via cannula and the mixture heated to 55 °C. After 2 hours, the black reaction was cooled to room temperature, diluted with brine, and extracted twice with pentane and once with 5% ether/pentanes. The combined organic extracts were dried over MgSO₄ and the solvent evaporated carefully. The crude material was purified by flash chromatography on silica gel with 15% ether/pentane. (0.652 g, 4.79 mmol, 72% yield): [α]_D = +29.2 (*c* 0.59, CHCl₃); IR (Germanium ATR): 2922, 1678, 1388, 881 cm⁻¹; ¹H NMR (499 MHz, Chloroform-*d*) δ 7.01 (ddd, *J* = 10.1, 5.8, 2.5 Hz, 1H), 6.11 – 5.98 (m, 1H), 4.83 (q, *J* = 1.6 Hz, 1H), 4.78 (s, 1H), 2.78 – 2.66 (m, 1H), 2.57 (dd, *J* = 16.2, 3.8 Hz, 1H), 2.53 – 2.44 (m, 1H), 2.41 – 2.27 (m, 2H), 1.77 (d, *J* = 1.5 Hz, 3H); ¹³C NMR (126 MHz, CDCl₃) δ 199.8, 149.8, 146.6, 129.7, 110.9, 43.2, 42.2, 31.1, 20.6; HRMS (ESI): Exact mass calc'd for C₉H₁₃O [M+H]⁺, 137.0966 Found 137.0962.



Compound III-112.

See Experimental Section **2.9.2** for the preparation and characterization of **III-112**.

3.6.2.2 Implementation of developed strategy for the synthesis tricyclic III-109



Compound III-150.

To a flame dried conical flask was added diisopropylamine (113 μ L, 0.81 mmol, 1.2 equiv) and THF (0.8 mL). The flask was cooled to -78 °C, and *n*-BuLi (freshly titrated to 2.04 M, 0.36 mL, 0.74 mmol, 1.1 equiv) was added. After 10 minutes, enone **III-111** (92.0 mg, 0.67

mmol, 1.0 equiv) in THF (0.3 mL) was added (0.1 mL rinse). The solution stirred for 30 minutes before slowly adding it via cannula to a flask containing $i\text{Pr}_2\text{SiCl}_2$ (120 μL , 0.67 mmol, 1.0 equiv) and THF (2.7 mL), also at $-78\text{ }^\circ\text{C}$, over 1 hour. Meanwhile, LDA was prepared exactly as above in a separate conical flask. After 10 minutes, enone **III-112** (92.0 mg, 0.67 mmol, 1.0 equiv) in THF (0.3 mL) was added (0.1 mL rinse). This solution stirred for 30 minutes before adding it slowly to the reaction flask via cannula over 1 hour (about 40 minutes following the completion of the first enolate addition). The mixture stirred at $-78\text{ }^\circ\text{C}$ for 45 min before warming to room temperature. Upon observed consumption of the starting materials by TLC (2h), the orange reaction was quenched with pH 7 buffer and extracted with pentanes. The combined organic layers were dried over MgSO_4 , and concentrated under reduced pressure. The crude material was placed on the vacuum manifold overnight and was used directly in the next reaction.

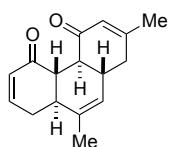
To a flame-dried round-bottom flask was added CAN (0.81 g, 1.47 mmol, 2.2 equiv), NaHCO_3 (0.25 g, 2.98 mmol, 4.4 equiv), ACN (22 mL, dried over activated sieves), and DMSO (95.2 μL , 1.34 mmol, 2.0 equiv). The mixture was cooled to $-30\text{ }^\circ\text{C}$ and stirred vigorously while the crude material in EtCN (3 mL, dried over activated sieves, 0.4 mL rinse) was added via cannula. Upon observed consumption of the starting silyl bis-enol ether by TLC (15 min), the orange mixture was diluted with saturated NaHCO_3 solution, extracted with CHCl_3 . The combined organic layers were dried over MgSO_4 filtered through Celite with EtOAc, and concentrated under reduced pressure to yield a 5:1 mixture of diastereomers. The crude material was purified by flash chromatography on silica gel using 5% EtOAc/hexane (major diastereomer: 73.0 mg, 0.27 mmol, 40% yield over two steps; total coupled yield: 88.8 mg, 0.33 mmol, 49% yield): $[\alpha]_{\text{D}} = +42.9$ (c 0.84, CHCl_3); IR (Germanium ATR): 2916, 1658, 1380, 1211, 916 cm^{-1} ; ^1H NMR (500 MHz,

Chloroform-*d*) δ 6.90 (ddd, $J = 10.0, 5.9, 2.4$ Hz, 1H), 5.99 (ddd, $J = 10.0, 2.8, 1.0$ Hz, 1H), 5.85 (q, $J = 1.5$ Hz, 1H), 5.59 (dt, $J = 17.0, 9.8$ Hz, 1H), 5.14 – 5.08 (m, 2H), 4.84 (dq, $J = 3.5, 1.8$ Hz, 2H), 3.52 (td, $J = 12.2, 4.9$ Hz, 1H), 3.44 – 3.30 (m, 1H), 2.63 (d, $J = 12.8$ Hz, 1H), 2.44 – 2.27 (m, 3H), 2.27 – 2.20 (m, 2H), 1.93 (d, $J = 1.2$ Hz, 3H), 1.66 (t, $J = 1.1$ Hz, 3H); ^{13}C NMR (126 MHz, CDCl_3) δ 200.3, 199.1, 159.3, 148.2, 145.5, 140.6, 130.2, 127.2, 117.6, 114.8, 49.3, 48.8, 48.1, 45.2, 38.4, 31.8, 24.2, 18.6; HRMS (ESI): Exact mass calc'd for $\text{C}_{18}\text{H}_{22}\text{O}_2\text{Na}$ $[\text{M}+\text{Na}]^+$, 293.1518. Found 293.1513.

Note: scaled up procedure for oxidative coupling:

While formation of the silyl bis-enol ether is a very scalable process, the developed oxidative coupling conditions are not as amenable to large scale ups, which would require re-optimization due to reagent solubility issues. Therefore, to bring forward larger amounts of material, the following procedure was followed: To a flame dried conical flask was added diisopropylamine (1.24 mL, 8.81 mmol, 1.2 equiv) and THF (10 mL). The flask was cooled to -78 °C, and *n*-BuLi (freshly titrated to 2.28 M, 3.55 mL, 8.08 mmol, 1.1 equiv) added. After 10 minutes, enone **III-111** (1.0 g, 7.34 mmol, 1.0 equiv) in THF (4 mL) was added (0.3 mL rinse). The solution stirred for 30 minutes before slowly adding it via cannula to a flask containing $\text{iPr}_2\text{SiCl}_2$ (1.32 mL, 7.34 mmol, 1.0 equiv) and THF (29 mL), also at -78 °C over 1.5 hours. Meanwhile, LDA was prepared exactly as above in a separate conical flask. After 10 minutes, enone **III-112** (1.0 g, 7.34 mmol, 1.0 equiv) in THF (4 mL) was added (0.3 mL rinse). This solution stirred for 30 minutes before adding it slowly to the reaction flask via cannula over 1 hour (45 min following the completion of the first enolate addition). The mixture stirred at -78 °C for 45 min and then was warmed to room temperature. Upon observed consumption of the starting materials by TLC (1.5 h from when

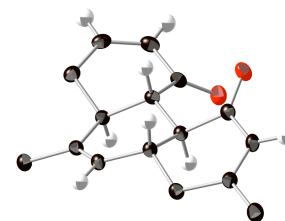
warmed to room temperature), the orange reaction was quenched with pH 7 buffer and extracted with pentanes. The combined organic layers were dried over MgSO_4 and concentrated under reduced pressure. The crude material was placed on the vacuum manifold overnight. The crude silyl bis-enol ether was split into seven equal portions (0.404 g, 1.05 mmol) and each was used in the following manner: To a flame-dried 100 mL flask was added CAN (1.27 g, 2.31 mmol, 2.2 equiv), NaHCO_3 (0.39 g, 4.62 mmol, 4.4 equiv), ACN (35 mL, 0.03 M), and DMSO (0.15 mL, 2.10 mmol, 2.0 equiv). The mixture was cooled to $-30\text{ }^\circ\text{C}$, and stirred vigorously while the silyl bis-enol ether in EtCN (5 mL) was added to the reaction via cannula (0.3 mL rinse). Upon observed consumption of the starting silyl bis-enol ether by TLC (15 min), the orange mixture was diluted with saturated NaHCO_3 solution, extracted with CHCl_3 . The combined organic layers were dried over MgSO_4 filtered through celite with EtOAc, and concentrated under reduced pressure to yield a ~7:1 mixture of diastereomers. The combined crude material from all seven partitions was purified by flash chromatography on silica gel using 5% EtOAc/hexane (major diastereomer: 0.97 g, 3.6 mmol, 49% over two steps; total coupled yield: 1.1 g, 4.10 mmol, 56%).



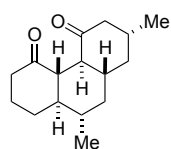
Compound III-110.

To a flame-dried flask was added Grubbs II from the glove box (16 mg, 0.02 mmol, 10 mol %). **III-150** (40.0 mg, 0.15 mmol, 1.0 equiv) in DCM (2.5 mL, with an additional 0.4 mL rinse) was added to the flask via cannula and the reaction heated to $40\text{ }^\circ\text{C}$. Upon observed consumption of the starting material by TLC (22h), 10 μL DMSO were added, and the mixture stirred for 2h. The solvent was evaporated, and the crude material was purified by flash chromatography on silica gel with 20% EtOAc/hexanes (30.5 mg, 0.126 mmol, 84% yield). Solid crystals for X-ray crystallography were obtained by slow evaporation of ethyl acetate. $[\alpha]_D =$

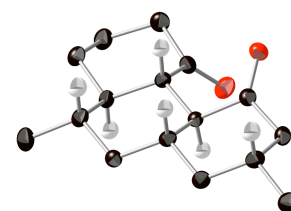
+561.6 (*c* 1.13, CHCl₃); IR (Germanium ATR): 2923, 1670, 1681, 1379, 1176, 843 cm⁻¹; ¹H NMR (500 MHz, Chloroform-*d*) δ 6.81 (ddd, *J* = 10.0, 5.6, 2.1 Hz, 1H), 6.10 (ddd, *J* = 10.0, 3.1, 0.9 Hz, 1H), 5.90 (dd, *J* = 2.7, 1.4 Hz, 1H), 5.28 (q, *J* = 1.8 Hz, 1H), 2.78 – 2.66 (m, 2H), 2.56 (dd, *J* = 12.4, 10.8 Hz, 1H), 2.52 – 2.38 (m, 2H), 2.34 (dd, *J* = 18.0, 4.0 Hz, 1H), 2.27 – 2.12 (m, 2H), 1.93 (d, *J* = 1.2 Hz, 3H), 1.70 (dt, *J* = 2.4, 1.2 Hz, 3H); ¹³C NMR (126 MHz, CDCl₃) δ 200.3, 199.6, 157.2, 145.3, 134.4, 130.5, 127.1, 124.8, 47.6, 45.9, 42.0, 39.7, 37.8, 32.5, 23.7, 20.3; HRMS (ESI): Exact mass calc'd for C₁₆H₁₈O₂Na [M+Na]⁺, 265.1205. Found 265.1199.



X-ray structure

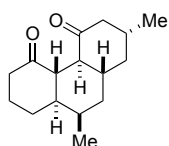
**Compound III-109.**

III-110 (100 mg, 0.41 mmol, 1.0 equiv) was diluted in MeOH (14 mL, 0.03 M). Pd/C (44.0 mg, 0.041 mmol, 10 mol %) was added. H₂ was bubbled through the solution for 1 minute, and then the reaction was left to stir at room temperature under H₂ overnight. The reaction was then purged with N₂ for 1h before filtering through Celite with EtOAc. The solvent was evaporated, and the crude material purified by flash chromatography on silica gel with 20% EtOAc/hexanes to yield a 3:1 mixture of diastereomers (95.0 mg, 0.38 mmol, 93% yield). The two diastereomers were separated by preparative HPLC using a C18 column and a 40-75% ACN/H₂O gradient solvent system. The structures of the major and minor products were elucidated by X-ray crystallography. Solid crystals were obtained by slow evaporation of ether. Major isomer: [α]_D = +41.2 (*c* 1.14, CHCl₃); IR (Germanium ATR): 2911, 1707, 1455 cm⁻¹; ¹H NMR (500 MHz, Chloroform-*d*) δ 2.57 – 2.37 (m, 3H), 2.37 – 2.29 (m, 2H), 2.28 – 2.19 (m, 1H), 2.19 –

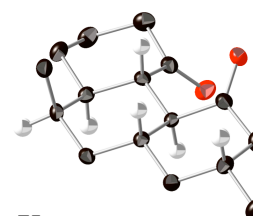


X-ray structure

2.06 (m, 2H), 1.86 (dq, $J = 11.9, 6.3$ Hz, 1H), 1.77 (dtd, $J = 13.2, 3.5, 1.8$ Hz, 1H), 1.68 (dt, $J = 13.1, 3.4$ Hz, 1H), 1.60 (tdd, $J = 14.2, 11.8, 3.3$ Hz, 2H), 1.44 (qt, $J = 11.8, 3.2$ Hz, 1H), 1.38 – 1.25 (m, 2H), 1.20 (q, $J = 12.2$ Hz, 1H), 1.12 – 1.03 (m, 1H), 1.03 (d, $J = 6.6$ Hz, 3H), 0.93 (d, $J = 6.3$ Hz, 3H); ^{13}C NMR (126 MHz, CDCl_3) δ 211.5, 210.9, 53.1, 52.6, 50.9, 50.2, 42.3, 42.1, 42.1, 41.8, 37.3, 35.4, 29.8, 27.7, 22.6, 19.9; HRMS (ESI): Exact mass calc'd for $\text{C}_{16}\text{H}_{24}\text{O}_2\text{Na}$ $[\text{M}+\text{Na}]^+$, 271.1674. Found 271.1670.

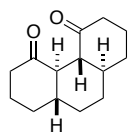
**Compound III-114.**

^1H NMR (500 MHz, Chloroform-*d*) δ 2.65 (t, $J = 11.3$ Hz, 1H), 2.46 (ddd, $J = 18.5, 12.2, 6.0$ Hz, 1H), 2.33 (td, $J = 11.2, 9.9, 5.4$ Hz, 3H), 2.23 (t, $J = 12.4$ Hz, 1H), 2.11 (dq, $J = 9.2, 3.2$ Hz, 1H), 1.98 –

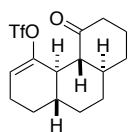
**X-ray structure**

1.80 (m, 2H), 1.76 – 1.67 (m, 1H), 1.66 – 1.52 (m, 6H), 1.35 (td, $J = 13.1, 4.3$ Hz, 1H), 1.18 (q, $J = 12.1$ Hz, 1H), 1.02 (d, $J = 6.5$ Hz, 3H), 0.92 (d, $J = 7.2$ Hz, 3H); ^{13}C NMR (126 MHz, CDCl_3) δ 212.1, 210.9, 52.9, 50.3, 47.2, 47.0, 42.3, 42.2, 40.4, 36.5, 35.4, 32.4, 30.5, 27.7, 22.6, 13.2; HRMS (ESI): Exact mass calc'd for $\text{C}_{16}\text{H}_{24}\text{O}_2\text{Na}$ $[\text{M}+\text{Na}]^+$, 271.1674. Found 271.1670.

3.6.3 Triflate strategy – model system

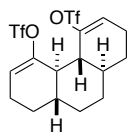
**Compound III-117.**

See Experimental Section 2.9.6 for the preparation and characterization of **III-117**.

**Compound III-120.**

A 1 M solution of LDA was prepared by cooling a mixture of diisopropylamine (0.31 mL, 2.2 mmol) in THF (2 mL) to -78 °C, and adding *n*-BuLi (0.9 mL, 2.25 M solution in hexanes, 2.0 mmol). After 10 minutes at this temperature, a portion of this solution (0.31 mL, 0.31 mmol, 1.5 equiv) was added to a solution of **III-117** (45 mg, 0.20 mmol) in THF (1.3 mL) at -78 °C. The

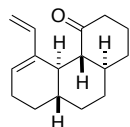
mixture stirred for 10 minutes before Comins' reagent was added (157 mg, 0.40 mmol, 2.0 equiv). After an hour at this temperature, the reaction was diluted with water, and extracted with ether. The combined organic extracts were washed with brine, dried over MgSO₄, and the solvent evaporated under reduced pressure. The crude material was purified by flash chromatography on silica gel using a gradient from hexane to 20% EtOAc/hexane to yield the pure desired product (36.6 mg, 0.104 mmol, 52%): [α]_D = -32.1 (*c* 0.96, CHCl₃); IR (Germanium ATR): 2927, 2856, 1718, 1409, 1204, 1139, 874 cm⁻¹; ¹H NMR (499 MHz, Chloroform-*d*) δ 5.71 (q, *J* = 3.6 Hz, 1H), 2.67 (tq, *J* = 10.4, 3.3 Hz, 1H), 2.53 (ddd, *J* = 13.4, 11.6, 6.4 Hz, 1H), 2.42 – 2.34 (m, 2H), 2.29 – 2.22 (m, 2H), 2.12 (dddt, *J* = 13.2, 6.5, 4.4, 2.2 Hz, 1H), 1.83 – 1.65 (m, 5H), 1.60 – 1.50 (m, 1H), 1.50 – 1.35 (m, 2H), 1.33 – 1.22 (m, 2H), 1.08 (tdd, *J* = 12.9, 11.6, 3.2 Hz, 1H); ¹³C NMR (126 MHz, CDCl₃) δ 212.5, 149.9, 119.6, 118.4, 117.1, 55.7, 47.2, 42.6, 40.3, 39.8, 33.7, 33.1, 31.6, 29.3, 28.6, 23.8; LRMS (ESI): Exact mass calc'd for C₁₅H₁₉F₃O₄SNa [M+Na]⁺, 375.0854. Found 375.08. Note: Also reisolated pure starting material: 20 mg, 0.091 mmol.



Compound III-119.

To a solution of **III-120** (17 mg, 0.05 mmol) in DCM (0.5 mL) at 0 °C was added 2,6-di-*tert*-butylpyridine (20 μ L, 0.09 mmol, 1.8 equiv), followed by the dropwise addition of Tf₂O (16 μ L, 0.09 mmol, 1.8 equiv). The reaction was allowed to warm to room temperature over night, after which time the starting material was observed to be consumed by TLC. The mixture was then diluted with water and extracted with DCM. The combined organic extracts were dried over MgSO₄ and the solvent evaporated under reduced pressure. The crude material was purified by flash chromatography on silica gel using a gradient from hexanes to 10% EtOAc/hexanes to yield the pure product (17.2 mg, 0.036, 72%): IR (Germanium ATR): 2929, 1446, 1206, 1025, 797 cm⁻¹

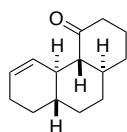
¹H NMR (500 MHz, Chloroform-*d*) δ 5.93 (s, 1H), 2.31 – 2.13 (m, 3H), 1.97 – 1.78 (m, 1H), 1.72 – 1.57 (m, 2H), 1.49 – 1.29 (m, 2H); ¹³C NMR (126 MHz, CDCl₃) δ 147.9, 122.6, 122.3, 119.8, 117.2, 114.7, 51.0, 45.8, 33.5, 29.1, 24.4; LRMS (ESI): Exact mass calc'd for C₁₆H₁₈F₆O₆S₂Na [M+Na]⁺, 507.0347. Found 507.03.



Compound III-126.

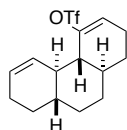
Lithium chloride (17 mg, 0.39 mmol, 6.0 equiv) was added to a round-bottom flask and flame dried twice. The flask was placed in the glove box, and CuCl (33 mg, 0.33 mmol, 5.0 equiv) and Pd(PPh₃)₄ (7.5 mg, 0.0065 mmol, 10 mol %) added. A solution of **III-120** (23 mg, 0.065 mmol) in DMSO (0.7 mL) and tributyl(vinyl)tin (29 μ L, 0.10 mmol, 1.5 equiv) was added to the flask outside of the glove box, using THF (0.2 mL) to rinse the solution. This mixture was cooled to in a liquid nitrogen bath and placed under vacuum for 10 minutes, then removed from the vacuum, warmed to room temperature, and purged with argon. This freeze-pump-thaw process was repeated four times before allowing the reaction to stir at room temperature for 1 hour, after which time it was heated to 60 °C. Upon observed consumption of the starting material by TLC (5.5 h), the reaction was cooled to room temperature, diluted with brine, and extracted with ether. The combined organic extracts were dried over MgSO₄, and the solvent evaporated under reduced pressure. The crude material was purified by flash chromatography on silica gel using a gradient from pentane to 5% ether/pentane to yield the pure product (9.7 mg, 0.042 mmol, 65%): [α]_D = –68.2 (*c* 0.05, CHCl₃); IR (Germanium ATR): 2920, 2852, 1712, 1455, 1261, 891 cm⁻¹; ¹H NMR (500 MHz, Chloroform-*d*) δ 6.03 – 5.94 (m, 1H), 5.66 (d, *J* = 3.5 Hz, 1H), 5.05 (dd, *J* = 16.9, 2.5 Hz, 1H), 4.74 (dd, *J* = 10.5, 2.5 Hz, 1H), 2.50 – 2.33 (m, 3H), 2.22 (t, *J* = 11.0 Hz, 1H), 2.17 – 2.09 (m, 3H), 1.81 – 1.70 (m, 3H), 1.68 – 1.58 (m, 2H), 1.51 – 1.36 (m, 3H), 1.28 – 1.19 (m, 2H),

1.06 (qd, $J = 12.7, 3.1$ Hz, 1H); ^{13}C NMR (126 MHz, CDCl_3) δ 215.3, 141.3, 140.1, 125.2, 113.1, 58.5, 48.0, 43.3, 40.2, 39.4, 34.1, 33.7, 32.4, 30.5, 28.9, 26.2; LRMS (ESI): Exact mass calc'd for $\text{C}_{16}\text{H}_{22}\text{ONa}$ $[\text{M}+\text{Na}]^+$, 253.1568. Found 253.10.



Compound III-129.

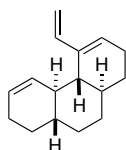
To a solution of **III-120** (106 mg, 0.30 mmol) in DMF (1.7 mL) was added $\text{Pd}(\text{OAc})_2$ (3.1 mg, 0.014 mmol, 4 mol %), PPh_3 (9 mg, 0.034 mmol, 10 mol %), and NEt_3 (0.15 mL, 1.1 mmol, 3.2 equiv). Formic acid (13 μL , 0.34 mmol, 1.1 equiv) was added to this mixture, and the yellow reaction was heated to 60 $^\circ\text{C}$. After observed consumption of the starting material by TLC (1.75 h), the black mixture was cooled to room temperature, diluted with water, and extracted with pentane twice and 5% ether/pentane twice. The combined organic layers were dried over MgSO_4 , and the solvent evaporated under reduced pressure. The crude material was purified by flash chromatography on silica gel using a gradient from pentane to 5% ether/pentane to yield pure product (37.3 mg, 0.18 mmol, 60%): $[\alpha]_{\text{D}} = -103.5$ (c 0.51, CHCl_3); IR (Germanium ATR): 2913, 2850, 1707, 1447, 1167, 1050, 732 cm^{-1} ; ^1H NMR (500 MHz, Chloroform- d) δ 5.70 – 5.51 (m, 2H), 2.40 – 2.29 (m, 2H), 2.10 – 1.94 (m, 5H), 1.85 – 1.71 (m, 2H), 1.71 – 1.55 (m, 3H), 1.50 – 1.41 (m, 2H), 1.42 – 1.32 (m, 1H), 1.32 – 1.22 (m, 1H), 1.15 (qt, $J = 11.0, 2.2$ Hz, 1H), 1.05 (qd, $J = 12.4, 3.4$ Hz, 1H); ^{13}C NMR (126 MHz, CDCl_3) δ 213.1, 130.2, 127.4, 59.2, 46.6, 43.2, 40.0, 39.4, 34.3, 33.7, 32.5, 30.1, 28.1, 26.1; LRMS (ESI): Exact mass calc'd for $\text{C}_{14}\text{H}_{20}\text{ONa}$ $[\text{M}+\text{Na}]^+$, 227.1412. Found 226.98.



Compound III-130.

To a solution of **III-129** (25 mg, 0.12 mmol) in DCM (1.2 mL) at 0 $^\circ\text{C}$ was added 2,6-di-*tert*-butylpyridine (39 μL , 0.18 mmol, 1.5 equiv), followed by the dropwise addition of Tf_2O

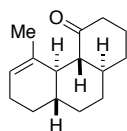
(31 μ L, 0.18 mmol, 1.5 equiv). The reaction was warmed to room temperature after 30 minutes. After observed consumption of the starting material by TLC (4h), the light brown reaction was diluted with water and extracted with DCM. The combined organic extracts were dried over $MgSO_4$, and the solvent evaporated under reduced pressure. The crude material as purified by flash chromatography on silica gel using pentane to yield the pure product (37.3 mg, 0.11 mmol, 92%): $[\alpha]_D = -11.0$ (c 0.05, $CHCl_3$); IR (Germanium ATR): 2963, 1260, 1091, 1018, 798 cm^{-1} ; 1H NMR (500 MHz, Chloroform- d) δ 6.17 – 6.06 (m, 1H), 5.82 (d, $J = 3.9$ Hz, 1H), 5.72 – 5.64 (m, 1H), 2.27 – 2.14 (m, 2H), 2.14 – 1.98 (m, 3H), 1.95 (d, $J = 10.8$ Hz, 1H), 1.78 – 1.67 (m, 2H), 1.67 – 1.58 (m, 2H), 1.51 – 1.42 (m, 1H), 1.42 – 1.29 (m, 4H), 1.29 – 1.18 (m, 1H); ^{13}C NMR (126 MHz, $CDCl_3$) δ 152.3, 129.4, 128.2, 121.1, 117.4, 48.6, 46.0, 43.9, 41.5, 33.8, 33.4, 30.6, 29.4, 25.7, 24.5; LRMS (ESI): Exact mass calc'd for $C_{15}H_{20}F_3O_3S$ $[M+H]^+$, 337.1085. Found 337.21.



Compound III-128.

Lithium chloride (28 mg, 0.65 mmol, 6.0 equiv) was added to a round-bottom flask and flame dried twice. The flask was placed in the glove box, and $CuCl$ (54 mg, 0.55 mmol, 5.0 equiv) and $Pd(PPh_3)_4$ (13 mg, 0.011 mmol, 10 mol %) added. A solution of **III-130** (36.6 mg, 0.109 mmol) in DMSO (0.9 mL) and tributyl(vinyl)tin (48 μ L, 0.16 mmol, 1.5 equiv) was added to the flask outside of the glove box, using THF (0.2 mL) to rinse the solution. This mixture was cooled to in a liquid nitrogen bath and placed under vacuum for 10 minutes, then removed from the vacuum, warmed to room temperature, and purged with argon. This freeze-pump-thaw process was repeated four times before allowing the reaction to stir at room temperature for 1 hour, after which time it was heated to 60 $^{\circ}C$. Upon observed consumption of the starting material by TLC (2.5 h), the reaction was cooled to room temperature, diluted with brine, and extracted with 50%

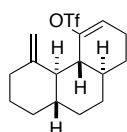
ether/ pentane. The combined organic extracts were dried over MgSO_4 , and the solvent evaporated under reduced pressure. The crude material was purified by flash chromatography on silica gel using pentane to yield the pure product (20.5 mg, 0.096 mmol, 88%): $[\alpha]_D = -25.6$ (c 0.1, CHCl_3); IR (Germanium ATR): 2923, 2856, 1722, 1010, 910 cm^{-1} ; ^1H NMR (500 MHz, Chloroform- d) δ 6.38 (ddd, $J = 17.4, 11.0, 1.8$ Hz, 1H), 6.04 (dq, $J = 10.3, 2.1$ Hz, 1H), 5.79 (dtd, $J = 5.0, 2.4, 1.2$ Hz, 1H), 5.60 – 5.51 (m, 1H), 5.13 (dd, $J = 17.1, 2.1$ Hz, 1H), 4.82 (dd, $J = 10.6, 2.1$ Hz, 1H), 2.21 – 1.97 (m, 4H), 1.85 – 1.69 (m, 3H), 1.63 (dddd, $J = 23.2, 12.5, 6.1, 2.4$ Hz, 3H), 1.44 – 1.25 (m, 4H), 1.25 – 1.12 (m, 2H); ^{13}C NMR (126 MHz, CDCl_3) δ 141.8, 141.5, 132.3, 127.7, 126.3, 110.7, 48.0, 45.6, 42.4, 41.9, 34.2, 33.8, 30.9, 30.7, 26.2, 26.0; LRMS (ESI): Exact mass calc'd for $\text{C}_{16}\text{H}_{22}\text{Na}$ $[\text{M}+\text{Na}]^+$, 237.1619. Found 237.00.



Compound III-133.

To a flame-dried round-bottom flask was added AsPh_3 (10 mg, 0.033 mmol, 40 mol %), $\text{Pd}(\text{PhCN})_2\text{Cl}_2$ (5 mg, 0.013 mmol, 17 mol %), CuI (10 mg, 0.053 mmol, 67 mol %) and NMP (0.4 mL) and the solution was heated to 85 $^\circ\text{C}$, turning red upon heating. After reaching this temperature, the reaction stirred for 5 minutes before adding **III-120** (27.4 mg, 0.078 mmol) in NMP (0.3 mL with an additional 0.2 mL rinse), followed by tetramethyltin (23 μL , 0.16 mmol, 2.0 equiv). After 2.5 hours, the reaction was observed by TLC to be incomplete, so an additional 1 mg of AsPh_3 , $\text{Pd}(\text{PhCN})_2\text{Cl}_2$, and CuI was added, as well as an additional 20 μL of tetramethyl tin. The reaction stirred for 2 hours before TLC indicated a complete reaction. The mixture was then cooled to room temperature, diluted with saturated KF solution, and extracted with ether. The combined organic extracts were dried over MgSO_4 , and the solvent evaporated under reduced pressure. The crude material was purified by flash

chromatography on silica gel using 2% ether/pentane to yield the pure product (15.4 mg, 0.071 mmol, 91%): $[\alpha]_D = -54.1$ (*c* 0.54, CHCl_3); IR (Germanium ATR): 2915, 2852, 1711, 1439, 1171 cm^{-1} ; ^1H NMR (499 MHz, Chloroform-*d*) δ 5.34 (s, 1H), 2.51 (ddd, $J = 13.1, 10.9, 6.3$ Hz, 1H), 2.40 – 2.30 (m, 2H), 2.23 (t, $J = 11.0$ Hz, 1H), 2.17 – 2.09 (m, 1H), 2.10 – 1.99 (m, 2H), 1.82 – 1.69 (m, 3H), 1.67 – 1.54 (m, 2H), 1.53 – 1.33 (m, 6H), 1.28 – 1.17 (m, 2H), 1.05 (qd, $J = 12.7, 3.1$ Hz, 1H); ^{13}C NMR (126 MHz, CDCl_3) δ 215.4, 136.4, 124.1, 58.8, 48.5, 43.3, 40.9, 39.7, 34.3, 33.8, 32.5, 30.8, 29.2, 26.1, 23.7; LRMS (ESI): Exact mass calc'd for $\text{C}_{15}\text{H}_{23}\text{O}$ $[\text{M}+\text{H}]^+$, 219.1749. Found 219.03.

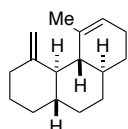


Compound III-134.

To a solution of **III-133** (14.2 mg, 0.065 mmol) in DCM (0.7 mL) at 0 °C was added 2,6-di-*tert*-butylpyridine (22 μL , 0.10 mmol, 1.5 equiv), followed by the dropwise addition of Tf_2O (24 μL , 0.14 mmol, 2.2 equiv). After 30 minutes the reaction was warmed to room temperature. Upon observed consumption of the starting material by TLC (1.25 h), the brown reaction was diluted with water and extracted with DCM. The combined organic extracts were dried over MgSO_4 , and the solvent evaporated under reduced pressure. The crude material was purified by flash chromatography on silica gel using pentane (16.1 mg, 0.046 mmol, 71%): $[\alpha]_D = -58.9$ (*c* 0.08, CHCl_3); IR (Germanium ATR): 2925, 2855, 1414, 1206, 1141, 878 cm^{-1} ; ^1H NMR (500 MHz, Chloroform-*d*) δ 5.73 (q, $J = 3.7$ Hz, 1H), 4.77 (s, 1H), 4.53 (s, 1H), 2.47 – 2.38 (m, 1H), 2.36 – 2.23 (m, 3H), 2.09 – 2.00 (m, 1H), 1.85 (dt, $J = 11.0, 4.3, 2.3$ Hz, 1H), 1.79 – 1.65 (m, 4H), 1.64 – 1.58 (m, 1H), 1.56 – 1.53 (m, 1H), 1.48 – 1.36 (m, 2H), 1.35 – 1.23 (m, 1H), 1.20 – 1.03 (m, 3H); ^{13}C NMR (126 MHz, CDCl_3) δ 153.0, 150.9, 119.7, 118.7, 104.9, 48.1, 46.7, 42.8, 41.0,

37.9, 35.1, 33.4, 32.3, 30.0, 29.4, 23.7; LRMS (ESI): Exact mass calc'd for $C_{16}H_{21}F_3O_3SNa$ $[M+Na]^+$, 373.1061. Found 373.04.

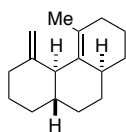
The identity of this compound was also confirmed by accessing from **III-140**: To a solution of **III-140** (5 mg, 0.023 mmol) in DCM (5 mL) at 0 °C was added 2,6-di-*tert*-butylpyridine (10 μ L, 0.046 mmol, 2.0 equiv), followed by the dropwise addition of Tf_2O (10 μ L, 0.060 mmol, 2.6 equiv). The light brown reaction was warmed to room temperature after 30 minutes. Upon observed consumption of the starting material by TLC (another 30 minutes), the reaction was diluted with water and extracted with DCM. The combined organic extracts were dried over $MgSO_4$, and the solvent evaporated under reduced pressure. The crude material was purified by flash chromatography on silica gel using a solvent gradient from pentane to 2% ether/pentane to yield the same product as isolated from the above reaction.



Compound III-135.

To a flame-dried round-bottom flask was added $AsPh_3$ (6 mg, 0.020 mmol, 43 mol %), $Pd(PhCN)_2Cl_2$ (6 mg, 0.016 mmol, 35 mol %), CuI (10 mg, 0.053 mmol, 1.1 equiv) and NMP (0.3 mL) and the solution was heated to 85 °C, turning red upon heating. After reaching this temperature, the reaction stirred for 5 minutes before adding **III-134** (16.1 mg, 0.046 mmol) in NMP (0.2 mL with an additional 0.1 mL rinse), followed by tetramethyltin (20 μ L, 0.15 mmol, 3.3 equiv). After 2.5 hours, the reaction was observed by TLC to be incomplete, so an additional 1 mg of $AsPh_3$, $Pd(PhCN)_2Cl_2$, and CuI was added, as well as an additional 20 μ L of tetramethyl tin. The reaction stirred for 3 hours before TLC indicated a complete reaction. The mixture was then cooled to room temperature, diluted with saturated KF solution, and extracted with 50% ether/pentane. The combined organic extracts were dried over

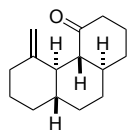
MgSO₄, and the solvent evaporated under reduced pressure. The crude material was purified by flash chromatography on silica gel using pentane to yield the pure product (6.0 mg, 0.028 mmol, 61%): $[\alpha]_D = -60.9$ (*c* 0.20, CHCl₃); IR (Germanium ATR): 2920, 2855, 1260, 1093, 1018, 800 cm⁻¹; ¹H NMR (500 MHz, Chloroform-*d*) δ 5.37 (t, *J* = 2.5 Hz, 1H), 4.75 (s, 1H), 4.62 (s, 1H), 2.34 (ddt, *J* = 12.3, 4.3, 1.9 Hz, 1H), 2.17 – 2.07 (m, 3H), 2.07 – 1.98 (m, 1H), 1.87 (ddp, *J* = 11.5, 4.5, 2.2 Hz, 1H), 1.75 – 1.66 (m, 2H), 1.67 – 1.63 (m, 4H), 1.62 – 1.53 (m, 2H), 1.49 – 1.34 (m, 2H), 1.31 – 1.12 (m, 3H), 1.11 – 1.01 (m, 2H); ¹³C NMR (126 MHz, CDCl₃) δ 155.5, 138.8, 124.3, 104.9, 50.7, 47.6, 42.9, 40.7, 38.5, 35.7, 34.0, 33.2, 31.4, 29.9, 25.7, 23.8; HRMS (EI): Exact mass calc'd for C₁₆H₂₄ [M]⁺, 216.1878. Found 216.1872.



Compound III-136.

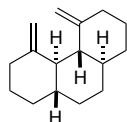
To a solution of **III-135** (6 mg, 0.028 mmol) in DCM (0.5 mL) at 0 °C was added 2,6-di-*tert*-butylpyridine (11 μ L, 0.05 mmol, 1.5 equiv), followed by the dropwise addition of Tf₂O (15 μ L, 0.09 mmol, 3.0 equiv). After 30 minutes the reaction was warmed to room temperature. Upon observed consumption of the starting material by TLC (30 minutes), the brown reaction was diluted with water and extracted with DCM. The combined organic extracts were dried over MgSO₄, and the solvent evaporated under reduced pressure. The crude material was purified by flash chromatography on silica gel using pentane (3 mg, 0.014 mmol, 50%): IR (Germanium ATR): 2921, 2856, 1446, 1378, 755 cm⁻¹; ¹H NMR (500 MHz, Chloroform-*d*) δ 4.69 (s, 1H), 4.33 (s, 1H), 2.31 (ddt, *J* = 12.5, 4.4, 2.1 Hz, 1H), 2.09 – 1.0 (m, 18H), 1.50 – 1.45 (m, 3H); ¹³C NMR (126 MHz, CDCl₃) δ 151.2, 134.6, 126.9, 105.9, 48.8, 45.5, 39.4, 38.2, 35.8, 35.3, 33.9, 32.2, 31.7, 29.3, 21.7, 21.0.

3.6.4 Olefination strategy – model system



Compound III-140.

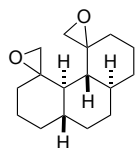
KO^tBu (12 mg, 0.11 mmol, 3.6 equiv) and benzene (0.6 mL) were added to a flame-dried round bottom flask. The mixture was cooled to 0 °C and Ph₃PMeBr (34 mg, 0.095 mmol, 3.2 equiv) was added. This mixture was heated to 70 °C for 1.5 hours, before cooling again to 0 °C, adding **III-117** (6.5 mg, 0.03 mmol) in benzene (0.1 mL with an additional 0.1 mL rinse), and reheating the reaction to 70 °C over night. After 19 hours, the mixture was cooled to room temperature, quenched with water, and extracted with 50% ether/pentane. The combined organic extracts were dried over MgSO₄ and the solvent evaporated under reduced pressure. The crude material was purified by flash chromatography on silica gel with hexane (3.8 mg, 0.0174 mmol, 58%): [α]_D = -58.8 (*c* 0.43, CHCl₃); IR (Germanium ATR): 2920, 2851, 1704, 1446, 891 cm⁻¹; ¹H NMR (500 MHz, Chloroform-*d*) δ 4.63 (q, *J* = 1.4 Hz, 1H), 4.04 (q, *J* = 1.2 Hz, 1H), 2.52 – 2.40 (m, 2H), 2.39 – 2.28 (m, 2H), 2.17 – 2.09 (m, 2H), 2.03 – 1.97 (m, 1H), 1.88 – 1.65 (m, 5H), 1.60 (dq, *J* = 9.4, 3.0 Hz, 1H), 1.54 – 1.44 (m, 2H), 1.35 (qt, *J* = 12.8, 4.0 Hz, 1H), 1.28 – 1.16 (m, 2H), 1.14 – 1.00 (m, 2H); ¹³C NMR (126 MHz, CDCl₃) δ 212.8, 151.8, 103.9, 56.7, 46.6, 45.6, 44.2, 43.2, 37.5, 34.6, 34.0, 33.6, 33.3, 28.8, 28.6; LRMS (ESI): Exact mass calc'd for C₁₅H₂₂ONa [M+Na]⁺, 241.1568. Found 241.07.



Compound III-139.

Sublimed KO^tBu (0.17 g, 1.48 mmol, 2.2 equiv) and benzene (3 mL) were added to a flame-dried round bottom flask. The mixture was cooled to 0 °C and Ph₃PMeBr (0.57 g, 1.6 mmol, 2.4 equiv) was added. This mixture was heated to 80 °C for 1 hour, after which it was cooled to 0 °C, and **III-117** (150 mg, 0.68 mmol) in benzene (0.7 mL with an additional 0.3 mL rinse) was

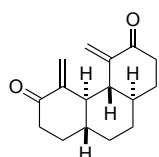
added. The mixture was then reheated to 80 °C over night. After 13 hours, the mixture was cooled to room temperature, quenched with water, and extracted with 50% ether/pentane. The combined organic extracts were dried over MgSO₄ and the solvent evaporated carefully under reduced pressure due to the potential volatility of the product. The crude material was purified by flash chromatography on silica gel with pentane to 10% ether/pentane (66.8 mg, 0.31 mmol, 46%): IR (Germanium ATR): 2919, 2853, 1714 (broad), 1445, 884 cm⁻¹; ¹H NMR (500 MHz, Chloroform-*d*) δ 4.69 (s, 1H), 4.33 (s, 1H), 2.31 (ddt, *J* = 12.5, 4.3, 2.1 Hz, 1H), 2.06 – 1.97 (m, 1H), 1.88 – 1.80 (m, 2H), 1.71 (dtd, *J* = 12.6, 4.4, 2.3 Hz, 1H), 1.63 – 1.57 (m, 1H), 1.39 (ddt, *J* = 25.8, 12.9, 4.1 Hz, 1H), 1.30 – 1.04 (m, 3H); ¹³C NMR (126 MHz, CDCl₃) δ 151.2, 106.0, 48.8, 45.5, 38.2, 35.3, 33.9, 29.3; LRMS (ESI): Exact mass calc'd for C₁₆H₂₅ [M+H]⁺, 217.1956. Found 217.07. In this unoptimized reaction on the model system, the mono olefin product **III-140** was also isolated (57.2 mg, 0.26 mmol, 39%). This reaction was optimized using the material to produce the natural product.



Compound III-143.

CrO₃ (120 mg, 1.20 mmol, 24 equiv) was added to a flame-dried flask and diluted with DCM (0.5 mL). The mixture was cooled to –20 °C, and 3,5-dimethylpyrazole (115 mg, 1.20 mmol, 24 equiv) was added quickly in one portion. After stirring at this temperature for 15 minutes, **III-139** (10 mg, 0.046 mmol) in DCM (0.3 mL with an additional 0.2 mL rinse) was added and the red-brown mixture was maintained at this temperature over night. After 21 hours, the mixture was diluted with 3 M NaOH solution and stirred for 1 hour before extracting with DCM. The combined organic extracts were washed with 1 M HCl, dried over MgSO₄, and the solvent evaporated under reduced pressure. The crude material was purified by flash

chromatography on silica gel with 10% ether/pentane (7 mg, 0.028 mmol, 61%): IR (Germanium ATR): 2922, 2848, 1730, 1448, 1250, 755 cm^{-1} ; ^1H NMR (500 MHz, Chloroform-*d*) δ 2.80 (d, $J = 4.3$ Hz, 1H), 2.65 (d, $J = 4.3$ Hz, 1H), 1.85 – 1.76 (m, 1H), 1.75 – 1.64 (m, 3H), 1.56 – 1.52 (m, 1H), 1.27 – 1.10 (m, 3H), 1.06 – 0.97 (m, 2H); ^{13}C NMR (126 MHz, CDCl_3) δ 61.5, 55.4, 40.2, 40.1, 34.7, 34.2, 32.4, 24.1; LRMS (ESI): Exact mass calc'd for $\text{C}_{16}\text{H}_{24}\text{O}_2\text{Na}$ $[\text{M}+\text{Na}]^+$, 271.1674. Found 271.15.

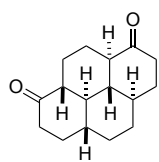


Compound III-141.

To compound **III-139** (23 mg, 0.106 mmol) in EtOH (0.8 mL) and DCM (0.4 mL) was added selenium dioxide (54 mg, 0.49 mmol, 4.5 equiv). The mixture was heated to 78 °C. Upon observed consumption of the starting material by TLC (12 hours), the reaction was cooled to room temperature and the solvent evaporated under reduced pressure. The crude material was purified by flash chromatography on silica gel using 30% EtOAc/hexane, yielding a mixture of diastereomers that was taken forward to the oxidation step (18.3 mg, 0.074 mmol 70%).

To a flame dried round-bottom flask was added DMP (97 mg, 0.23 mmol, 3.0 equiv). To this flask was added the mixture of diastereomers (19 mg, 0.076 mmol) in DCM (1 mL with an additional 1 mL rinse). Upon observed consumption of the starting materials by TLC (4 hours), the yellow reaction was poured into saturated $\text{Na}_2\text{S}_2\text{O}_3$ solution and extracted with DCM. The combined organic extracts were washed with saturated NaHCO_3 , dried over MgSO_4 , and the solvent evaporated under reduced pressure. The crude material was purified by flash chromatography on silica gel with 25% EtOAc/hexane to yield the pure product (16.4 mg, 0.067 mmol, 88%): IR (Germanium ATR): 2924, 2863, 1695, 1614, 1105, 936 cm^{-1} ; ^1H NMR (500 MHz, Chloroform-*d*) δ 5.72 – 5.63 (m, 1H), 4.98 – 4.90 (m, 1H), 2.68 (ddd, $J = 16.8, 5.7, 2.5$ Hz, 1H), 2.43 (ddd, $J =$

16.8, 12.0, 7.4 Hz, 1H), 2.29 – 2.22 (m, 1H), 2.05 (ddt, $J = 12.9, 7.1, 2.8$ Hz, 1H), 1.92 – 1.83 (m, 1H), 1.70 – 1.55 (m, 2H), 1.27 – 1.20 (m, 1H); ^{13}C NMR (126 MHz, CDCl_3) δ 204.0, 148.7, 119.2, 46.9, 40.9, 40.3, 32.8, 31.6; LRMS (ESI): Exact mass calc'd for $\text{C}_{16}\text{H}_{21}\text{O}_2$ $[\text{M}+\text{H}]^+$, 245.1542. Found 245.10.

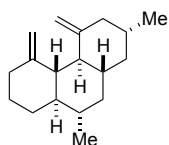


Compound III-123.

Employing reductive cyclization conditions developed by Yoon and coworkers,²⁹⁹

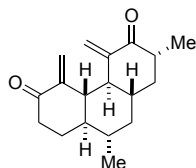
III-141 (8.0 mg, 0.033 mmol, 1.0 equiv) was dissolved in freshly distilled ACN (1 mL). $\text{Ru}(\text{bpy})_3\text{Cl}_2 \cdot \text{H}_2\text{O}$ (1 mg, 0.0013 mmol, 4 mol %) was added, followed by HCO_2H (7 μL , 0.17 mmol, 5.0 equiv) and $i\text{Pr}_2\text{NEt}$ (58 μL , 0.33 mmol, 10.0 equiv). The orange mixture was placed in the dark, cooled in a liquid nitrogen bath, placed under vacuum for 10 minutes, removed from vacuum and warmed to room temperature, and purged with N_2 . This freeze-pump-thaw process was repeated three times, after which the orange reaction was irradiated with a 23 W (1600 lumen) compact fluorescent lamp at room temperature while stirring vigorously. Upon observed consumption of the UV-active starting material by TLC, (4.5h), the solvent was evaporated under reduced pressure. The crude material was purified by flash chromatography on silica gel using 30% EtOAc/hexane to yield pure product (6.8 mg, 0.028 mmol, 85%): IR (Germanium ATR): 2925, 2855, 1710, 1169, 1084 cm^{-1} ; ^1H NMR (500 MHz, Chloroform- d) δ 2.42 – 2.35 (m, 2H), 2.07 – 1.94 (m, 3H), 1.85 – 1.80 (m, 1H), 1.54 – 1.36 (m, 2H), 1.30 – 1.22 (m, 1H), 1.17 – 1.02 (m, 2H); ^{13}C NMR (126 MHz, CDCl_3) δ 211.9, 53.0, 52.3, 41.3, 40.2, 34.0, 32.2, 23.7; LRMS (ESI): Exact mass calc'd for $\text{C}_{16}\text{H}_{23}\text{O}_2$ $[\text{M}+\text{H}]^+$, 247.1698. Found 247.10.

3.6.5 Successful synthesis of Corey dione



Compound III-138.

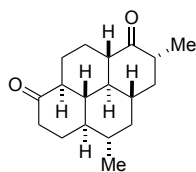
KO^tBu (84.0 mg, 0.75 mmol, 3.6 equiv, sublimed and stored in the glove box freezer) was added to a flame-dried round-bottom flask. Benzene (1 mL) was added, followed by Ph₃PMeBr (278.0 mg, 0.78 mmol, 3.7 equiv). The yellow mixture was heated to 80 °C for 1h before cooling to room temperature and adding **III-109** (53.0 mg, 0.21 mmol) in benzene (0.8 mL, with an additional 0.3 mL rinse). The reaction was heated back to 80 °C. Upon observed consumption of the starting material, and the characterized mono-olefinated product (15.5h), the orange reaction was cooled to room temperature, diluted with water, and extracted with 50% ether/pentane. The combined organic extracts were dried over MgSO₄, and the solvent evaporated under reduced pressure. The crude material was purified by flash chromatography on silica gel using hexane. (42.3 mg, 0.173 mmol, 82% yield): [α]_D = +65.2 (*c* 0.24, CHCl₃); IR (Germanium ATR): 2911, 2850, 1645, 1444, 883 cm⁻¹; ¹H NMR (500 MHz, Chloroform-*d*) δ 4.69 (s, 2H), 4.33 (s, 1H), 4.31 (s, 1H), 2.35 – 2.25 (m, 2H), 2.08 (dd, *J* = 13.3, 3.6 Hz, 1H), 2.00 (td, *J* = 12.8, 4.7 Hz, 1H), 1.94 – 1.82 (m, 2H), 1.79 (t, *J* = 10.6 Hz, 1H), 1.73 – 1.63 (m, 2H), 1.59 – 1.49 (m, 2H), 1.35 (qt, *J* = 13.1, 4.3 Hz, 1H), 1.20 (dddd, *J* = 22.1, 12.6, 9.9, 6.3, 3.2 Hz, 2H), 1.12 – 1.00 (m, 1H), 0.92 (d, *J* = 6.3 Hz, 4H), 0.88 (q, *J* = 5.0 Hz, 3H), 0.85 – 0.79 (m, 2H); ¹³C NMR (126 MHz, CDCl₃) δ 151.6, 150.7, 106.1, 105.7, 51.8, 48.5, 48.3, 46.6, 43.9, 43.7, 43.2, 38.2, 37.2, 35.7, 31.7, 29.5, 22.6, 20.4; HRMS (EI): Exact mass calc'd for C₁₈H₂₈ [M]⁺, 244.2191. Found 244.2173.



Compound III-137.

To **III-138** (30.0 mg, 0.12 mmol, 1.0 equiv) in EtOH (0.8 mL) and DCM (0.4 mL) was added SeO₂ (58.0 mg, 0.52 mmol, 4.0 equiv). The mixture was heated

to 78 °C. Upon observed consumption of the starting material and the previously characterized mono-oxidation products by TLC (40 h), the yellow reaction was cooled to room temperature and the solvent evaporated. The crude material in DCM (2 mL, with an additional 0.5 mL rinse) was then added to a flame-dried round-bottom flask with DMP (157.0 mg, 0.37 mmol, 3.0 equiv). Upon observed consumption of the starting material by TLC, with both alcohol diastereomers converging to one UV-active product (4h), the mixture was diluted with saturated Na₂S₂O₃ solution and extracted with DCM. The combined organic extracts were washed with saturated NaHCO₃ solution, dried over MgSO₄, and the solvent evaporated under reduced pressure. This crude material was purified by flash chromatography on silica gel using 10% EtOAc/hexane (16.4 mg, 0.06 mmol, 50% yield over two steps): $[\alpha]_D^{25} = +165.4$ (*c* 0.73, CHCl₃); IR (Germanium ATR): 2922, 2853, 1694, 1615, 1260, 1915, 801 cm⁻¹; ¹H NMR (500 MHz, Chloroform-*d*) δ 5.71 (d, *J* = 1.7 Hz, 1H), 5.48 (d, *J* = 1.7 Hz, 1H), 4.95 (d, *J* = 2.0 Hz, 1H), 4.82 (d, *J* = 2.0 Hz, 1H), 2.69 (ddd, *J* = 16.3, 6.5, 3.1 Hz, 1H), 2.49 – 2.29 (m, 4H), 2.21 (t, *J* = 10.4 Hz, 1H), 2.09 (ddd, *J* = 13.4, 6.7, 2.7 Hz, 1H), 1.79 – 1.67 (m, 2H), 1.59 (s, 1H), 1.57 – 1.47 (m, 1H), 1.44 – 1.30 (m, 2H), 1.22 (ddd, *J* = 21.6, 10.6, 3.2 Hz, 1H), 1.14 (d, *J* = 6.5 Hz, 3H), 1.02 (d, *J* = 6.3 Hz, 3H); ¹³C NMR (126 MHz, CDCl₃) δ 206.6, 203.7, 149.6, 148.3, 119.2, 117.4, 48.2, 47.0, 46.4, 45.4, 41.6, 41.3, 41.1, 39.7, 36.8, 28.2, 20.1, 15.1; HRMS (EI): Exact mass calc'd for C₁₈H₂₄O₂ [M]⁺, 272.1776. Found 272.1757.



Compound III-45.

Employing reductive cyclization conditions developed by Yoon and coworkers,²⁹⁹ **III-137** (21.0 mg, 0.077 mmol, 1.0 equiv) was dissolved in freshly distilled ACN (1.6 mL). Ru(bpy)₃Cl₂•H₂O (2.0 mg, 0.0027 mmol, 3.5 mol %) was added, followed

by HCO₂H (15 μ L, 0.39 mmol, 5.0 equiv) and iPr₂NEt (134 μ L, 0.77 mmol, 10.0 equiv). The orange mixture was cooled in a liquid nitrogen bath, placed under vacuum for 10 minutes, removed from vacuum and warmed to room temperature, and purged with N₂. This freeze-pump-thaw process was repeated three times, after which the orange reaction was irradiated with a 23 W (1600 lumen) compact fluorescent lamp at room temperature. Upon observed consumption of the UV-active starting material by TLC, (20h), the solvent was evaporated under reduced pressure. The crude material was purified by flash chromatography on silica gel using 10% EtOAc/hexane (19.4 mg, 0.071 mmol, 92% yield): $[\alpha]_D = +16.0$ (*c* 0.35, CHCl₃); IR (Germanium ATR): 2924, 2862, 1707, 1453 cm⁻¹; ¹H NMR (499 MHz, Chloroform-*d*) δ 2.51 – 2.30 (m, 4H), 2.06 – 1.94 (m, 5H), 1.74 (dt, *J* = 13.1, 3.5 Hz, 1H), 1.66 (tdt, *J* = 11.6, 7.1, 3.5 Hz, 1H), 1.35 – 1.04 (m, 8H), 1.00 (d, *J* = 6.5 Hz, 3H), 0.98 (d, *J* = 6.5 Hz, 3H), 0.86 (q, *J* = 12.1 Hz, 1H); ¹³C NMR (126 MHz, CDCl₃, referenced to 77.0 ppm) δ 213.0, 212.0, 53.6, 52.7, 52.2, 52.1, 46.3, 44.3, 43.0, 41.2, 41.0, 40.4, 36.4, 31.0, 23.7, 23.6, 19.9, 14.4; HRMS (ESI): Exact mass calc'd for C₁₈H₂₆O₂Na [M+Na]⁺, 297.1831. Found 297.1827. All spectroscopic data for this compound agrees with previously reported values.²⁸⁶

Chapter 4

Future Directions for the Continued Development and Application of the “Couple and Close”

Strategy

4 Chapter 4

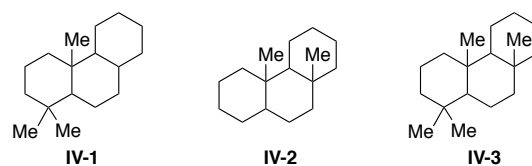
4.1 Introduction

The developed couple and close methodology has provided access to a suite of *trans-anti-trans* carbocyclic scaffolds with varying substitution and composition, as discussed in Chapter 2. The strategy enabled the concise synthesis of diterpene (+)-7,20-diisocyanoadociane, demonstrating the potential for this approach to be applied to the synthesis of different complex molecules. In this chapter, a discussion of the future development and application of this general synthetic strategy will be outlined.

4.2 Further methodology development

Although the established conditions for this general strategy were successful in the generation of straightforward substitution patterns within the scaffolds, there are avenues for the continued development to expand the approach. It has often been observed in oxidative coupling that the alteration of substrates, particularly with regard to the steric environment, can provide vastly different coupling capabilities. This was specifically seen through the challenging substitution patterns that were discussed in Section 2.5.3, some of which are shown in Figure 4.1. However, the large majority of natural products contain these particular substitution patterns, and as such, the development of conditions to allow their access through this sequence is instrumental to the enhancement of the strategy, and will expose a wealth of possible targets.

Figure 4.1 Generally desirable carbocyclic scaffolds



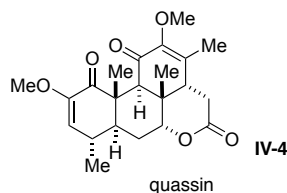
4.3 Potential natural product targets

With the ability to achieve challenging substitution patterns prevalent in numerous natural product families, there are many avenues for potential application of the platform to natural product synthesis. As the complexity and steric bulk of the individual substrates increases, the oxidative coupling and ring-closing metathesis steps will become more challenging and will likely require optimization for each individual system. A few of the structurally interesting targets that are potentially accessible with the execution of the couple and close strategy are listed herein.

4.3.1 Quassin

Isolated from plant species *Simaroubaceae*, the quassinoids have attracted the attention of scientists for their complex carbocyclic structures with a dense array of stereocenters, and for their wide range of biological activities. They have exhibited potent antineoplastic activity, as well as antiviral, antimalarial, antifeedant, antiamebic, antituberculosis, and insecticidal abilities.^{259, 302} The first synthesis of quassin **IV-4**, shown in Figure 4.2, was achieved by Grieco and coworkers, which has been followed by a number of successful syntheses.^{178, 302-305} The *trans-anti-trans* tricyclic 1,4-diketone embedded within this core structure is particularly attractive, mapping directly onto scaffolds that are potentially accessible through the sequence.

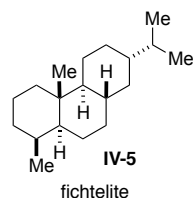
Figure 4.2 Quassin



4.3.2 Fichtelite

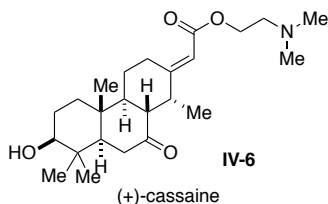
Hydrocarbon fichtelite (**IV-5**, Figure 4.3) was isolated from the remains of a pine trunk in Fictelgebirge, Bavaria, and the absolute stereochemistry of the molecule was determined by Burgstahler and Marx in their synthesis from abietic acid.³⁰⁶⁻³⁰⁷ The molecule has been synthesized by Johnson and coworkers, employing cationic polyene cyclizations as discussed in Section 1.2.1.1,²⁵⁻²⁶ and by Taber and Saleh, through an intramolecular Diels–Alder reaction, as discussed in Section 1.4.2.2.¹⁸⁵ The *trans-anti-trans* nature of this polycyclic molecule should enable the facile implementation of the couple and close strategy, should conditions be discovered to allow the coupling to proceed with both substitution in the 4- and α -positions.

Figure 4.3 Fichtelite



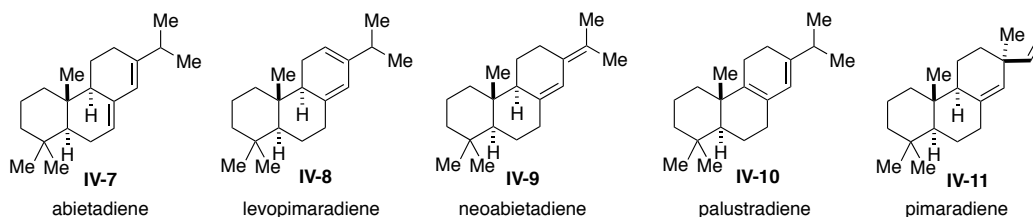
4.3.3 Cassaine

(+)-Cassaine **IV-6** (Figure 4.4) was isolated from the bark of *Erythrophleum guineense* in 1935 and the structure was confirmed by Turner and coworkers in the late 1950s, who went on to achieve the first total synthesis of the molecule.³⁰⁸ Aside from this seminal synthesis, Deslongchamps and coworkers have accomplished two syntheses of this molecule with varying strategies, as discussed in Sections 1.3.1¹³⁵ and 1.4.1.¹⁷²⁻¹⁷³ As an inhibitor of Na⁺ and K⁺-ATPase, the compound is of interest due to its cardiotoxic activity. The tricyclic *trans-anti-trans* core structure of the molecule lends itself as a potential target for the general couple and close strategy.

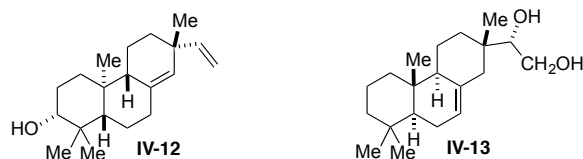
Figure 4.4 Cassaine

4.3.4 Conifer oleoresin diterpenoids

The viscous resin produced by conifers is composed of a variety of tricyclic terpenes, mostly made of abietic, levopimaric, neoabietic, and palustric, and pimaric acids, which are known to possess defensive properties against predators and pathogens.³⁰⁹⁻³¹¹ These 4-carboxylic acids are likely biosynthetically produced from the corresponding diterpenoid hydrocarbons, as shown in Figure 4.5, which possess the *trans-anti* relationship about the ring fusions of the tricyclic core and differ in the location of unsaturation.

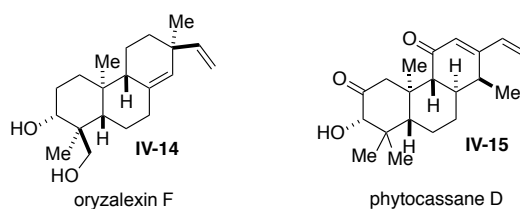
Figure 4.5 Conifer oleoresin hydrocarbons

There are numerous variants of these general scaffold families isolated throughout nature with interesting properties. Figure 4.6 depicts two examples of bioactive pimarane diterpenoids, displaying potent antimicrobial activities (**IV-12**)³¹² and moderate cytotoxic activities (**IV-13**, with many other isolated compounds with bioactivities reported in the study).³¹³

Figure 4.6 Bioactive pimarane diterpenoids

4.3.5 *Phytoalexin diterpenoids*

With similar structures and substitution patterns to the diterpenoids discussed in the previous section, the compounds shown in Figure 4.7 were isolated from rice plant *Oryza sativa* and are known to be phytoalexins, or species that are not present in healthy plants but are produced in the event of an infection as a defense mechanism due to their antimicrobial action.¹⁵³ Oryzalexin F (**IV-14**)³¹⁴ and phytocassane D (**IV-15**, the synthesis of which was discussed in Section 1.4.1)¹⁵³ each possess the *trans-anti-trans* core with substitution in the 4-position and an angular α -methyl substituent.

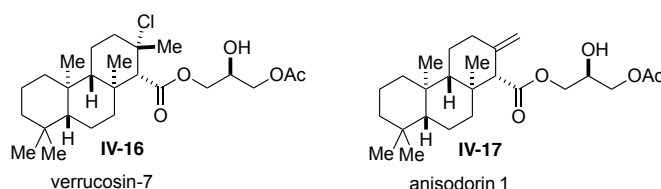
Figure 4.7 Phytoalexins from rice plants

4.3.6 *Acylglycerol diterpenes*

Cimino and coworkers have investigated marine mollusks, isolating diterpenes from the skin of the organisms and discovering novel glyceryl esters with interesting biological properties. As shown in Figure 4.8, verrucosin-type diterpenoids isolated from the Mediterranean Sea (i.e. **IV-16**)³¹⁵ exhibited potent kinase C activating properties. Structurally similar anisodorins (i.e. **IV-**

17)³¹⁶ were isolated from the Pacific Ocean, demonstrating the ability for related mollusks in different environments to also biosynthesize these acylglycerols.

Figure 4.8 Bioactive acylglycerols isolated from mollusks



4.3.7 Furan-containing diterpenes

Terpenes containing a fused furan appendage (or tetrahydrofuran or furanone functionalities) are common throughout nature with an array of interesting structures and biological activities, and as such have been the synthetic targets of many research groups (Figure 4.9). For example, spongian diterpenes display significant structural diversification among the class, a selection of which are shown in Figure 4.9a. Compound **IV-18** and derivatives were isolated from marine sponge *Dysidea* cf. *arenaria* that possess cytotoxic activity.³¹⁷ In 1997, Taylor and Toth reported the isolation of many marine diterpenoids with interesting spongian and structurally related scaffolds, with a representative example being 16-oxospongian **IV-19**, isolated from *A. sulphurea* sponges near Sydney, Australia.³¹⁸ Additionally, Garson and coworkers reported the isolation of a variety of these types of structures in 2011.³¹⁹

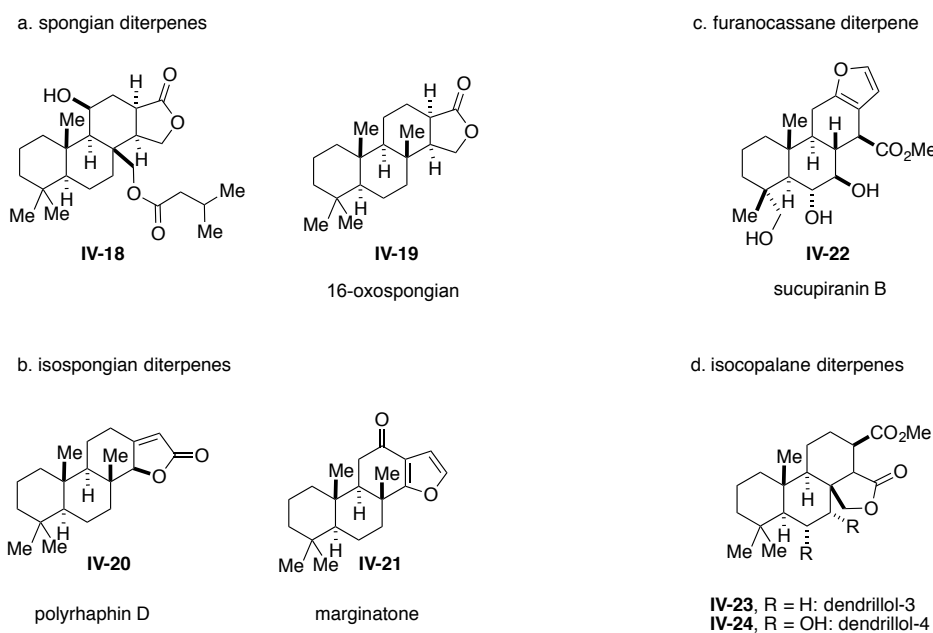
The structurally related isospongian diterpenes have also been of significant interest to the synthetic community. Figure 4.9b displays polyrhaphin d (**IV-20**), which was isolated from marine sponge *Aplysilla polyrhaphis* and synthesized by She and coworkers in 2016, as discussed in Section 1.4.1.¹⁶² A similar compound marginatone **IV-21** was isolated from the marine sponge

Aplysilla glacialis and has been synthesized by Ragoussis and coworkers³²⁰ and by Abad-Somovilla and coworkers.³²¹

Similar furanocassane diterpenoids (Figure 4.9c, **IV-22**) were recently isolated from the seeds of *Bowdichia virgilioides* in South America and exhibited cytotoxic and antimalarial properties.³²² These seeds and the accompanying bark is known to produce many species with a wide array of biological activities.

Finally, the isocopalane diterpenes from *Darwinella rosea* sponges near New Zealand shown in Figure 4.9d (dendrillol-3 **IV-23** and dendrillol-4 **IV-24**) were among the structurally intriguing compounds isolated in 1997 by Taylor and Toth.³¹⁸

Figure 4.9 Furan-containing diterpenes

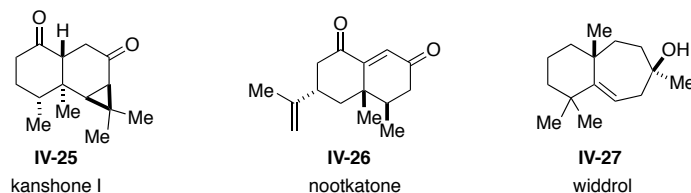


4.3.8 Bicyclic compounds

The oxidative coupling of cyclic fragments with acyclic methylvinyl ketone, or a related species, has the ability to provide bicyclic structures. These sesquiterpene molecules are prevalent

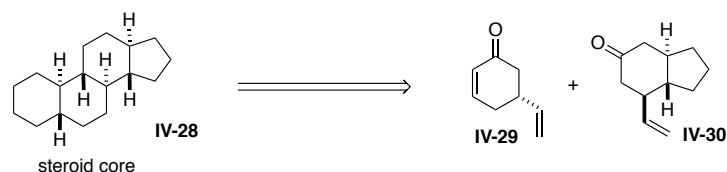
throughout nature and are accompanied by a range of biological activities. Figure 4.10 displays select examples that may be accessible through the couple and close strategy. Kanshone I (**IV-25**) was recently isolated alongside several other compounds from the Himalayan herb *Nardostachys chinensis* Batal, which is rich in sesquiterpene species.³²³ The isolated sesquiterpenes bear structural semblance to other species with known cytotoxic, antinociceptive, and antimalarial activities. Additionally, novel eudesmane sesquiterpenes were isolated from the fruit of the *Alpinia oxyphylla* plant, which is rich in terpene natural products. As an example, nootkatone **IV-26** exhibited anti-inflammatory activity in mouse peritoneal cells, as well as microglia inhibitory activity.³²⁴ The 6,7-fused widdrol **IV-27** was isolated from *Juniperus chinensis* and displayed notable anticancer activity.³²⁵

Figure 4.10 Putative bicyclic natural product targets

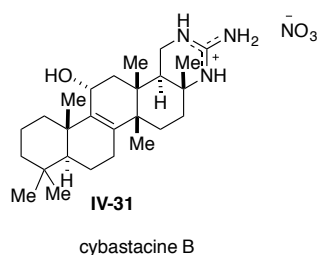


4.3.9 Steroid core

The all-*trans* core structure of steroids, as well as their extensive bioactivities, mark these species as attractive targets for implementation of the couple and close platform. As shown in Scheme 4.1, achieving **IV-28** would require the coupling of species such as **IV-29** and **IV-30**. As detailed in Scheme 2.26b, the coupling between an enone and a ketone is possible, so it is reasonable that this coupling would proceed and could be optimized. In this way, fragment **IV-30** could arrive from the vinyl cuprate addition to the corresponding 6,5-enone, prepared enantioselectively by List and Fonseca.³²⁶

Scheme 4.1 Access to the steroid nucleus**4.3.10 Larger polycyclic scaffolds**

The implementation of the developed strategy for the preparation of polycyclic scaffolds with larger ring systems may be imagined. Earlier this year, antibiotic sesterterpenes were isolated from *Nostoc* sp. cyanobacterium, with cybastacine B **IV-31** shown in Figure 4.11.³²⁷ Notably, the compound displayed significant antimicrobial activity. This desirable activity, paired with its unique pentacyclic structure with guanidinium functionality, make this natural product an interesting target, particularly as the discovery of novel antibiotic compounds is of increasing importance.

Figure 4.11 Cybastacine B**4.4 Conclusion**

There are numerous natural product families whose fused polycyclic core structures are potentially accessible through the developed oxidative coupling–ring-closing metathesis sequence. As discussed throughout this chapter, these natural products present display a wealth of interesting structural features and biological activities. In order to access the carbocyclic scaffolds making up

the majority of these targets, conditions must be developed for the oxidative coupling and ring-closing metathesis to cater to the increased steric environment of the corresponding coupling partners. Should these prevalent substitution patterns become accessible through the general strategy, an unlimited number of natural products can be investigated, enabling convergent and modular syntheses that may facilitate biological activity studies.

References

1. Lee, M. L.; Schneider, G. *J. Comb. Chem.* **2001**, *3*, 284–289.
2. Koehn, F. E.; Carter, G. T. *Nat. Rev. Drug Discov.* **2005**, *4*, 206–220.
3. Messer, R.; Fuhrer, C. A.; Haner, R. *Curr. Opin. Chem. Biol.* **2005**, *9*, 259–265.
4. Lovering, F.; Bikker, J.; Humblet, C. *J. Med. Chem.* **2009**, *52*, 6752–6756.
5. Walters, W. P.; Green, J.; Weiss, J. R.; Murcko, M. A. *J. Med. Chem.* **2011**, *54*, 6405–6416.
6. Langdon, S. R.; Brown, N.; Blagg, J. *J. Chem. Inf. Model.* **2011**, *51*, 2174–2185.
7. Duran-Frigola, M.; Mosca, R.; Aloy, P. *Chem. Biol.* **2013**, *20*, 674–684.
8. Tajabadi, F. M.; Campitelli, M. R.; Quinn, R. J. *Springer Sci. Rev.* **2013**, *1*, 141–151.
9. Aldeghi, M.; Malhotra, S.; Selwood, D. L.; Chan, A. W. E. *Chem. Biol. Drug. Des.* **2014**, *83*, 450–461.
10. Feher, M.; Schmidt, J. M. *J. Chem. Inf. Comput. Sci.* **2003**, *43*, 218–227.
11. Rodrigues, T.; Reker, D.; Schneider, P.; Schneider, G. *Nat. Chem.* **2016**, *8*, 531–541.
12. Abe, I.; Rohmer, M.; Prestwich, G. D. *Chem. Rev.* **1993**, *93*, 2189–2206.
13. Wendt, K. U.; Schulz, G. E.; Corey, E. J.; Liu, D. R. *Angew. Chem. Int. Ed.* **2000**, *39*, 2812–2833.
14. Nes, W. D. *Chem. Rev.* **2011**, *111*, 6423–6451.
15. Baunach, M.; Franke, J.; Hertweck, C. *Angew. Chem. Int. Ed.* **2015**, *54*, 2604–2626.
16. Johnson, W. S. *Acc. Chem. Res.* **1968**, *1*, 1–8.
17. Stork, G.; Burgstahler, A. W. *J. Am. Chem. Soc.* **1955**, *77*, 5068–5077.
18. Eschenmoser, A.; Ruzicka, L.; Jeger, O.; Arigoni, D. *Helv. Chim. Acta.* **1955**, *38*, 1890–1904.
19. Johnson, W. S. *Angew. Chem. Int. Ed.* **1976**, *15*, 9–17.
20. Johnson, W. S. *Bioorg. Chem.* **1976**, *5*, 51–98.

21. Yoder, R. A.; Johnston, J. N. *Chem. Rev.* **2005**, *105*, 4730–4756.
22. Johnson, W. S. *Tetrahedron* **1991**, *47*, R11–R50.
23. Johnson, W. S.; Kinnel, R. B. *J. Am. Chem. Soc.* **1966**, *88*, 3861–3862.
24. Abrams, G. D.; Bartlett, W. R.; Fung, V. A.; Johnson, W. S. *Bioorg. Chem.* **1971**, *1*, 243–268.
25. Johnson, W. S.; Jensen, N. P.; Hooz, J. *J. Am. Chem. Soc.* **1966**, *88*, 3859–3860.
26. Johnson, W. S.; Jensen, N. P.; Hooz, J.; Leopold, E. J. *J. Am. Chem. Soc.* **1968**, *90*, 5872–5881.
27. Johnson, W. S.; Schaaf, T. K. *J. Chem. Soc. Chem. Commun.* **1969**, 611–612.
28. Johnson, W. S.; Harbert, C. A.; Ratcliffe, B. E.; Stipanovic, R. D. *J. Am. Chem. Soc.* **1976**, *98*, 6188–6193.
29. Johnson, W. S.; Fletcher, V. R.; Chenera, B.; Bartlett, W. R.; Tham, F. S.; Kullnig, R. K. *J. Am. Chem. Soc.* **1993**, *115*, 497–504.
30. Johnson, W. S.; Dubois, G. E. *J. Am. Chem. Soc.* **1976**, *98*, 1038–1039.
31. Johnson, W. S.; Brinkmeyer, R. S.; Kapoor, V. M.; Yarnell, T. M. *J. Am. Chem. Soc.* **1977**, *99*, 8341–8343.
32. Zhao, Y. J.; Chng, S. S.; Loh, T. P. *J. Am. Chem. Soc.* **2007**, *129*, 492–493.
33. Zhao, Y. J.; Loh, T. P. *J. Am. Chem. Soc.* **2008**, *130*, 10024–10029.
34. Johnson, W. S.; Li, T. T.; Harbert, C. A.; Bartlett, W. R.; Herrin, T. R.; Staskun, B.; Rich, D. H. *J. Am. Chem. Soc.* **1970**, *92*, 4461–4463.
35. Prestwic, G. D.; Labovitz, J. N. *J. Am. Chem. Soc.* **1974**, *96*, 7103–7105.
36. Gravestock, M. B.; Johnson, W. S.; Mccarry, B. E.; Parry, R. J.; Ratcliffe, B. E. *J. Am. Chem. Soc.* **1978**, *100*, 4274–4282.
37. Camelio, A. M.; Johnson, T. C.; Siegel, D. *J. Am. Chem. Soc.* **2015**, *137*, 11864–11867.
38. Slegeris, R.; Dudley, G. B. *Tetrahedron* **2016**, *72*, 3666–3672.
39. Corey, E. J.; Russey, W. E.; Demontel, Pr. *J. Am. Chem. Soc.* **1966**, *88*, 4750–4751.
40. Van Tamelen, E. E.; Willett, J. D.; Clayton, R. B.; Lord, K. E. *J. Am. Chem. Soc.* **1966**, *88*, 4752–4754.

41. Goldsmith, D. J.; Phillips, C. F. *J. Am. Chem. Soc.* **1969**, *91*, 5862–5870.
42. Vantamelen, E. E.; Leiden, T. M. *J. Am. Chem. Soc.* **1982**, *104*, 2061–2062.
43. Corey, E. J.; Lin, S. Z. *J. Am. Chem. Soc.* **1996**, *118*, 8765–8766.
44. Corey, E. J.; Luo, G. L.; Lin, L. S. Z. *J. Am. Chem. Soc.* **1997**, *119*, 9927–9928.
45. Corey, E. J.; Luo, G. L.; Lin, L. U. S. Z. *Angew. Chem. Int. Ed.* **1998**, *37*, 1126–1128.
46. Zhao, J. F.; Zhao, Y. J.; Loh, T. P. *Chem. Commun.* **2008**, 1353–1355.
47. Suzuki, K.; Yamakoshi, H.; Nakamura, S. *Chem. Eur. J.* **2015**, *21*, 17605–17609.
48. Tian, Y.; Xu, X.; Zhang, L.; Qu, J. *Org. Lett.* **2016**, *18*, 268–271.
49. Elkin, M.; Szewczyk, S. M.; Scruse, A. C.; Newhouse, T. R. *J. Am. Chem. Soc.* **2017**, *139*, 1790–1793.
50. Ishihara, K.; Ishibashi, H.; Yamamoto, H. *J. Am. Chem. Soc.* **2001**, *123*, 1505–1506.
51. Ishihara, K.; Ishibashi, H.; Yamamoto, H. *J. Am. Chem. Soc.* **2002**, *124*, 3647–3655.
52. Kumazawa, K.; Ishihara, K.; Yamamoto, H. *Org. Lett.* **2004**, *6*, 2551–2554.
53. Lin, S. C.; Chein, R. J. *J. Org. Chem.* **2017**, *82*, 1575–1583.
54. Fan, L. W.; Han, C. Y.; Li, X. R.; Yao, J. S.; Wang, Z. N.; Yao, C. C.; Chen, W. H.; Wang, T.; Zhao, J. F. *Angew. Chem. Int. Ed.* **2018**, *57*, 2115–2119.
55. Surendra, K.; Corey, E. J. *J. Am. Chem. Soc.* **2012**, *134*, 11992–11994.
56. Ungarean, C. N.; Southgate, E. H.; Sarlah, D. *Org. Biomol. Chem.* **2016**, *14*, 5454–5467.
57. Sakakura, A.; Ukai, A.; Ishihara, K. *Nature* **2007**, *445*, 900–903.
58. Sawamura, Y.; Nakatsuji, H.; Sakakura, A.; Ishihara, K. *Chem. Sci.* **2013**, *4*, 4181–4186.
59. Snyder, S. A.; Treitler, D. S. *Angew. Chem. Int. Ed.* **2009**, *48*, 7899–7903.
60. Snyder, S. A.; Treitler, D. S.; Brucks, A. P. *J. Am. Chem. Soc.* **2010**, *132*, 14303–14314.
61. Snyder, S. A.; Treitler, D. S.; Schall, A. *Tetrahedron* **2010**, *66*, 4796–4804.
62. Zhao, Y. J.; Tan, L. J. S.; Li, B.; Li, S. M.; Loh, T. P. *Chem. Commun.* **2009**, 3738–3740.
63. Harring, S. R.; Livinghouse, T. *Tetrahedron Lett.* **1989**, *30*, 1499–1502.

64. Edstrom, E. D.; Livinghouse, T. *J. Org. Chem.* **1987**, *52*, 949–951.
65. Desjardins, S.; Andrez, J. C.; Canesi, S. *Org. Lett.* **2011**, *13*, 3406–3409.
66. Desjardins, S.; Maertens, G.; Canesi, S. *Org. Lett.* **2014**, *16*, 4928–4931.
67. Maertens, G.; Desjardins, S.; Canesi, S. *Org. Biomol. Chem.* **2016**, *14*, 6744–6750.
68. Zhang, Y. T.; Wu, G. Z.; Agnel, G.; Negishi, E. *J. Am. Chem. Soc.* **1990**, *112*, 8590–8592.
69. Sokol, J. G.; Korapala, C. S.; White, P. S.; Becker, J. J.; Gagné, M. R. *Angew. Chem. Int. Ed.* **2011**, *50*, 5657–5660.
70. Geier, M. J.; Gagné, M. R. *J. Am. Chem. Soc.* **2014**, *136*, 3032–3035.
71. McCulley, C. H.; Geier, M. J.; Hudson, B. M.; Gagné, M. R.; Tantillo, D. J. *J. Am. Chem. Soc.* **2017**, *139*, 11158–11164.
72. Schafroth, M. A.; Sarlah, D.; Krautwald, S.; Carreira, E. M. *J. Am. Chem. Soc.* **2012**, *134*, 20276–20278.
73. Deng, J.; Zhou, S. P.; Zhang, W. H.; Li, J.; Li, R. F.; Li, A. *J. Am. Chem. Soc.* **2014**, *136*, 8185–8188.
74. Zhou, S. P.; Chen, H.; Luo, Y. J.; Zhang, W. H.; Li, A. *Angew. Chem. Int. Ed.* **2015**, *54*, 6878–6882.
75. Sethofer, S. G.; Mayer, T.; Toste, F. D. *J. Am. Chem. Soc.* **2010**, *132*, 8276–8277.
76. Yeh, M. C. P.; Lin, M. N.; Chou, Y. S.; Lin, T. C.; Tseng, L. Y. *J. Org. Chem.* **2011**, *76*, 4027–4033.
77. Rong, Z. T.; Echavarren, A. M. *Org. Biomol. Chem.* **2017**, *15*.
78. Breslow, R.; Barrett, E.; Mohacsi, E. *Tetrahedron Lett.* **1962**, 1207–1211.
79. Breslow, R.; Groves, J. T.; Olin, S. S. *Tetrahedron Lett.* **1966**, 4717–4719.
80. Breslow, R.; Olin, S. S.; Groves, J. T. *Tetrahedron Lett.* **1968**, 1837–1840.
81. Justicia, J.; de Cienfuegos, L. A.; Campana, A. G.; Miguel, D.; Jakoby, V.; Gansauer, A.; Cuerva, J. M. *Chem. Soc. Rev.* **2011**, *40*, 3525–3537.
82. Julia, M. *Acc. Chem. Res.* **1971**, *4*, 386–392.
83. Lallemand, J. Y.; Julia, M.; Mansuy, D. *Tetrahedron Lett.* **1973**, 4461–4464.

84. Hoffmann, U.; Gao, Y. M.; Pandey, B. P.; Klinge, S.; Warzecha, K. D.; Kruger, C.; Roth, H. D.; Demuth, M. *J. Am. Chem. Soc.* **1993**, *115*, 10358–10359.
85. Heinemann, C.; Xing, X. C.; Warzecha, K. D.; Ritterskamp, P.; Gorner, H.; Demuth, M. *Pure Appl. Chem.* **1998**, *70*, 2167–2176.
86. Ozser, M. E.; Icil, H.; Makhynya, Y.; Demuth, M. *Eur. J. Org. Chem.* **2004**, 3686–3692.
87. Xing, X. C.; Demuth, M. *Synlett* **1999**, 987–990.
88. Xing, X. C.; Demuth, M. *Eur. J. Org. Chem.* **2001**, 537–544.
89. Heinemann, C.; Demuth, M. *J. Am. Chem. Soc.* **1999**, *121*, 4894–4895.
90. Chen, L. G.; Gill, G. B.; Pattenden, G. *Tetrahedron Lett.* **1994**, *35*, 2593–2596.
91. Chen, L. G.; Gill, G. B.; Pattenden, G.; Simonian, H. *J. Chem. Soc., Perkin Trans. 1* **1996**, 31–43.
92. Pattenden, G.; Roberts, L.; Blake, A. J. *J. Chem. Soc., Perkin Trans. 1* **1998**, 863–868.
93. Boehm, H. M.; Handa, S.; Pattenden, G.; Roberts, L.; Blake, A. J.; Li, W. S. *J. Chem. Soc., Perkin Trans. 1* **2000**, 3522–3538.
94. Andemichael, Y. W.; Huang, Y.; Wang, K. K. *J. Org. Chem.* **1993**, *58*, 1651–1652.
95. Myers, A. G.; Kuo, E. Y.; Finney, N. S. *J. Am. Chem. Soc.* **1989**, *111*, 8057–8059.
96. Zhang, Q. W.; Mohan, R. M.; Cook, L.; Kazanis, S.; Peisach, D.; Foxman, B. M.; Snider, B. B. *J. Org. Chem.* **1993**, *58*, 7640–7651.
97. Snider, B. B. *Chem. Rev.* **1996**, *96*, 339–363.
98. Snider, B. B.; Kiselgof, J. Y.; Foxman, B. M. *J. Org. Chem.* **1998**, *63*, 7945–7952.
99. Zoretic, P. A.; Weng, X. Y.; Caspar, M. L.; Davis, D. G. *Tetrahedron Lett.* **1991**, *32*, 4819–4822.
100. Zoretic, P. A.; Shen, Z. Q.; Wang, M.; Ribeiro, A. A. *Tetrahedron Lett.* **1995**, *36*, 2925–2928.
101. Zoretic, P. A.; Wang, M.; Zhang, Y. Z.; Shen, Z. Q.; Ribeiro, A. A. *J. Org. Chem.* **1996**, *61*, 1806–1813.
102. Yang, D.; Ye, X. Y.; Xu, H.; Pang, K. W.; Zou, N.; Letcher, R. M. *J. Org. Chem.* **1998**, *63*, 6446–6447.

103. Yang, D.; Ye, X. Y.; Gu, S.; Xu, M. *J. Am. Chem. Soc.* **1999**, *121*, 5579–5580.
104. Justicia, J.; Rosales, A.; Bunuel, E.; Oller-Lopez, J. L.; Valdivia, N.; Haidour, A.; Oltra, J. E.; Barrero, A. F.; Cardenas, D. J.; Cuerva, J. M. *Chem. Eur. J.* **2004**, *10*, 1778–1788.
105. Morcillo, S. P.; Miguel, D.; Resa, S.; Martin-Lasanta, A.; Millan, A.; Choquesillo-Lazarte, D.; Garcia-Ruiz, J. M.; Mota, A. J.; Justicia, J.; Cuerva, J. M. *J. Am. Chem. Soc.* **2014**, *136*, 6943–6951.
106. Rosales, A.; Munoz-Bascon, J.; Morales-Alcazar, V. M.; Castilla-Alcala, J. A.; Oltra, J. E. *RSC Adv.* **2012**, *2*, 12922–12925.
107. Rendler, S.; MacMillan, D. W. C. *J. Am. Chem. Soc.* **2010**, *132*, 5027–5029.
108. Jasperse, C. P.; Curran, D. P.; Fevig, T. L. *Chem. Rev.* **1991**, *91*, 1237–1286.
109. Hung, K.; Hu, X. R.; Maimone, T. J. *Nat. Prod. Rep.* **2018**, *35*, 174–202.
110. Funk, R. L.; Vollhardt, K. P. C. *J. Am. Chem. Soc.* **1980**, *102*, 5253–5261.
111. Lecker, S. H.; Nguyen, N. H.; Vollhardt, K. P. C. *J. Am. Chem. Soc.* **1986**, *108*, 856–858.
112. Cruciani, P.; Aubert, C.; Malacria, M. *J. Org. Chem.* **1995**, *60*, 2664–2665.
113. Groth, U.; Richter, N.; Kalogerakis, A. *Eur. J. Org. Chem.* **2003**, 4634–4639.
114. Petit, M.; Aubert, C.; Malacria, M. *Org. Lett.* **2004**, *6*, 3937–3940.
115. Hakuba, H.; Kitagaki, S.; Mukai, C. *Tetrahedron* **2007**, *63*, 12639–12645.
116. Myers, A. G.; Zheng, B. *J. Am. Chem. Soc.* **1996**, *118*, 4492–4493.
117. Movassaghi, M.; Ahmad, O. K. *J. Org. Chem.* **2007**, *72*, 1838–1841.
118. Cope, A. C.; Martin, M. M.; Mckerverey, M. A. *Quart. Rev. Chem. Soc.* **1966**, *20*, 119–152.
119. Dauben, W. G.; Michno, D. M.; Olsen, E. G. *J. Org. Chem.* **1981**, *46*, 687–690.
120. Deslongchamps, P. *Pure Appl. Chem.* **1992**, *64*, 1831–1847.
121. Lamothe, S.; Ndibwami, A.; Deslongchamps, P. *Tetrahedron Lett.* **1988**, *29*, 1639–1640.
122. Lamothe, S.; Ndibwami, A.; Deslongchamps, P. *Tetrahedron Lett.* **1988**, *29*, 1641–1644.
123. Cantin, M.; Xu, Y. C.; Deslongchamps, P. *Can. J. Chem.* **1990**, *68*, 2144–2152.

124. Xu, Y. C.; Roughton, A. L.; Plante, R.; Goldstein, S.; Deslongchamps, P. *Can. J. Chem.* **1993**, *71*, 1152–1168.
125. Xu, Y. C.; Roughton, A. L.; Soucy, P.; Goldstein, S.; Deslongchamps, P. *Can. J. Chem.* **1993**, *71*, 1169–1183.
126. Ndibwami, A.; Lamothe, S.; Guay, D.; Plante, R.; Soucy, P.; Goldstein, S.; Deslongchamps, P. *Can. J. Chem.* **1993**, *71*, 695–713.
127. Ndibwami, A.; Lamothe, S.; Soucy, P.; Goldstein, S.; Deslongchamps, P. *Can. J. Chem.* **1993**, *71*, 714–725.
128. Marinier, A.; Deslongchamps, P. *Tetrahedron Lett.* **1988**, *29*, 6215–6218.
129. Marinier, A.; Deslongchamps, P. *Can. J. Chem.* **1992**, *70*, 2350–2364.
130. Marsault, E.; Toro, A.; Nowak, P.; Deslongchamps, P. *Tetrahedron* **2001**, *57*, 4243–4260.
131. Germain, J.; Deslongchamps, P. *J. Org. Chem.* **2002**, *67*, 5269–5278.
132. Soucy, P.; L'Heureux, A.; Toro, A.; Deslongchamps, P. *J. Org. Chem.* **2003**, *68*, 9983–9987.
133. Toro, A.; Deslongchamps, P. *J. Org. Chem.* **2003**, *68*, 6847–6852.
134. Jung, M. E.; Zhang, T. H.; Lui, R. M.; Gutierrez, O.; Houk, K. N. *J. Org. Chem.* **2010**, *75*, 6933–6940.
135. Phoenix, S.; Reddy, M. S.; Deslongchamps, P. *J. Am. Chem. Soc.* **2008**, *130*, 13989–13995.
136. Pattenden, G.; Smithies, A. J.; Walter, D. S. *Tetrahedron Lett.* **1994**, *35*, 2413–2416.
137. Begley, M. J.; Pattenden, G.; Smithies, A. J.; Walter, D. S. *Tetrahedron Lett.* **1994**, *35*, 2417–2420.
138. Jahn, U.; Curran, D. P. *Tetrahedron Lett.* **1995**, *36*, 8921–8924.
139. Jones, P.; Pattenden, G. *Synlett* **1997**, 398–400.
140. Handa, S.; Pattenden, G. *Contemp. Org. Synth.* **1997**, *4*, 196–215.
141. Pattenden, G.; Stoker, D. A.; Thomson, N. M. *Org. Biomol. Chem.* **2007**, *5*, 1776–1788.
142. Cardente, M. A. G.; McCulloch, S.; Pattenden, G. *Comptes Rendus Acad. Sci.* **2001**, *4*, 571–574.

143. Pattenden, G.; Gonzalez, M. A.; McCulloch, S.; Walter, A.; Woodhead, S. J. *Proc. Natl. Acad. Sci. U.S.A.* **2004**, *101*, 12024–12029.
144. Pattenden, G.; Stoker, D. A.; Winne, J. M. *Tetrahedron* **2009**, *65*, 5767–5775.
145. Bradshaw, B.; Bonjoch, J. *Synlett* **2012**, 337–356.
146. Eagan, J. M.; Hori, M.; Wu, J. B.; Kanyiva, K. S.; Snyder, S. A. *Angew. Chem. Int. Ed.* **2015**, *54*, 7842–7846.
147. Spencer, T. A.; Smith, R. A. J.; Storm, D. L.; Villarica, R. M. *J. Am. Chem. Soc.* **1971**, *93*, 4856–4864.
148. Spencer, T. A.; Weaver, T. D.; Villarica, R. M.; Friary, R. J.; Posler, J.; Schwartz, M. A. *J. Org. Chem.* **1968**, *33*, 712–719.
149. Ireland, R. E.; Beslin, P.; Giger, R.; Hengartner, U.; Kirst, H. A.; Maag, H. *J. Org. Chem.* **1977**, *42*, 1267–1276.
150. Ireland, R. E.; Hengartner, U. *J. Am. Chem. Soc.* **1972**, *94*, 3652–3653.
151. Ireland, R. E.; Mander, L. N. *J. Org. Chem.* **1967**, *32*, 689–696.
152. Stork, G.; Meisels, A.; Davies, J. E. *J. Am. Chem. Soc.* **1963**, *85*, 3419–3425.
153. Yajima, A.; Mori, K. *Eur. J. Org. Chem.* **2000**, 4079–4091.
154. Yajima, A.; Mori, K. *Tetrahedron Lett.* **2000**, *41*, 351–354.
155. Ushakov, D. B.; Raja, A.; Franke, R.; Sasse, F.; Maier, M. E. *Synlett* **2012**, 1358–1360.
156. Yu, J.; Yu, B. A. *Chin. Chem. Lett.* **2015**, *26*, 1331–1335.
157. Honda, T.; Favalaro, F. G.; Janosik, T.; Honda, Y.; Suh, N.; Sporn, M. B.; Gribble, G. W. *Org. Biomol. Chem.* **2003**, *1*, 4384–4391.
158. Honda, T.; Murae, T.; Ohta, S.; Kurata, Y.; Kawai, H.; Takahashi, T.; Itai, A.; Iitaka, Y. *Chem. Lett.* **1981**, 299–302.
159. Takikawa, H.; Imamura, Y.; Sasaki, M. *Tetrahedron* **2006**, *62*, 39–48.
160. Nakazaki, K.; Hayashi, K.; Hosoe, S.; Tashiro, T.; Kuse, M.; Takikawa, H. *Tetrahedron* **2012**, *68*, 9029–9034.
161. Stork, G.; Rosen, P.; Goldman, N.; Coombs, R. V.; Tsuji, J. *J. Am. Chem. Soc.* **1965**, *87*, 275–286.

162. Wang, Z. M.; Xing, Z. M.; Liu, L.; Zhang, H.; Zhong, Z. L.; Xie, X. G.; She, X. G. *ChemistrySelect*. **2016**, *1*, 2225–2227.
163. Pinkerton, D. M.; Bernhardt, P. V.; Savage, G. P.; Williams, C. M. *Asian J. Org. Chem.* **2017**, *6*, 583–597.
164. Pinkerton, D. M.; Vanden Berg, T. J.; Bernhardt, P. V.; Williams, C. M. *Chem. Eur. J.* **2017**, *23*, 2282–2285.
165. Volpe, T.; Revial, G.; Pfau, M.; Dangelo, J. *Tetrahedron Lett.* **1987**, *28*, 2367–2370.
166. Shimizu, T.; Hiranuma, S.; Okubo, T.; Yoshioka, H. *Chem. Pharm. Bull.* **1993**, *41*, 1524–1529.
167. Hamilton, R. J.; Mander, L. N. *Aust. J. Chem.* **1991**, *44*, 927–938.
168. Reingold, I. D.; Butterfield, A. M.; Daglen, B. C.; Walters, R. S.; Allen, K.; Scheuring, S.; Kratz, K.; Gembicky, M.; Baran, P. *Tetrahedron Lett.* **2005**, *46*, 3835–3837.
169. Bhar, S. S.; Ramana, M. M. V. *J. Org. Chem.* **2004**, *69*, 8935–8937.
170. Lavalley, J. F.; Deslongchamps, P. *Tetrahedron Lett.* **1988**, *29*, 5117–5118.
171. Lepage, O.; Deslongchamps, P. *J. Org. Chem.* **2003**, *68*, 2183–2186.
172. Ravindar, K.; Caron, P.-Y.; Deslongchamps, P. *Org. Lett.* **2013**, *15*, 6270–6273.
173. Ravindar, K.; Caron, P.-Y.; Deslongchamps, P. *J. Org. Chem.* **2014**, *79*, 7979–7999.
174. Mackay, E. G.; Sherburn, M. S. *Synthesis* **2015**, *47*, 1–21.
175. Kakushima, M.; Allain, L.; Dickinson, R. A.; White, P. S.; Valenta, Z. *Can. J. Chem.* **1979**, *57*, 3354–3356.
176. Kakushima, M.; Das, J.; Reid, G. R.; White, P. S.; Valenta, Z. *Can. J. Chem.* **1979**, *57*, 3356–3358.
177. Das, J.; Kubela, R.; Macalpine, G. A.; Stojanac, Z.; Valenta, Z. *Can. J. Chem.* **1979**, *57*, 3308–3319.
178. Vidari, G.; Ferrino, S.; Grieco, P. A. *J. Am. Chem. Soc.* **1984**, *106*, 3539–3548.
179. Ling, T.; Kramer, B. A.; Palladino, M. A.; Theodorakis, E. A. *Org. Lett.* **2000**, *2*, 2073–2076.
180. Ling, T. T.; Chowdhury, C.; Kramer, B. A.; Vong, B. G.; Palladino, M. A.; Theodorakis, E. A. *J. Org. Chem.* **2001**, *66*, 8843–8853.

181. Coltart, D. M.; Danishefsky, S. J. *Org. Lett.* **2003**, *5*, 1289–1292.
182. Anada, M.; Hanari, T.; Kakita, K.; Kurosaki, Y.; Katsuse, K.; Sunadoi, Y.; Jinushi, Y.; Takeda, K.; Matsunaga, S.; Hashimoto, S. *Org. Lett.* **2017**, *19*, 5581–5584.
183. Spino, C.; Crawford, J. *Tetrahedron Lett.* **1994**, *35*, 5559–5562.
184. Spino, C.; Crawford, J.; Bishop, J. *J. Org. Chem.* **1995**, *60*, 844–851.
185. Taber, D. F.; Saleh, S. A. *J. Am. Chem. Soc.* **1980**, *102*, 5085–5088.
186. Juhl, M.; Monrad, R.; Sotofte, I.; Tanner, D. *J. Org. Chem.* **2007**, *72*, 4644–4654.
187. Tartakoff, S. S.; Vanderwal, C. D. *Org. Lett.* **2014**, *16*, 1458–1461.
188. Nannini, L. J.; Nemat, S. J.; Carreira, E. M. *Angew. Chem. Int. Ed.* **2018**, *57*, 823–826.
189. Pinkney, P. S.; Nesty, G. A.; Wiley, R. H.; Marvel, C. S. *J. Am. Chem. Soc.* **1936**, *58*, 972–976.
190. Overman, L. E.; Ricca, D. J.; Tran, V. D. *J. Am. Chem. Soc.* **1993**, *115*, 2042–2044.
191. Overman, L. E.; Ricca, D. J.; Tran, V. D. *J. Am. Chem. Soc.* **1997**, *119*, 12031–12040.
192. Taber, D. F.; Sheth, R. B. *J. Org. Chem.* **2008**, *73*, 8030–8032.
193. Du, K.; Guo, P.; Chen, Y.; Cao, Z.; Wang, Z.; Tang, W. J. *Angew. Chem. Int. Ed.* **2015**, *54*, 3033–3037.
194. Kim, W. S.; Du, K.; Eastman, A.; Hughes, R. P.; Micalizio, G. C. *Nat. Chem.* **2018**, *10*, 70–77.
195. Guo, F. H.; Clift, M. D.; Thomson, R. J. *Eur. J. Org. Chem.* **2012**, 4881–4896.
196. Csaky, A. G.; Plumet, J. *Chem. Soc. Rev.* **2001**, *30*, 313–320.
197. Baran, P. S.; Guerrero, C. A.; Ambhaikar, N. B.; Hafensteiner, B. D. *Angew. Chem. Int. Ed.* **2005**, *44*, 606–609.
198. Baran, P. S.; Hafensteiner, B. D.; Ambhaikar, N. B.; Guerrero, C. A.; Gallagher, J. D. *J. Am. Chem. Soc.* **2006**, *128*, 8678–8693.
199. DeMartino, M. P.; Chen, K.; Baran, P. S. *J. Am. Chem. Soc.* **2008**, *130*, 11546–11560.
200. Martin, C. L.; Overman, L. E.; Rohde, J. M. *J. Am. Chem. Soc.* **2008**, *130*, 7568–7569.
201. Herzon, S. B.; Lu, L.; Woo, C. M.; Gholap, S. L. *J. Am. Chem. Soc.* **2011**, *133*, 7260–7263.

202. Ekebergh, A.; Karlsson, I.; Mete, R.; Pan, Y.; Borje, A.; Martensson, J. *Org. Lett.* **2011**, *13*, 4458–4461.
203. You, L.; Liang, X. T.; Xu, L. M.; Wang, Y. F.; Zhang, J. J.; Su, Q.; Li, Y. H.; Zhang, B.; Yang, S. L.; Chen, J. H.; Yang, Z. *J. Am. Chem. Soc.* **2015**, *137*, 10120–10123.
204. Ghosh, S.; Chaudhuri, S.; Bisai, A. *Org. Lett.* **2015**, *17*, 1373–1376.
205. Quesnelle, C. A.; Gill, P.; Kim, S. H.; Chen, L. B.; Zhao, Y. F.; Fink, B. E.; Saulnier, M.; Frennesson, D.; DeMartino, M. P.; Baran, P. S.; Gavai, A. V. *Synlett* **2016**, *27*, 2254–2258.
206. Ivanoff, D.; Spasoff, A. *Bull. Soc. Chim. Fr.* **1935**, *2*, 76–78.
207. Rathke, M. W.; Lindert, A. *J. Am. Chem. Soc.* **1971**, *93*, 4605–4506.
208. Ito, Y.; Konoike, T.; Saegusa, T. *J. Am. Chem. Soc.* **1975**, *97*, 2912–2914.
209. Ito, Y.; Konoike, T.; Harada, T.; Saegusa, T. *J. Am. Chem. Soc.* **1977**, *99*, 1487–1493.
210. Kobayashi, Y.; Taguchi, T.; Tokuno, E. *Tetrahedron Lett.* **1977**, 3741–3742.
211. Frazier, R. H.; Harlow, R. L. *J. Org. Chem.* **1980**, *45*, 5408–5411.
212. Brocksom, T. J.; Petraghani, N.; Rodrigues, R.; Lascalateixeira, H. *Synthesis* **1975**, 396–397.
213. Kise, N.; Tokioka, K.; Aoyama, Y.; Matsumura, Y. *J. Org. Chem.* **1995**, *60*, 1100–1101.
214. Ojima, I.; Brandstadter, S. M.; Donovan, R. J. *Chem. Lett.* **1992**, 1591–1594.
215. Babler, J. H.; Haack, R. A. *Synth. Commun.* **1983**, *13*, 905–911.
216. Guo, F. H.; Konkol, L. C.; Thomson, R. J. *J. Am. Chem. Soc.* **2011**, *133*, 17100–17100.
217. Konkol, L. C.; Guo, F. H.; Sarjeant, A. A.; Thomson, R. J. *Angew. Chem. Int. Ed.* **2011**, *50*, 9931–9934.
218. Baran, P. S.; DeMartino, M. P. *Angew. Chem. Int. Ed.* **2006**, *45*, 7083–7086.
219. Nguyen, P. Q.; Schafer, H. J. *Org. Lett.* **2001**, *3*, 2993–2995.
220. Casey, B. M.; Flowers, R. A. *J. Am. Chem. Soc.* **2011**, *133*, 11492–11495.
221. Do, H. Q.; Hung, T. V.; Daugulis, O. *Organometallics* **2012**, *31*, 7816–7818.
222. Ito, Y.; Konoike, T.; Saegusa, T. *J. Am. Chem. Soc.* **1975**, *97*, 649–651.

223. Baciocchi, E.; Casu, A.; Ruzziconi, R. *Tetrahedron Lett.* **1989**, *30*, 3707–3710.
224. Paolobelli, A. B.; Latini, D.; Ruzziconi, R. *Tetrahedron Lett.* **1993**, *34*, 721–724.
225. Fujii, T.; Hirao, T.; Ohshiro, Y. *Tetrahedron Lett.* **1992**, *33*, 5823–5826.
226. Ryter, K.; Livinghouse, T. *J. Am. Chem. Soc.* **1998**, *120*, 2658–2659.
227. Amaya, T.; Maegawa, Y.; Masuda, T.; Osafune, Y.; Hirao, T. *J. Am. Chem. Soc.* **2015**, *137*, 10072–10075.
228. Rathke, M. W.; Weipert, P. D. *Synth. Commun.* **1991**, *21*, 1337–1351.
229. Schmittel, M.; Burghart, A.; Malisch, W.; Reising, J.; Sollner, R. *J. Org. Chem.* **1998**, *63*, 396–400.
230. Schmittel, M.; Haeuseler, A. *J. Organomet. Chem.* **2002**, *661*, 169–179.
231. Clift, M. D.; Taylor, C. N.; Thomson, R. J. *Org. Lett.* **2007**, *9*, 4667–4669.
232. Konkol, L. C.; Jones, B. T.; Thomson, R. J. *Org. Lett.* **2009**, *11*, 5550–5553.
233. Clift, M. D.; Thomson, R. J. *J. Am. Chem. Soc.* **2009**, *131*, 14579–14583.
234. Vega, M. M.; Crain, D. M.; Konkol, L. C.; Thomson, R. J. *Tetrahedron Lett.* **2015**, *56*, 3228–3230.
235. Avetta, C. T.; Konkol, L. C.; Taylor, C. N.; Dugan, K. C.; Stern, C. L.; Thomson, R. J. *Org. Lett.* **2008**, *10*, 5621–5624.
236. Jones, B. T.; Avetta, C. T.; Thomson, R. J. *Chem. Sci.* **2014**, *5*, 1794–1798.
237. Narasaka, K.; Okauchi, T.; Tanaka, K.; Murakami, M. *Chem. Lett.* **1992**, 2099–2102.
238. Jang, H. Y.; Hong, J. B.; MacMillan, D. W. C. *J. Am. Chem. Soc.* **2007**, *129*, 7004–7005.
239. Beeson, T. D.; Mastracchio, A.; Hong, J. B.; Ashton, K.; MacMillan, D. W. C. *Science* **2007**, *316*, 582–585.
240. Graham, T. H.; Jones, C. M.; Jui, N. T.; MacMillan, D. W. C. *J. Am. Chem. Soc.* **2008**, *130*, 16494–16495.
241. Kim, H.; MacMillan, D. W. C. *J. Am. Chem. Soc.* **2008**, *130*, 398–399.
242. Li, Q. J.; Fan, A. L.; Lu, Z. Y.; Cui, Y. X.; Lin, W. H.; Jia, Y. X. *Org. Lett.* **2010**, *12*, 4066–4069.

243. Li, Q. J.; Jiang, J. Q.; Fan, A. L.; Cui, Y. X.; Jia, Y. X. *Org. Lett.* **2011**, *13*, 312–315.
244. Tokuda, M.; Shigei, T.; Itoh, M. *Chem. Lett.* **1975**, 621–624.
245. Moeller, K. D. *Synlett* **2009**, 1208–1218.
246. Bolze, P.; Dickmeiss, G.; Jorgensen, K. A. *Org. Lett.* **2008**, *10*, 3753–3756.
247. Sarakinos, G.; Corey, E. J. *Org. Lett.* **1999**, *1*, 811–814.
248. Asaoka, M.; Shima, K.; Takei, H. *J. Chem. Soc. Chem. Commun.* **1988**, 430–431.
249. Asaoka, M.; Sonoda, S.; Fujii, N.; Takei, H. *Tetrahedron* **1990**, *46*, 1541–1552.
250. Torosyan, S. A.; Gimalova, F. A.; Valeev, R. F.; Miftakhov, M. S. *Russ. J. Org. Chem.* **2011**, *47*, 682–686.
251. Furrow, M. E.; Myers, A. G. *J. Am. Chem. Soc.* **2004**, *126*, 5436–5445.
252. Asaba, T.; Katoh, Y.; Urabe, D.; Inoue, M. *Angew. Chem. Int. Ed.* **2015**, *54*, 14457–14461.
253. Barros, M. T.; Maycock, C. D.; Ventura, M. R. *J. Org. Chem.* **1997**, *62*, 3984–3988.
254. Yamamoto, E.; Gokuden, D.; Nagai, A.; Kamachi, T.; Yoshizawa, K.; Hamasaki, A.; Ishida, T.; Tokunaga, M. *Org. Lett.* **2012**, *14*, 6178–6181.
255. Hong, S. H.; Day, M. W.; Grubbs, R. H. *J. Am. Chem. Soc.* **2004**, *126*, 7414–7415.
256. Hong, S. H.; Sanders, D. P.; Lee, C. W.; Grubbs, R. H. *J. Am. Chem. Soc.* **2005**, *127*, 17160–17161.
257. Hong, D. S.; Kurzrock, R.; Supko, J. G.; He, X. Y.; Naing, A.; Wheler, J.; Lawrence, D.; Eder, J. P.; Meyer, C. J.; Ferguson, D. A.; Mier, J.; Konopleva, M.; Konoplev, S.; Andreeff, M.; Kufe, D.; Lazarus, H.; Shapiro, G. I.; Dezube, B. J. *Clin. Cancer Res.* **2012**, *18*, 3396–3406.
258. Sporn, M. B.; Liby, K.; Yore, M. M.; Suh, N.; Albin, A.; Honda, T.; Sundararajan, C.; Gribble, G. W. *Drug Dev. Res.* **2007**, *68*, 174–182.
259. Guo, Z.; Vangapandu, S.; Sindelar, R. W.; Walker, L. A.; Sindelar, R. D. *Curr. Med. Chem.* **2005**, *12*, 173–190.
260. Robinson, E. E.; Thomson, R. J. *J. Am. Chem. Soc.* **2018**, *140*, 1956–1965.
261. Pangborn, A. B.; Giardello, M. A.; Grubbs, R. H.; Rosen, R. K.; Timmers, F. J. *Organometallics* **1996**, *15*, 1518–1520.

262. Armarego, W. L. F.; Chai, C. L. L., *Purification of Laboratory Chemicals*. 6th ed.; Elsevier/Butterworth-Heinemann: Boston, 2009.
263. Zhao, L.; Wang, J. L.; Zheng, H. Y.; Li, Y.; Yang, K.; Cheng, B.; Jin, X. J.; Yao, X. J.; Zhai, H. B. *Org. Lett.* **2014**, *16*, 6378–6381.
264. Edenborough, M. S.; Herbert, R. B. *Nat. Prod. Rep.* **1988**, *5*, 229–245.
265. Scheuer, P. J. *Acc. Chem. Res.* **1992**, *25*, 433–439.
266. Simpson, J. S.; Garson, M. J. *Org. Biomol. Chem.* **2004**, *2*, 939–948.
267. Garson, M. J.; Simpson, J. S. *Nat. Prod. Rep.* **2004**, *21*, 164–179.
268. Laurent, D.; Pietra, F. *Mar. Biotechnol.* **2006**, *8*, 433–447.
269. Fattorusso, E.; Taglialatela-Scafati, O. *Mar. Drugs* **2009**, *7*, 130–152.
270. Schnermann, M. J.; Shenvi, R. A. *Nat. Prod. Rep.* **2014**, *32*, 543–577.
271. Baker, J. T.; Wells, R. J.; Oberhansli, W. E.; Hawes, G. B. *J. Am. Chem. Soc.* **1976**, *98*, 4010–4012.
272. Fookes, C. J. R.; Garson, M. J.; Macleod, J. K.; Skelton, B. W.; White, A. H. *J. Chem. Soc., Perkin Trans. 1* **1988**, 1003–1011.
273. Garson, M. J. *J. Chem. Soc. Chem. Commun.* **1986**, 35–36.
274. Hagadone, M. R.; Scheuer, P. J.; Holm, A. *J. Am. Chem. Soc.* **1984**, *106*, 2447–2448.
275. Dumdei, E. J.; Flowers, A. E.; Garson, M. J.; Moore, C. J. *Comp. Biochem. Physiol.* **1997**, *118*, 1385–1392.
276. Simpson, J. S.; Garson, M. J. *Tetrahedron Lett.* **1998**, *39*, 5819–5822.
277. *World Malaria Report 2017*; World Health Organization: 2017; pp 1–196.
278. Dondorp, A. M.; Nosten, F.; Yi, P.; Das, D.; Phyto, A. P.; Tarning, J.; Lwin, K. M.; Ariey, F.; Hanpithakpong, W.; Lee, S. J.; Ringwald, P.; Silamut, K.; Imwong, M.; Chotivanich, K.; Lim, P.; Herdman, T.; An, S. S.; Yeung, S.; Singhasivanon, P.; Day, N. P. J.; Lindegardh, N.; Socheat, D.; White, N. J. *N. Engl. J. Med.* **2009**, *361*, 455–467.
279. Taylor, W. R. J.; White, N. J. *Drug Saf.* **2004**, *27*, 25–61.
280. Rosenthal, P. J. *N. Engl. J. Med.* **2008**, *358*, 1829–1836.
281. Su, X. Z.; Miller, L. H. *Sci. China Life Sci.* **2015**, *58*, 1175–1179.

282. Kumar, S.; Guha, M.; Choubey, V.; Maity, P.; Bandyopadhyay, U. *Life Sci.* **2007**, *80*, 813–828.
283. Wright, A. D.; Wang, H. Q.; Gurrath, M.; Konig, G. M.; Kocak, G.; Neumann, G.; Loria, P.; Foley, M.; Tilley, L. *J. Med. Chem.* **2001**, *44*, 873–885.
284. Roepe, P. D. *Trends Parasitol.* **2014**, *30*, 130–135.
285. Wright, A. D.; Konig, G. M.; Angerhofer, C. K.; Greenidge, P.; Linden, A.; Desqueyroux-Faundez, R. *J. Nat. Prod.* **1996**, *59*, 710–716.
286. Corey, E. J.; Magriotis, P. A. *J. Am. Chem. Soc.* **1987**, *109*, 287–289.
287. Fairweather, K. A.; Mander, L. N. *Org. Lett.* **2006**, *8*, 3395–3398.
288. Miyaoka, H.; Okubo, Y.; Muroi, M.; Mitome, H.; Kawashima, E. *Chem. Lett.* **2011**, *40*, 246–247.
289. Roosen, P. C.; Vanderwal, C. D. *Angew. Chem. Int. Ed.* **2016**, *55*, 7180–7183.
290. Lu, H. H.; Pronin, S. V.; Antonova-Koch, Y.; Meister, S.; Winzeler, E. A.; Shenvi, R. A. *J. Am. Chem. Soc.* **2016**, *138*, 7268–7271.
291. Corey, E. J.; Ohno, M.; Mitra, R. B.; Vatakencherry, P. A. *J. Am. Chem. Soc.* **1964**, *86*, 478–485.
292. Pronin, S. V.; Reiher, C. A.; Shenvi, R. A. *Nature* **2013**, *501*, 195–199.
293. Iwasaki, K.; Wan, K. K.; Oppedisano, A.; Crossley, S. W. M.; Shenvi, R. A. *J. Am. Chem. Soc.* **2014**, *136*, 1300–1303.
294. Chung, S. K. *J. Org. Chem.* **1979**, *44*, 1014–1016.
295. Sharma, P. K.; Kumar, S.; Kumar, P.; Nielsen, P. *Tetrahedron Lett.* **2007**, *48*, 8704–8708.
296. Brown, C. A.; Ahuja, V. K. *J. Org. Chem.* **1973**, *38*, 2226–2230.
297. Yoon, N. M. *Pure Appl. Chem.* **1996**, *68*, 843–848.
298. Nicolaou, K. C.; Ellery, S. P.; Chen, J. S. *Angew. Chem. Int. Ed.* **2009**, *48*, 7140–7165.
299. Du, J. N.; Espelt, L. R.; Guzei, I. A.; Yoon, T. P. *Chem. Sci.* **2011**, *2*, 2115–2119.
300. Corey, E. J.; Sneen, R. A. *J. Am. Chem. Soc.* **1956**, *78*, 6269–6278.
301. Matthews, R. S.; Girgenti, S. J.; Folkers, E. A. *J. Chem. Soc. Chem. Commun.* **1970**, 708–709.

302. Shing, T. K. M.; Jiang, Q. *J. Org. Chem.* **2000**, *65*, 7059–7069.
303. Stojanac, N.; Valenta, Z. *Can. J. Chem.* **1991**, *69*, 853–855.
304. Kim, M.; Kawada, K.; Gross, R. S.; Watt, D. S. *J. Org. Chem.* **1990**, *55*, 504–511.
305. Shing, T. K. M.; Jiang, Q.; Mak, T. C. W. *J. Org. Chem.* **1998**, *63*, 2056–2057.
306. Burgstahler, A. W.; Marx, J. N. *J. Org. Chem.* **1969**, *34*, 1562–1566.
307. Burgstahler, A. W.; Marx, J. N. *Tetrahedron Lett.* **1964**, 3333–3338.
308. Turner, R. B.; Buchardt, O.; Herzog, E.; Morin, R. B.; Riebel, A.; Sanders, J. M. *J. Am. Chem. Soc.* **1966**, *88*, 1766–1775.
309. Lee, H. J.; Ravn, M. M.; Coates, R. M. *Tetrahedron* **2001**, *57*, 6155–6167.
310. Keeling, C. I.; Madilao, L. L.; Zerbe, P.; Dullat, H. K.; Bohlmann, J. *J. Biol. Chem.* **2011**, *286*, 21145–21153.
311. Norin, T.; Winell, B. *Phytochemistry* **1971**, *10*, 2818–2821.
312. Porto, S. T.; Rangel, R.; Furtado, A. N.; De Carvalho, C. T.; Martins, H. C.; Veneziani, C. R.; Da Costa, B. F.; Vinholis, H. A.; Cunha, R. W.; Heleno, C. V.; Ambrosio, R. S. *Molecules* **2009**, *14*.
313. Wang, X.; Yu, H.; Zhang, Y.; Lu, X.; Wang, B.; Liu, X. *Chem. Biodivers.* **2017**, *15*, e1700276.
314. Kato, H.; Kodama, O.; Akatsuka, T. *Phytochemistry* **1994**, *36*, 299–301.
315. Gavagnin, M.; Ungur, N.; Castelluccio, F.; Cimino, G. *Tetrahedron* **1997**, *53*, 1491–1504.
316. Gavagnin, M.; Ungur, N.; Castelluccio, F.; Muniain, C.; Cimino, G. *J. Nat. Prod.* **1999**, *62*, 269–274.
317. Shingaki, M.; Wauke, T.; Ahmadi, P.; Tanaka, J. *Chem. Pharm. Bull.* **2016**, *64*, 272–275.
318. Taylor, W. C.; Toth, S. *Aust. J. Chem.* **1997**, *50*, 895–902.
319. Suciati; Lambert, L. K.; Garson, M. J. *Aust. J. Chem.* **2011**, *64*, 757–765.
320. Kolypadi, M.; Liapis, M.; Ragoussis, V. *Tetrahedron* **2005**, *61*, 2003–2010.
321. Gris, A.; Cabedo, N.; Navarro, I.; de Alfonso, I.; Agulló, C.; Abad-Somovilla, A. *J. Org. Chem.* **2012**, *77*, 5664–5680.

322. Endo, Y.; Kasahara, T.; Harada, K.; Kubo, M.; Etoh, T.; Ishibashi, M.; Ishiyama, A.; Iwatsuki, M.; Ootoguro, K.; Omura, S.; Akisue, G.; Hirano, T.; Kagechika, H.; Fukuyama, Y.; Ohsaki, A. *J. Nat. Prod.* **2017**, *80*, 3121–3128.
323. Liu, M.-L.; Duan, Y.-H.; Zhang, J.-B.; Yu, Y.; Dai, Y.; Yao, X.-S. *Tetrahedron* **2013**, *69*, 6574–6578.
324. Jiang, B.; Wang, W.-J.; Li, M.-P.; Huang, X.-J.; Huang, F.; Gao, H.; Sun, P.-H.; He, M.-F.; Jiang, Z.-J.; Zhang, X.-Q.; Ye, W.-C. *Bioorg. Med. Chem. Lett.* **2013**, *23*, 3879–3883.
325. Kwon, H. J.; Hong, Y. K.; Park, C.; Choi, Y. H.; Yun, H. J.; Lee, E. W.; Kim, B. W. *Cancer Lett.* **2010**, *290*, 96–103.
326. Fonseca, M. T. H.; List, B. *Angew. Chem. Int. Ed.* **2004**, *43*, 3958–3960.
327. Cabanillas, A. H.; Tena Pérez, V.; Maderuelo Corral, S.; Rosero Valencia, D. F.; Martel Quintana, A.; Ortega Doménech, M.; Rumbero Sánchez, Á. *J. Nat. Prod.* **2018**, *81*, 410–413.